

Dissertation

**submitted to the
Combined Faculties for the Natural Sciences and for Mathematics
of the Ruperto-Carola University of Heidelberg, Germany
for the degree of
Doctor of Natural Sciences**

presented by
Diplom-Biologin Verena Schmeiser
born in Regensburg, Germany
Oral-examination:

**Regulated by the interplay of multiple
CLASP domains,
the localization of the TOGL2 domain to
microtubules drives spindle formation in
*Saccharomyces cerevisiae***

Referees:

Prof. Dr. Felix Wieland

PD Dr. Johannes Lechner

For my parents

TABLE OF CONTENTS

TABLE OF CONTENTS	I
ABBREVIATIONS	VI
SUMMARY	IX
ZUSAMMENFASSUNG	XI
1 INTRODUCTION	1
1.1 The cell cycle in <i>S. cerevisiae</i>	1
1.2 The cell cycle phases in <i>S. cerevisiae</i>	3
1.2.1 G1-phase.....	3
1.2.2 S-phase	4
1.2.2.1 The DNA replication and damage checkpoint	5
1.2.2.2 Capturing of unattached KTs	6
1.2.2.3 SPB duplication and separation	8
1.2.3 G2- and metaphase	8
1.2.3.1 The tension checkpoint.....	10
1.2.3.2 The spindle assembly checkpoint.....	12
1.2.3.3 The bipolar metaphase spindle	14
1.2.4 Anaphase	15
1.2.4.1 The Cdc14 early anaphase release.....	17
1.2.4.2 Formation of the spindle midzone	17
1.2.5 Telophase and exit from mitosis	18
1.3 The kinetochore	19
1.3.1 The centromere	19
1.3.2 The inner kinetochore	20
1.3.3 The linker layer	20
1.3.4 The outer kinetochore.....	21
1.4 CLASP proteins and the <i>S. cerevisiae</i> Stu1	22
1.5 The aim of the study	25
2 MATERIALS	26
2.1 Organisms	26
2.1.1 <i>Escherichia coli</i> strains	26
2.1.2 <i>Saccharomyces cerevisiae</i> strains.....	26
2.2 Plasmids	30
2.3 Oligonucleotides	32
2.4 Antibodies	34

2.5 Equipment	35
2.6 Chemicals, Enzymes and Disposals	35
2.7 Service Providers, Web Services and Software	35
3 METHODS.....	37
3.1 Cultivation conditions for Microorganisms.....	37
3.1.1 <i>Escherichia coli</i>	37
3.1.2 <i>Saccharomyces cerevisiae</i>	37
3.1.2.1 Regular growth conditions	37
3.1.2.2 Growth conditions for SILAC approaches.....	38
3.2 Molecular Biology	39
3.2.1 Polymerase chain reaction (PCR).....	39
3.2.1.1 Preparative amplification of DNA fragments for cloning	39
3.2.1.2 Preparative amplification of DNA fragments by overlap extension mutagenesis ...	39
3.2.1.3 Preparative amplification of DNA fragments for PCR-mediated tagging of proteins ..	40
3.2.1.4 Analytical amplification of DNA fragments	41
3.2.2 Agarose gel electrophoresis	41
3.2.3 DNA precipitation.....	41
3.2.4 Cloning procedures.....	41
3.2.5 Purification of DNA fragments.....	41
3.2.6 Determination of DNA contents.....	42
3.2.7 Ligation of DNA fragments.....	42
3.2.8 Preparation of chemically competent <i>E. coli</i> cells.....	42
3.2.9 Transformation of <i>E. coli</i> cells.....	42
3.2.10 Isolation of plasmid DNA from <i>E. coli</i>	42
3.2.11 Transformation of <i>S. cerevisiae</i> cells	43
3.2.12 Construction of genomically modified <i>S. cerevisiae</i> strains.....	43
3.2.13 System for the integration of Stu1 mutants in the endogenous DNA locus .	43
3.2.14 Labeling of CEN DNA.....	44
3.2.15 Isolation of chromosomal DNA from <i>S. cerevisiae</i>	44
3.3 Cell biology.....	45
3.3.1 Methods for <i>S. cerevisiae</i> cell synchronization.....	45
3.3.1.1 G1 arrest	45
3.3.1.2 G2- /metaphase arrest with unattached kinetochores	45
3.3.1.3 Metaphase arrest	45
3.3.1.4 Anaphase arrest.....	45
3.3.2 Stu1 shutdown conditions	45

3.3.3 Stu1 overexpression	46
3.3.4 Chromosomal loss assay.....	46
3.3.5 Fluorescent Microscopy	46
3.3.5.1 Cell preparation for microscopy.....	46
3.3.5.2 Live-cell imaging	46
3.3.5.3 Analysis of microscope images	46
3.3.5.3.1 Processing of microscope images.....	47
3.3.5.3.2 Generation of intensity profiles	47
3.3.5.3.3 Generation of box-whisker-plots.....	47
3.4 Protein Biochemistry	47
3.4.1 Protein expression and purification from <i>E. coli</i> cells	47
3.4.2 Protein extraction from <i>S. cerevisiae</i> cells	49
3.4.3 Determination of protein concentrations via Bradford assay	49
3.4.4 Immunoprecipitation of Flag-Stu1 with M2 α -Flag Magnetic Beads.....	49
3.4.5 Immunoprecipitation of Stu1-ProtA with IgG beads.....	50
3.4.6 Immunoprecipitation of Stu1-ProtA with IgG beads with SILAC	51
3.4.7 <i>In vitro</i> phosphatase treatment	51
3.4.8 <i>In vitro</i> kinase assay	51
3.4.9 SDS polyacrylamide gel electrophoresis (SDS-PAGE)	52
3.4.9.1 Glycine SDS-PAGE	52
3.4.9.2 NuPAGE® Novex Bis-Tris SDS-PAGE	52
3.4.10 Coomassie staining	52
3.4.10.1 Colloidal Coomassie staining of SDS-gels.....	52
3.4.10.2 Regular coomassie staining for SDS-gels or PVDF	52
3.4.11 Western blot analysis	53
3.4.12 Mass Spectrometry	53
3.5 <i>In silico</i> analysis.....	54
3.5.1 Secondary structure prediction	54
3.5.2 Isoelectric point calculator	54
4 RESULTS	55
4.1 Stu1 domains and their functions.....	55
4.1.1 Introduction of putative Stu1 domains.....	55
4.1.2 The role of Stu1 domains for spindle localization and formation in meta- and anaphase.....	56
4.1.2.1 The TOGL2 domain is sufficient for tubulin interaction	56
4.1.2.2 Stu1 requires the TOGL2 and ML domain for the efficient formation of metaphase spindles.....	58

4.1.2.3	The CL domain specifies Stu1 localization to the MT overlap in metaphase	61
4.1.2.4	The TOGL2 and ML domain are dispensable for midzone localization of Stu1 in anaphase	62
4.1.3	The role of Stu1 domains for unattached KT localization	64
4.1.3.1	The CL domain specifies Stu1 localization to unattached KTs.....	64
4.1.3.2	Efficient capturing does not require Stu1 localization to unattached KTs – but TOGL2 activity	66
4.1.3.3	The TOGL2 domain might be required for the temporal regulation of KT-generated MTs	67
4.1.4	Stu1's localization and role at metaphase KTs.....	69
4.1.4.1	The ML domain is required for proper KT attachment to MTs.....	69
4.1.4.2	The CL domain inhibits Stu1's ability to stabilize kMTs.....	70
4.1.4.3	The CL domain makes kMT length dependent on tension	72
4.1.5	Disturbed (k)MT dynamics result in bipolar attachment defects	72
4.1.6	Deletion of the TOGL2 domain cannot be rescued by the CLASP1 TOGL2 or Stu2 TOG1 domain.....	76
4.2	Various cell cycle dependent phosphorylations of Stu1 indicate a complex way of regulation.....	78
4.2.1	Stu1 phosphorylation in mitosis causes a mobility shift on SDS-PAGE.....	78
4.2.2	Stu1 gets phosphorylated and dephosphorylated throughout the cell cycle ..	79
4.2.3	Ipl1 and Mps1 phosphorylate Stu1 <i>in vitro</i>	82
4.2.4	Analysis of Stu1 phosphorylation mutants	84
4.2.4.1	Analysis of Stu1 phosphomutants created according to SILAC results.....	85
4.2.4.2	Phosphorylation site S1113 is responsible for the conformational change causing the mobility shift on SDS-PAGE.....	88
4.2.4.3	Analysis of single mutations of Stu1 phosphorylation sites	89
4.2.4.4	Analysis of Stu1 phosphomutants according to predicted kinases.....	91
4.2.4.5	Analysis of Stu1 phosphorylation sites located in the CL domain	93
5	DISCUSSION	95
5.1	An interplay of Stu1 domains regulates Stu1 localization and controls TOGL2 activity.....	95
5.1.1	Metaphase spindle formation requires the TOGL2 activity of binding free tubulin.....	95
5.1.2	MT lattice binding via the ML domain is required for metaphase, but not anaphase spindle formation.....	98
5.1.3	Stu1 localizes to attached KTs in metaphase and regulates kMT formation..	99
5.1.4	The CL domain specifies Stu1 for unattached KTs	101

5.1.5 TOGL2 activity and the ML domain, but not KT localization are prerequisites for efficient capturing of unattached KTs.....	101
5.1.6 The TOGL2 and ML domain contribute to faithful KT attachment.....	103
5.1.7 Sequestration of Stu1 at unattached KTs prevents precocious SPB separation to ensure bipolar attachment	105
5.1.8 The regulatory interplay between the CL domain and the ML domain.....	107
5.2 Phosphorylation might contribute to regulate the MT affinity of Stu1	110
5.2.1 Cell cycle specific phosphorylations within the ML and the CL domain contribute to regulate Stu1 localization	110
5.2.2 Phosphorylation of the CL domain might contribute to a balanced Stu1 sequestration at unattached KTs	111
5.2.3 Phosphorylation of Stu1 in the ML domain.....	113
5.2.4 Phosphorylation of putative Cdk1 sites	115
5.2.5 Phosphorylation of the main cell cycle dependent sites	116
5.2.6 Problems of reproducibility due to strain variations	117
6 REFERENCES.....	118
ACKNOWLEDGEMENT/DANKSAGUNG	137

ABBREVIATIONS

2TY	2x tryptone/yeast extract
aa	amino acid
AP	alkaline phosphatase
APC/C	anaphase promoting complex/cyclosome
APS	ammonium persulfate
ATP	adenosine triphosphate
α -factor	alpha factor
bp	base pair
β -EtSH	β -mercaptoethanol
CEN	centromere
CFP	cyan fluorescent protein
CHIP	chromatin immunoprecipitation
CIP	calf intestine alkaline phosphatase
CL	C-terminal loop
D3	domain three
D4	domain four
DMSO	dimethyl sulfoxide
DNA	deoxyribonucleic acid
dNTP	deoxyribonucleoside triphosphate
DOC	sodium deoxycholate
DTT	dithiothreitol
EDTA	ethylenediaminetetraacetic acid
FEAR	Cdc fourteen early anaphase release
FOA	5'-fluoroorotic acid
g	gravitational force (9.80665 ms ⁻²)
Gal	galactose
GFP	green fluorescent protein
Glc	glucose
HRP	horseradish peroxidase
IgG	immunoglobulin G
IPTG	Isopropyl- β -D-thiogalactopyranosid
kDa	kilo dalton
kMT	kinetochore microtubule

KT	kinetochore
KT5	kinetochore of chromosome V
LB	lysogeny broth
MBD	microtubule binding domain
ML	minimal microtubule binding loop
mpH ₂ O	millipore H ₂ O
MT	microtubule
MW	molecular weight or relative molecular mass
NFM	non-fluorescent media
Nz	nocodazole
OD	optical density
PBS	phosphate buffered saline
PCR	polymerase chain reaction
PEG	polyethylene glycol
PMSF	phenylmethylsulfonyl fluoride
ProtA-tag	immunoglobulin G (IgG) binding domain of protein A from <i>Staphylococcus aureus</i>
PVDF	polyvinylidenedifluoride
Raff	raffinose
RNase A	bovine pancreatic ribonuclease A
SAC	spindle assembly checkpoint
SDS	sodium dodecyl sulfate
SDS-PAGE	sodium dodecyl sulfate polyacrylamide gel electrophoresis
SOB	super optimal broth
SOC	super optimal broth with catabolite repression
SPB	spindle pole body
SPOC	spindle position checkpoint
TAE	Tris-acetate-EDTA
TE	Tris-EDTA
TEMED	tetramethylethylenediamine
tetO/tetR	tetracycline operator/tetracycline repressor
TOG	tumor overexpressed gene
TOGL	TOG-like
Tris	tris(hydroxymethyl)-aminomethan
TPCK	tosyl phenylalanyl chloromethyl ketone
ts	temperature-sensitive

uaKT	unattached kinetochore
WT	wild type
YNB	yeast nitrogen base
YPD	yeast extract/ peptone/ dextrose

SUMMARY

The kinetochore (KT) is a complex structure that enables attachment of chromosomes to spindle microtubules (MTs). Several MT associated proteins (MAPs) contribute to the KT-MT interface and regulate the dynamics of kinetochore microtubules (kMTs). In addition, these MAPs localize to interpolar MTs and regulate spindle stability. One of these proteins is the *S. cerevisiae* CLASP (cytoplasmic linker associated protein) Stu1, an essential protein that has several functions during mitosis and therefore localizes differently in the course of each cell division. The aim of this work was to investigate which domains of Stu1 are important for its cell cycle specific localization, how this contributes to a coordinated action of Stu1 and how localization and function of Stu1 are regulated. Structural predictions of Stu1 suggest the organization in six domains. The following observations were made with the focus on three of them: the TOGL2 domain, the minimal MT-binding loop (ML) and the C-terminal loop (CL).

The TOGL2 domain solely achieves binding of $\alpha\beta$ -tubulin and drives spindle formation

Co-immunoprecipitations identified the TOGL2 domain to be sufficient to bind free $\alpha\beta$ -tubulin. This feature of the TOGL2 domain is essential and solely responsible for the important role of Stu1 in driving spindle formation. Thus, the TOGL2 domain ensures the function of Stu1 as a MT polymerase or rescue factor. Domain swapping experiments demonstrated that the function of the TOGL2 domain of Stu1 is very specific and cannot be easily taken over by another TOG domain.

MT binding via the ML domain is required for efficient metaphase spindle formation, but is dispensable for midzone localization

Besides the TOGL2 domain, efficient spindle formation in metaphase additionally depends on the binding of Stu1 to the MT lattice via the ML domain. Thereby, the CL domain specifies Stu1 localization to the region of the MT overlap. Midzone localization of Stu1 in anaphase, however, is independent of the ML domain and therefore must be ensured in a manner that is not based on MT binding.

An interplay of the CL domain with the ML domain specifies Stu1's sequestration at unattached KTs

The CL domain was found to specify Stu1 for the sequestration at unattached KTs, most likely by inhibiting the MT binding affinity of the ML domain. Thus, the CL domain indirectly prevents spindle formation in the presence of unattached KTs.

Efficient KT capture relies on unperturbed MT dynamics ensured by the Stu1 TOGL2 activity

Capturing experiments of the CL deletion mutant revealed that Stu1 localization to unattached KTs is not a prerequisite for efficient capturing. However, the ML domain and especially the TOGL2 activity are mandatory in this respect. The contribution of Stu1 to unperturbed MT dynamics seems to be more important for the capturing process than KT localization. This may involve the polymerization of capturing kMTs but also, as analyzed, the temporal regulation of KT-generated MTs.

The CL domain makes kMT length dependent on the tension on the KT-MT interface

The localization of Stu1 to attached KTs is a prerequisite for the polymerization of kMTs. In this respect, the CL domain was found to inhibit Stu1's ability to stabilize kMTs and to make the kMT length dependent on tension on the KT-MT interface.

The CL domain prevents precocious spindle formation to ensure biorientation

The data showed that the CL domain facilitates bipolar attachment by ensuring unperturbed dynamics of inter polar MTs. Therefore, the CL domain seems to fine-tune the MT polymerizing activity of Stu1 by regulating the MT affinity of the ML domain.

Stu1 phosphorylation within the CL domain contributes to Stu1 regulation

Finally, this work revealed that phosphorylation of Stu1 contributes to the regulation of Stu1. SILAC analyses identified 15 phosphorylation sites that mainly reside within the ML and the CL domain of Stu1 and are putative target sites of various serine/ threonine kinases like Cdk1, polo-like kinase, Ipl1 and Mps1. Furthermore, these analyses demonstrated that Stu1 gets phosphorylated and dephosphorylated throughout the cell cycle suggesting a regulatory role for kinases. Consistent with that, *in vitro* kinase assays identified Stu1 N- and C-terminus as targets of Ipl1 and Mps1 kinases. Analyses of phosphomutants eventually suggested that phosphorylation of the CL domain contributes to the regulatory impact of the CL domain on the MT affinity of the ML domain.

Taken together, the present study supports the theory that Stu1, similar to other CLASP proteins acts as a local modulator for MT dynamics and stability. While the TOGL2 domain accomplishes the essential function of tubulin incorporation in MT plus-ends, the other domains are required to regulate the localization of Stu1 and (probably therefore) control the MT polymerizing activity.

ZUSAMMENFASSUNG

Das Kinetochor (KT) ist eine komplexe Struktur, die die Anhaftung von Mikrotubuli (MT) an Chromosomen ermöglicht. Mehrere MT-assoziierte Proteine (MAPs) tragen zu dieser Schnittstelle zwischen KT und MT bei und regulieren die Dynamik von Kinetochor-Mikrotubuli (kMT). Diese MAPs lokalisieren außerdem an interpolare MT und regulieren die Spindelstabilität. Eines dieser Proteine ist das essentielle CLASP Stu1 der Bäckerhefe, das während der Mitose gleich mehrere Funktionen hat und deshalb im Laufe des Zellzyklus unterschiedlich lokalisiert. Ziel dieser Arbeit war es herauszufinden, welche Proteindomänen für diese Zellzyklus-abhängige Lokalisierung von Bedeutung sind, wie dies wiederum dazu beiträgt die Aktivität von Stu1 zu koordinieren und wie sowohl Lokalisierung als auch Funktion dabei geregelt werden. Vorhersagen für die Struktur von Stu1 legen eine Unterteilung in sechs Domänen nahe. Bei den im Folgenden beschriebenen Beobachtungen standen drei davon im Fokus: die TOGL2 Domäne, der minimalen MT-Binde-Loop (ML) und der C-terminale Loop (CL).

Die TOGL2 Domäne alleine bindet $\alpha\beta$ -Tubulin und treibt die Spindelbildung voran

Co-Immunopräzipitationen zeigten, dass die TOGL2 Domäne für die Bindung von $\alpha\beta$ -Tubulin ausreicht. Dieses Merkmal der TOGL2 Domäne ist essentiell und alleinig für die wichtige Rolle von Stu1 in der Spindelbildung verantwortlich. Auf diese Weise sorgt die TOGL2 Domäne für die Funktion von Stu1 als MT-Polymerase oder -Retungsfaktor. Der Austausch der TOGL2 Domäne zeigte, dass ihre Funktion sehr spezifisch ist und nicht einfach von anderen TOG Domänen übernommen werden kann.

Die MT-Bindung mittels der ML Domäne wird für effiziente Metaphasen-Spindelbildung benötigt, ist aber später für die Lokalisierung zur Spindelmitte unwichtig

Eine effiziente Spindelbildung in der Metaphase ist neben der TOGL2 Domäne auch von der Stu1-Bindung an die MT-Oberfläche mittels der ML Domäne abhängig. Dabei bestimmt die CL Domäne die Lokalisierung von Stu1 an die überlappenden interpolaren MT. Die Lokalisierung zur Spindelmitte während der Anaphase ist jedoch unabhängig von der ML Domäne und muss daher auf eine Weise gewährleistet werden, die nicht auf MT-Bindung beruht.

Eine Wechselwirkung zwischen CL Domäne und ML Domäne bestimmt die Stu1 Lokalisierung an nicht-anhaftende KTe

Indem sie wahrscheinlich die Affinität der ML Domäne für die MT-Bindung inhibiert, stellt die CL Domäne die Bindung von Stu1 an nicht-anhaftende KTe sicher. Dadurch verhindert die CL Domäne indirekt die Spindelbildung solange nicht-anhaftende KTe vorhanden sind.

Effizientes Einfangen der KTe beruht auf ungestörter MT Dynamik, die durch die TOGL2 Aktivität sichergestellt wird

„Capturing“-Experimente mit der CL-Deletionsmutante zeigten, dass die Lokalisierung von Stu1 an nicht-anhaftende KTe keine Voraussetzung für ein effizientes Einfangen der KTe ist. Die ML Domäne und vor allem die TOGL2 Domäne sind in diesem Zusammenhang allerdings zwingend notwendig. Die Beteiligung von Stu1 an ungestörter MT Dynamik scheint für das Einfangen wichtiger zu sein als die KT-Lokalisierung.

Die CL Domäne macht die Länge der kMT von der Spannung an der Grenzfläche zwischen KT und MT abhängig

Die Lokalisierung von Stu1 an anhaftende KTe ist eine Voraussetzung für die Polymerisierung der kMT. In dieser Hinsicht zeigte sich, dass die CL Domäne die Fähigkeit von Stu1 inhibiert kMT zu stabilisieren und die Länge der kMT abhängig von der Spannung an der KT-MT Grenzfläche macht.

Die CL Domäne verhindert verfrühte Spindelbildung, um bipolare Anhaftung sicherzustellen

Es konnte gezeigt werden, dass die CL Domäne die bipolare Anhaftung erleichtert indem sie eine ungestörte Dynamik der interpolaren MT gewährleistet. Daher scheint die CL Domäne die Aktivität von Stu1 bei der MT-Polymerisierung zu steuern indem sie die Affinität der ML Domäne für die MT reguliert.

Phosphorylierung innerhalb der CL Domäne trägt zur Regulation von Stu1 bei

In dieser Arbeit konnte gezeigt werden, dass die Phosphorylierung von Stu1 zu dessen Regulation beiträgt. Mittels SILAC-Analyse wurden 15 Phosphorylierungsstellen identifiziert, die größtenteils innerhalb der ML und der CL Domäne von Stu1 liegen und mögliche Ziele verschiedener Serin/Threonin-Kinasen wie der Cdk1, der Polokinase, Ipl1 und Mps1 sind. Darüber hinaus zeigte sich, dass Stu1 während des Zellzyklus sowohl phosphoryliert, als auch dephosphoryliert wird. Passend dazu werden der N- und C-Terminus von Stu1 *in vitro* von Ipl1 und Mps1 phosphoryliert. Die Analyse von Phosphorylierungsmutanten legte schließlich nahe, dass die Phosphorylierung der CL Domäne zum regulatorischen Effekt der CL Domäne auf die MT Affinität der ML Domäne beiträgt.

Zusammengefasst unterstützt diese Arbeit die Theorie, dass Stu1, ähnlich wie andere CLASP Proteine, als ein lokaler Modulator für MT-Dynamik und -Stabilität fungiert. Während die TOGL2 Domäne die essentielle Funktion der MT-Inkorporation in MT übernimmt, werden die anderen Domänen dafür benötigt die Lokalisierung von Stu1 zu regulieren und steuern daher die Aktivität der MT Polymerisierung.

1 INTRODUCTION

Eukaryotic cells undergo mitotic cell divisions resulting in two genetically identical cells. Therefore, the chromosomes containing the genetic information have to be faithfully duplicated and segregated. Incorrect chromosome segregation can lead to aneuploidy and cell death caused by chromosome loss. The highly regulated cell cycle machinery ensures the precise spatial and temporal coordination of events taking place to activate processes during cell division. Microtubules (MTs) that attach to chromosomes via the kinetochore (KT) thereby enable chromosome separation and distribution. Defective attachment of chromosomes is one of the most prominent causes of chromosomal instability. Studies over the last years have advanced the knowledge about the interface between KTs and MT plus-ends giving more insight in the mechanisms of attachment, its regulation and error correction.

In higher eukaryotes cell cycle deregulations and aneuploidy are the reasons for several congenital disorders and cancer. Tumor cells accumulate mutations that generate uncontrolled cell proliferation, missegregated chromosomes and chromosome instability. Thus, an important prerequisite to improve cancer therapeutic strategies that target the cell division cycle is to increase our understanding of the concerted mechanisms during mitosis (Manchado, E. et al., 2012).

The current work focused on the eukaryotic model organism *Saccharomyces cerevisiae*. Thus in the following, the key aspects of the cell cycle in budding yeast are discussed.

1.1 The cell cycle in *S. cerevisiae*

Each cell cycle has the function to accurately duplicate the genetic information of the mother cell and proliferate it to the daughter cell. Thereby the DNA, arranged in 16 chromosomes, has to get replicated and equally distributed between mother and daughter cell in a highly ordered and regulated process that can be divided into four discrete cell cycle phases (Fig. 1-1). The phases of DNA synthesis (S) and mitosis (M), separated from each other by the gap phases G1 (gap 1) and G2 (gap 2).

Thereby the first three consecutive phases of the cell cycle (G1, S and G2) are collectively referred to as interphase and represent the most time consuming part of the cell cycle. During all three phases, the cells grow by producing proteins and cytoplasmic organelles. Assuming that the environmental conditions like nutrients, space and temperature are sufficient, cells in G1 prepare for DNA replication by the synthesis of

proteins required for duplication of the genetic material in the following S-phase. In response to insufficient environmental requirements however, mitosis is prevented and cells move into a quiescent stage called G₀. After accurate DNA replication and spindle pole body (SPB, microtubule organizing centers in higher eukaryotes) duplication in S-phase, cells move into the second pause called G₂-phase and prepare for their entry into M-phase. In contrast to higher eukaryotes, *S. cerevisiae* cells undergo a closed mitosis. This implies that the nuclear envelope stays intact during mitosis and cells therefore have no distinct G₂-phase or G₂/M-transition. In higher eukaryotes, the nuclear envelope breakdown indicates the start of M-phase.

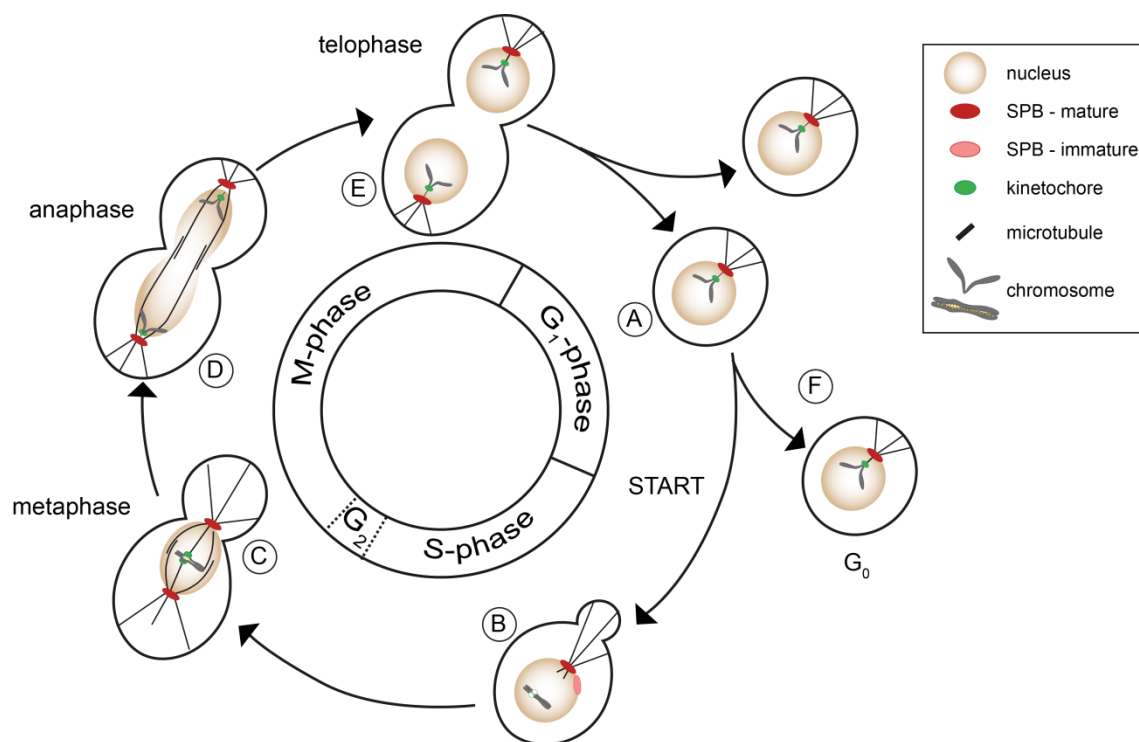


Fig. 1-1. Model of the *S. cerevisiae* cell cycle.

During one cell cycle, cells progress through the phase of G₁ (gap 1), S (synthesis) and G₂ (gap 2), also taken together as interphase and the phase of chromosome segregation and cell division, called mitosis or M-phase. Whereas the G₁- and G₂-phase are mainly used for cell growth and expression of required mRNA and proteins (A), S-phase serves for DNA replication, SPB duplication and bud formation (B). Mitosis is characterized by the formation of a short spindle with bipolar attached sister-KTs in metaphase (C) and cleavage of cohesin followed by spindle elongation and chromosome segregation in anaphase (D). Subsequently one cell cycle is completed by cytokinesis and cell division in telophase (E). Under insufficient environmental conditions mitosis is stalled before S-phase and cells move into the quiescent G₀ state (F).

The aim of mitosis is to distribute the replicated chromosomes between mother and daughter cell, a process that is arranged in five mainly consecutive phases: pro-, prometa-, meta-, ana- and telophase. However, *S. cerevisiae* cells have no specific

prophase where chromosomes condense and prometaphase is not distinctly separable from late S-phase. During late S-/prometaphase sister chromatids get attached to MTs emanating from the SPB and separated SPBs initiate the formation of the spindle apparatus. In addition, bud formation is initiated. In metaphase, sister chromatids bi-orient to opposing SPBs and a stable bipolar spindle is established. During anaphase, the separation of chromosomes is accomplished when sister chromatids get separated and the spindle apparatus pulls them to the opposite poles of the cell. In telophase, which represents the end of mitosis, the spindle apparatus disassembles and cells undergo cytokinesis. This process divides the nucleus, the cytoplasm, the organelles and the cell membrane and results in two genetically identical cells. During all these steps various checkpoints guarantee the completion of the previous cell cycle step before the next one can start (Nasmyth, K., 1993, 1996a, 1996b; Israels, E. D., 2000; Pinheiro, D. et al., 2012).

In the following, the current knowledge of the processes taking place at each cell cycle phase and the regulatory function of the involved cell cycle checkpoints are described.

1.2 The cell cycle phases in *S. cerevisiae*

1.2.1 G1-phase

During G1-phase, cells grow and prepare for S-phase by the synthesis of mRNAs and proteins required for DNA replication. In early G1-phase, haploid *S. cerevisiae* cells are able to respond to mating pheromones, which induce the expression of genes involved in the conjugation process and prevent the progression into S-phase. If no mating partner is available and cells have achieved a minimum size, mitosis is initiated by passing the G1/S-transition (START) (Nasmyth, K., 1993). In budding yeast, KTs are attached to SPBs almost throughout the entire cell cycle (Fig. 1-2 A) (Guacci, V. et al., 1997; Winey, M. et al., 2001). Thereby the centromeres are clustered in the vicinity of the SPB by the attachment to relatively short MTs (Jin, Q. W. et al., 2000). The SPBs are embedded within the nuclear envelope and are the origin for the nucleation of almost all kinds of MTs (Winey, M. et al., 2001; Jaspersen, S. L. et al., 2004). The SPB duplication takes place in three major steps described as the SPB duplication pathway. The first step already takes place early in G1. SPBs start to prepare for duplication by the elongation of the so called half-bridge which initially connects the old and the new SPB. In addition, the satellite material required to form the new SPB in the

following S-phase gets assembled at the distal end of the half bridge (Jaspersen, S. L. et al., 2004).

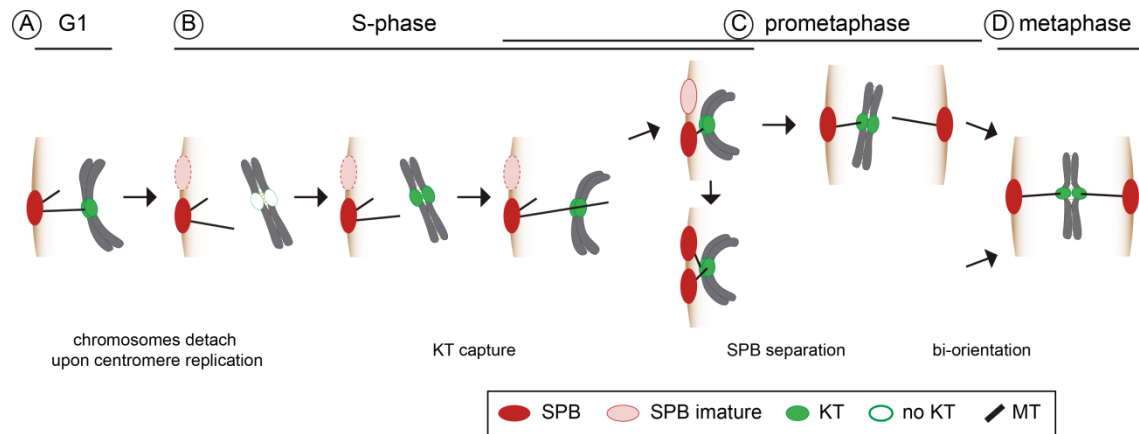


Fig. 1-2. Scheme of mitosis from G1 to metaphase.

(A) In G1, all chromosomes are attached to MTs via the KT. (B) For centromere replication in S-phase, KTs have to disassemble and consequently chromosomes detach. After KT assembly, unattached KTs get captured by MTs mainly emanating from the old SPB. (C) SPB separation and re-orientation of sister chromatids allow for the formation of bipolar spindle in metaphase (D). According to Kitamura, E. et al. (2007).

1.2.2 S-phase

In S-phase, chromosomes replicate, SPB duplication is completed and required proteins are transported to the prospective bud site to initiate budding (Nasmyth 1993; Winey and O'Toole 2001). To allow centromere replication in early S-phase, KTs have to disassemble and as a consequence, chromosomes get detached from MTs for a short period of time (1-2 min) (McCarroll, R. M. et al., 1988; Pearson, C. G. et al., 2004; Tanaka, K. et al., 2005; Kitamura, E. et al., 2007). Once the replication of the centromeric region is completed, the KT reassembles and reconnects preferentially to a MT emanating from the old SPB (Fig. 1-2 B), because the new, immature SPB is not able to form MTs yet (Janke, C. et al., 2002; Tanaka, T. U. et al., 2002; Kitamura, E. et al., 2007). As soon as the new SPB gets operative, KTs reorient between the old and the new SPB with the help of the tension checkpoint machinery (Fig. 1-2 C) (Tanaka, T. U. et al., 2002). The processes of capturing unattached KTs and SPB duplication and separation are subjects of intensive research and are described in detail below (see 1.2.2.2 and 1.2.2.3).

To guarantee an accurate DNA replication during S-phase this process is controlled by two distinct checkpoints, called the DNA replication and the DNA damage checkpoint.

1.2.2.1 The DNA replication and damage checkpoint

DNA damage occurs throughout every cell's life by the exposure to radiation, reactive oxygen species or replication across nicked DNA. To ensure the cell's survival, DNA damage has to be sensed and repaired during every cell cycle.

Whereas the DNA damage checkpoint delays cell cycle progress in response to DNA damage in G1- or G2-phase, the DNA replication checkpoint gets activated when the DNA replication fork stalls as a result of nucleotide deficiency or DNA alkylation in S-phase. Both DNA checkpoints can delay cell cycle progression and arrest the cells prior to anaphase onset at the G2/M transition in budding yeast. Therefore, the checkpoints do not only sense the damage signal, but also transfer the signal in order to activate the mechanisms for cell delay and DNA repair. The main key players in this respect are the sensor kinase Mec1 (homolog of the human ataxia telangiectasia and Rad3-related, ATR) and the effector kinase Rad53 (CHK2 in human cells). They also play a crucial role during an unperturbed S-phase by stabilizing the replication forks (Harrison, J. C. et al., 2006).

Initial processing of DNA-damages by the DNA repair machinery, but also stalling of the replication fork in response to replication stress, results in single stranded DNA (ssDNA) that promotes binding of the single-stranded-binding protein RPA (replication protein A) and further activating factors that recruit the kinase Mec1. Mec1 promotes the DNA repair mechanism by phosphorylating the histone variant H2AX which recruits Rad9 to the region of modified histones. After phosphorylation of Rad9 by Mec1, the effector kinases Chk1 (checkpoint kinase 1) and Rad53 (CHK 2 in human cells) (Navadgi-Patil, V. M. et al., 2011) get recruited and activated by Mec1. Whereas Rad53 is required for a DNA damage response throughout the cell cycle, the kinase Chk1 is mainly involved in the G2/M-phase. Another checkpoint mechanism can directly recognize blunt-ended DNA as a result of double-strand chromosomal breaks by the binding of the MRX (Mre11-Rad50-Xrs2) complex and recruitment of the kinase Tel1 (homolog of the human ataxia-telangiectasia mutated, ATM). Similar to Mec1, this kinase activates the DNA repair by histone phosphorylation and subsequent recruitment and activation of Rad53 (Harrison, J. C. et al., 2006). The generation of ssDNA during the DNA damage repair additionally activates the RPA-dependent recruitment of Mec1.

In response to the stalled replication, the Rad53-dependent mechanism further stabilizes the existing replication fork and suppresses the activation of late origins of replication, causing a delay in DNA synthesis. Upon all kinds of DNA damage responses, the activation of Rad53 initiates the damage-inducible gene expression and inhibits homologous recombination (Santocanale, C. et al., 1998; Segurado, M. et al., 2009). In

addition, precocious chromosome segregation is prevented by the direct regulation of the spindle dynamics by modulating the levels and activities of the MT-associated proteins Cin8, Stu2 and Kip3 (Krishnan, V. et al., 2004). Entry into mitosis is further restrained by the prevented degradation of securin (Pds1 in budding yeast). Pds1 is stabilized by its Mec1-, Rad9- and Chk1-dependent hyperphosphorylation that inhibits its ubiquitination and therefore degradation. This is supported by blocking the interaction between Pds1 and Cdc20 in a Rad53 dependent manner, most likely by the direct phosphorylation of Cdc20. Besides that, Rad53 delays anaphase entry and hinders mitotic exit through the inhibition of Cdc5, probably achieved by its direct phosphorylation. This might decrease APC activity and maintains the Clb2/Cdk1 activity. As a result, cells stably arrest with the sister chromatids of replicated chromosomes bipolarly attached to a short mitotic spindle (Sanchez, Y., 1999; Harrison, J. C. et al., 2006).

1.2.2.2 Capturing of unattached KTs

During S-phase, another important step that follows the replication of the centromeric region is the reattachment of chromosomes to MTs, a process that is called capturing. Capturing of the reassembled, but unattached KTs is thought to be evolutionary conserved within eukaryotic cells (Hayden, J. H. et al., 1990; Rieder, C. L. et al., 1990; Tanaka, K. et al., 2005; Franco, A. et al., 2007; Gachet, Y. et al., 2008) and is achieved within the following steps reviewed in Tanaka, T. U. (2010). Initially, the KTs make lateral contact with the MT lattice of MTs emanating from the SPB (kinetochore-MT, kMT). This facilitates the first encounter of kMTs and KTs by providing a larger surface for the KTs to contact the MTs. The initial contact between the kMT and the KT was suggested to be achieved by a simple search-and-capture mechanism, but the efficiency of this mechanism suggests additional processes that support capturing. Wollman et al. propose that in vertebrate cells a gradient of RanGTP generates a spatial bias for kMT growth (Wollman, R. et al., 2005). But *S. cerevisiae* cells are thought to be too small to create a gradient of RanGTP (Kitamura, E. et al., 2010). Therefore other mechanisms, also suitable for short distances, facilitate KT capture. One of these mechanisms are KT-generated MTs (Fig. 1-3). These MTs frequently emanate from the KTs themselves, particularly when the KT-MT interaction is delayed, and facilitate the loading of KTs on the kMT lattice. Thereby the two types of MTs can achieve the first contact in two different orientations along their length: in a parallel or antiparallel manner (Maiato, H. et al., 2004; Kitamura, E. et al., 2010). In budding yeast, the plus-ends of these kMTs are facing away from the KTs, whereas the minus-ends reside at the unattached KTs. Stu2 (the budding yeast XMAP215/ ch-TOG ortholog) localizes to

these unattached KT's and is crucial for the nucleation and the extension of the KT-generated MTs. Localization of Stu2 on the other hand is dependent on an intact KT structure. The elongation of KT-generated MTs however additionally requires the two MT plus-end tracking proteins Bim1 and Bik1 (Kitamura, E. et al., 2010). As soon as the KT's are loaded on the kMTs, KT-generated MTs rapidly depolymerize and disappear, probably by Stu2 leaving the KT and dispersing along the kMT (Kitamura, E. et al., 2010).

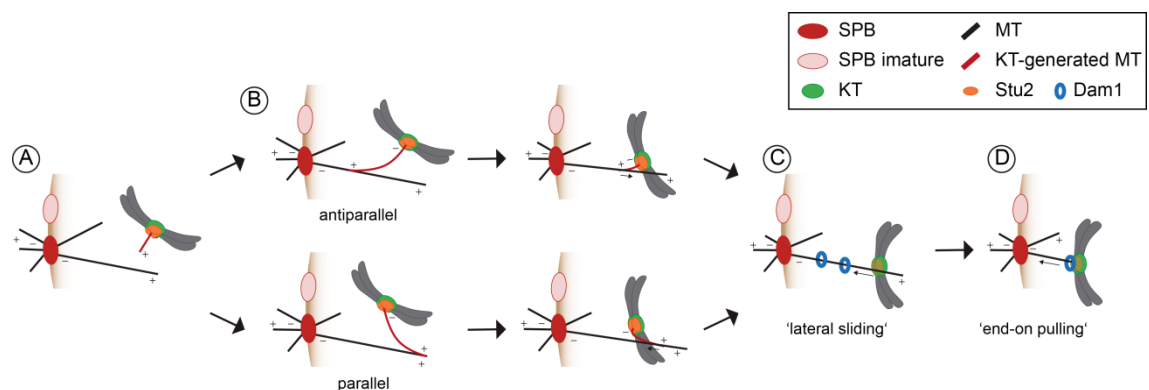


Fig. 1-3. Capturing of unattached KT's is facilitated by KT-generated MTs.

(A) KT's form KT-generated MTs in a Stu2 dependent manner. (B) KT-generated MTs and kMT can achieve the first contact in an antiparallel or parallel manner. (C) Chromosomes get moved towards the SPB by lateral sliding along the kMT. (D) When kMTs shrink, this movement is converted into 'end-on pulling' by the Dam1 complex. According to Kitamura, E. et al. (2010).

Subsequently, KT's slide along the kMTs towards the SPB promoted by the force of minus-end directed motor proteins like the kinesin Kar3 in budding yeast (Tanaka, K. et al., 2005, 2007) or dynein in vertebrates (King, J. M. et al., 2000; Yang, Z. et al., 2007). When kMTs shrink and reach the KT, the lateral attachment is often turned into a more stable end-on attachment by connecting the KT to the plus-end of the kMT (Tanaka, K. et al., 2007). This end-on pulling is dependent on the Dam1 complex and allows a faster transport of the KT. The Dam1 complex localizes along the kMT and accumulates at the plus-end as a result of the depolymerizing kMT. Upon end-on attachment the Dam1 complex gets loaded on the KT and is thought to convert the MT depolymerization into a KT-pulling force (Tanaka, K. et al., 2007). Thereby it is thought that multiple Dam1 complexes assemble in a ring structure encircling the end-on attached MT as observed in *in vitro* analyses (Miranda, J. J. L. et al., 2005; Westermann, S. et al., 2005). Consequently, further depolymerization of the kMT pulls KT's to the SPB (Tanaka, T. U., 2010).

1.2.2.3 SPB duplication and separation

In order to prepare for the bi-orientation of the captured sister-KTs and for the formation of a bipolar spindle in metaphase, SPB duplication is completed during S-phase. In this second step of SPB duplication, the satellite material forms the duplication plaque, a layered structure that reminds of the cytoplasmic part of the mature SPB. A major part of this plaque consists of the self-assembled Spc42 which is induced upon phosphorylation (Bullitt, E. et al., 1997; Adams, I. R. et al., 1999). The third major step of SPB duplication is the insertion of the duplication plaque into the nuclear envelope and the subsequent formation of the nuclear part of the SPB. Therefore, duplicated SPBs reside side-by-side within the nuclear envelope linked by a complete inter-SPB bridge until late S-phase (Byers and Goetsch, 1975; Lim, H. H. et al., 1996; Lim, H. H. et al., 2009). SPB duplication was found to be a mostly conservative mechanism, meaning that the old SPB stays intact whereas the emerging SPB is formed completely new (Pereira, G. et al., 2001).

As DNA replication is close to be completed, SPB separation is initiated by dissolving the connecting bridge between the old and the new SPB. The nuclear MTs have to assemble to enable the two kinesin-like motor proteins Cin8 and Kip1 to push the SPBs apart. They generate an outward directed force as they crosslink the antiparallel interpolar MTs and slide them apart (Jacobs, C. W. et al., 1988; Hoyt, M. A. et al., 1992; Roof, D. M. et al., 1992). Thereby the minus-end directed motor protein Kar3 counteracts the forces of Cin8 and Kip1 (Saunders, W. S. et al., 1992; Hoyt, M. A. et al., 1993). In addition, another pathway containing the MT-bundling protein Ase1 regulates spindle assembly in parallel to the Cin8 and Kip1 motor pathways. Ase1 and other spindle midzone proteins crosslink the interdigitating antiparallel MTs prior to SPB separation. This allows the motor proteins to induce the outward forces that contribute to break the inter-SPB bridge and separate SPBs (Kotwaliwale, C. V. et al., 2007). In anaphase Ase1 localizes to the MT overlap of the spindle midzone and recruits further MAP proteins. The MAP protein Stu1, a the non-motor MT-binding protein was also found to be required for SPB separation and spindle formation (Yin, H. et al., 2002). At late S-phase SPBs have slightly moved apart and a very short spindle is assembled (Lim, H. H. et al., 2009).

1.2.3 G2- and metaphase

After DNA replication and a first slight SPB separation have been successfully completed in S-phase, cells proceed into G2/metaphase. Since the nuclear envelope does not break down and chromosome condensation is not evident in budding yeast, bipolar

spindle formation is the main indicator for the beginning of mitosis in these cells. The aim of metaphase is to form a stable bipolar spindle with each sister chromatid attached to one kMT emanating from opposite SPBs to ensure accurate chromosome segregation (Fig. 1-2 D).

Therefore, the sister-KTs of the still monopolar attached chromosomes have to attach to MTs emanating from the opposing SPB and achieve bi-orientation (bipolar or amphitelic attachment) (Fig. 1-4). Two mechanisms seem to promote bipolar attachment. One is the avoidance of aberrant attachments due to the back-to-back geometry of the sister-KTs (Östergren, G., 1951; Indjeian, V. B. et al., 2007; Sakuno, T. et al., 2009) and the other one is the tension dependent error-correction. If the sister-KT accidentally gets attached to the MT extending from the same SPB (syntelic attachment), these errors have to be corrected before SPBs separate at anaphase onset. Therefore, the tension checkpoint (see 1.2.3.1) and the spindle assembly checkpoint (SAC; see 1.2.3.2) collaborate to accomplish the turnover and correction of KT-MT attachments (Tanaka, T. U. et al., 2002).

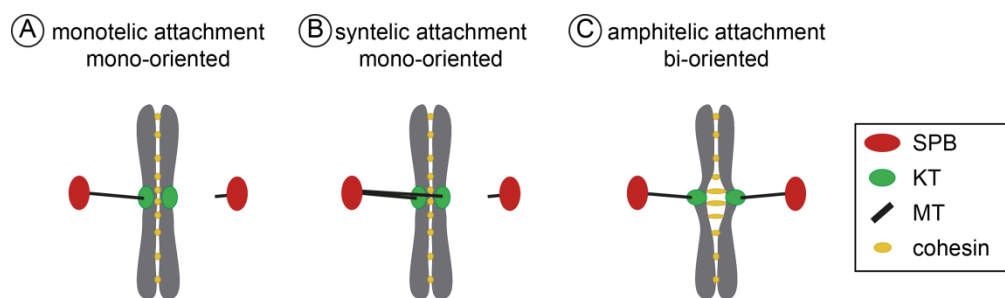


Fig. 1-4. Model of the possible modes of KT-MT attachment in *S. cerevisiae*.

(A) Monotelic attachment: only one sister-KT is attached to a SPB, the other one is unattached. **(B)** Syntelic attachment: Both sister-KTs are attached to the same SPB. **(C)** Amphitelic or bipolar attachment: Sister-KTs are attached to MTs emanating from opposing SPBs. According to Tanaka, T. U. (2008).

Another prerequisite for sister-KT bi-orientation is the stable connection of sister-KTs by the cohesin complexes that withstand the pulling forces of the kMTs (Tanaka, T. U. et al., 2000; Dewar, H. et al., 2004). Only when bipolar attachment and therefore tension across the sister-KT is achieved, a stable connection between KTs and SPB via the MT is formed (Nicklas, R. B. et al., 1969; Tanaka, T. U. et al., 2002; Dewar, H. et al., 2004). As a consequence, a very dynamic equilibrium is maintained between the forces of the kMTs that pull sister-KTs towards the opposing SPBs and the forces of the cohesin that holds the sister-KTs together. This determines a certain level of tension on the KT-MT interface and is mandatory for a stable bipolar spindle (Skibbens, R.

V. et al., 1993; Inoué, S. et al., 1995). Thereby the Dam1 complex is required to sustain bi-orientation most likely by withstanding the forces of the depolymerizing kMTs and transferring them into pulling forces on the KT (Janke, C. et al., 2002).

1.2.3.1 The tension checkpoint

In order to prevent the unequal distribution of chromatids, the tension checkpoint has to sense erroneous attached sister-KTs (monotelic and syntelic) that lack tension. When the new SPBs become operative, cells have to achieve re-orientation between the old and the new SPB and particularly bipolar attachment when a spindle is formed. Therefore, erroneous KT-MT attachments, sensed by the lack of tension on the KT-MT interface, get destabilized by Aurora B (Ipl1 in budding yeast) kinase-mediated phosphorylation (Fig.1-5) (Biggins, S. et al., 1999; Tanaka, T. U. et al., 2002; Dewar, H. et al., 2004). This activates the spindle assembly checkpoint (SAC) by either creating unattached KTs (Pinsky, B. A. et al., 2006) or by the phosphorylation of Mad3 (King, E. M. J. et al., 2007).

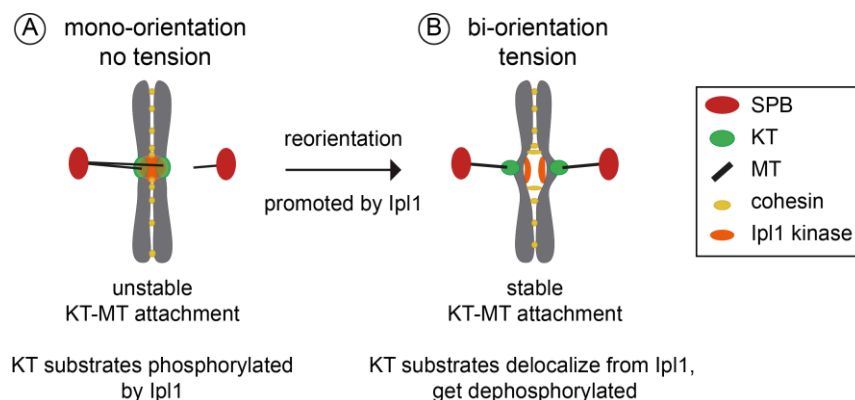


Fig. 1-5. Model of the error correction of KT-MT attachments.

(A) The Ipl1 kinase induces the turnover of syntelic KT-MT attachments that lack tension by the phosphorylation of KT components. This promotes the bi-orientation of sister-KTs. (B) Upon bipolar attachment the tension on the KT-MT interface delocalizes KT substrates from the Ipl1 kinase and therefore stabilizes the KT-MT attachment. According to Tanaka, T. U. (2010).

Ipl1 kinase together with Bir1, Sli15 and Nbl1 (Survivin, INCENP and borealin in higher eukaryotes) forms the Ipl1 complex, also called chromosome passenger complex (CPC). Whereas Ipl1 is the catalytic subunit of the complex, the other proteins are regulatory subunits for Ipl1 localization and activity (Ruchaud, S. et al., 2007; Carmena, M. et al., 2009).

To date, the only identified substrates of Ipl1 that are involved in bi-orientation of KT's are the two major MT binding complexes, Dam1 (Cheeseman, I. M. et al., 2002; Zhang, K. et al., 2005) and Ndc80 (Akiyoshi, B. et al., 2009a). The phosphorylation of the Dam1 or the Ndc80 protein by Ipl1 directly weakens the interaction with MTs. Additionally phospho-mimetic Dam1 was shown to destabilize the kMT tip, indirectly contributing to the KT release (Sarangapani, K. K. et al., 2013). Phosphorylation of these two proteins seems to be important, but additional Aurora B substrates like KLN1 of higher eukaryotes (Spc105 in budding yeast) are suggested to be involved in the release (Akiyoshi, B. et al., 2009a; Liu, D. et al., 2010; Welburn, J. P. I. et al., 2010). Upon bipolar attachment and tension on the KT-MT interface, these substrates get dephosphorylated by the antagonizing protein phosphatase 1 (PP1, Glc7 in budding yeast) (Francisco, L. et al., 1994; Pinsky, B. A., Kotwaliwale, C. V., et al., 2006; Liu, D. et al., 2010).

Since Ipl1 localizes to the inner KT that faces the centromeric DNA (see 1.3), a mechanism based on the spatial distance between the kinase and the substrates at the outer KT providing the interaction with the MT is suggested. If the sister-KT's are not under tension, the substrates at the KT-MT interface are in close proximity to the highly active Ipl1 kinase and get phosphorylated (Fig. 1-5). However, when sister-KT's are under tension Ipl1 is spatially distant and the substrates get dephosphorylated (Tanaka, T. U. et al., 2002; Liu, D. et al., 2009; Lampson, M. A. et al., 2011). Nevertheless this model bears some caveats. It is still unclear how Ipl1 activity is suppressed to achieve a general initial KT-MT attachment that always lacks tension. A possible explanation would be a balance between Ipl1 activity and the activity of the antagonizing PP1 (Glc7 in budding yeast) (Pinsky, B. A., Kotwaliwale, C. V., et al., 2006; Rosenberg, J. S. et al., 2011). On the other hand Ipl1 just recently was found to contribute to bi-orientation even when its absent from the inner KT (Campbell, C. S. et al., 2013). Therefore another possible model proposes a tension-dependent activity of Ipl1 where tension is directly sensed by the Ipl1 binding partners Bir1 and Sli15 (Sandall, S. et al., 2006). An alternative mechanism suggests that MTs and KT proteins that come in closer proximity to Ipl1 when tension is missing, activate the Aurora B kinase (Rosasco-Nitcher, S. E. et al., 2008).

Besides the bi-orientation via Ipl1, also Mps1 kinase contributes to the bi-orientation of sister KT's (Maure, J.-F. et al., 2007) and phosphorylates the Dam1 and Ndc80 protein (Shimogawa, M. M. et al., 2006; Kemmler, S. et al., 2009). Since Mps1 localizes to the outer KT, a mechanism different from the one suggested for Ipl1 might regulate bi-orientation. Thereby it is unclear whether Mps1 acts in a separate pathway together

with Bub1 and Sgo1 (Storchová, Z. et al., 2011) or if these proteins contribute to the rapid accumulation and activation of Ipl1 (Jelluma, N. et al., 2008; van der Waal, M. S. et al., 2012). So far it is known that the recruitment of the Ipl1 complex (CPC) to the inner KT depends on the interaction of Bir1 with Sgo1 (Kawashima, S. A. et al., 2007), whereas Sgo1 itself localizes to the histone H2A after phosphorylation by Bub1 (Kawashima, S. A. et al., 2010). This is similar to another recruitment pathway of Ipl1 where phosphorylated histone H3, modified by the Haspin kinase, binds Bir1 (Tanaka, T. U., 2010; Yamagishi, Y. et al., 2010).

1.2.3.2 The spindle assembly checkpoint

One of the most important surveillance mechanisms of the cell cycle is the spindle assembly checkpoint (SAC) that delays cell cycle progression until all sister chromatids are bipolar attached. Upon defective KT-MT attachments, more precisely unattached KTs, the SAC induces a cell cycle arrest by the inhibition of Cdc20, an activator of the ubiquitin ligase anaphase-promoting complex/cyclosome (APC/C) (Yu, H., 2007; Biggins, S., 2013). The inactive APC/C therefore fails to initiate the downstream mitotic events by the polyubiquitination of cyclin B and securin (Pds1 in budding yeast) that labels them for degradation by the 26S proteasome (King, R. W. et al., 1995; Peters, J.-M., 2002). Cyclin B, an activator of the cyclin dependent kinase (Cdk1) in mitosis (Nurse, P., 1990) has to be degraded to induce anaphase (King, R. W. et al., 1994). Securin inhibits the protease separase (Esp1 in budding yeast) that cleaves the cohesin complex that holds sister chromatids together. Degradation of securin is required to initialize anaphase (Cohen-Fix, O. et al., 1996; Uhlmann, F. et al., 1999).

Genetic screens identified the *MAD* (mitotic-arrest deficient) genes *MAD1*, 2 and 3 (BubR1 in human), the *BUB* (budding uninhibited by benzimidazole) genes *BUB1* and *BUB3* and *MPS1* (multipolar spindle 1) as genes that are involved in the checkpoint signaling (Hoyt, M. A. et al., 1991; Li, R. et al., 1991; Weiss, E. et al., 1996). In contrast to animal cells, only *MPS1* is essential during a normal cell cycle in budding yeast. Nevertheless deletions of the other checkpoint proteins cause segregation defects of various strength (Biggins, S., 2013).

Since all checkpoint proteins except of Mad3 localize at the KT, the checkpoint signal is most likely generated there (Musacchio, A. et al., 2007). Whereas Bub1 and Bub3 are always found at KTs in mitosis, Mad1 and Mad2 specifically localize only to unattached KTs (Waters, J. C. et al., 1998; Gillett, E. S. et al., 2004). Thereby the KT subcomplexes Ndc80 and COMA (see 1.3) contribute to the SAC, probably by recruiting the checkpoint proteins in a direct or indirect way (McClelland, M. L. et al., 2003;

Matson, D. R. et al., 2012). If this recruitment and/or the KT structure is impaired, the SAC activity is inhibited (Musacchio, A. et al., 2007).

The Mps1 kinase interacts most likely with Ndc80 at the KT (Kemmler, S. et al., 2009) and is thought to be the most upstream signal that recruits further checkpoint proteins to the KTs. Bub1 and Bub3 localize to the KT upon the phosphorylation of Spc105 by Mps1 (Fig. 1-6) (London, N. et al., 2012; Shepperd, L. A. et al., 2012; Yamagishi, Y. et al., 2012). Mad1 and Mad2 recruitment is dependent on Mps1, Bub1 and Bub3, but the binding partner of Mad1 at the KT is still unknown. Mad2 is suggested to exist in two different forms, an conformational 'open' (Mad2-O) and 'closed' (Mad2-C) form (Shah, J. V et al., 2004; Antoni, A. De et al., 2005). Upon recruitment to Mad1, Mad2-O changes its conformation to Mad2-C that stably localizes to Mad1. The bound Mad2-C serves as a receptor for the transient binding of soluble Mad2-O that subsequently gets converted to Mad2-C. This allows Mad2-C to interact with Cdc20. The Cdc20-Mad2-C complex then dissociates from the KT and additionally serves as a structural equivalent of the KT bound Mad1-Mad2-C complex to promote the conformational change of Mad2-O to Mad2-C. Therefore the Mad1-Mad2-C complex is thought to serve as a template for the formation of the Cdc20-Mad2-C complex copy ("Mad2-template model") (Luo, X. et al., 2002; Antoni, A. De et al., 2005; Nezi, L. et al., 2006; Mapelli, M. et al., 2007).

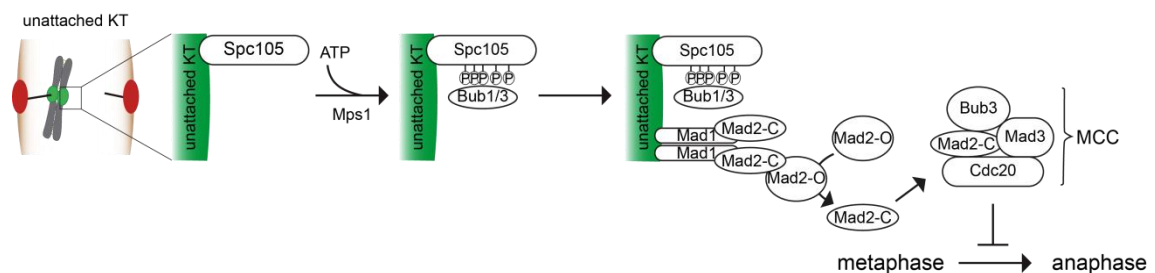


Fig. 1-6. The pathway of the spindle assembly checkpoint.

Phosphorylation of the KT protein Spc105 by Mps1 kinase recruits Bub1 and Bub3 to the unattached KT. Binding of Bub1/3 promotes the recruitment of the Mad1/ Mad2 complex accompanied by a conformational change of the open (Mad2-O) to the closed (Mad2-C) Mad2 form. Mad2-C interacts with Cdc20 and forms the mitotic checkpoint complex (MCC) consisting of Mad2-C, Cdc20, Bub3 and Mad3. This inhibits the APC activator Cdc20 and blocks the metaphase to anaphase transition. According to Biggins, S. (2013).

Formation of the Cdc20-Mad2-C complex is followed by the assembly of the effector of the SAC, the soluble mitotic checkpoint complex (MCC) comprised of Mad2-C, Mad3, Bub3 and Cdc20. As a consequence, Cdc20 and therefore the APC/C is inhibited (Sudakin, V. et al., 2001). Thereby it is worth to mention that MCC formation in-

duced by just one single unattached KT is sufficient to cause a cell cycle arrest (Rieder, C. L. et al., 1995).

Upon bipolar attachment of all chromosomes, Mad1 and Mad2 are removed from the KT. In metazoans the motor protein dynein is required to turn off the SAC by ‘stripping’ off the checkpoint proteins (Howell, B. J. et al., 2001; Wojcik, E. et al., 2001). The minus-directed motor protein Kar3 might have an equivalent function in *S. cerevisiae* (Musacchio, A. et al., 2007). In order to silence the checkpoint, the phosphatase PP1 reverses the Mps1 phosphorylation. Thereby it is a matter of debate if Spc105 or which other proteins are receptors for PP1 at the KT and if and how PP1 regulates Spc105 and other so far unknown checkpoint proteins.

Additionally, phosphorylation and de-phosphorylation events mediated by other kinases like Ipl1, Cdk1 or Bub1 or of other checkpoint proteins might contribute to the very complex regulatory mechanism of the SAC (Biggins, S., 2013).

1.2.3.3 The bipolar metaphase spindle

In budding yeast, the metaphase spindle has a length of about 1.5-2 μm and three different kinds of MTs ensure the maintenance, stability and position of the spindle. The minus-end of all these MTs is anchored to the SPB, whereas the plus-end faces away from the SPB. Exactly one kinetochore MT (kMT) emanating from the nuclear side of each SPB attaches to one of the sister-KTs of the 16 chromosomes. Three to four interpolar MTs extend from each opposing pole and interdigitate to an antiparallel overlap. This MT bundle at the spindle center stabilizes the spindle and supports its elongation during anaphase. In addition, two to three astral MTs emanate at the cytoplasmic side of the SPB and position the spindle within the cell (Winey, M. et al., 1995; Toole, E. T. O. et al., 1999).

Various motor proteins and microtubule-associated proteins (MAPs) contribute to the formation, stabilization and later elongation of the spindle by crosslinking and regulating the spindle MTs. Thereby the spindle length is always determined by the balance between the outward and the inward forces on the spindle (Winey, M. et al., 2012). Four kinesin-like proteins were found to act on the nuclear mitotic spindle: Cin8, Kip1, Kar3 and Kip3. The kinesin-5 family members Cin8 and Kip1 are plus-end directed motor proteins and have redundant functions. They provide outward pushing forces by sliding the antiparallel interpolar MTs apart. In addition, Cin8 was found to work as a main plus-end depolymerase that regulates the length-dependent disassembly of kMTs (Gardner, M. K. et al., 2008). Cin8 localization and therefore function is regulated by the MT-bundling protein Ase1 (Khmelniskii, A. et al., 2009). Kar3, a minus-end directed

kinesin-14, was found to antagonize these forces. Thereby it is unclear if Kar3 creates an inward force by walking to the minus-end or opposes the outward force by cross-linking the antiparallel interpolar MTs (Roof, D. M. et al., 1992; Saunders, W. S. et al., 1992; Saunders, W. et al., 1997). Kip3, a kinesin-8 family member, does not regulate the spindle length itself, but provides the clustering of kinetochores on the metaphase spindle by adjusting the kMT length (Varga, V. et al., 2006; Wargacki, M. et al., 2010). In addition, Kar3 and Kip3, together with two further kinesin-like proteins (Kip2 and Smy1) and one dynein (Dhc1) operate on the cytoplasmic MTs to position the spindle and the nucleus within the cell (Winey, M. and Bloom, K., 2012). Despite their specific functions, none of the kinesins is individually essential and yeast cells containing only two of the motor proteins are viable: Cin8 and Kar3 or Kip3 respectively (Cottingham, F. R. et al., 1999).

A highly diverse group of MT regulators are the MT-associated proteins (MAPs). A common feature of all these MAPs is that they are non-motor proteins that bind to MTs and most of them show plus-end tracking. There are five major proteins of different MAP-families in budding yeast: Bim1 (EB1), Bik1 (CLIP-170), Stu1 (CLASP), Stu2 (XMAP215) and Nip100 (p150^{glued}). For MT (or tubulin)-binding they use calponin homology (CH) domains, protein glycine-rich (CAP-GLY) domains and tumor overexpressing gene (TOG)-domains respectively. In addition, the MT-bundling protein Ase1 also localizes to the metaphase spindle and crosslinks interpolar MTs (Schuyler, S. C. et al., 2003). Their diversity in structure also reflects their various functions for the integrity of the spindle (Winey, M. et al., 2012). Due to their relevance for this work, CLASP proteins and particularly Stu1 and TOG domains are described in more detail below (see 1.4).

1.2.4 Anaphase

Following the formation of a stable bipolar spindle during metaphase, chromosomes get separated into mother and daughter cell in anaphase. When all sister-KTs are bipolar attached to the SPBs, the SAC is turned off and the APC/C gets activated. Subsequently the cleavage of the cohesin complex initiates anaphase (Uhlmann, F. et al., 1999) and kMTs depolymerize to pull the sister chromatids towards the SPBs (anaphase A). Almost simultaneously the spindle elongates rapidly and SPBs move apart (anaphase B) (Fig. 1-7) (Winey, M. et al., 1995; Toole, E. T. O. et al., 1999).

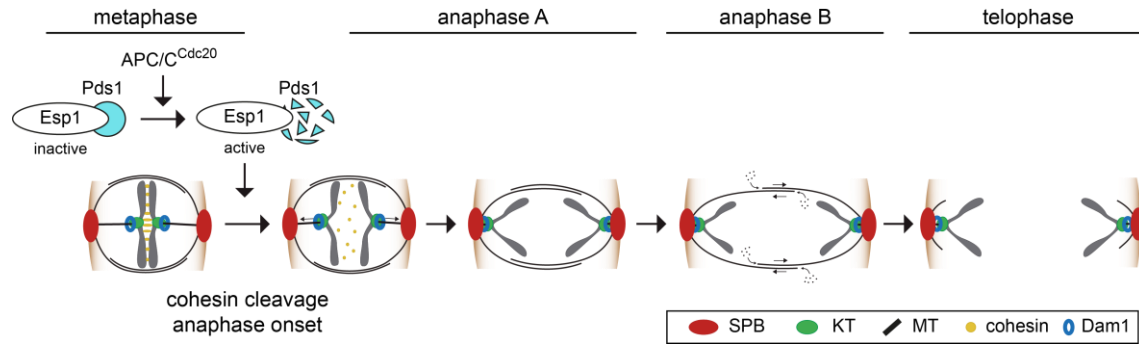


Fig. 1-7. Mitosis from anaphase onset until late anaphase.

Upon bipolar attachment of all sister-KTs, APC/C^{Cdc20} gets activated and promotes the degradation of Pds1 (securin). This activates Esp1 (separase) which subsequently cleaves the cohesin that holds sister chromatids together. As a consequence, sister chromatids rapidly get dragged to the opposing SPBs by the depolymerizing kMTs (anaphase A), followed by rapid sliding apart of the overlapping inter-polar MTs, decreasing the region of overlap (anaphase B). Formation of the midzone by the recruitment of various midzone proteins stabilizes the inter-polar MTs until their depolymerization in late anaphase/ telophase. According to Peters, J.-M. (2002).

At the metaphase to anaphase transition (Fig. 1-7), the ubiquitin protein ligase APC/C together with the activator protein Cdc20 mediate ubiquitination of Pds1 followed by its degradation (King, R. W. et al., 1995; Cohen-Fix, O. et al., 1996). Proteolysis of Pds1 subsequently activates the separase Esp1 to cleave the cohesin subunit Scc1 and the sister chromatids get segregated (Ciosk, R. et al., 1998; Uhlmann, F. et al., 1999). In budding yeast, the separation of the sister chromatids starts at the centromeric region and continues along the chromosomal arm until telomeres are reached (Renshaw, M. J. et al., 2010). Activation of Esp1 additionally promotes the release of the protein phosphatase Cdc14 from the nucleolus (FEAR, Cdc fourteen early anaphase release; see 1.2.4.1) (Sullivan, M. et al., 2003; Baskerville, C. et al., 2008).

As kMTs depolymerize, the pulling forces of the kMTs rapidly move the sister chromatids poleward (anaphase A). Simultaneously, the spindle midzone (see 1.2.4.2), the overlap region of inter-polar MTs emanating from opposing SPBs, is formed by the recruitment of motor proteins and MAPs (Glotzer, M., 2009). This stabilizes spindles by crosslinking inter-polar MTs and drives their elongation. Subsequently, the spindles elongate by sliding inter-polar MTs apart and the distance between the SPBs increases up to 10 μm (anaphase B) (Winey, M. et al., 1995; Toole, E. T. O. et al., 1999). Thereby spindles elongate in two phases: An initially fast elongation with a velocity of $\sim 1\mu\text{m}/\text{min}$ that brings the old SPB and one set of chromosomes in the daughter cell, and a second slower elongation phase until the final spindle length is reached (Kahana, J. A. et al., 1995; Yeh, E. et al., 1995).

1.2.4.1 The Cdc14 early anaphase release

During metaphase cells show a high activity of Cdk1 which is diminished in anaphase and substituted by an increased phosphatase activity. The main antagonizing phosphatase for Cdk1 phosphorylation in budding yeast is the Cdc14 phosphatase. Cdc14 is sequestered at the nucleolus by binding to the nucleolar protein Net1/Cfi1 most of the time during the cell cycle, but undergoes two cycles of release during anaphase. The first partial and transient release in early anaphase is achieved by the FEAR network consisting of Esp1, Slk19, the polo-like kinase (Cdc5), Spo12 and Bns1. Cdc5 inactivates the Cdk1 inhibitor Swe1 and therefore the phosphorylation of Net1 by Clb2-Cdk1 activates the Cdc14 release (Stegmeier, F. et al., 2002; Torres-Rosell, J. et al., 2005; Liang, F. et al., 2009). Subsequently, Cdc14 promotes a drastic change in MT dynamics and spindle stability by the dephosphorylation of spindle-associated targets like the MT-bundler Ase1, Sli15 (CPC), Ask1 (Dam1 complex) and Fin1 (Khmelinskii, A. et al., 2008).

1.2.4.2 Formation of the spindle midzone

Sliding apart the antiparallel interpolar MTs that overlap in the spindle midzone generates the forces for spindle elongation. In budding yeast, the spindle midzone of anaphase spindles initially consists of about 8 antiparallel interpolar MTs (3-4 emanating from each SPB) and this number decreases down to about 2 in late anaphase.

At anaphase onset, various proteins are recruited to the central region of the spindle to form the spindle midzone. Some of these proteins like the MT-bundling protein Ase1, the plus-end binding proteins Bim1 and Bik1, the motor proteins Cin8 and Kip3 and the MAP Stu1 already localize to the spindle in metaphase. Others like the FEAR-complex separase-Slk19 and Pds1 however get recruited to the spindle only upon anaphase onset.

After dephosphorylation by the separase-activated phosphatase Cdc14, Ase1 localizes to the spindle midzone and subsequently is essential to recruit additional midzone proteins. Therefore, Ase1 does not only stabilize the spindle by bundling interpolar MTs in an antiparallel fashion, but also acts as the main organizer of the spindle midzone. The Ase1-dependent binding of the Esp1-Slk19 complex then defines and restricts the localization of Ase1 and further midzone proteins to the center of the midzone (Khmelinskii, A. et al., 2007). The recruitment of Cin8 to the midzone promotes the sliding of antiparallel MTs for spindle elongation (Khmelinskii, A. et al., 2009). However, some proteins like the Ipl1 complex, but also Dam1 or Ndc10 stay localized along the

spindle in early anaphase and localize to the spindle midzone in late anaphase (Buvelot, S. et al., 2003; Bouck, D. C. et al., 2005; Nakajima, Y. et al., 2011).

1.2.5 Telophase and exit from mitosis

When chromosome segregation is completed, cells exit from mitosis. This critical cell cycle transition is concomitant with the disassembly of the spindle and subsequent cytokinesis. Only if the spindle is correctly aligned along the mother-bud polarity axis with one SPB in the mother cell and the other SPB reaching the cell cortex of the daughter cell, the spindle position checkpoint (SPOC) is satisfied and the mitotic exit network (MEN) gets active. This ensures that one chromosome set is indeed transferred to the bud, whereas the other chromosome set remains in the mother cell (Caydasi, A. K. et al., 2010). The degradation of Ase1 (Juang, Y.-L., 1997), but also the localization of the Ipl1-Sli15 complex to the midzone in late anaphase (Buvelot, S. et al., 2003) are thought to induce the disassembly of the spindle.

The signaling cascade of the MEN, which is regulated by the small Ras-like GTPase Tem1, activates the kinases Cdc15 and Dbf2 (in complex with its regulatory binding protein Mob1). This promotes the full release of Cdc14 from the nucleolus and therefore the complete inhibition of the Cdk1 activity in three pathways (Caydasi, A. K. et al., 2012). Firstly, dephosphorylation of Cdh1, which is the second activator protein of the APC/C, activates the APC-Cdh1 complex that achieves the degradation of the cyclin Clb2 (Jaspersen, S. L. et al., 1998). Secondly, the dephosphorylation of the transcription factor Swi5 induces the expression of the Cdk1 inhibitor Sic1 and thirdly, Sic1 is stabilized by its own dephosphorylation (Dumitrescu, T. P. et al., 2002).

When the Cdk1 is inactive, the kinases of the MEN and Cdc14 localize to the bud neck as the site of cell division, and initiate the cortical actomyosin ring contraction, septum formation and cytokinesis (Meitinger, F. et al., 2012).

1.3 The kinetochore

The KT is a complex structure that mediates the attachment of chromosomes to kMTs and regulates the progress of mitosis via the spindle assembly checkpoint. In all eukaryotes this complex is essential for accurate segregation of duplicated chromosomes to daughter cells. Although composed of more than 70 proteins, the *S. cerevisiae* KT is considered relatively simple since it provides only one MT binding site. Many components of the *S. cerevisiae* KT have orthologs in KTs of higher eukaryotes, especially the KT-MT interface appears to be very similar. Several MAPs contribute to this interface and regulate the dynamics of kMTs. In addition, the same MAPs also localize to interpolar microtubules and regulate spindle stability. The distinct subcomplexes of the KT form a structure that can be subdivided in the inner KT, the linker layer and the outer KT (Fig. 1-8). These KT subcomplexes are thought to be assembled in a hierarchal manner at a specific DNA region, called the centromere (Biggins, S., 2013).

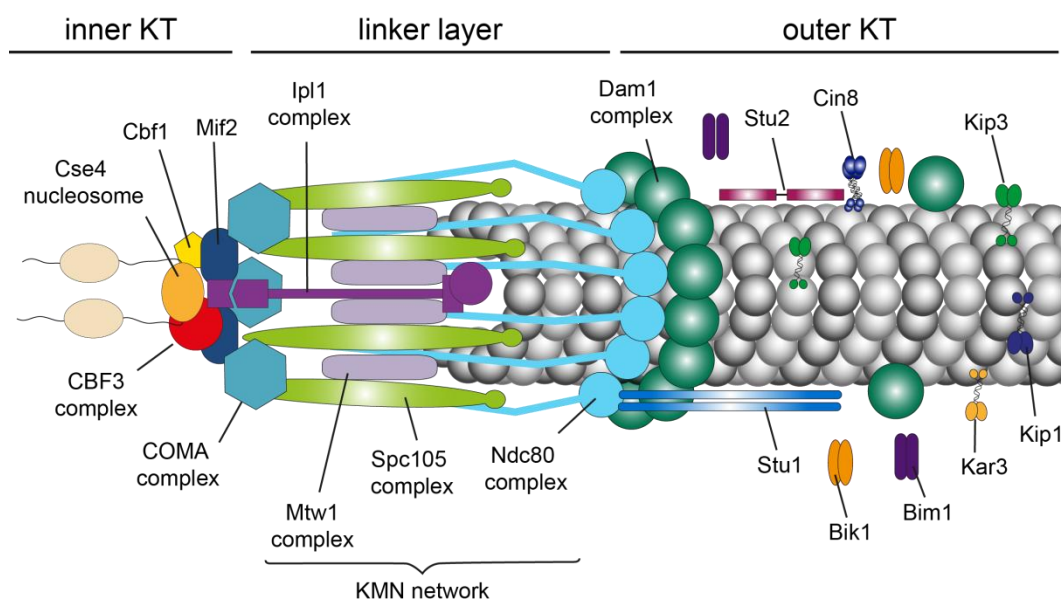


Fig. 1-8. Model of the kinetochore structure and the KT-MT interface.

Scheme indicating the rough position and stoichiometry of the *S. cerevisiae* KT subcomplexes. According to Westermann, S. et al. (2007) and Biggins, S. (2013).

1.3.1 The centromere

The centromere of budding yeast is a point-centromere with a defined DNA region of 125 bp. In contrast to most eukaryotic centromeres, epigenetic mechanisms might not contribute to their generation. However, a specific chromatin structure is the hall-

mark of all eukaryotic centromeres. Whereas regular nucleosomes consist of a histone octamer containing two copies of each H2A, H2B, H3 and H4, the centromeric nucleosome comprises a H3 variant called Cse4 (CENP-A in higher eukaryotes) (Palmer, D. K. et al., 1987; Stoler, S. et al., 1995). The point-centromere is composed of three conserved centromere-determining elements (CDE): CDEI, an 8 bp palindrome, CDEII, a 78 to 86 bp stretch of AT-rich DNA and CDEIII, a conserved 26 bp element (Hieter, P. et al., 1985; Cottarel, G. et al., 1989; Clarke, L., 1998). The centromeric DNA gets replicated early in S-phase (McCarroll, R. M. et al., 1988), most likely to give cells enough time for KT assembly followed by KT-MT attachment until the end of S-phase (Kitamura, E. et al., 2007). In order to build up the KT, the CDEI and CDEIII consensus sites initiate the assembly of the inner KT by the binding of Cbf1 and the CBF3 complex (Cai, M. et al., 1990; Lechner, J. et al., 1991).

1.3.2 The inner kinetochore

The inner KT is formed by the proteins that achieve the contact with the centromere and serve as a platform for the further assembly of the KT components. One of the key nucleating factors for the KT is the CBF3 complex, consisting of the four essential proteins Ndc10, Cep3, Ctf13 and Skp1 (Lechner, J. et al., 1991; Connelly, C. et al., 1996). A network of different subcomplexes called the constitutive centromere associated network (CCAN) was determined in vertebrates. Most of these identified proteins also have orthologs in budding yeast. These include Mif2 (Meeks-Wagner, D. et al., 1986; Meluh, P. B. et al., 1995), the histone H3 variant Cse4 and the CDEI binding protein Cbf1 (Cai, M. et al., 1990). The model that the inner KT could be structured as a loop around the Cse4-nucleosome arose from the finding that Ndc10 binds to CDEIII, but also to the CDEI binding protein Cbf1 (Cho, U.-S. et al., 2012; Biggins, S., 2013). An additional component of the inner KT is the Ipl1 complex, consisting of the Ipl1 kinase, Sli15, Bir1 and Nbl1. This complex localizes to the KT from G1 until anaphase via binding of Bir1 to the CBF3 complex (Yoon, H. et al., 1999) and Sli15 interaction with the COMA complex of the linker layer (Knockleby, J. et al., 2009).

1.3.3 The linker layer

The linker layer serves as a bridge between the centromere-binding proteins of the inner KT and the MT-binding proteins of the outer KT (Westermann, S. et al., 2007). A protein complex that is also counted to the CCAN, but is also part of the linker layer is the COMA complex containing of the proteins Ctf19, Okp1, Mcm21 and Ame1 (Ortiz, J.

et al., 1999; De Wulf, P. et al., 2003). Various additional proteins that bind to the CO-MA complex are taken together as the Ctf19 complex in budding yeast and are also counted among the CCAN. Additionally the essential subcomplexes Spc105/KNL-1/Blinkin complex (containing Spc105 and Kre28), the Mtw1/MIND/Mis12 (composed of Mtw1, Dsn1, Nnf1 and Nsl1) and Ndc80 complex (composed of Ndc80, Nuf2, Spc24, Spc25) contribute to the linker layer (Westermann, S. et al., 2007; Biggins, S., 2013). They can be summarized as the highly conserved KMN (KNL-1, Mis12, Ndc80) network that represents the main MT-binding site of the KT (Cheeseman, I. M. et al., 2006).

The Ndc80 complex is a heterotetramer with globular head domains that are connected by a long rod-shaped coiled-coil structure. The crucial function of MT binding is achieved by the interaction of the positively charged CH domains with the negatively charged MT interface (Wei, R. R. et al., 2005; Ciferri, C. et al., 2008). Phosphorylation of Ndc80 by the protein kinase Mps1 plays an important role for the activation of the SAC at the KT (Kemmler, S. et al., 2009). A loop that interrupts the rod of the Ndc80 protein is suggested to connect Ndc80 with the outer KT complex Dam1, but the exact role of this loop is still unclear (Maure, J.-F. et al., 2011). Besides the Dam1 complex also other proteins of the outer KT are dependent on Ndc80 either because they directly bind to Ndc80 or more likely because the KT-MT attachment is impaired upon Ndc80 disruption (Westermann, S. et al., 2007).

In addition, the Mtw1 complex forms an elongated structure with a globular head, interacting with the C-terminal globular head of Ndc80 (consisting of Spc24 and Spc25) (Maskell, D. P. et al., 2010). The Spc105 complex, similar to the Mtw1 complex does not show MT-binding activity on its own, but it is suggested to serve as a scaffold for further proteins of the outer KT. Therefore it binds Bub1 and Bub3 checkpoint proteins and may be a regulatory subunit for the PP1 phosphatase (Kiyomitsu, T. et al., 2007; Rosenberg, J. S. et al., 2011; London, N. et al., 2012).

1.3.4 The outer kinetochore

The outer KT is assembled of the proteins that form the interface between KTs and MTs and described the site where the chromosome movement is generated.

Like the Ndc80 complex, the outer kinetochore Dam1/DASH complex directly binds to MTs. This essential complex consists of 10 proteins and localizes to KTs in a KMN and MT dependent way (Janke, C. et al., 2002; Li, Y. et al., 2002). Thereby it is uncertain if the Dam1 complex assembles a ring-structure surrounding the MT protofilament

like it was detected *in vitro* (Miranda, J. J. L. et al., 2005; Westermann, S. et al., 2005). It is known that the interaction with the MT lattice requires the C-terminus of Dam1 and $\alpha\beta$ -tubulin (Westermann, S. et al., 2005). Lateral sliding of the Dam1 ring-structure along the MT lattice would allow to convert the energy of the depolymerizing MT into a pulling force of the end-on attached KT. Taken together, the Ndc80 complex and the Dam1 complex are thought to be the key player to promote a robust, but also dynamic interaction of KTs and MTs (Westermann, S. et al., 2007).

In addition, the checkpoint proteins Mps1, Mad1, Mad2, Bub1 and Bub3 count to the outer KT (Biggins, S., 2013). The four nuclear MT motor proteins Kar3, Cin8, Kip1 and Kip3 and several MAPs like Stu1, Stu2, Bik1 and Bim1 are further components of the outer KT. Most of them localize to the dynamic plus-ends of MTs and regulate MT dynamics and interactions of MTs with other cellular structures (Schuyler, S. C. et al., 2001; Tytell, J. D. et al., 2006; Wolyniak, M. J. et al., 2006). These proteins do not contribute to the core structure of the KT, but transiently localize to the KT to fulfill regulatory functions. They are required for KT-MT attachment and stabilization of interpolar MTs and kMTs (Lin, H. et al., 2001; Yin, H. et al., 2002; Biggins, S., 2013). Furthermore, some of them experience a dramatic reorganization to the spindle at the beginning of anaphase and thus stabilize the mitotic spindle. The *S. cerevisiae* CLASP homolog Stu1 (suppressor of β -tubulin) is an impressive example in this respect (Yin, H. et al., 2002; Ortiz, J. et al., 2009).

1.4 CLASP proteins and the *S. cerevisiae* Stu1

One of the proteins that contribute to the outer KT and therefore to the KT-MT interface is Stu1. This essential protein was originally found as a suppressor of a beta-tubulin mutation and turned out to be an essential component of the mitotic spindle (Pasqualone, D. et al., 1994; Yin, H. et al., 2002).

Stu1 belongs to the evolutionary conserved CLASP family, which includes CLASP1 and CLASP2 in vertebrates, MAST/orbit in *D. melanogaster*, Cls-2 in *C. elegans* and Cls1 in *S. pombe* (Akhmanova, A. et al., 2005). CLASP proteins are characterized by binding to MTs, preferentially to their plus-end tips and by promoting MT stability or polymerization by the incorporation of tubulin subunits (Maiato, H. et al., 2005). In all characterized organisms, CLASP proteins play an essential role for the formation and maintenance of a bipolar spindle (Pasqualone, D. et al., 1994; Inoue, Y. H. et al., 2000). The budding yeast Stu1 for example is required to drive and maintain the separation of the SPBs (Yin, H. et al., 2002). In contrast to the human CLASP1, Stu1 cannot be found at SPBs (centrosomes in higher eukaryotes) or outside the nucleus at astral

MTs, nor does it particularly localize to the plus-ends of MTs in a regular cell cycle (Maiato, H. et al., 2003; Ortiz, J. et al., 2009).

Recent findings revealed that in the progress of mitosis Stu1 first localizes to KTs, then binds to the metaphase spindle, focuses to the midregion of interpolar MTs in anaphase and diffusely surrounds SPBs in late anaphase (Ortiz, J. et al., 2009). More detailed analysis demonstrated that Stu1 specifically binds to unattached KTs and thus facilitates capturing of unattached KTs by MTs. The displacement of Stu1 from the KT and re-localization to interpolar MTs is putatively initiated when both sister KTs engage in MT interaction. Since detached KTs in competition with interpolar MTs apparently recruit almost all cellular Stu1, they might indirectly regulate the spindle formation. If Stu1 is absent from the spindle, SPBs stay in close proximity to each other and this is likely to facilitate bipolar KT attachment (Ortiz, J. et al., 2009).

Interestingly, CLASP1 was suggested to bind to the outer KT (called outer corona) of vertebrate cells to regulate kMT dynamics by providing tubulin for the incorporation into kMTs (Maiato, H. et al., 2003). CLASP2 has only partially redundant functions during mitosis and has a key role for efficient chromosome poleward movement. Nevertheless, CLASP1 and CLASP2 are thought to work together to ensure mitotic fidelity. They both are suggested to incorporate tubulin not only in kMTs when localizing to the KT, but also to plus-ends of interpolar MTs in anaphase (Pereira, A. L. et al., 2006).

In agreement with this, proteins of the CLASP family were found to use conserved TOG-like (TOGL) domains to directly bind tubulin, similar to the mechanism firstly discovered for Dis1/XMAP215 family members like the budding yeast Stu2. Two pairs of TOG domains of a protein dimer are thought to wrap around a tubulin heterodimer like a clamp. In combination with their ability to interact with the MT lattice, they recruit free tubulin to MTs and provide $\alpha\beta$ -tubulin for MT polymerization or stabilization (Al-Bassam, J. et al., 2006, 2010).

TOG domains are repeats of about 200 amino acids consisting of up to six HEAT motifs that arrange in parallel to form a characteristic flat paddle-like domain (Al-Bassam, J. et al., 2006). One HEAT repeat consists of one pair of antiparallel alpha-helical structures connected by a so called intra-HEAT repeat loop (Fig. 1-9 A). HEAT motifs were generally found as protein-protein interaction domains and are comprised within various proteins (Neuwald, A. F., 2000). The name originates from four proteins in which the repeat was detected: huntingtin, elongation factor 3 (EF3), the regulatory A subunit of protein phosphatase 2 A (PP2A) and IOR1 (Andrade, M. A. et al., 1995). Especially the intra-HEAT repeat loops appear to be highly conserved within the XMAP215 and CLASP family members (Fig. 1-9 B).

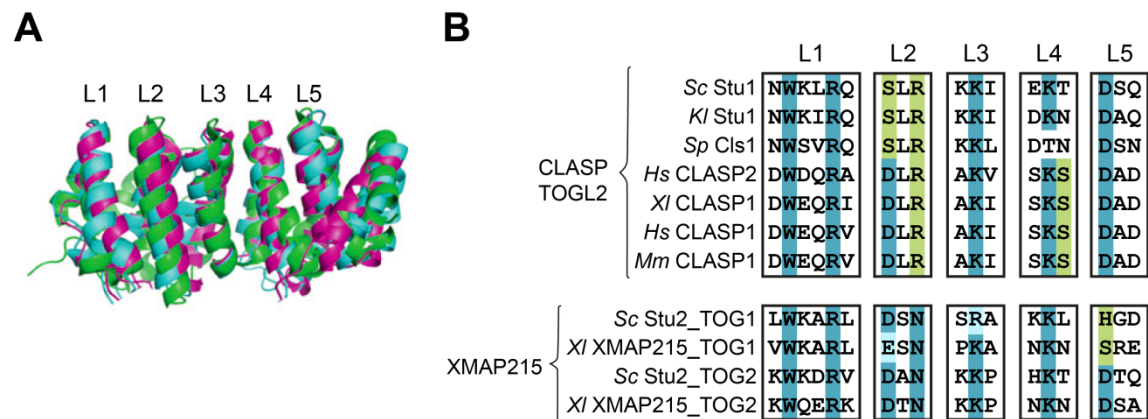


Fig. 1-9. TOG domains and the tubulin binding loops

(A) Overlaid crystal structure of TOG domains from the XMAP215 homologs *S. pombe* Stu2, *C. elegans* Zyg9 and *D. melanogaster* Msps with indicated intra-HEAT repeat loops (L1-L5). Six HEAT repeats, each consisting of two antiparallel alpha-helical structures that are connected via five intra-HEAT repeat loops, form a characteristic paddle-like domain. Adapted from Al-Bassam, J. et al. (2011). **(B)** Alignment of the highly conserved tubulin binding turns, the intra-HEAT repeat loops (L1-L5). Residues that are strictly conserved within TOG and TOGL domains of CLASP and XMAP215 proteins are highlighted in cyan, moderately ones in bright blue and weakly conserved ones in green. Alignments of indicated proteins of *Saccharomyces cerevisiae* (Sc), *Kluyveromyces lactis* (Kl), *Schizosaccharomyces pombe* (Sp), *Homo sapiens* (Hs), *Xenopus laevis* (Xl) and *Mus musculus* (Mm) were performed using ClustalW. Conservation is indicated according to Al-Bassam, J. et al. (2011).

In contrast to XMAP215/CLASP proteins of higher eukaryotes that contain five or three arrayed TOG domains at the N-terminal region of the protein, yeast proteins only have two TOG domain repeats (Ohkura, H. et al., 2001). Therefore, Stu2 or Cls1 function as a homodimer, in contrast to higher eukaryotes that act as a monomer (Al-Bassam, J. et al., 2006). Often an additional C-terminal coiled-coil region contributes to MT-binding or localization to the centrosome (SPB in budding yeast) or the KT. Whereas XMAP215 family members are suggested to have the function of a MT polymerase when localizing to MT plus-ends, CLASP family members are thought to stabilize MTs by promoting MT rescue and preventing MT catastrophe events (Al-Bassam, J. et al., 2011). For instance, the *S. pombe* CLASP Cls1 locally increases MT rescue frequency and decreases MT catastrophe frequency *in vitro*. Thereby, unimpaired tubulin binding by the TOGL domains is critical for the MT rescue activity of Cls1 (Al-Bassam, J. et al., 2010).

Along with other CLASP proteins, Stu1 was also suggested to contain TOGL domains at the N-terminal part of the protein (Al-Bassam, J. et al., 2011), but nothing is known about the biological significance of these domains for the function of Stu1.

1.5 The aim of the study

The *S. cerevisiae* CLASP homolog Stu1 is an essential protein that localizes to different molecular structures and has various functions during mitosis. But only little is known about the structural requirements that direct and regulate Stu1 and about their mechanism of action. Earlier studies demonstrated that the determined MT-binding domain (MBD) of Stu1 (Yin, H. et al., 2002) is essential for cell viability and binding to MTs also *in vivo*. Additionally, the MBD seems to ensure a proper KT-MT attachment (Ortiz, J. et al., 2009). The C-terminal domain was found to be required for the localization to unattached KTs (Ortiz, J. et al., 2009). This work had the purpose to contribute to a better understanding of the function of Stu1 as an essential midzone protein, its role in spindle dynamics and capturing, but also the basic mechanisms of the regulation of this protein. One strategy to characterize the impact of different domains on the localization and function of Stu1 at KTs and at the spindle was to evaluate the phenotypes of various deletion mutants. Another strategy was to analyze the impact of modifications like phosphorylation on the properties of Stu1 in order to gain more insight in the regulatory mechanism of this protein. Identified phosphorylation sites were analyzed in regards to their biological significance for the function of Stu1.

2 MATERIALS

2.1 Organisms

2.1.1 *Escherichia coli* strains

Strain	Genotype	Reference
DH5 α	<i>F</i> endA1 <i>glnV44</i> <i>thi-1</i> <i>recA1</i> <i>relA1</i> <i>gyrA96</i> <i>deoR</i> <i>nupG</i> Φ 80 <i>lacZ</i> Δ M15 Δ (<i>lacZYA-argF</i>)U169, <i>hsdR17</i> (<i>r_K⁻ m_K⁺</i>), λ -	
XL1-Blue	<i>endA1</i> <i>gyrA96</i> (<i>na^R</i>) <i>thi-1</i> <i>recA1</i> <i>relA1</i> <i>lac</i> <i>glnV44</i> <i>F'</i> [::Tn10 <i>proAB⁺</i> <i>lacI^f</i> Δ (<i>lacZ</i>)M15] <i>hsdR17</i> (<i>r_K⁻ m_K⁺</i>)	Stratagene

2.1.2 *Saccharomyces cerevisiae* strains

Strain	Genotype	Reference
YPH499	<i>MATa</i> <i>ade2-101ochre</i> <i>trp1-Δ63</i> <i>leu2-Δ1</i> <i>ura3-52</i> <i>his3-Δ200</i> <i>lys2-801ambre</i>	<i>Sikorski and Hieter (1989)</i>
YMS231	<i>MATa</i> Δ <i>sst1</i> <i>ade2-101ochre</i> <i>trp1-Δ63</i> <i>leu2-Δ1</i> <i>ura3-52</i> <i>his3-Δ200</i> <i>lys2-801ambre</i>	this lab
YMS299	<i>MATa</i> Δ <i>sst1</i> <i>ade2-101ochre</i> <i>trp1-Δ63</i> <i>leu2-Δ1</i> <i>ura3-52</i> <i>his3-Δ200</i> <i>lys2-801ambre</i> <i>PDS1-9MYC::kITRP1</i>	this lab
YSK633	<i>MATalpha</i> <i>ade2-101ochre</i> <i>trp1-Δ63</i> <i>leu2-Δ1</i> <i>ura3-52</i> <i>his3-Δ200</i> <i>lys2-801ambre</i> <i>cyh2R</i> [CF CEN6 URA3 SUP11 CYH2S] Δ <i>mad2::kITRP1</i>	this lab
YBK2137	<i>MATa</i> Δ <i>sst1</i> <i>ade2-101ochre</i> <i>trp1-Δ63</i> <i>leu2-Δ1</i> <i>ura3-52</i> <i>his3-Δ200</i> Δ <i>stu1::HIS3MX6</i> <i>lys2-801ambre::pSTU1-FLAG-stu1(aa261-aa762)-NLS-GFP::LYS2</i>	this lab
YBK2139	<i>MATa</i> Δ <i>sst1</i> <i>ade2-101ochre</i> <i>trp1-Δ63</i> <i>leu2-Δ1</i> <i>ura3-52</i> <i>his3-Δ200</i> Δ <i>stu1::HIS3MX6</i> <i>lys2-801ambre::pSTU1-FLAG-stu1(aa261-aa569)-NLS-GFP::LYS2 + pCF1137 (pSTU1-STU1-Term)</i>	this lab
YBK2241	<i>MATa</i> Δ <i>sst1</i> <i>trp1-Δ63</i> <i>leu2-Δ1</i> <i>ura3-52</i> <i>his3-Δ200</i> <i>lys2-801ambre</i> <i>stu1Δ(995-1180)-CFP::KANMX6</i> <i>SPC72-3mCherry::hphNT1</i> <i>ade2-101ochre::TetR-GFP::ADE2</i> <i>CEN5-tetO2x112::URA3 LEU2::pMET25-CDC20 Δcin8::natNT2</i>	this lab
YBK2242	<i>MATa</i> Δ <i>sst1</i> <i>trp1-Δ63</i> <i>leu2-Δ1</i> <i>ura3-52</i> <i>his3-Δ200</i> <i>lys2-801ambre</i> <i>STU1-CFP::KANMX6</i> <i>SPC72-3mCherry::hphNT1</i> <i>ade2-101ochre::TetR-GFP::ADE2</i> <i>CEN5-tetO2x112::URA3 HIS3MX6::pMET25-CDC20 Δcin8::natNT2</i>	this lab
YCF1778	<i>MATa</i> Δ <i>sst1</i> <i>ade2-101ochre</i> <i>trp1-Δ63</i> <i>leu2-Δ1</i> <i>ura3-52</i> <i>his3-Δ200</i> <i>STU1-ProtA-7HIS::HIS3MX6</i> <i>lys2-801ambre::pGAL1-FLAG-stu1(K428A,K429A)-NLS-GFP::LYS2</i>	this lab
YCF2177	<i>MATalpha</i> <i>ade2-101ochre</i> <i>trp1-Δ63</i> <i>leu2-Δ1</i> <i>ura3-52</i> <i>his3-Δ200</i> <i>lys2-801ambre</i> <i>cyh2R</i> [CF CEN6 URA3 SUP11 CYH2S]	this lab
YCF2226	<i>MATa</i> Δ <i>sst1</i> <i>ade2-101ochre</i> <i>trp1-Δ63</i> <i>leu2-Δ1</i> <i>ura3-52</i> <i>his3-Δ200</i> Δ <i>stu1::HIS3MX6</i> <i>lys2-801ambre::pSTU1-FLAG-STU1-NLS-GFP::LYS2</i> <i>cdc20::LEU2-pMET25-CDC20</i>	this lab
YJO1164	<i>MATa</i> Δ <i>sst1</i> <i>ade2-101ochre</i> <i>trp1-Δ63</i> <i>leu2-Δ1</i> <i>ura3-52</i> <i>his3-Δ200</i> <i>lys2-801ambre</i> <i>STU1-ProtA-7HIS::HIS3MX6</i>	this lab
YJO1334	<i>MATa</i> Δ <i>sst1</i> <i>trp1-Δ63</i> <i>leu2-Δ1</i> <i>ura3-52</i> <i>his3-Δ200</i> <i>ade2-101ochre::TetR-GFP::ADE2</i> <i>CEN5-tetO2x112::URA3</i> <i>SPC72-Cherry::hphNT1</i> <i>stu1::kITRP1-pGAL-UbiR-STU1-CFP::KANMX4</i>	this lab
YJO1392	<i>MATa</i> Δ <i>sst1</i> <i>ade2-101ochre</i> <i>trp1-Δ63</i> <i>leu2-Δ1</i> <i>ura3-52</i> <i>his3-Δ200</i> <i>lys2-801ambre</i> <i>STU1-ProtA-7HIS::HIS3MX6</i> <i>cdc20::KANMX4-pMET25-CDC20</i>	this lab
YVS1408	<i>MATa</i> Δ <i>sst1</i> <i>ade2-101ochre</i> <i>trp1-Δ63</i> <i>leu2-Δ1</i> <i>ura3-52</i> <i>his3</i> <i>STU1-NLS-EGFP::kITRP1</i> <i>lys2-801ambre::CFP-TUB1::LYS2</i> <i>AME1-Cherry::hphNT1</i>	this work
YVS1421	<i>MATa</i> Δ <i>sst1</i> <i>ade2-101ochre</i> <i>trp1-Δ63</i> <i>leu2-Δ1</i> <i>ura3-52</i> <i>his3-Δ200</i> Δ <i>stu1::HIS3MX6</i> <i>lys2-801ambre::CFP-TUB1::LYS2</i> <i>AME1-Cherry::hphNT1</i>	this work
YVS1459	<i>MATa</i> Δ <i>sst1</i> <i>ade2-101ochre</i> <i>trp1-Δ63</i> <i>leu2-Δ1</i> <i>ura3-52</i> <i>his3-Δ200</i> <i>lys2-801ambre</i> <i>cdc15-1</i> <i>ura3::GFP-TUB1::URA3</i> <i>STU1-ProtA-7HIS::HIS3MX6</i>	this work
YVS1536	<i>MATa</i> Δ <i>sst1</i> <i>ade2-101ochre</i> <i>trp1-Δ63</i> <i>leu2-Δ1</i> <i>ura3-52</i> <i>his3-Δ200</i> <i>stu1</i> (S497A, S602A, S690A, S745A, S1001A, S1018A, T1034A, T1047A, S1060A, S1113A, T1134A, S1167A)-EGFP::kITRP1 <i>lys2-801ambre::CFP-TUB1::LYS2</i> <i>AME1-Cherry::hphNT1</i>	this work
YVS1543	<i>MATa</i> Δ <i>sst1</i> <i>ade2-101ochre</i> <i>trp1-Δ63</i> <i>leu2-Δ1</i> <i>ura3-52</i> <i>his3-Δ200</i> <i>lys2-801ambre</i> Δ <i>stu1::HIS3MX6 + pCF1137 (pSTU1-STU1-Term)</i>	this work
YVS1553	<i>MATa</i> Δ <i>sst1</i> <i>ade2-101ochre</i> <i>trp1-Δ63</i> <i>leu2-Δ1</i> <i>ura3-52</i> <i>his3-Δ200</i> <i>stu1</i> (T1047A)-EGFP::kITRP1 <i>lys2-801ambre::CFP-TUB1::LYS2</i> <i>AME1-Cherry::hphNT1</i>	this work
YVS1554	<i>MATa</i> Δ <i>sst1</i> <i>ade2-101ochre</i> <i>trp1-Δ63</i> <i>leu2-Δ1</i> <i>ura3-52</i> <i>his3-Δ200</i> <i>stu1</i> (T1134A)-EGFP::kITRP1 <i>lys2-801ambre::CFP-TUB1::LYS2</i> <i>AME1-Cherry::hphNT1</i>	this work
YVS1562	<i>MATa</i> Δ <i>sst1</i> <i>ade2-101ochre</i> <i>trp1-Δ63</i> <i>leu2-Δ1</i> <i>ura3-52</i> <i>his3-Δ200</i> <i>stu1</i> (S602E)-EGFP::kITRP1 <i>lys2-801ambre::CFP-TUB1::LYS2</i> <i>AME1-Cherry::hphNT1</i>	this work

Saccharomyces cerevisiae strains continued

Strain	Genotype	Reference
YVS1565	<i>MATa</i> Δ ss1 <i>ade2-101ochre</i> <i>trp1-Δ63</i> <i>leu2-Δ1</i> <i>ura3-52</i> <i>his3-Δ200</i> <i>stu1</i> (S602A)-EGFP::kiTRP1 <i>lys2-801ambre</i> ::CFP-TUB1::LYS2 <i>AME1-Cherry</i> ::hphNT1	this work
YVS1580	<i>MATa</i> Δ ss1 <i>ade2-101ochre</i> <i>trp1-Δ63</i> <i>leu2-Δ1</i> <i>ura3-52</i> <i>his3-Δ200</i> <i>lys2-801ambre</i> <i>arg4Δ</i> ::loxP-KANMX4-loxP <i>STU1-ProtA-7HIS</i> ::HIS3MX6	this work
YVS1582	<i>MATa</i> Δ ss1 <i>ade2-101ochre</i> <i>trp1-Δ63</i> <i>leu2-Δ1</i> <i>ura3-52</i> <i>his3-Δ200</i> <i>lys2-801ambre</i> <i>cdc15-1</i> <i>ura3</i> ::GFP1-TUB1::URA3 <i>arg4Δ</i> ::loxP-KANMX4-loxP <i>STU1-ProtA-7HIS</i> ::HIS3MX6	this work
YVS1596	<i>MATa</i> Δ ss1 <i>ade2-101ochre</i> <i>trp1-Δ63</i> <i>leu2-Δ1</i> <i>ura3-52</i> <i>his3-Δ200</i> <i>stu1</i> (S1113A)-EGFP::kiTRP1 <i>lys2-801ambre</i> ::CFP-TUB1::LYS2 <i>AME1-Cherry</i> ::hphNT1	this work
YVS1597	<i>MATa</i> Δ ss1 <i>ade2-101ochre</i> <i>trp1-Δ63</i> <i>leu2-Δ1</i> <i>ura3-52</i> <i>his3-Δ200</i> <i>stu1</i> (S1113E)-EGFP::kiTRP1 <i>lys2-801ambre</i> ::CFP-TUB1::LYS2 <i>AME1-Cherry</i> ::hphNT1	this work
YVS1611	<i>MATa</i> Δ ss1 <i>ade2-101ochre</i> <i>trp1-Δ63</i> <i>leu2-Δ1</i> <i>ura3-52</i> <i>his3-Δ200</i> <i>stu1</i> (S497A)-EGFP::kiTRP1 <i>lys2-801ambre</i> ::CFP-TUB1::LYS2 <i>AME1-Cherry</i> ::hphNT1	this work
YVS1613	<i>MATa</i> Δ ss1 <i>ade2-101ochre</i> <i>trp1-Δ63</i> <i>leu2-Δ1</i> <i>ura3-52</i> <i>his3-Δ200</i> <i>stu1</i> (S497E)-EGFP::kiTRP1 <i>lys2-801ambre</i> ::CFP-TUB1::LYS2 <i>AME1-Cherry</i> ::hphNT1	this work
YVS1614	<i>MATa</i> Δ ss1 <i>ade2-101ochre</i> <i>trp1-Δ63</i> <i>leu2-Δ1</i> <i>ura3-52</i> <i>his3-Δ200</i> <i>stu1</i> (T1047A, S1113A, T1134A)-EGFP::kiTRP1 <i>lys2-801ambre</i> ::CFP-TUB1::LYS2 <i>AME1-Cherry</i> ::hphNT1	this work
YVS1615	<i>MATa</i> Δ ss1 <i>ade2-101ochre</i> <i>trp1-Δ63</i> <i>leu2-Δ1</i> <i>ura3-52</i> <i>his3-Δ200</i> <i>stu1</i> (S745E)-EGFP::kiTRP1 <i>lys2-801ambre</i> ::CFP-TUB1::LYS2 <i>AME1-Cherry</i> ::hphNT1	this work
YVS1616	<i>MATa</i> Δ ss1 <i>ade2-101ochre</i> <i>trp1-Δ63</i> <i>leu2-Δ1</i> <i>ura3-52</i> <i>his3-Δ200</i> <i>stu1</i> (K428A, K429A)-EGFP::kiTRP1 <i>lys2-801ambre</i> ::CFP-TUB1::LYS2 <i>AME1-Cherry</i> ::hphNT1	this work
YVS1626	<i>MATa</i> Δ ss1 <i>ade2-101ochre</i> <i>trp1-Δ63</i> <i>leu2-Δ1</i> <i>ura3-52</i> <i>his3-Δ200</i> <i>stu1</i> (T1047E, S1113E, T1134E)- EGFP::kiTRP1 <i>lys2-801ambre</i> ::CFP-TUB1::LYS2 <i>AME1-Cherry</i> ::hphNT1	this work
YVS1627	<i>MATa</i> Δ ss1 <i>ade2-101ochre</i> <i>trp1-Δ63</i> <i>leu2-Δ1</i> <i>ura3-52</i> <i>his3-Δ200</i> <i>stu1</i> (S497E, T1047A, S1113A, T1134A)-EGFP::kiTRP1 <i>lys2-801ambre</i> ::CFP-TUB1::LYS2 <i>AME1-Cherry</i> ::hphNT1	this work
YVS1628	<i>MATa</i> Δ ss1 <i>ade2-101ochre</i> <i>trp1-Δ63</i> <i>leu2-Δ1</i> <i>ura3-52</i> <i>his3-Δ200</i> <i>stu1</i> (S497A, T1047E, S1113E, T1134E)-EGFP::kiTRP1 <i>lys2-801ambre</i> ::CFP-TUB1::LYS2 <i>AME1-Cherry</i> ::hphNT1	this work
YVS1634	<i>MATa</i> Δ ss1 <i>ade2-101ochre</i> <i>trp1-Δ63</i> <i>leu2-Δ1</i> <i>ura3-52</i> <i>his3-Δ200</i> <i>stu1</i> (S745A)-EGFP::kiTRP1 <i>lys2-801ambre</i> ::CFP-TUB1::LYS2 <i>AME1-Cherry</i> ::hphNT1	this work
YVS1648	<i>MATa</i> Δ ss1 <i>ade2-101ochre</i> <i>trp1-Δ63</i> <i>leu2-Δ1</i> <i>ura3-52</i> <i>his3-Δ200</i> <i>stu1</i> (S497A, S745E, T1047E, S1113E, T1134E)-EGFP::kiTRP1 <i>lys2-801ambre</i> ::CFP-TUB1::LYS2 <i>AME1-Cherry</i> ::hphNT1	this work
YVS1649	<i>MATa</i> Δ ss1 <i>ade2-101ochre</i> <i>trp1-Δ63</i> <i>leu2-Δ1</i> <i>ura3-52</i> <i>his3-Δ200</i> <i>stu1</i> (S497E, S745A, T1047A, S1113A, T1134A)-EGFP::kiTRP1 <i>lys2-801ambre</i> ::CFP-TUB1::LYS2 <i>AME1-Cherry</i> ::hphNT1	this work
YVS1651	<i>MATa</i> Δ ss1 <i>ade2-101ochre</i> <i>trp1-Δ63</i> <i>leu2-Δ1</i> <i>ura3-52</i> <i>his3-Δ200</i> <i>stu1Δ</i> (995-1180)-EGFP::kiTRP1 <i>lys2-801ambre</i> ::CFP-TUB1::LYS2 <i>AME1-Cherry</i> ::hphNT1	this work
YVS1662	<i>MATa</i> Δ ss1 <i>ade2-101ochre</i> <i>trp1-Δ63</i> <i>leu2-Δ1</i> <i>ura3-52</i> <i>his3-Δ200</i> <i>stu1</i> (S265A, S276A, T277A, S497E, S745A, T1047A, S1113A, T1134A)-EGFP::kiTRP1 <i>lys2-801ambre</i> ::CFP-TUB1::LYS2 <i>AME1-Cherry</i> ::hphNT1	this work
YVS1718	<i>MATa</i> Δ ss1 <i>ade2-101ochre</i> <i>trp1-Δ63</i> <i>leu2-Δ1</i> <i>his3-Δ200</i> <i>ura3-52</i> ::CFP-TUB1::URA3 <i>AME1-Cherry</i> ::hphNT1 <i>lys2-801ambre</i> ::pGAL1- <i>STU1-NLS-GFP</i> ::LYS2	this work
YVS1718	<i>MATa</i> Δ ss1 <i>ade2-101ochre</i> <i>trp1-Δ63</i> <i>leu2-Δ1</i> <i>ura3-52</i> <i>his3-Δ200</i> <i>lys2-801ambre</i> <i>STU1-ProtA-7HIS</i> ::HIS3MX6	this work
YVS1743	<i>MATa</i> Δ ss1 <i>ade2-101ochre</i> <i>trp1-Δ63</i> <i>leu2-Δ1</i> <i>ura3-52</i> <i>his3-Δ200</i> <i>stu1</i> (S265E, S276E, T277E, S497A, S745E, T1047E, S1113E, T1134E)-EGFP::kiTRP1 <i>lys2-801ambre</i> ::CFP-TUB1::LYS2 <i>AME1-Cherry</i> ::hphNT1	this work
YVS1757	<i>MATa</i> Δ ss1 <i>ade2-101ochre</i> <i>trp1-Δ63</i> <i>leu2-Δ1</i> <i>ura3-52</i> <i>his3-Δ200</i> <i>stu1</i> (S1001A)-EGFP::kiTRP1 <i>lys2-801ambre</i> ::CFP-TUB1::LYS2 <i>AME1-Cherry</i> ::hphNT1	this work
YVS1768	<i>MATa</i> Δ ss1 <i>ade2-101ochre</i> <i>trp1-Δ63</i> <i>leu2-Δ1</i> <i>ura3-52</i> <i>his3-Δ200</i> <i>stu1</i> (S997A, S1000A, S1001A, S1003A, T1005A, S1018A, T1034A, T1047A, S1060A, S1113A, T1134A, S1167A)-EGFP::kiTRP1 <i>lys2-801ambre</i> ::CFP-TUB1::LYS2 <i>AME1-Cherry</i> ::hphNT1	this work
YVS1772	<i>MATa</i> Δ ss1 <i>ade2-101ochre</i> <i>trp1-Δ63</i> <i>leu2-Δ1</i> <i>ura3-52</i> <i>his3-Δ200</i> <i>stu1Δ</i> (aa301-aa569)-EGFP::kiTRP1 <i>lys2-801ambre</i> ::CFP-TUB1::LYS2 <i>AME1-Cherry</i> ::hphNT1 + pCF1137 (pSTU1- <i>STU1-Term</i>)	this work
YVS1814	<i>MATa</i> Δ ss1 <i>ade2-101ochre</i> <i>trp1-Δ63</i> <i>leu2-Δ1</i> <i>ura3-52</i> <i>his3-Δ200</i> <i>stu1</i> (W339A, R342A, K428A, K429A)-EGFP::kiTRP1 <i>lys2-801ambre</i> ::CFP-TUB1::LYS2 <i>AME1-Cherry</i> ::hphNT1 + pCF1137 (pSTU1- <i>STU1-Term</i>)	this work
YVS1919	<i>MATa</i> Δ ss1 <i>ade2-101ochre</i> <i>trp1-Δ63</i> <i>leu2-Δ1</i> <i>ura3-52</i> <i>his3-Δ200</i> <i>STU1-ProtA-7HIS</i> ::HIS3MX6 <i>lys2-801ambre</i> ::pGAL1- <i>FLAG-stu1</i> (W339A, R342A, K428A, K429A)- <i>NLS-GFP</i> ::LYS2	this work
YVS1933	<i>MATa</i> Δ ss1 <i>ade2-101ochre</i> <i>trp1-Δ63</i> <i>leu2-Δ1</i> <i>ura3-52</i> <i>his3-Δ200</i> <i>stu1</i> (S276A, T277A, S602A)- EGFP::kiTRP1 <i>lys2-801ambre</i> ::CFP-TUB1::LYS2 <i>AME1-Cherry</i> ::hphNT1	this work
YVS1971	<i>MATa</i> Δ ss1 <i>ade2-101ochre</i> <i>trp1-Δ63</i> <i>leu2-Δ1</i> <i>ura3-52</i> <i>his3-Δ200</i> <i>STU1-ProtA-7HIS</i> ::HIS3MX6 <i>lys2-801ambre</i> ::pGAL1- <i>FLAG-stu1</i> (aa261-aa569)- <i>NLS-GFP</i> ::LYS2	this work
YVS1972	<i>MATa</i> Δ ss1 <i>ade2-101ochre</i> <i>trp1-Δ63</i> <i>leu2-Δ1</i> <i>ura3-52</i> <i>his3-Δ200</i> <i>STU1-ProtA-7HIS</i> ::HIS3MX6 <i>lys2-801ambre</i> ::pGAL1- <i>FLAG-stu1Δ</i> (301-560)- <i>NLS-GFP</i> ::LYS2	this work
YVS1986	<i>MATa</i> Δ ss1 <i>ade2-101ochre</i> <i>trp1-Δ63</i> <i>leu2-Δ1</i> <i>ura3-52</i> <i>his3</i> <i>stu1Δ</i> (aa717-aa994)-EGFP::kiTRP1 <i>lys2-801ambre</i> ::CFP-TUB1::LYS2 <i>AME1-Cherry</i> ::hphNT1	this work
YVS1994	<i>MATa</i> Δ ss1 <i>ade2-101ochre</i> <i>trp1-Δ63</i> <i>ura3-52</i> <i>his3-Δ200</i> <i>stu1</i> (W339A, R342A, K428A, K429A)- EGFP::kiTRP1 <i>lys2-801ambre</i> ::CFP-TUB1::LYS2 <i>AME1-Cherry</i> ::hphNT1 <i>leu2-Δ1</i> ::pGAL1- <i>UbiR-STU1</i> ::LEU2	this work

Saccharomyces cerevisiae strains continued

Strain	Genotype	Reference
YVS2000	<i>MATa</i> Δ ss1 ade2-101ochre trp1- Δ 63 leu2- Δ 1 ura3-52 his3- Δ 200 stu1(S602A)-ECFP::KANMX6 lys2-801 GFP-TUB1::TRP1 SPC72-Cherry::hphNT1	this work
YVS2001	<i>MATa</i> Δ ss1 ade2-101ochre trp1- Δ 63 leu2- Δ 1 ura3-52 his3 stu1 Δ (aa570-aa716)-EGFP::kITRP1 lys2-801ambre::CFP-TUB1::LYS2 AME1-Cherry::hphNT1	this work
YVS2028	<i>MATa</i> Δ ss1 ade2-101ochre trp1- Δ 63 leu2- Δ 1 ura3-52 his3- Δ 200 lys2-801ambre STU1-CFP::KANMX6 SPC72-3mCherry::hphNT1 ade2-101ochre::TetR-GFP::ADE2 CEN5-tetO2x112::URA3	this work
YVS2029	<i>MATa</i> Δ ss1 trp1- Δ 63 leu2- Δ 1 ura3-52 his3- Δ 200 lys2-801ambre stu1 Δ (aa995-aa1180)-CFP::KANMX6 SPC72-3mCherry::hphNT1 ade2-101ochre::TetR-GFP::ADE2 CEN5-tetO2x112::URA3	this work
YVS2046	<i>MATa</i> Δ ss1 ade2-101ochre trp1- Δ 63 leu2- Δ 1 ura3-52 his3- Δ 200 stu1 Δ (aa570-aa716, aa995-aa1180)-EGFP::kITRP1 lys2-801ambre::CFP-TUB1::LYS2 AME1-Cherry::hphNT1	this work
YVS2078	<i>MATa</i> Δ ss1 ade2-101ochre leu2- Δ 1 ura3-52 his3- Δ 200 lys2-801ambre ade1::pURA3-TetR-3xCFP::hphNT1 CEN5-tetO2x112::URA3 SPC72-Cherry::natNT2 trp1- Δ 63::GFP-TUB1::TRP1 KANMX6::pGAL1-UbiR-STU1	this work
YVS2085	<i>MATa</i> Δ ss1 ade2-101ochre trp1- Δ 63 leu2- Δ 1 ura3-52 his3- Δ 200 ade1::pURA3-TetR-3xCFP-HPH1 CEN5-tetO2x112::URA3 SPC72-Cherry::natNT2 trp1- Δ 63::GFP-TUB1::TRP1 KANMX6::pGAL1-UbiR-STU1 lys2-801ambre::pSTU1-FLAG-STU1-NLS::LYS2	this work
YVS2086	<i>MATa</i> Δ ss1 ade2-101ochre leu2- Δ 1 ura3-52 his3- Δ 200 ade1::pURA3-TetR-3xCFP-HPH1 CEN5-tetO2x112::URA3 SPC72-Cherry::natNT2 trp1- Δ 63::GFP-TUB1::TRP1 KANMX6::pGAL1-UbiR-STU1 lys2-801ambre::pSTU1-FLAG-stu1(W339A, R342A, K428A, K429A)-NLS::LYS2	this work
YVS2087	<i>MATa</i> Δ ss1 ade2-101ochre trp1- Δ 63 leu2- Δ 1 ura3-52 his3- Δ 200 ade1::pURA3-TetR-3xCFP-HPH1 CEN5-tetO2x112::URA3 SPC72-Cherry::natNT2 GFP-TUB1::TRP1 KANMX6::pGAL1-UbiR-STU1 lys2-801ambre::pSTU1-FLAG-stu1 Δ (aa301-aa560)-NLS::LYS2	this work
YVS2104	<i>MATa</i> Δ ss1 trp1- Δ 63 leu2- Δ 1 ura3-52 his3- Δ 200 lys2-801ambre stu1 Δ (995-1180)-CFP::KANMX6 SPC72-3mCherry::hphNT1 ade2-101ochre::TetR-GFP::ADE2 CEN5-tetO2x112::URA3 LEU2-pMET25-CDC20	this work
YVS2113	<i>MATa</i> Δ ss1 ade2-101ochre trp1- Δ 63 leu2- Δ 1 ura3-52 his3- Δ 200 lys2-801ambre stu1(S1113A)-CFP::KANMX6 SPC72-3mCherry::hphNT2 ade2-101ochre::TetR-GFP::ADE2 CEN5-tetO2x112::URA3	this work
YVS2114	<i>MATa</i> Δ ss1 ade2-101ochre trp1- Δ 63 leu2- Δ 1 ura3-52 his3- Δ 200 lys2-801ambre stu1(S1113E)-CFP::KANMX6 SPC72-3mCherry::hphNT2 ade2-101ochre::TetR-GFP::ADE2 CEN5-tetO2x112::URA3	this work
YVS2152	<i>MATa</i> Δ ss1 ade2-101ochre trp1- Δ 63 leu2- Δ 1 ura3-52 his3- Δ 200 lys2-801ambre stu1 Δ (aa995-aa1180)-EGFP::kITRP1 ade1::pURA3-TetR-3xCFP::hphNT1 SPC72-3mcherry::natNT2 CEN5-tetO2x112::URA3	this work
YVS2153	<i>MATa</i> Δ ss1 ade2-101ochre trp1- Δ 63 leu2- Δ 1 ura3-52 his3- Δ 200 lys2-801ambre stu1 Δ (aa570-aa716)-EGFP::kITRP1 SPC72-3mCherry::natNT2 ade1::pURA3-TetR-3xCFP::hphNT1 CEN5-tetO2x112::URA3	this work
YVS2154	<i>MATa</i> Δ ss1 ade2-101ochre trp1- Δ 63 leu2- Δ 1 ura3-52 his3- Δ 200 lys2-801ambre stu1 Δ (aa570-aa716, aa995-aa1180)-EGFP::kITRP1 ade1::pURA3-TetR-3xCFP::hphNT1 SPC72-3mcherry::natNT2 CEN5-tetO2x112::URA3	this work
YVS2156	<i>MATa</i> Δ ss1 ade2-101ochre trp1- Δ 63 leu2- Δ 1 ura3-52 his3- Δ 200 lys2-801ambre stu1(S997A, S1000A, S1001A, S1003A, T1005A, S1018A, T1034A, T1047A, S1060A, S1113A, T1134A, S1167A)-EGFP::kITRP1 SPC72-3mCherry::natNT2 ade1::pURA3-TetR-3xCFP::hphNT1 CEN5-tetO2x112::URA3	this work
YVS2159	<i>MATa</i> Δ ss1 ade2-101ochre trp1- Δ 63 leu2- Δ 1 ura3-52 his3- Δ 200 lys2-801ambre stu1(T1047E, S1113E, T1134E)-EGFP::kITRP1 SPC72-3mCherry::natNT2 ade1::pURA3-TetR-3xCFP::hphNT1 CEN5-tetO2x112::URA3	this work
YVS2160	<i>MATa</i> Δ ss1 ade2-101ochre trp1- Δ 63 leu2- Δ 1 ura3-52 his3- Δ 200 lys2-801ambre stu1(S1001A, T1034A, T1047A, T1134A)-EGFP::kITRP1 SPC72-3mCherry::natNT2 ade1::pURA3-TetR-3xCFP::hphNT1 CEN5-tetO2x112::URA3	this work
YVS2161	<i>MATa</i> Δ ss1 ade2-101ochre trp1- Δ 63 leu2- Δ 1 ura3-52 his3- Δ 200 lys2-801ambre stu1(S497A, S745A, S1167A)-EGFP::kITRP1 SPC72-3mCherry::natNT2 ade1::pURA3-TetR-3xCFP::hphNT1 CEN5-tetO2x112::URA3	this work
YVS2162	<i>MATa</i> Δ ss1 ade2-101ochre trp1- Δ 63 leu2- Δ 1 ura3-52 his3- Δ 200 lys2-801ambre stu1(S276A, T277A, S602A)-EGFP::kITRP1 SPC72-3mCherry::natNT2 ade1::pURA3-TetR-3xCFP::hphNT1 CEN5-tetO2x112::URA3	this work
YVS2163	<i>MATa</i> Δ ss1 ade2-101ochre leu2- Δ 1 ura3-52 his3- Δ 200 trp1- Δ 63::GFP-TUB1::TRP1 SPC72-3mCherry::natNT2 ade1::pURA3-TetR-3xCFP::hphNT1 CEN5-tetO2x112::URA3 KANMX6::pGAL1-UbiR-STU1 lys2-801ambre::pSTU1-FLAG-stu1(aa261-aa569)-NLS::LYS2	this work
YVS2199	<i>MATa</i> Δ ss1 ade2-101ochre trp1- Δ 63 leu2- Δ 1 ura3-52 his3- Δ 200 lys2-801ambre stu1(T1047A, S1113A, T1134A)-EGFP::kITRP1 SPC72-3mCherry::natNT2 ade1::pURA3-TetR-3xCFP::hphNT1 CEN5-tetO2x112::URA3	this work
YVS2199	<i>MATa</i> Δ ss1 ade2-101ochre trp1- Δ 63 leu2- Δ 1 ura3-52 his3- Δ 200 lys2-801ambre stu1(T1047A, S1113A, T1134A)-EGFP::kITRP1 ade1::pURA3-TetR-3xCFP::hphNT1 SPC72-3mCherry::natNT2 CEN5-tetO2x112::URA3	this work
YVS2201	<i>MATalpha</i> ade2-101ochre trp1- Δ 63 leu2- Δ 1 ura3-52 his3- Δ 200 cyh2R [CF: GEN6 URA3 CYH2S SUP11] stu1 Δ ::HIS3MX6 lys2-801ambre::pSTU1-FLAG-stu1 Δ (aa995-aa1180)-NLS-GFP::LYS2	this work

Saccharomyces cerevisiae strains continued

Strain	Genotype	Reference
YVS2206	<i>MATa</i> Δ ss1 <i>ade2-101ochre</i> <i>trp1-Δ63</i> <i>leu2-Δ1</i> <i>ura3-52</i> <i>his3-Δ200</i> <i>lys2-801ambre</i> <i>stu1</i> (S602E)-EGFP::klTRP1 SPC72-3mCherry::natNT2 <i>ade1</i> ::pURA3-TetR-3xCFP::hphNT1 CEN5-tetO2x112::URA3	this work
YVS2209	<i>MATa</i> Δ ss1 <i>ade2-101ochre</i> <i>trp1-Δ63</i> <i>leu2-Δ1</i> <i>ura3-52</i> <i>his3-Δ200</i> <i>lys2-801ambre</i> <i>stu1</i> Δ (aa570-aa716)-EGFP::klTRP1 <i>ade1</i> ::pURA3-TetR-3xCFP::hphNT1 SPC72-3mcherry::natNT2 CEN5-tetO2x112::URA3 LEU2::pMET25-CDC20	this work
YVS2210	<i>MATa</i> Δ ss1 <i>ade2-101ochre</i> <i>trp1-Δ63</i> <i>leu2-Δ1</i> <i>ura3-52</i> <i>his3-Δ200</i> <i>lys2-801ambre</i> <i>stu1</i> Δ (aa570-aa716, aa995-aa1180)-EGFP::klTRP1 <i>ade1</i> ::pURA3-TetR-3xCFP::hphNT1 SPC72-3mcherry::natNT2 CEN5-tetO2x112::URA3 LEU2::pMET25-CDC20	this work
YVS2211	<i>MATa</i> Δ ss1 <i>ade2-101ochre</i> <i>trp1-Δ63</i> <i>leu2-Δ1</i> <i>ura3-52</i> <i>his3-Δ200</i> <i>lys2-801ambre</i> STU1-CFP::KANMX6 SPC72-3xHA::HIS3MX6 <i>ade2-101ochre</i> ::TetR-GFP::ADE2 CEN5-tetO2x112::URA3 SPC42-EQFP::hphNT1	this work
YVS2212	<i>MATa</i> Δ ss1 <i>ade2-101ochre</i> <i>trp1-Δ63</i> <i>leu2-Δ1</i> <i>ura3-52</i> <i>his3-Δ200</i> <i>lys2-801ambre</i> <i>stu1</i> Δ (995-1180)-CFP::KANMX6 SPC72-3xHA::HIS3MX6 <i>ade2-101ochre</i> ::TetR-GFP::ADE2 CEN5-tetO2x112::URA3 SPC42-EQFP::hphNT1	this work
YVS2213	<i>MATa</i> Δ ss1 <i>ade2-101ochre</i> <i>trp1-Δ63</i> <i>ura3-52</i> <i>his3-Δ200</i> Δ stu1::HIS3MX6 <i>ade1</i> ::pURA3-TetR-3xCFP::hphNT1 SPC72-3mcherry::natNT2 <i>lys2-801ambre</i> ::pStu1-Flag-STU1-NLS::LYS2 CEN5-tetO2x112::URA3 <i>leu2-Δ1</i> ::GFP-TUB1::LEU2	this work
YVS2214	<i>MATa</i> Δ ss1 <i>ade2-101ochre</i> <i>trp1-Δ63</i> <i>leu2-Δ1</i> <i>ura3-52</i> <i>his3-Δ200</i> Δ stu1::HIS3MX6 <i>ade1</i> ::pURA3-TetR-3xCFP::hphNT1 SPC72-3mcherry::natNT2 <i>lys2-801ambre</i> ::pStu1-Flag-stu1 Δ (aa995-aa1180)-NLS::LYS2 CEN5-tetO2x112::URA3 <i>leu2-Δ1</i> ::GFP-TUB1::LEU2	this work
YVS2220	<i>MATa</i> alpha <i>ade2-101ochre</i> <i>trp1-Δ63</i> <i>leu2-Δ1</i> <i>ura3-52</i> <i>his3-Δ200</i> <i>cyh2R</i> [CF: CEN6 URA3 CYH2S SUP11] Δ stu1::HIS3MX6 <i>lys2-801ambre</i> ::pSTU1-FLAG-stu1 Δ (aa717-aa996)-NLS-GFP::LYS2	this work
YVS2222	<i>MATa</i> alpha <i>ade2-101ochre</i> <i>trp1-Δ63</i> <i>leu2-Δ1</i> <i>ura3-52</i> <i>his3-Δ200</i> <i>cyh2R</i> [CF: CEN6 URA3 CYH2S SUP11] Δ stu1::HIS3MX6 <i>lys2-801ambre</i> ::pSTU1-FLAG-stu1 Δ (aa570-aa716)-NLS-GFP::LYS2	this work
YVS2230	<i>MATa</i> Δ ss1 <i>ade2-101ochre</i> <i>trp1-Δ63</i> <i>leu2-Δ1</i> <i>his3-Δ200</i> <i>lys2-801ambre</i> <i>ura3-52</i> ::CFP-TUB1::URA3 AME1-3mCherry::hphNT1 KANMX6::pGAL1-UbiR-STU1	this work
YVS2231	<i>MATa</i> Δ ss1 <i>ade2-101ochre</i> <i>trp1-Δ63</i> <i>leu2-Δ1</i> <i>his3-Δ200</i> <i>ura3-52</i> ::CFP-TUB1::URA3 AME1-3mCherry::hphNT1 KANMX6::pGAL1-UbiR-STU1 <i>lys2-801ambre</i> ::pSTU1-FLAG-stu1(W339A, R342A, K428A, K429A)-NLS-GFP::LYS2	this work
YVS2232	<i>MATa</i> Δ ss1 <i>ade2-101ochre</i> <i>trp1-Δ63</i> <i>leu2-Δ1</i> <i>his3-Δ200</i> <i>ura3-52</i> ::CFP-TUB1::URA3 AME1-3mCherry::hphNT1 KANMX6::pGAL1-UbiR-STU1 <i>lys2-801ambre</i> ::pSTU1-FLAG-stu1 Δ (aa301-aa569)-NLS-GFP::LYS2	this work
YVS2234	<i>MATa</i> Δ ss1 <i>ade2-101ochre</i> <i>trp1-Δ63</i> <i>leu2-Δ1</i> <i>his3-Δ200</i> <i>ura3-52</i> ::TUBI-CFP::URA3 AME1-3mCherry::hphNT1 KANMX6::pGAL1-UbiR-STU1 <i>lys2-801ambre</i> ::pSTU1-FLAG-(aa261-aa716)-NLS-GFP::LYS2	this work
YVS2294	<i>MATa</i> Δ ss1 <i>ade2-101ochre</i> <i>trp1-Δ63</i> <i>leu2-Δ1</i> <i>lys2-801ambre</i> <i>ura3-52</i> ::CFP-TUB1::URA3 AME1-3mCherry::hphNT1 KANMX6::pGAL1-UbiR-STU1 pSTU1-FLAG-stu1 Δ (aa301-aa569)::Hs_CLASP1-TOGL2(aa284-aa552)-NLS-GFP::LYS2	this work
YVS2295	<i>MATa</i> Δ ss1 <i>ade2-101ochre</i> <i>trp1-Δ63</i> <i>leu2-Δ1</i> <i>lys2-801ambre</i> <i>ade1</i> ::pURA3-TetR-3xCFP::hphNT1 CEN5-tetO2x112::URA3 SPC72-Cherry::natNT2 <i>stu1</i> ::KANMX6-pGAL1-UbiR-STU1 pSTU1-FLAG-stu1 Δ (aa301-aa569)::Hs_CLASP1-TOG2(aa284-aa552)-NLS-GFP::LYS2	this work
YVS2296	<i>MATa</i> Δ ss1 <i>ade2-101ochre</i> <i>trp1-Δ63</i> <i>leu2-Δ1</i> <i>lys2-801ambre</i> <i>ade1</i> ::pURA3-TetR-3xCFP::hphNT1 CEN5-tetO2x112::URA3 SPC72-Cherry::natNT2 <i>stu1</i> ::KANMX6-pGAL1-UbiR-STU1 pSTU1-FLAG-stu1 Δ (aa301-aa569)::STU2-TOG1(aa1-aa318)-NLS-GFP::LYS2	this work
YVS2298	<i>MATa</i> Δ ss1 <i>ade2-101ochre</i> <i>trp1-Δ63</i> <i>leu2-Δ1</i> <i>lys2-801ambre</i> ::pSTU1-FLAG-stu1(S602E)-NLS-GFP::LYS2 <i>ade1</i> ::pURA3-TetR-3xCFP::hphNT1 SPC72-3mcherry::natNT2 CEN5-tetO2x112::URA3	this work
YVS2301	<i>Mata</i> <i>ade2-101ochre</i> <i>leu2-Δ1</i> <i>ura3-52</i> <i>his3-Δ200</i> Δ stu1::HIS3MX6 <i>ade1</i> ::pURA3-TetR-3xCFP::hphNT1 SPC72-3mcherry::natNT2 <i>lys2-801ambre</i> ::pSTU1-Flag-STU1-NLS::LYS2 CEN5-tetO2x112::URA3 <i>trp1-Δ63</i> :12xGFP-Lacl::TRP1 CEN15-lacOx256::LEU2-CEN15	this work
YVS2302	<i>Mata</i> <i>ade2-101ochre</i> <i>leu2-Δ1</i> <i>ura3-52</i> <i>his3-Δ200</i> Δ stu1::HIS3MX6 <i>ade1</i> ::pURA3-TetR-3xCFP::hphNT1 SPC72-3mcherry::natNT2 <i>lys2-801ambre</i> ::pSTU1-Flag-stu1 Δ (aa995-aa1180)-NLS::LYS2 CEN5-tetO2x112::URA3 <i>trp1-Δ63</i> ::12xGFP-Lacl::TRP1 CEN15-lacOx256::LEU2-CEN15	this work
YVS2304	<i>Mata</i> <i>ade2-101ochre</i> <i>trp1-Δ63</i> <i>leu2-Δ1</i> <i>ura3-52</i> <i>his3-Δ200</i> SPC72-3mcherry::hphNT1 <i>lys2-801ambre</i> ::pSTU1-FLAG-stu1 Δ (aa301-aa569)-NLS-GFP::LYS2 pSTU1-FLAG-stu1 Δ (aa1181-aa1513)-ZIPPER-NLS-ECFP::KANMX4	this work
YVS2311	<i>MATa</i> Δ ss1 <i>ade2-101ochre</i> <i>trp1-Δ63</i> <i>leu2-Δ1</i> <i>his3-Δ200</i> <i>lys2-801ambre</i> <i>ura3-52</i> ::CFP-TUB1::URA3 STU1-GFP::HIS3MX6 <i>cdc20</i> ::LEU2-pMET25-CDC20 ASE1-Cherry::hphNT1	this work
YVS2313	<i>MATa</i> Δ ss1 <i>ade2-101ochre</i> <i>trp1-Δ63</i> <i>leu2-Δ1</i> <i>ura3-52</i> <i>his3-Δ200</i> Δ stu1::HIS3MX6 <i>lys2-801ambre</i> ::pSTU1-FLAG-stu1 Δ (aa995-aa1180)-NLS-GFP::LYS2 CDC20::LEU2-pMET25-CDC20 <i>ura3-52</i> ::CFP-TUB1::URA3 ASE1-Cherry::natNT2	this work
YVS2316	<i>MATa</i> Δ ss1 <i>ade2-101ochre</i> <i>trp1-Δ63</i> <i>leu2-Δ1</i> <i>ura3-52</i> <i>his3-Δ200</i> Δ stu1::HIS3MX6 <i>ade1</i> ::pURA3-TetR-3xCFP::hphNT1 SPC72-3mcherry::natNT2 <i>lys2-801ambre</i> ::pSTU1-FLAG-STU1-NLS::LYS2 CEN5-tetO2x112::URA3 ASE1-GFP::KANMX6	this work
YVS2317	<i>MATa</i> Δ ss1 <i>ade2-101ochre</i> <i>trp1-Δ63</i> <i>leu2-Δ1</i> <i>ura3-52</i> <i>his3-Δ200</i> Δ stu1::HIS3MX6 <i>ade1</i> ::pURA3-TetR-3xCFP::hphNT1 SPC72-3mcherry::natNT2 <i>lys2-801ambre</i> ::pSTU1-FLAG-stu1 Δ (aa995-aa1180)-NLS::LYS2 CEN5-tetO2x112::URA3 ASE1-GFP::KANMX6	this work

Saccharomyces cerevisiae strains continued

Strain	Genotype	Reference
YVS2334	<i>MATa Δsst1 ade2-101ochre trp1-Δ63 leu2-Δ1 lys2-801ambre ura3-52::CFP-TUB1::URA3 AME1-3mCherry::hphNT1 KANMX6::pGAL1-Ubi-R-STU1 pSTU1-FLAG-stu1Δ(aa301-aa569)::STU2-TOG1(aa1-aa318)-NLS-GFP::LYS2</i>	this work
YVS2336	<i>MATa Δsst1 ade2-101ochre trp1-Δ63 leu2-Δ1 ura3-52 his3-Δ200 lys2-801ambre STU1-CFP::KANMX6 SPC72-3mCherry::hphNT1 ade2-101ochre::TetR-GFP::ADE2 CEN5-tetO2x112::URA3 Δase1::HIS3MX6</i>	this work
YVS2338	<i>MATa Δsst1 ade2-101ochre trp1-Δ63 leu2-Δ1 ura3-52 his3-Δ200 lys2-801ambre stu1Δ(995-1180)-CFP::KANMX6 SPC72-3mCherry::hphNT1 ade2-101ochre::TetR-GFP::ADE2 CEN5-tetO2x112::URA3 Δase1::HIS3MX6</i>	this work

Strain Legend - figures

Figure	Strains
Tab. 4-1	YVS1408, YVS1772, YVS1814, YVS2001, YVS1987, YVS1651, YBK2137, YBK2139, YCF2177, YSK633, YVS2201, YVS2220, YVS2222
Fig. 4-2	YVS1718, YJO1164, YVS1971, YVS1972, YVS1919, YCF1778
Fig. 4-3	YVS1408, YVS2230, YVS2232, YVS2001, YV1987, YVS1651, YVS2046, YVS2231, YVS2234, YCF2170, YVS2104, YVS2209, YVS2210, YVS1772, YVS1814
Fig. 4-4	YVS2311, YVS2313
Fig. 4-5	YVS1408, YVS2001, YV1987, YVS1651, YVS2046, YVS2304
Fig. 4-6	YVS1408, YVS2232, YVS2231, YVS2001, YV1987, YVS1651, YVS2046, YVS2028, YVS2029, YVS2152, YVS2154
Fig. 4-7	YVS2085, YVS2078, YJO1334, YVS2087, YVS2086, YVS2028, YVS2153, YVS2029, YVS2154
Fig. 4-8	YVS2085, YVS2078, YVS2087, YVS2086
Fig. 4-9	YVS2001, YVS2231, YVS2234
Fig. 4-10	YCF2170, YVS2104, YVS2028, YVS2153, YVS2029, YBK2242, YBK2241
Fig. 4-11	YCF2170, YVS2104, YBK2242, YBK2241
Fig. 4-12	YVS2028, YVS2029, YVS2336, YVS2338
Fig. 4-13	YVS2028, YVS2029, YVS2336, YVS2338, YVS2152, YVS2316, YVS2317
Fig. 4-14	YVS2301, YVS2302, YVS2211, YVS2212
Fig. 4-15	YVS2334, YVS2294, YVS2295, YVS2296
Fig. 4-16	YMS231, YMS299
Fig. 4-17	YVS1580, YVS1582, YJO1164, YJO1392, YVS1459
Fig. 4-20	pCF1377, pVS1437, pET28-lp1-Sli15, pBL902
Fig. 4-22	YVS1408, YVS1536
Fig. 4-23	YVS1408, YVS1628, YVS1627, YVS1648, YVS1649, YVS1743, YVS1662
Fig. 4-24	YVS1408, YVS1596, YVS1597, YVS2028, YVS2113, YVS2114
Fig. 4-25	YVS1408, YVS1611, YVS1613, YVS1565, YVS1562, YVS1634, YVS1615, YVS1757, YVS1553, YVS1554, YVS2028, YVS2111, YVS2206, YVS2298
Fig. 4-26	YVS1408, YVS1462, YVS1564, YVS1614, YVS1626, YVS1933, YVS2028, YVS2161, YVS2160, YVS2199, YVS2159, YVS2162
Fig. 4-27	YVS1408, YVS1768, YVS2028, YVS2156

2.2 Plasmids

Plasmid	Description	Purpose
pASF125	<i>pTUB1-GFP-TUB1::URA3</i>	URA3 integration
pBK1487	<i>pSTU1-FLAG- stu1(aa261- 762)-NLS-GFP in YDpK</i>	LYS2 integration
pBK1503	<i>Δcin8::NatNT2 in pUC18</i>	deletion of CIN8
pBK1506	<i>pSTU1-FLAG-stu1Δ(aa301-aa569)::STU2-TOG1(aa1-aa318)-NLS-GFP in YDpK</i>	LYS2 integration
pBK1508	<i>pSTU1-FLAG-stu1Δ(aa301-aa569)::Hs_CLASP1-TOGL2(aa284-aa552)-NLS-GFP in YDpK</i>	LYS2 integration
pBL902	<i>pT7-10xHIS-Mps1- in pET16b</i>	expression
pBL929	<i>KANMX6::pGAL1-UbiR</i>	template for N-terminal pGAL1-UbiR tagging
pBSII/SK	ori, lacZ, bla	subcloning of PCR fragments
pCF1137	<i>pSTU1-STU1-Term</i>	CEN plasmid
pCF1377	<i>pT7-6xHIS-SUMO1-stu1(aa716-aa1513)-EGFP</i>	expression

Plasmids continued

Plasmid	Description	Purpose
pCF1421	<i>pGAL1-FLAG-Stu1(aa261-aa569)-NLS-GFP</i> in YDpK	<i>LYS2</i> integration
pCJ092	<i>TetR-GFP::ADE2</i>	<i>ADE2</i> integration
pCM79-2	<i>pFA6a-3mCherry::hphNT1</i>	fluorescent tagging
pCM80-1	<i>pFA6a-3mcherry::natNT2</i>	fluorescent tagging
pDB075	<i>ADE1::pURA3-TetR-3xCFP::HPH1</i>	<i>ADE1</i> integration
pET28-lpl1-Sli15	<i>pT7-IPL1-6xHIS-SLI15-6xHIS</i>	expression
pHM105-6	<i>EQFP::hphNT1</i>	fluorescent tagging
pJO719	<i>kiTRP1::pGAL1-UbiR</i>	template for <i>N</i> -terminal <i>pGAL1-UbiR</i> tagging
pMK1168	<i>KANMX4::pMET25-CDC20</i>	integration <i>N</i> -terminal tagging <i>CDC20</i>
pMK1169	<i>HIS3MX6::pMET25-CDC20</i>	expression of P1 phage <i>Cre</i> protein (recombinase) for marker recycling
pSH47	<i>pGAL1-P1CRE</i>	<i>TRP1</i> integration
pSM1026	<i>pTUB1-GFP-TUB1::TRP1</i>	template for loxP- <i>KANMX4-loxP</i> cassette
pUG6	ori, loxP- <i>KANMX4-loxP</i>	<i>KANMX4-loxP</i> cassette
pVS1181	<i>pSTU1-stu1(S497A)-EGFP::kiTRP1</i> in pBSII/SK	endogenous integration
pVS1182	<i>pSTU1-stu1(S1001A)-EGFP::kiTRP1</i> in pBSII/SK	endogenous integration
pVS1233	<i>pSTU1-stu1(S497A, S602A, S690A, S745A, S1001A, S1018A, T1034A, T1047A, S1060A, S1113A, T1134A, S1167A)-EGFP::kiTRP1</i> in pBSII/SK	endogenous integration
pVS1241	<i>pSTU1-stu1(S602A)-EGFP::kiTRP1</i> in pBSII/SK	endogenous integration
pVS1242	<i>pSTU1-stu1(E1043V, T1047A)-EGFP::kiTRP1</i> in pBSII/SK	endogenous integration
pVS1243	<i>pSTU1-stu1(T1134A)-EGFP::kiTRP1</i> in pBSII/SK	endogenous integration
pVS1246	<i>pSTU1-stu1(S1113A)-EGFP::kiTRP1</i> in pBSII/SK	endogenous integration
pVS1248	<i>pSTU1-stu1(S602E)-EGFP::kiTRP1</i> in pBSII/SK	endogenous integration
pVS1275	<i>pSTU1-stu1(S1113E)-EGFP::kiTRP1</i> in pBSII/SK	endogenous integration
pVS1285	<i>pSTU1-stu1(T1047A, S1113A, T1134A)-EGFP::kiTRP1</i> in pBSII/SK	endogenous integration
pVS1286	<i>loxP-LYS2-loxP</i>	template for loxP- <i>LYS2-loxP</i> cassette
pVS1286	<i>pSTU1-stu1(S497E)-EGFP::kiTRP1</i> in pBSII/SK	endogenous integration
pVS1287	<i>pSTU1-stu1(S745A)-EGFP::kiTRP1</i> in pBSII/SK	endogenous integration
pVS1288	<i>pSTU1-stu1(S745E)-EGFP::kiTRP1</i> in pBSII/SK	endogenous integration
pVS1292	<i>pSTU1-stu1(S497E, T1047A, S1113A, T1134A)-EGFP::kiTRP1</i> in pBSII/SK	endogenous integration
pVS1295	<i>pSTU1-stu1(S497A, T1047E, S1113E, T1134E)-EGFP::kiTRP1</i> in pBSII/SK	endogenous integration
pVS1296	<i>pSTU1-stu1(T1047E, S1113E, T1134E)-EGFP::kiTRP1</i> in pBSII/SK	endogenous integration
pVS1303	<i>pSTU1-stu1(S497E, S745A, T1047A, S1113A, T1134A)-EGFP::kiTRP1</i> in pBSII/SK	endogenous integration
pVS1304	<i>pSTU1-stu1(S497A, S745E, T1047E, S1113E, T1134E)-EGFP::kiTRP1</i> in pBSII/SK	endogenous integration
pVS1309	<i>pSTU1-stu1Δ(aa995-aa1180)-EGFP::kiTRP1</i> in pBSII/SK	endogenous integration
pVS1310	<i>pSTU1-stu1(S265E, S276E, T277E, S497A, S745E, T1047E, S1113E, T1134E)-EGFP::kiTRP1</i> in pBSII/SK	endogenous integration
pVS1312	<i>pSTU1-stu1(S265A, S276A, T277A, S497E, S745A, T1047A, S1113A, T1134A)-EGFP::kiTRP1</i> in pBSII/SK	endogenous integration
pVS1322	<i>pGAL1-FLAG-stu1(K428A, K429A)-NLS-GFP</i> in YDpK	<i>LYS2</i> integration
pVS1325	<i>pGAL1-FLAG-STU1-GFP</i> in YDpK	<i>LYS2</i> integration
pVS1328	<i>pSTU1-stu1Δ(416aa-716aa, aa995-aa1180)-EGFP::kiTRP1</i> in pBSII/SK	endogenous integration
pVS1338	<i>pTUB1-GFP-TUB1::LEU2</i>	<i>LEU2</i> integration
pVS1345	<i>pSTU1-STU1-CFP::KANMX6</i> in pBSII/SK	endogenous integration
pVS1346	<i>pSTU1-stu1Δ(aa995-aa1180)-CFP::KANMX6</i> in pBSII/SK	endogenous integration
pVS1359	<i>pSTU1-stu1(S997A, S1000A, S1001A, S1003A, T1005A, S1018A, T1034A, T1047A, S1060A, S1113A, T1134A, S1167A)-EGFP::kiTRP1</i> in pBSII/SK	endogenous integration
pVS1362	<i>pSTU1-stu1Δ(aa301-aa569)-EGFP::kiTRP1</i> in pBSII/SK	endogenous integration
pVS1369	<i>pSTU1-stu1(W339A, R342A, K428A, K429A)-GFP::kiTRP1</i> in pBSII/SK	endogenous integration
pVS1391	<i>pSTU1-stu1(S602A)-CFP::KANMX6</i> in pBSII/SK	endogenous integration
pVS1400	<i>pSTU1-stu1Δ(aa717-aa994)-EGFP::kiTRP1</i> in pBSII/SK	endogenous integration
pVS1410	<i>pGAL1-FLAG-stu1Δ(aa301-aa560)-NLS-GFP</i> in YDpK	<i>LYS2</i> integration

Oligonucleotides continued

Name	Sequence (5'-3')	Description
STU1-fUbiR-26	GACAGGCATATTTAGCGGTAATTATTAGGGTTTTGGAGAGACCTTGATTCTTC Agcgcggaataacgactcac	N-terminal tagging
STU1-rUbiR-27	TCGTCTGGATGTGTATTAGTGTGCTGTTATTATTGGTCTCATTGTTGAAGGACG Aggatccgtgcctaccacct	N-terminal tagging
STU1-28	ACTAAAAGAAAAGTTgcTGCCCCCTCTTCgTCgACTGCCGCCA	S690A ; Sal1 fw
STU1-29	TGGCGGCAGTcGAcGAAGGAGGGGCAgcAACTTTTCTTTTAGT	S690A ; Sal1 rev
STU1-30	GGGGATGAGGAAGCCGACGATGCTGTcGACGAAAATGATG	S1018A ; Sal1 fw
STU1-31	CATCATTTTCGTcGACAGCATCGTGGcTTCCTCATCCCC	S1018A ; Sal1 rev
STU1-32	GTTGAAAAAGAACAagcgtACAGACAGCGTAGTT	S1060A ; Afe1 fw
STU1-33	AACTACGCTGTCTGTAgcgtTGTCTTTTCCAAC	S1060A ; Afe1 rev
STU1-36	CAATTCAAATACAACggCGCCAACCTCAAAG	S497A ; Nar1 fw
STU1-37	CTTTGAGGTTGGCGccGTTGATTTGAATTG	S497A ; Nar1 rev
STU1-38	GTTTCGATGTCAagcgCTCCAATCTCATAAAAAG	S745A ; Afe1 fw
STU1-39	CTTTAATGAGATTGGAGcgtTGACATCGAAAAC	S745A ; Afe1 rev
STU1-40	CTAGAGAAAAGcgCTGTAAGCTTCACTCC	S1001A ; Afe1 fw
STU1-41	GGAGTGAAGCTTACAGcgCTTCTCTAG	S1001A ; Afe1 rev
STU1-48	CTGATTTGAATTTAgcTGAgATTTTCAAACAGTGG	S1113A ; -XmnI fw
STU1-49	CCACTGTTTTGAAAAATcTCAgcTAAATTCAAATCAG	S1113A ; -XmnI rev
STU1-44	GAGAAAACCGTAACACCGAG	analytical PCR
STU1-45	GCTAGCTGATTTTGACATTG	analytical PCR
STU1-46	CTGATTTGGAAACcATGgCACCAATCAAATAAACG	S1167A ; NcoI fw
STU1-47	CGTTTATTTTGATTGGTgCAtgGTTTCAAATCAG	S1167A ; NcoI rev
STU1-50	GCATGGAAATGgCcATGATTAATCCCTTCAAAC	T1034A ; MscI fw
STU1-51	GTTTTGAAGGGATTAATCATgGcCATTTCATGC	T1034A ; MscI rev
STU1-52	GACGATAATGAACCggCcGTAATAATCAGTACAGATC	T1134A ; Eco52I fw
STU1-53	GATCTGACTGAATTTTAcgGccGGTTCATTATCGTC	T1134A ; Eco52I rev
STU1-55	CTTGAAACTGATAAAgCACTAGAGcTcAAGAATAACG	T1047A ; SacI fw
STU1-56	CGTTATTCTTgAgCTCTAGTgctTTTATCAGTTTCCAAG	T1047A ; SacI rev
STU1-57	CTTcTAGAAAACCgctTTTACTGGAGCAGAAAAGG	S602A ; XbaI fw
STU1-58	CCTTTCTGCTCCAGTAAAgcGGTcTTTcTaGAAG	S602A ; XbaI rev
STU1-59	CTTCAAGAAAACCgagcTcCTGGAGCAGAAAAGGAAC	S602E ; SacI fw
STU1-60	GTTCTTTTCTGCTCCAGgAgctcGGTTTTTCTTGAAG	S602E ; SacI rev
STU1-61	CTTGAAACTGATAAAgagCTAGAGcTcAAGAATAACG	T1047E ; SacI fw
STU1-62	CGTTATTCTTgAgCTCTAGcctTTTATCAGTTTCCAAG	T1047E ; SacI rev
STU1-63	CTGATTTGAATTTAgagGAgATTTTCAAACAGTGG	S1113E ; -XmnI fw
STU1-64	CCACTGTTTTGAAAAATcTcctTAAATTCAAATCAG	S1113E ; -XmnI rev
STU1-65	GAAGGACGATAATGACCCgagGTAATAATCAGTACAGATC	T1134E ; Aval fw
STU1-66	GATCTGACTGAATTTTAcctcgGGGTCATTATCGTCCTTC	T1134E ; Aval rev
STU1-67	CACAGGACCAGCATGGTgCACAGAAGATAAAgCGACCTTGTGACGAAGAGT ACG	S276A ; ApaLI fw
STU1-68	CGTACTCTTCGTCAAACAAGGTCGcTTTATCTTCTTGTGcACCATGCTGGTCTGT G	S276A ; ApaLI rev
STU1-71	CTTTAAGGTAGAAGACATCATTgCTAGAGAAgcTgCTGTAgcCTTCgCTCCATCGA CAATAAA	S997A, S1000A, S1001A, S1003A, T1005A ; -XbaI, -HindIII fw
STU1-72	TTTATTGTCGATGGGAGcGAAGgcTACAGcAgcTTCTCTAGcAATGATGTCTTCTAC CTTAAAG	S997A, S1000A, S1001A, S1003A, T1005A ; -XbaI, -HindIII rev
STU1-73	GAACAagtgcTACAGACgcCGTAGTTATTCATGATG	S1060A, S1063A ; -AfeI fw
STU1-74	CATCATGAATAACTACGgcGTCTGTAgcactTGTTTC	S1060A, S1063A ; -AfeI rev
STU1-75	ACTAAAAGAAAAGTTgagGCcCTCCTTCTTCTACTGCCGCCA	S690E ; Ehel fw
STU1-76	TGGCGGCAGTAGAAGAAGGAGGcGCctcAACTTTTCTTTTAGT	S690E ; Ehel rev
STU1-77	CAATTCAAATACAACtgaGCCAACCTCAAAG	S497E ; BpII fw
STU1-78	CTTTGAGGTTGGCtcAGTTGATTTGAATTG	S497E ; BpII rev

Oligonucleotides continued

Name	Sequence (5'-3')	Description
STU1-81	GTTTCGATGTCATCTgagCCAATCTCATTAAAAG	S745E; BpII fw
STU1-82	CTTTTAATGAGATTGGctcAGATGACATCGAAAC	S745E; BpII rev
STU1-83	GAAC TTGTTATCATCTACCgcGgcAAATCTCTTCACAAACTGC	K428A, K429A; SacII fw
STU1-84	GCAGTTTGTGAAGAGATTgcCgcGGTAGATGATAACAAGTTC	K428A, K429A; SacII rev
STU1-86	AATTCATAAGcTTAGCAAAGgCACAGGACCAGCATTGGTTCAC	S265A; HindIII fw
STU1-87	GTGAACCATGCTGGTCCTGTGcCTTTGCTAAgCTTATGAATT	S265A; HindIII rev
STU1-88	GCAAAAATTCATAAGcTTAGCAAAGgagCAGGACCAGCATGGTTCACAAGAAG	S265E; HindIII fw
STU1-89	CTTCTGTGAACCATGCTGGTCCTGctcCTTTGCTAAgCTTATGAATTTTGC	S265E; HindIII rev
STU1-90	CCAGCATGGaTcCAAGAAGATAAAgcgCCTTGTGACGAAGAGTACGAG	S276A, T277A; BamHI fw
STU1-91	CTCGTACTCTTCGTCAAACAAGGccgcTTTATCTTCTTGgGAtCCATGCTGG	S276A, T277A; BamHI rev
STU1-92	CAGGACCAGCATGGTTCACAAGAAGATAAAgaggagTcTTTGACGAAGAGTACGA GTTTC	S276E, T277E; SacI fw
STU1-93	GAAACTCGTACTCTTCGTCAAAGAgctcctcTTTATCTTCTTGGAACCATGCTGGTC CTG	S276E, T277E; SacI rev
STU1-94	ACTGTGATCCTTTGgtctctaccttaaagttggcatc	ΔCL(aa995 - 1180)
STU1-95	CTTTAAGGTAGAAGACcaaaggatcacagtaagagag	ΔCL (aa995 - 1180)
STU1-100	ATCAAAGGTGGAAACGGCCATGG	analytical PCR
STU1-102	CCTGGAAACTTGATAGTTgttgttgataactcggc	ΔTOGL2 (aa 300-569)
STU1-103	GCAGTTATCAAACAACaactatcaagttccagggtgctc	ΔTOGL2 (aa 300-569)
STU1-108	CAGAACAAAATgcGAAGCTgcGCAATCAAATATAATTG	W339A, R342A; HindIII fw
STU1-109	CAATTATATTTGATTGCgcaAGCTTCgcATTTTGTCTCG	W339A, R342A; HindIII rev
STU1-115	CTTTCTCTAGAAATGATgattgggttgacgaaagtc	ΔD3 (aa717-994)
STU1-116	TTCCGTCAAACCAAATCcatcttagagaaagtc	ΔD3 (aa717-994)
STU1-NotI-118	GCATCATTGCGGCCGcGTAAAGGGTTTCATATTCAC	NotI, in YDpK
STU1-NotI-119	TTGTATTGCGGCCGCaATGTCGTCTTCAACAATGA	NotI, in YDpK
STU1-128	GATAACTCATCAGTCAAGTctatattcaaatgagcagggtgctc	ΔML (aa570-716)
STU1-129	GCAATCCCTGCTCATTTGAATATAgacttgactgatgattatc	ΔML (aa570-716)
STU1-130	ATGTCGTCCTTCAACAATGAGACC	analytical PCR

2.4 Antibodies

Name	Description	Company/ Reference
αFLAG	mouse, 1:10.000, M2	Sigma
αmyc	mouse, 1:10.000, 9E10	Convence
αStu1	rabbit, 1:2.000 mix of N-terminal and C-terminal antibody1:1	Ortiz, J. et al. (2009)
αmouse ^{HRP}	sheep, 1:10.000, HRP conjugate	Sigma
αmouse ^{AP}	goat, 1:15.000, AP conjugate	Sigma
αmouse ^{Alexa680}	goat, 1:10.000, Alexa 680 conjugate	Invitrogen
αrabbit ^{HRP}	goat, 1:10.000, HRP conjugate	Sigma
αrabbit ^{AP}	goat, 1:15.000, AP conjugate	Sigma
αrabbit ^{Alexa680}	goat, 1:10.000, Alexa 680 conjugate	Invitrogen

2.5 Equipment

Equipment	Company
Power supply PowerPac basic, Protein electrophoresis equipment Mini PROTEAN, Semi-Dry blotting apparatus	BioRad
Table centrifuges (5417C, 5417 R, 5424), Thermo mixer	Eppendorf
Pulverisette6	Fritsch
Platform shaker Heidolph Polymax 1040, Vortexer Heidolph Reax top	Heidolph
Rotina 46R Centrifuge	Hettich
Power Supply	Hölzel-diagnostics
Shaker Vibrax VXR basic, universal hot plate magnetic stirrer RCT basic	IKA
Incubator Shaker MULTITRON	Infors
XCell SureLock™ Mini-Cell Electrophoresis System	Invitrogen
Circulating bath E100	Lauda
Precision Balance	Mettler-Toledo
Water purification system Milli Q plus	Millipore
Olympus CellR Imaging Station.	Olympus
Microfluidizer	Parker/Watts FluidAir
pH-metre WTW pH 526 MultiCal	Sigma-Aldrich
Sorvall centrifuge	Sorvall
Tube Rotator SB3	Stuart
Thermal cycler	Techne
Spectrophotometer Genesys 10 Bio, Safety bench Heraeus, Savant Speed Vac SPD111v	Thermo
Light-microscope Axiolab	Zeiss

2.6 Chemicals, Enzymes and Disposals

Standard chemicals were purchased from AppliChem (Darmstadt, Germany), Becton Dickinson (Heidelberg, Germany), Fermentas/Thermo Scientific (Darmstadt, Germany), Merck (Darmstadt, Germany), New England Biolabs (Höchst, Germany), Carl Roth (Karlsruhe, Germany), Serva (Heidelberg, Germany) or Sigma-Aldrich (Steinheim, Germany). Suppliers of special reagents are mentioned in the corresponding method section. Disposable lab ware was purchased from Greiner bio-one (Kremsmünster, Austria), Kisker (Steinfurt, Germany) or Sarstedt (Nümbrecht, Germany).

2.7 Service Providers, Web Services and Software

Service providers

DNA sequencing

eurofins mwg/operon (Hamburg, Germany)

Protein mass spectrometry

Protein Mass Spectrometry Facility (BZH, University of Heidelberg) in cooperation with the Core Facility for Mass Spectrometry and Proteomics (ZMBH, University of Heidelberg)

Web services

ExPASy	http://expasy.org/
ClustalW2	http://www.ebi.ac.uk/Tools/msa/clustalw2/
Google Scholar	http://scholar.google.de/
NCBI	http://www.ncbi.nlm.nih.gov/
<i>Saccharomyces</i> genome database	http://www.yeastgenome.org/

Software

DNA/ protein sequence analysis	BioEdit, MegAlign, SeqBuilder
Illustrations	Adobe Illustrator, Adobe Photoshop
Microscope image processing	Fiji, Olympus xcellence software
Primer Database	Amplify
Reference Manager	Mendeley (Mendeley Ltd.)
Strain Database	FileMaker Pro

3 METHODS

3.1 Cultivation conditions for Microorganisms

3.1.1 *Escherichia coli*

E. coli cultures were grown in 2TY or LB liquid media or on LB plates [18 g/l agar] at 37 °C overnight. The culture medium was supplemented with 100 µg/ml ampicillin to keep selective pressure on the plasmid. For protein expression in *E. coli*, media was supplemented with 30 µg/ml Kanamycin and/or 34 µg/ml Chloramphenicol. Glycerol stocks were prepared by the addition of glycerol to 800 µl of an overnight culture to a final concentration of 15 % (v/v), frozen in liquid nitrogen and stored at -80 °C. Optical density (OD) was measured using a photometer at a wavelength of 600 nm.

2TY medium	LB medium
10 g/l yeast extract	5 g/l yeast extract
16 g/l tryptone	10 g/l tryptone
5 g/l NaCl	10 mM NaCl
pH 7.0	2.5 mM KCl
	10 mM MgCl ₂ /MgSO ₄ pH 7.0
SOC medium	
5 g/l yeast extract	
20 g/l tryptone	
0.5 g/l NaCl	
2.5 mM KCl	
10 mM MgCl ₂	
0.4 % (w/v) glucose	

3.1.2 *Saccharomyces cerevisiae*

3.1.2.1 Regular growth conditions

Raffinose media contained 2 % (w/v) raffinose. Galactose media was supplemented with 2 % (w/v) raffinose and the indicated amount of galactose (indicated by x %). For better cell growth, medium was supplemented with 100 mg/ml adenine and 30 mg/ml uracil (indicated with +2) and additional 50 mg/l tryptophane (indicated with +3).

Media used for microscope experiments was filter sterilized instead of autoclaved. When antibiotics were used for selection, media was supplemented with 0.02 % (w/v) Geneticin (Sigma-Aldrich, Steinheim, Germany), 0.04 % (w/v) Hygromycin (Cayla-In VivoGen, Toulouse, France) and 0.01 % Nourseothricin (Werner Bioagents, Jena, Germany) respectively. Synthetic media was prepared with Kaiser Drop-out supplement (Formedium, Norfolk, UK) and was used in amounts as recommended by the manufacturer (indicated by y) (Kaiser, C. et al., 1994). 5-Fluoroorotic acid (5-FOA) (Apollo Scientific, Tokyo, Japan) was used for *URA3* based counter selection of cells. For plates, media was supplemented with 2 % agar.

Unless not indicated differently yeast cultures were grown overnight in media containing 2 % (w/v) glucose at 25 °C. Strains containing pGAL-*UbiR-STU1* constructs were

routinely grown in 0.8 % galactose to ensure cell survival. Plates were incubated at 25 °C for several days. Optical density of liquid cultures was determined at 578 nm (OD₅₇₈). For long-term storage yeast cells were grown on plates for several days, cells were scraped off the plates and resuspended in glycerol to a final concentration of 15 % (v/v), frozen in liquid nitrogen and stored at -80 °C.

Yeast rich media

YPD/R+2 (+3)	YPRG (x %)+2 (+3)
10 g/l yeast extract	10 g/l yeast extract
20 g/l peptone	20 g/l peptone
2 % (w/v) glucose/ raffinose	2 % (w/v) raffinose
100 mg/l adenine	x % (w/v) galactose
30 mg/l uracil	100 mg/l adenine
(50 mg/l tryptophane)	30 mg/l uracil
	(50 mg/l tryptophane)

Yeast synthetic media

SCD/R	SCRG (x %)
6.75 g/l yeast nitrogen base wo aa	6.75 g/l yeast nitrogen base wo aa
y g/l SC -(his/leu/lys/trp/ura/met)	y g/l SC -(his/leu/lys/trp/ura/met)
2 % (w/v) glucose	2 % (w/v) raffinose
100 mg/l adenine	x % (w/v) galactose
	100 mg/l adenine

SCD +FOA	SCRG (x %) +FOA
6.75 g/l yeast nitrogen base wo aa	6.75 g/l yeast nitrogen base wo aa
0.79 g/l SC complete	0.79 g/l SC complete
2 % (w/v) glucose	2 % (w/v) raffinose
1 g/l 5-FOA	x % (w/v) galactose
	1 g/l 5-FOA

3.1.2.2 Growth conditions for SILAC approaches

SILAC (stable isotope labeling by amino acids in cell culture) was used to compare two *S. cerevisiae* cultures arrested in two different cell cycle stages.

To be able to distinguish the proteins purified simultaneously from the two different cultures, amino acids with substituted stable isotopic nuclei were supplemented to the media to be incorporated into the proteins. Thus one of the cultures contained a 'light' and the other one a 'heavy' form of a particular amino acid (¹³C and ¹⁵N labeled lysine and arginine). To avoid that the strains used are capable to produce their own lysine or arginine, strains contained an early amber stop codon in lysine and were knocked out for arginine.

Cells used for SILAC approaches were grown in the synthetic medium containing the 'heavy' or 'light' form of amino acids for a minimum of ten cell divisions to ensure efficient incorporation of these amino acids in the newly synthesized proteins prior to harvesting. Stock solutions of supplemented amino acids were filter sterilized instead of autoclaved. For the SILAC approaches performed within the thesis the α -factor arrested cells were grown in synthetic media containing the 'heavy' form of amino acids whereas the comparative culture was grown in media containing the 'light' form of ami-

no acids. To be able to arrest cells in nocodazole, these cells exceptionally were cultivated in YPD+2 media.

Synthetic media with 'heavy' or 'light' amino acids

SDC 'heavy'/'light'

6.75 g/l	yeast nitrogen base wo aa
0.68 g/l	SC - arg, - lys, - ade
2 % (w/v)	glucose
50 mg/l	adenine
20 mg/l	arginine ('heavy' or 'light')
20 mg/l	lysine ('heavy' or 'light')

3.2 Molecular Biology

3.2.1 Polymerase chain reaction (PCR)

PCRs were routinely performed adjusting the annealing temperature (X) and the extension time according to the T_m of the oligonucleotides, the used polymerase and the length of the expected PCR product.

3.2.1.1 Preparative amplification of DNA fragments for cloning

DNA fragments required for cloning procedures were amplified using Phusion High Fidelity DNA Polymerase (Fermentas, Darmstadt, Germany) with the supplied buffers.

50 μ l reaction contained	program
10-50 ng plasmid DNA or genomic DNA	98 °C 3 min
1x Phusion Buffer	98 °C 30 s
200 μ M of each dNTP	X °C 45 s 25-30 cycles
1 μ M of each oligonucleotide	72 °C 30 s/kb
0.5 U Phusion DNA Polymerase	72 °C 10 min
ad 50 μ l mpH ₂ O	10 °C pause

3.2.1.2 Preparative amplification of DNA fragments by overlap extension mutagenesis

To carry out site-specific mutagenesis or deletion of DNA fragments, overlap extension mutagenesis was performed as described in (Ho, S. N. et al., 1989). Phusion High Fidelity DNA Polymerase was used as in 3.2.1.1. Products of the first amplification reactions were used as templates and oligonucleotides for the second round of amplification. No additional oligonucleotides were added for the second round. A scheme of how single amino acid substitutions were generated is shown in Fig. 3-1.

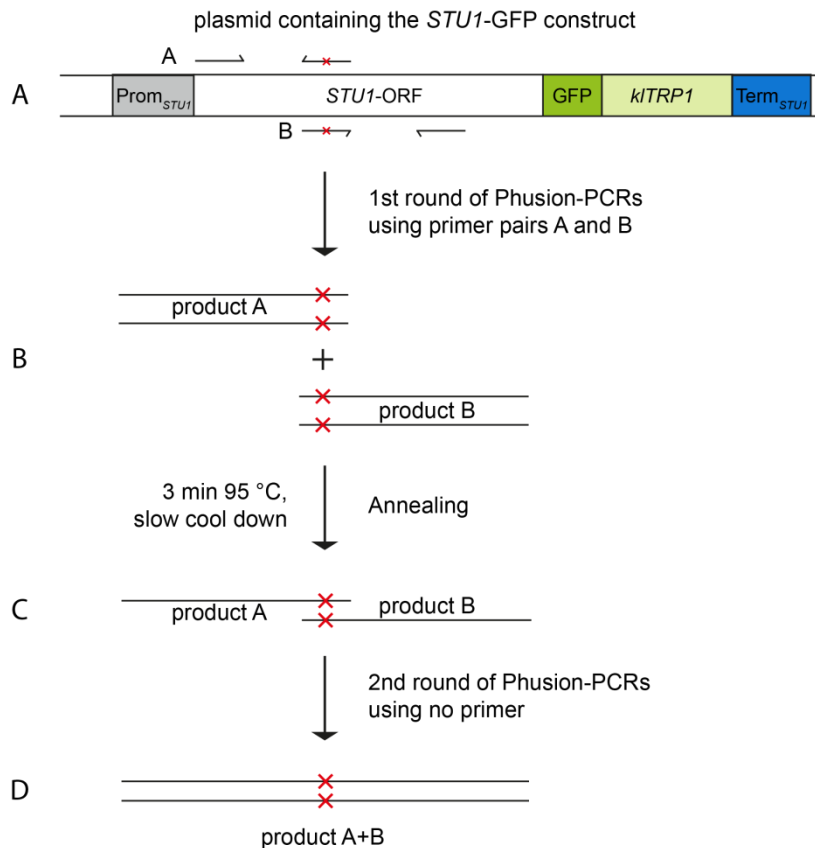


Figure 3-1. Scheme of site-directed mutagenesis.

(A) A plasmid containing the *STU1-GFP::kITRP1* construct was used as a template for the preparative amplification of the DNA fragments. Primer pairs A and B, with the reverse primer of pair A and the forward primer of pair B containing the DNA sequence resulting in the requested amino acid substitution (indicated by the red crosses) were used for the first round of amplification. **(B)** PCR-products A and B were mixed in approximately equimolar amounts, denatured and slowly cooled down to RT to allow the overlapping DNA regions to anneal. **(C)** Annealed products were used for a second round of PCR amplification without addition of further primers. **(D)** This resulted in the full-length PCR product containing the base pair substitutions.

3.2.1.3 Preparative amplification of DNA fragments for PCR-mediated tagging of proteins

DNA fragments transformed into *S. cerevisiae* cells to perform PCR-mediated tagging of proteins were amplified using the Long PCR Enzyme Mix (Fermentas, Darmstadt, Germany) and supplied buffers.

50 μ l reaction contained	program	
0,5-1 μ g plasmid DNA	95 °C 3 min	
1x Long PCR Buffer	95 °C 20 s	
2.75 mM MgCl ₂	54 °C 45 s	10 cycles
500 μ M of each dNTP	68 °C 2 min 30 s	
1 μ M of each primer	95 °C 30 s	
2.5 U Long PCR Enzyme Mix	54 °C 45 s	15 cycles
ad 50 μ l mpH ₂ O	68 °C 2 min 30 s + 20 s/cycle	
	72 °C 10 min	
	10 °C pause	

1 µl of the PCR was checked by agarose gel electrophoresis, the rest of the reaction was ethanol precipitated, the pellet was dried at RT and stored at -20 °C. Before transformation the DNA pellet was resuspended in 10 µl mpH₂O.

3.2.1.4 Analytical amplification of DNA fragments

Analytical amplification of DNA fragments was used to verify correct clones of *E. coli* and *S. cerevisiae*. Colonies of *E. coli* cells were resuspended in 5 µl mpH₂O, incubated at 95 °C for 3 min and used as template DNA. To verify *S. cerevisiae* cells, gDNA was isolated as described in 3.2.15. 0.5 µl of gDNA were used as template. 10x Taq polymerase buffer contained 100 mM Tris-Cl pH 8.3, 500 mM KCl and 15 mM MgCl₂.

25 µl reaction contained		program	
	DNA as indicated above	98 °C	3 min
1x	Taq polymerase buffer	98 °C	30 s
200 µM	of each dNTP	X °C	45 s
0.5 µM	of each oligonucleotide	72 °C	30 s/kb
1 µl	homemade Taq polymerase	72 °C	10 min
ad 50 µl	mpH ₂ O	10 °C	pause

25-30 cycles

3.2.2 Agarose gel electrophoresis

To separate DNA fragments, agarose gel electrophoresis was routinely performed with 1 % agarose (Roth, Karlsruhe, Germany) using TAE-buffer (40 mM Tris acetate, 1 mM EDTA pH 8.0) at a constant voltage of about 120 V. DNA molecular weight size markers (Fermentas, Darmstadt, Germany) were used to determine the size of the DNA fragments.

3.2.3 DNA precipitation

DNA precipitation was carried out by adding mpH₂O to a final volume of 100 µl, supplementing the sample with 10 µl of 10 mM LiCl and 300 µl of EtOH (100 %, 4 °C). After incubation for 30 min until overnight at 4 °C, the DNA pellet was collected by centrifugation (20,000 g, 20 min, 4 °C) and air-dried.

3.2.4 Cloning procedures

DNA manipulations like DNA restriction, phosphatase treatment, kinase treatment or blunting of DNA fragments were carried out using restriction enzymes, calf intestinal phosphatase, T4 polynucleotide kinase, T4 DNA polymerase and Klenow fragment from Fermentas or New England Biolabs (NEB, Frankfurt/Main, Germany), respectively following the manufacturer's instructions.

3.2.5 Purification of DNA fragments

DNA fragments were purified using the GeneJet™ PCR purification Kit or the GeneJET™ Gel Extraction Kit from Fermentas following the manufacturer's instructions.

3.2.6 Determination of DNA contents

The amount of DNA contents was determined by agarose gel electrophoresis in comparison with applied DNA molecular weight size markers.

3.2.7 Ligation of DNA fragments

DNA fragments were ligated using T4 DNA ligase from Fermentas using the provided buffers.

20 μ l reaction contained

50 ng	linear vector DNA
100 ng	insert DNA
2:1 molar ratio over plasmid	
1x	T4 DNA ligase buffer
5 %	PEG 4000
1 U	T4 DNA Ligase
ad 20 μ l	mpH ₂ O

Linear vector DNA, insert DNA and mpH₂O were incubated for 3 min at 42 °C. Subsequently remaining reaction components were added and incubated for 1 h at RT. 5 μ l of the ligation reaction were transformed into chemically competent *E. coli* cells.

3.2.8 Preparation of chemically competent *E. coli* cells

Chemically competent *E. coli* cells were prepared according to Inoue, H. et al. (1990). 60 μ l aliquots contained about 0.54 OD cells. Transformation rates were determined with 0.1 ng pUC18 and ranged between 6.4×10^7 and 1.0×10^8 colonies/ μ g DNA.

3.2.9 Transformation of *E. coli* cells

60 μ l aliquots of chemically competent *E. coli* cells were thawed on ice, free plasmid DNA or 5 μ l ligation reaction was added and tubes were incubated on ice for 30 min. Subsequently cells were heat-shocked for 60 s at 42 °C in a water bath, cooled down on ice for 2 min and supplemented with 440 μ l of SOC media. After incubation for 60 min (37 °C, 180 rpm) cells were transferred on selective plates.

3.2.10 Isolation of plasmid DNA from *E. coli*

Plasmids were isolated using the alkaline extraction procedure adopted from Birnboim, H. C. et al., (1979). *E. coli* cultures of 3-5 ml were grown overnight at 37 °C in 2 TY medium supplemented with antibiotic to select for the corresponding plasmid. Cells were harvested (10 min, 2.770 g) and cell pellets were resuspended in 300 μ l P1 buffer complemented with 0.1 mg /ml RNase A. 300 μ l of P2 buffer were added, tubes were gently mixed and incubated for 4 min at RT. Cell lysis was stopped with 300 μ l P3 buffer, solutions were gently mixed by inversion and incubated on ice for 10 min. Cell debris was pelleted (20 min, 20,000 g) at 4 °C, supernatants were transferred to fresh tubes and DNA was precipitated by the addition of 0.7x volume of 2-propanol. After incubation for 10 min at RT, tubes were centrifuged at RT (20 min, 20,000 g), superna-

tants were discarded and pellets were washed with 70 % (v/v) ethanol. Pellets were air-dried at RT and isolated DNA was dissolved in 30-50 μ l of TE. Plasmid DNA was stored at -20 °C.

P1 buffer	P2 buffer	P3 buffer
50 mM Tris-Cl pH 8.0	0.2 M NaOH	2.6 M potassium acetate pH 5.2
10 mM EDTA	1 % (w/v) SDS	(pH was set with 2.6 M acetic acid)
TE buffer		
10 mM Tris-Cl pH 8.0		
1 mM EDTA		

3.2.11 Transformation of *S. cerevisiae* cells

S. cerevisiae cells were transformed according to Gietz, D. R. et al. (1995). Routinely, 5 OD cells of a logarithmically growing culture were transformed with 0.1-1 μ g of free plasmid DNA, 10 OD cells were transformed with 0.5-5 μ g of linearised vector DNA or one reaction of amplified DNA fragment as described in 3.2.1.3. Per OD cells 10 μ g single stranded DNA were used. Heat-shock was performed at 37 °C for 15 min. Unless cells were transformed with free plasmid DNA, cells were incubated in the according media without selective pressure for 1-3 h at 25 °C for recovery. Subsequently, cells were evenly distributed on plates selective for the integrated DNA and incubated for several days at 25 or 30 °C.

LiSorb	LiPEG
10 mM Tris-Cl pH 8.0	10 mM Tris-Cl pH 8.0
100 mM LiAc	100 mM LiAc
1 mM EDTA	1 mM EDTA
1 M Sorbitol	45 % PEG 4000

3.2.12 Construction of genomically modified *S. cerevisiae* strains

Genomically modified *S. cerevisiae* strains were generated by homologous recombination (Longtine, M. et al., 1998). Linear vector DNA was generated by linearising DNA by restriction digest. DNA fragments for PCR-mediated tagging were generated by PCR according to 3.2.1.3. Oligonucleotides contained ~60 nucleotides identical to the upstream and downstream region of the genomic integration locus.

3.2.13 System for the integration of *Stu1* mutants in the endogenous DNA locus

A shuffle strain constructed as depicted in the scheme below was used to integrate the mutated *STU1* constructs into the endogenous *STU1* DNA locus.

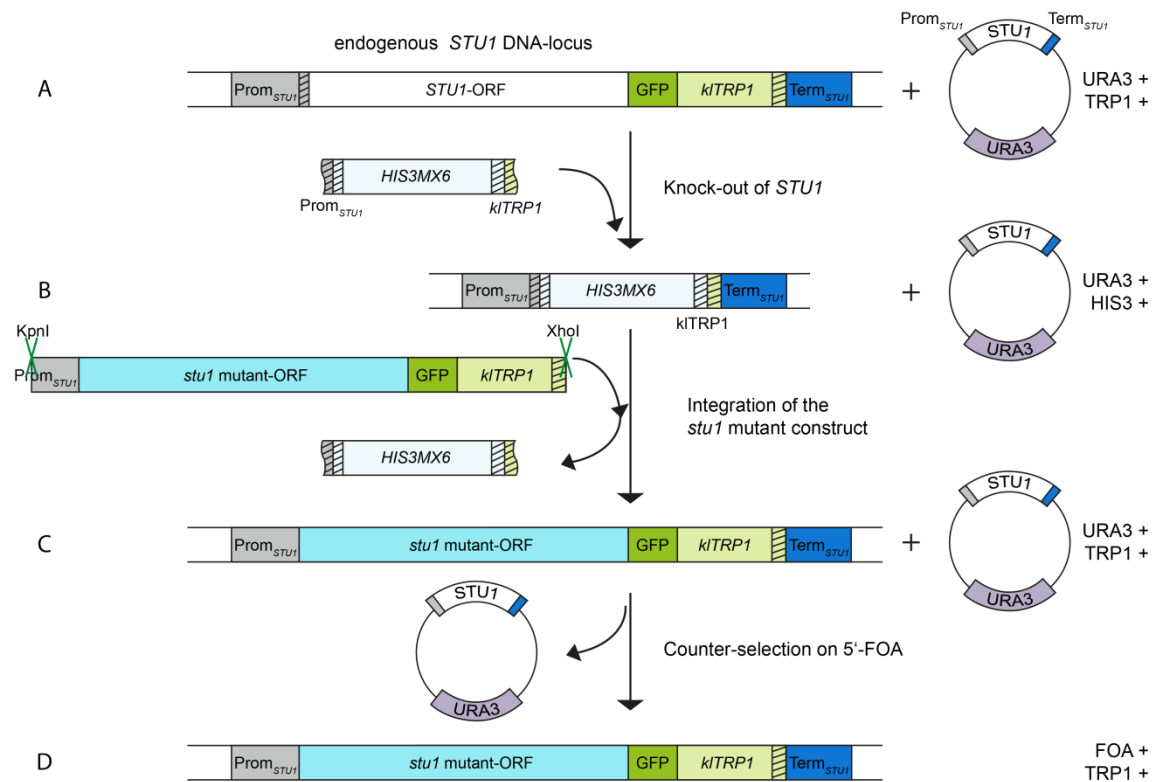


Figure 3-2. Scheme of the integration system for mutated *STU1* constructs in the endogenous *STU1* locus.

(A) The endogenous *STU1*-ORF was substituted with a *HIS3MX6* cassette after integration of a CEN-plasmid containing the *STU1*-ORF and a *URA3* marker. **(B)** The linearised *STU1* mutant construct was integrated by replacing the *HIS3MX6* cassette. **(C)** To test if the integrated *STU1* construct supports viability and to select for cells that lost the CEN plasmid that contains the *STU1*-ORF, cells were counter selected on FOA. **(D)** The mutated *STU1* construct is integrated at the endogenous locus representing the only *STU1* copy in the cell. Striped areas indicate homologous sequences responsible for recombination.

3.2.14 Labeling of CEN DNA

CEN5 was labeled fluorescently with CFP or GFP by using the tetO/tetR system (Michaelis, C. et al., 1997). A multitude of tetracycline operators (tetO) were integrated 1.4 kb upstream of the centromere 5. Tetracycline repressor (tetR) fused to a fluorescent tag was integrated in the locus of the selective marker and both were constitutively expressed. By recruitment of the tetR-CFP/GFP to the tetO, the region very close to the *CEN5* can be visualized by fluorescent microscopy. In a very similar way the lacO/lacR system (Straight, A. F. et al., 1996) was used to visualize the centromere 15. A multitude of lac operators (lacO) were integrated upstream of the centromere 15 and the lac repressor (lacR) was fused to 12xGFP.

3.2.15 Isolation of chromosomal DNA from *S. cerevisiae*

For the isolation of yeast genomic DNA cells were picked from plates or pelleted from liquid cultures and resuspended in 100 μ l of NTES buffer (10 mM TrisCl pH 8.0, 100 mM NaCl, 1 mM EDTA pH 8.0 and 1 % SDS). Glass beads were added and probes were incubated on a shaker for 20 min at 4 $^{\circ}$ C. After cells lysis, 100 μ l of phe-

nol:chloroform:isoamyl alcohol (25:24:1) were added, tubes were vortexed for 30 s and centrifuged at RT (5 min, 20,000g). 50 μ l of the aqueous layer were transferred to a fresh tube and supplemented with 25 μ l of chloroform. Tubes were vortexed and centrifuged again at RT (5 min, 20000g). 10 μ l of the aqueous layer containing the genomic DNA were transferred carefully to a fresh tube. 0.5 μ l of genomic DNA were used to perform analytical amplification of DNA fragments. If genomic DNA was used as a template for preparative amplification of DNA fragments DNA was purified by ethanol precipitation in addition.

3.3 Cell biology

3.3.1 Methods for *S. cerevisiae* cell synchronization

3.3.1.1 G1 arrest

Logarithmically growing cultures were diluted to an OD of 0.5. Cultures were arrested in G1 by the addition of 200 ng/ml alpha factor (α -factor, Applichem) for 2 h if not indicated differently. When cells were grown in media containing galactose incubation time was extended to 2.5 h.

3.3.1.2 G2- /metaphase arrest with unattached kinetochores

To achieve cells arrested in G2-/metaphase with unattached KT, cells were released from α -factor arrest by washing the cell pellet twice with mpH₂O and once with fresh medium (RT, 1 min, 2,100 g). Subsequently, cells were resuspended in fresh medium containing 15 μ g/ml nocodazole (Nz, Applichem) and incubated for 3 h.

3.3.1.3 Metaphase arrest

Cells containing *CDC20* under the control of a *pMET25* promoter were routinely kept in SDC media without methionine (SDC -met) to ensure cell survival. To arrest the cells in metaphase, they were depleted of Cdc20 as follows. Logarithmically growing cells were washed once (RT, 1 min, 2100 g) with YPD+3 +2 mM methionine (Met) and subsequently released into the same medium to achieve an OD of 0.5. Cells were incubated for 2-5 h.

3.3.1.4 Anaphase arrest

A temperature sensitive *cdc15-1* mutant was used to arrest cells in anaphase. A logarithmically growing culture was diluted to an OD of 0.5 and shifted to the non-permissive temperature of 37 °C. Cells were analyzed after 3 h of incubation.

3.3.2 Stu1 shutdown conditions

For the analyses of cells absent of Stu1 or cells containing nonviable Stu1 mutants cells were depleted of WT Stu1. Cells containing the *pGAL-UbiR-STU1* construct were routinely grown in 0.8 % galactose. Incubation at 0.1 % galactose over night reduced levels of *STU1* expression before the experiment. To start the shutdown, logarithmically growing cells were washed twice with YPD+3 (RT, 1 min, 2,100 g) and released into

YPD+3 to achieve an OD of 0.5. Cells were incubated for 3 h before cells were treated for further cell cycle arrests.

3.3.3 Stu1 overexpression

In order to overexpress Stu1 from a galactose inducible promoter, cells were grown in 2 % raffinose prior to the experiment. Expression was then induced by the addition of 2 % galactose and incubation for 8-10 hours.

3.3.4 Chromosomal loss assay

Chromosomal loss assays were performed using cells carrying a chromosomal fragment as described in Shero, J. et al., (1991). To select for the chromosomal fragment, cells were routinely grown in SCD -ura, shifted to YPD+2 for 3 h and diluted to 1×10^3 OD/ml. Cells were plated on YPD plates supplemented with 4 % glucose and incubated at 30 °C for 3-4 days. Colonies that showed red sectors covering at least half of the size of the colony were counted as colonies that had lost the CF. A minimum of 5,000 colonies were counted per strain.

3.3.5 Fluorescent Microscopy

3.3.5.1 Cell preparation for microscopy

Cells used for microscope experiments were grown in medium that was filter-sterilized instead of autoclaved. In preparation for the microscope 1 ml of yeast culture was harvested (1 min, 1,300 g) and cells were washed 2-3 times with mpH₂O before they were resuspended in 8-15 µl non-fluorescent media (NFM) containing glucose and galactose respectively. When treated with nocodazole, cells were kept on ice to avoid formation of microtubules. For Cdc20-depleted cells NFM medium was supplemented with 2 mM methionine.

NFM			NFM Gal		
0.79 g/l	SC complete		0.79 g/l	SC complete	
2 %	glucose		2 %	galactose	
0.9 g/l	KH ₂ PO ₄		0.9 g/l	KH ₂ PO ₄	
0.23 g/l	K ₂ HPO ₄		0.23 g/l	K ₂ HPO ₄	
0.5 g/l	MgSO ₄		0.5 g/l	MgSO ₄	
3.5 g/l	(NH ₄) ₂ SO ₅	pH 5.5	3.5 g/l	(NH ₄) ₂ SO ₅	pH 5.5

3.3.5.2 Live-cell imaging

To perform live-cell imaging, fluorescently labeled proteins were visualized using the Olympus CellR Imaging Station. The microscope was equipped with a piezo, an automated Z-stage, an emission filter wheel and a sensitive ORCA/ER cooled CCD camera. Images were taken using a 100x oil immersion objective. Routinely nine picture stacks with a distance of 0.25-0.30 µl were acquired. Images were taken with a resolution of 15.625 pixels/µm and a bit depth of 16 bit.

3.3.5.3 Analysis of microscope images

Images were processed and analyzed using the image processing program Fiji.

3.3.5.3.1 Processing of microscope images

Routinely images were processed by Z-stack projection and adjustment of color balance. Color channels were adjusted individually with a linear LUT that covered the full range of data. Measurements of spindle length or SPB distances were carried out using the “measure” tool of Fiji.

3.3.5.3.2 Generation of intensity profiles

Intensity profiles created along the spindle axis were generated using the “plot profile” tool. Therefore cells with about the same spindle length were chosen. Data points were obtained every 0.064 μm . Received data was normalized and converted to values between 0 as the minimum and 1 as the maximum. Values of each data point received from the indicated number of cells were averaged and depicted in the graph.

3.3.5.3.3 Generation of box-whisker-plots

Box-whisker-plots were created to depict the distance of SPBs, the inter-KT distance and the kMT lengths shown in Fig 4-10. The boxes cover 50 % of the data (quartile 2 and 3) and the horizontal line represents the median of the whole range of data. Whiskers span the whole range of data (quartile 1 to 4) with a maximum of 1.5x interquartile range. The interquartile range is defined as the calculated difference between the maximum value of the quartile 3 and the minimum value of the quartile 2. Upper and lower maximal outliers are indicated as crosses. P-values were calculated using a two-tailed unpaired t-test.

3.4 Protein Biochemistry

3.4.1 Protein expression and purification from *E. coli* cells

Rosetta BL21 cells containing the particular expression construct were routinely grown on LB medium containing 30 mg/ml Kanamycin and 34 mg/ml Chloramphenicol. The *E. coli* culture was inoculated from fresh plates to an OD of 0.05, grown for about 2 h at 37 °C (180 rpm) to an OD of 0.5-0.6 and cooled down for 5 min on ice. Protein expression was induced with 1 mM IPTG for 3 h at 25 °C (180 rpm). Subsequently cells were harvested by centrifugation (Sorvall SLC 6000, 20 min, 4 °C, 5,000 rpm), washed once with Lysis buffer containing 2 mM PMSF and 2 mM DTT and thoroughly resuspended in 15 ml of Lysis buffer additionally containing all protease inhibitors. Cells were lysed using the micro fluidizer two times. Lysates were clarified by two sequent centrifugation steps (Sorvall SS34, 30 min, 4 °C, 23,500 g). Supernatant was supplemented with 400 μl of 50 % Ni-NTA beads (Qiagen) that were pre-equilibrated in lysis buffer and incubated at 4 °C for 3 h under constant rotation (4 rpm). Beads with bound proteins were washed by gravity flow using a column. Subsequent washing steps with 20 ml of lysis buffer, 20 ml of wash buffer I, 20 ml of wash buffer II and 10 ml of wash buffer III were performed before eluting the purified protein in 5 times 1 ml fractions of elution buffer. All washing and elution buffers contained 2 mM PMSF and 2 mM DTT.

Buffers for purification of 6His-Stu1:

Lysis buffer		buffer was supplemented prior to use with	
25 mM	HEPES pH 8.0	2 mM	DTT
500 mM	KCl	2 mM	PMSF
0.1 %	NP-40	10 µg/ml	Pepstatin A
5 mM	Imidazole	10 µg/ml	Leupeptin
		40 µg/ml	TPCK
		10 µg/ml	Aprotinin
		2 mM	Benzamidin

Wash buffer I pH 8.0		Wash buffer II pH 8.0	
25 mM	HEPES pH 8.0	25 mM	HEPES pH 8.0
500 mM	KCl	500 mM	KCl
0.1 %	NP-40	0.1 %	NP-40
10 mM	Imidazole	40 mM	Imidazole

Wash buffer III pH 8.0		Elution buffer pH 8.0	
25 mM	HEPES pH 8.0	25 mM	HEPES pH 8.0
375 mM	KCl	250 mM	KCl
0.1 %	NP-40	0.1 %	NP-40
60 mM	Imidazole	500 mM	Imidazole
		20 %	glycerol

Purified 6xHis-Stu1 C-terminus was a gift from Caroline Funk.

Buffers for Purification of Ipl1-6xHis-Sli15-6xHis:

Lysis buffer		buffer was supplemented prior to use with	
50 mM	NaPO ₄ pH 8.0	2 mM	DTT
300 mM	NaCl	2 mM	PMSF
		10 µg/ml	Pepstatin A
		10 µg/ml	Leupeptin
		40 µg/ml	TPCK
		10 µg/ml	Aprotinin
		2 mM	Benzamidin

Wash buffer pH 8.0		Elution buffer pH 8.0	
50 mM	NaPO ₄ pH 8.0	50 mM	NaPO ₄ pH 8.0
300 mM	NaCl	300 mM	NaCl
5 %	glycerol	5 %	glycerol
20 mM	Imidazole	250 mM	Imidazole
5 mM	β-mercaptoethanol	5 mM	β-mercaptoethanol

To further purify the Ipl1-6His-Sli15-6His construct, the elution fraction containing the highest amount of protein was centrifuged for 15 min at 20.000 g at 4 °C and the supernatant was separated by gel filtration using a Superose 6 10/300 Column. Fractions of 0.5 ml were collected. Fractions containing the highest amounts of Stu1 (14-16) were combined and concentrated by the factor of ten by centrifugation (12 min, 4,000 rpm) using a VIVASPIN2 (Sartorius) column. Sli15, but not Ipl1 could be detected by Western blot, as the result of a stop codon at the end of Ipl1 (verified by sequencing), but was active as determined by the phosphorylation of Sli15.

Buffers for Purification of His-Mps1:

Lysis buffer	buffer was supplemented prior to use with
50 mM HEPES pH 8.0	protease inhibitors
200 mM NaCl	
5 mM Imidazole	
Wash buffer pH 8.0	Elution buffer pH 8.0
50 mM HEPES pH 8.0	50 mM HEPES pH 8.0
200 mM NaCl	200 mM NaCl
20 mM Imidazole	400 mM Imidazole
	10 % glycerol

Purified 6His-Mps1 was a gift from Manuel Stach. The protein was expressed using 0.8 mM IPTG for 4 h at 23 °C. For purification, cobalt beads were used. To remove imidazole, the buffer was exchanged for 50 mM HEPES pH 8.0, 200 mM NaCl and 10 % glycerol using a PD10 desalting column (GE Healthcare).

3.4.2 Protein extraction from *S. cerevisiae* cells

Cells were grown overnight and treated according to the experimental setup. Routinely 10-20 ml of the culture were harvested (4°C, 3 min, 2100 g), washed once with 500 µl of ESB buffer (80 mM Tris-Cl pH 6.8, 2 % SDS, 10 % glycerol, freshly supplemented with 1 mM PMSF and 6.5 mM DTT) and resuspended in 50-100 µl ESB buffer. After incubation for 3 min at 95 °C cells were put on ice for 2 min and frozen in liquid nitrogen. For cell lysis probes were thawed on ice, supplemented with glass beads ($\phi = 0.4-0.6$ nm, Sartorius) and vigorously mixed on a Vibrax shaker at 4 °C for 30-40 min. Cells lysis was microscopically verified. The lysate was collected through the punctured bottom into a fresh tube by centrifugation at 4 °C (20 s, 500 g). Tubes were centrifuged at 4 °C for 30 min (20000 g) to clarify the lysate. Supernatants were transferred into fresh tubes.

3.4.3 Determination of protein concentrations via Bradford assay

Protein concentrations were determined photometrically. 1 µl of the sample (whole cell extract) was added to 100 µl of mpH₂O and 1 ml of Bradford Solution (100 mg/l Coomassie Brilliant Blue G250 (Serva), 5 % EtOH, 4.25 % H₃PO₄). 0-25 µg of IgG rabbit (Sigma) or 0-12.5 µg BSA were used for calibration.

3.4.4 Immunoprecipitation of Flag-Stu1 with M2 α -Flag Magnetic Beads

To purify Flag-Stu1 from *S. cerevisiae* a protocol applied to isolate KT_s (Akiyoshi, B. et al., 2009b) was adapted. Cells containing pGAL-Flag-STU1-GFP constructs were grown in YPR+2 and supplemented with 2 % galactose to induce expression of Flag-Stu1-GFP. After about 10 h cells were harvested (4 °C, 5 min, 2,100 g), washed with ice-cold mpH₂O, transferred to a round bottom tube and resuspended in buffer BH/0.1 – 2.5 times the volume of OD cells (for example 450 OD cells were resuspended in 1.125 ml). Cell lysis was performed by the addition of about 70 % volume glass beads and cells were vigorously shaken at 4 °C (30 min, 2,000 rpm). The lysates were col-

lected through the punctured bottom into fresh falcon tubes by centrifugation at 4 °C (20 s, 500 g) and transferred to 1.5 ml tubes. Lysates were clarified for 30 min (4 °C, 20,000 g) and supernatants were transferred to fresh tubes. Flag-tagged Stu1 was immunoprecipitated using M2 α -Flag Magnetic Beads (Sigma) in the amount of 1/10 of the volume of OD cells. Lysate and beads were rotated for 3 h at 4 °C (10 rpm). Beads were washed six times with BH/0.1. Proteins were eluted under gentle agitation at RT for 25 min (500 rpm) with 3Flag peptide (Sigma) in BH/0.1 at a final concentration of 0.5 ng/ μ l. Subsequently, samples were visualized by SDS-PAGE and Western Blot analysis.

BH/0.1		buffer was supplemented prior to use with	
25 mM	HEPES pH 8.0		2 mM DTT
2 mM	MgCl ₂	protease inhibitors	20 μ g/ml Leupeptin
0.1 mM	EDTA pH 8.0		20 mg/ml Pepstatin A
0.5 mM	EGTA pH 8.0		20 μ g/ml Chymostatin
0.1 %	NP-40		0.2 mM PMSF
150 mM	KCl	phosphatase inhibitors	1 mM Sodiumpyrophosphate
10 %	glycerol		2 mM Na- β -glycerophosphate
			0.1 mM Vanadate
			5 mM NaF
			100 nM Microcystein

3.4.5 Immunoprecipitation of Stu1-ProtA with IgG beads

For large-scale protein purifications 2-3 l of *S. cerevisiae* cells containing a Stu1-ProtA construct were grown under the conditions of the respective experiment in YPD+2. Cells were harvested at 4 °C (SLC-4000, 15 min, 5,000 rpm) using a Sorvall centrifuge, washed once with ice-cold mpH₂O and once with 1x pellet volume Lysis buffer (5 min, 2,100 g). Pellets were resuspended in Lysis buffer⁺ (supplemented with protease and phosphatase inhibitors) to a final concentration of 200-350 OD/ml and cells were lysed with glass beads using a bead mill (Pulverisette6, Fritsch). Cells were broken three times at 500 rpm for 4 min at 4 °C with a pause of 2 min in between the lysis cycles. Lysates were clarified with three sequential centrifugation steps of 25 min using a Sorvall centrifuge (SS-34, 1x 17,000 g, 2x 20,500 g). Lysates were supplemented with 300-400 μ l 50 % human IgG beads resuspended in lysis buffer and incubated for 3.5 h at 4 °C on a tube rotator (10 rpm). Subsequently beads were washed with 10 ml of lysis buffer and 10 ml of wash buffer supplemented with 1 mM PMSF, followed by a washing step with 0.5 ml of NH₄OAc pH 5.0. Purified proteins were eluted with two times 0.5 ml of 0.5 M HAc pH 3.4 and completely dried using a speed vac (Savant). Purified proteins were run on NuPAGE® gels for mass spectrometric analyses.

Lysis buffer		buffer was supplemented prior to use with	
50 mM	Tris-Cl pH 8.0		2 mM DTT
5 mM	MgCl ₂	protease inhibitors	1 mM PMSF
140 mM	KCl		2 mM Benzamidin
0.1 %	NP-40		5 μ g/ml Leupeptin
10 %	glycerol		10 μ g/ml Pepstatin A
			10 μ g/ml Aprotinin
			40 μ g/ml TPCK
		phosphatase inhibitors	60 mM Na- β -glycerophosphate

1 mM Vanadate
10 mM NaF

Wash buffer

10 mM Tris-Cl pH 8.0
250 mM LiCl
1 mM EDTA
0.5 % NP-40

3.4.6 Immunoprecipitation of Stu1-ProtA with IgG beads with SILAC

SILAC approaches were used for *in vivo* incorporation of a label into proteins to quantitatively analyze protein phosphorylation by mass spectrometry. Cells were grown as described in 3.1.2.2. G1-arrested cells were compared with nocodazole-arrested cells and *cdc15-1* arrested cells respectively (described in 3.3.1). To be able to combine equal amounts of cells, additional to the OD also the cell number of each culture was determined by using a hemocytometer. After combining the cultures, Stu1-ProA was immunoprecipitated as described in 3.4.5.

3.4.7 *In vitro* phosphatase treatment

For phosphatase treatment 75 μ g of protein extracts from *S. cerevisiae* (3.4.2) were treated with 100 U of CIP (Fermentas) in 1x CIP Buffer (10 mM Tris-Cl pH 7.5, 10 mM $MgCl_2$) for 30 min at 37 °C. Before SDS-PAGE, EDTA pH 8.0 was added to a final concentration of 10 mM. Samples were supplemented with final 1x SDS sample buffer and heated for 3 min at 95 °C.

3.4.8 *In vitro* kinase assay

For *in vitro* kinase assays 90 ng of Stu1 N-terminal or C-terminal fragments purified from *E. coli* (3.4.1) were incubated with final 1x kinase buffer (25 mM HEPES pH 7.5, 150 mM KCl, 4 mM $MgCl_2$, 10 % glycerol) and 65 ng of kinase Ipl1-Sli15 and Mps1 purified from *E. coli* respectively. 5x kinase buffer was supplemented with 0.05 mM cold ATP and 10 mM DTT prior to the experiment. For the samples containing radioactive labeled ATP the samples were supplemented with 2.5 μ Ci γ -[^{32}P]-ATP (SRP501; specific activity: 6000 Ci/mmol, 10 μ Ci/ μ l; Hartmann Analytic, Braunschweig, Germany) per 50 μ l reaction that was added to the kinase buffer. Samples were carefully mixed and incubated for 1 h at 30 °C. To stop the kinase reaction, probes were completed with final 1x SPB and heated for 3 min at 95 °C followed by SDS-PAGE (3.4.9.1). After the gel run proteins were fixed by incubating the gel in 10 % HAc for 5 min and two times 15 min in fixing solution (40 % MeOH, 2 % HAc, 0.4 % glycerol). Subsequently, gels were washed for 5 min in 5 % glycerol, dried on Whatman[®] paper for 1 h at 80 °C and low pressure (Slab Gel Dryer SGD4050; Bachofer Laboratoriumsgeräte, Reutlingen, Germany). The incorporation of ^{32}P was visualized by exposing the dried gel to a film for several hours until overnight at -80 °C.

For the identification of phosphorylation sites by mass spectrometry, kinase assays were performed without γ -[^{32}P]-ATP. Despite of that, 0.2 mM cold ATP was used. Additionally, the amount of substrate was raised to 550-600 ng and 35 ng of Mps1 was used.

3.4.9 SDS polyacrylamide gel electrophoresis (SDS-PAGE)

Depending on the later processing of protein samples, extracts were separated by either glycine SDS-PAGE or NuPAGE Novex Bis-Tris SDS-PAGE.

3.4.9.1 Glycine SDS-PAGE

Protein extracts that were visualized by general coomassie staining or western blot analysis were separated using 6-10 % glycine SDS polyacrylamide gels (Laemmli, U. K., 1970). Samples were mixed prior to loading with 4x sample buffer (1x: 62.5 mM Tris-Cl pH 6.8, 10 % glycerol, 5 % β -EtSH, 2 % SDS, 0.02 % bromophenol blue) and incubated for 4 min at 95 °C. The gel run was performed at constant 135 V for 1 h 20 min until 2 h 20 min.

6-12 % separating gel		4 % stacking gel	
0.377 M	TrisHCl pH 8.8	0.125 M	TrisHCl pH 6.8
0.1 % (w/v)	SDS	0.1 % (w/v)	SDS
6-12 % (v/v)	Bis-Acrylamid (37.5:1)	4 % (v/v)	Bis-Acrylamid (37.5:1)
0.05 % (w/v)	APS	0.065 % (w/v)	APS
0.05 % (w/v)	TEMED	0.15 % (v/v)	TEMED
SDS-Running buffer			
25 mM	Tris-Cl		
192 mM	Glycine		
0.1 % (w/v)	SDS		

3.4.9.2 NuPAGE® Novex Bis-Tris SDS-PAGE

Purified proteins for mass spectrometric analyses were separated using a 4-12 % NuPAGE® Novex Bis-Tris gradient gel (Invitrogen). Samples were prepared according to the manufacturer's instructions with 1x NuPAGE® SDS Sample Buffer and 0.05 M DTT and incubated for 10 min at 70 °C. The NuPAGE® MOPS buffer in the inner chamber was supplemented with 500 μ l NuPAGE® Antioxidant. The gel run was performed for 1 h 40 min at 80 V constant.

3.4.10 Coomassie staining

3.4.10.1 Colloidal Coomassie staining of SDS-gels

Colloidal Coomassie staining of polyacrylamide gels was performed with Coomassie Brilliant Blue (Carl Roth GmbH). After electrophoresis, gels were fixed with 2 % HAc in 40 % MeOH for 1 h. Subsequently, gels were incubated in Colloidal Coomassie solution (0.8 % Coomassie Brilliant Blue in 20 % MeOH) for 1-24 h and destained in mpH_2O .

3.4.10.2 Regular coomassie staining for SDS-gels or PVDF

SDS gels or PVDF membranes were coomassie stained to visualize the marker and the amount of transferred proteins after Western blot analysis. Gels and membranes were stained in Coomassie Staining solution for 10-20 min followed by destaining with the Destaining solution.

Coomassie staining solutions

SDS-gel	PVDF membrane	
0.25 % (w/v)	0.2 % (w/v)	Coomassie Blue G250
50 % (v/v)	50 % (v/v)	MeOH
10 % (v/v)	10 % (v/v)	HAc

Destaining solutions

SDS-gel	PVDF membrane	
30 % (v/v)	50 % (v/v)	MeOH
7 % (v/v)	10 % (v/v)	HAc

3.4.11 Western blot analysis

For Western blot analyses proteins were transferred onto PVDF membranes (Millipore) with 16 V constant using a Trans-Blot® SD Semi-Dry Transfer Cell (BioRad, München, Germany). Time of blotting depended on the size of the protein of interest and varied between 1-2 h. Transfer buffer contained 48 mM Tris pH 9.2, 39 mM glycine, 0.025 % (w/v) SDS and 20 % (v/v) MeOH. Transfer efficiency was monitored by staining the gel as described in 3.4.10.2. Membranes were blocked with 5 % milk powder in PBS-T for 1 h at RT or 4 °C overnight to avoid unspecific antibody binding. For immunodecoration, primary and secondary antibodies were diluted in PBS-T containing 3 % milk powder (for dilutions see 2.4). For detection using the Licor system, secondary antibodies were supplemented with 0.02 % SDS. Membranes were incubated for 1-2 h at RT or overnight at 4 °C. In between the antibody incubation times membranes were washed three times for 10 min with PBS-T.

Protein-antibody complexes were visualized dependent on the secondary antibody using the Immobilon Western Chemiluminescent HRP Substrate (Millipore) or the Immobilon Western AP Substrate (Millipore), X-ray films Fujifilm Super RX (Fujifilm, Düsseldorf, Germany) and the X-ray film processor SRX-101A (Konica Minolta, Langenhagen, Germany). Protein-antibody complexes with fluorescently labeled secondary antibodies were detected by the LI-COR Odyssey® Infrared Imaging System (Licor, Lincoln, USA).

PBS		PBS-T
1.8 g/l	Na ₂ HPO ₄ *2H ₂ O	PBS with 0.1 % Tween20
0.24 g/l	KH ₂ PO ₄	
8 g/l	NaCl	
0.2 g/l	KCl	
		pH 7.4

3.4.12 Mass Spectrometry

Mass spectrometric analyses were carried out by the Protein Mass Spectrometry Facility of the BZH in cooperation with the Core Facility for Mass Spectrometry and Proteomics of the ZMBH at the University of Heidelberg.

For the determination of Stu1 phosphorylation sites, the bands of interest were cut out from the Coomassie-stained SDS-PAGE gel. The gel slice was reduced, alkylated and in-gel trypsin digested according to an adapted protocol from Rosenfeld, J. et al. (1992). The gel slice was washed once with mpH₂O (10 min, RT), followed by a shrink-

age step with acetonitrile (15 min, RT). Then cysteine residues were reduced with 10 mM DTT in 100 mM NH_4HCO_3 (30 min, 56 °C), followed by another shrinkage step with acetonitrile (15 min, RT). Cysteine residues were alkylated with 55 mM iodoacetamide (20 min, RT, darkness). Subsequently, the gel slice was washed with 100 mM NH_4HCO_3 (15 min, RT) and another shrinkage step was performed using acetonitrile (15 min, RT). For the proteolytic digest, the gel slice was incubated with 20 ng/ μl trypsin over night at 37 °C. Trypsin cuts specifically after the basic amino acids arginine and lysine. Subsequently, the pH of the tryptic digest was adjusted to pH 1-3 using trifluoroacetic acid.

Each peptide mixture was separated by HPLC (nanoAcquity, Waters) and analyzed by mass spectrometry using a LTQ-Orbitrap (Linear Trap Quadrupole-Orbitrap, Thermo Scientific). After a survey scan (300-2000 amu) the double or multiple charged peptide masses of the 3-6 most prominent peptides were selected for fragmentation (selected ion monitoring). To increase the sensitivity of this selection for phosphorylated peptides, a parent mass list was used containing all possible phosphorylated peptides that emerge upon Stu1 digestion with trypsin. Analysis and data interpretation of the peptide mixture was done using Mascot Daemon and Distiller (Matrix Science).

To evaluate the differences of phosphorylation comparing Stu1 from two different cell cycle arrests, the ratio of the intensity of the 'light' and the 'heavy' peptide was calculated for each phosphorylated peptide and the corresponding unphosphorylated peptide. To correct for unequally combined amounts of Stu1, the overall ratio of 'light' to 'heavy' Stu1 was calculated based on unmodified peptides. The L/H ratio for the nocodazole-arrest/G1 SILAC assay was 5.5 and 7.14 for the anaphase/G1 SILAC assay. Therefore, the L/H ratio of each peptide was corrected by division with this ratio. Peptides were considered to be highly significant when the L/H ratio of the phosphorylated peptide was higher than 10 and the L/H ratio of the corresponding unmodified peptide was smaller than 0.5. This indicated that the phosphorylated peptide was highly enriched in a certain cell cycle stage, whereas the corresponding unphosphorylated peptide was depleted. Peptides that were found phosphorylated with an L/H ratio between 2 and 10 and unmodified with a ratio between 0.5 and 1 were considered as less strong, but still significant.

3.5 *In silico* analysis

3.5.1 Secondary structure prediction

Secondary structure prediction was based on the amino acid sequence using the SYMPRED server (<http://www.ibi.vu.nl/programs/sympredwww/>). For the PSI-BLAST the database NR and a combination of PROFsec, SSPro 2.01, YASPIN and PSIPred was chosen as secondary structure prediction methods. POLYVIEW 2D (Porollo, A. A. et al., 2004) was used for visualization.

3.5.2 Isoelectric point calculator

The theoretical isoelectric point (pI) of single Stu1 domains was calculated using the ExPASy Compute pI/Mw tool (Bjellqvist, B. et al., 1993, 1994; Gasteiger, E. et al., 2005).

4 RESULTS

4.1 Stu1 domains and their functions

The *S. cerevisiae* CLASP homolog Stu1 is an essential protein that localizes to different cell structures and fulfills various functions during mitosis (Pasqualone, D. et al., 1994; Khmelinskii, A. et al., 2007; Ortiz, J. et al., 2009). Stu1 is a large protein consisting of 1513 amino acids that can be divided into different subdomains. In the following thesis some of these subdomains will be characterized in more detail.

4.1.1 Introduction of putative Stu1 domains

Based on homology with Stu1 orthologs (Al-Bassam, J. et al., 2011) and secondary structure predictions (Fig. 4-1), Stu1 can be subdivided into six structural different domains. Structural homology to other CLASP proteins suggest two TOG-like (TOGL) domains at the very N-terminus of Stu1 (TOGL1 and TOGL2). These two domains are followed by a presumable unstructured region containing a basic serine-rich stretch (the minimal MT-binding loop, ML) and a domain consisting of mainly alpha helical structures (domain three, D3). Another alpha helical domain at the very C-terminus (domain four, D4) is attached via a second rather unstructured region (the C-terminal loop, CL).

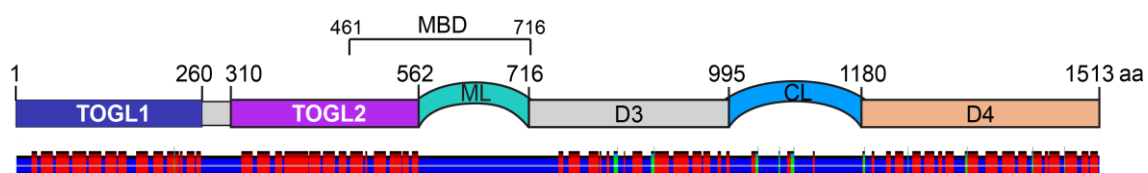


Figure 4-1. Putative domain organization of Stu1.

Helical structures (red), unstructured regions (blue) and beta-sheets (green) were predicted using the SYMPRED server and visualized by POLYVIEW 2D (see 3.5.1). The subdomains TOGL1, TOGL2, ML, D3, CL and D4 and the corresponding amino acid regions are depicted. The MBD consisting of part of the TOGL2 and the ML domain is indicated.

Whereas the TOGL1 domain was found to be less conserved, but essential for Stu1 binding to KTs (Funk, C. et al., submitted), the intra-HEAT repeat loops of TOGL2 show a high sequence conservation when compared with other CLASP proteins (see Fig. 1-9 B; Al-Bassam, J. et al., 2011). A part of the TOGL2 and the ML domain were suggested to embody the MT-binding domain (MBD) of Stu1 (Yin, H. et al., 2002, see Fig. 4-1). Just very recently, the C-terminal D4 domain was identified to enable Stu1

dimerization, a prerequisite for efficient meta- and anaphase spindle formation, but also KT binding. In addition, this domain is able to drive the midzone localization of Stu1 most likely via the direct interaction with another so far unidentified midzone protein (Funk, C. et al., submitted).

To which extent the TOGL2, ML, D3 and CL domains contribute to the localization of Stu1 to MTs and KTs will be analyzed in detail below. Therefore, deletion mutants of single or multiple Stu1 domains were created and characterized further. Complementation assays demonstrated that TOGL2 is the only essential domain (Table 4-1) (Funk, C. et al., submitted). Point-mutations of four of the most highly conserved amino acids within the intra HEAT-repeat loops of TOGL2 (W339, R342, K428, K429) (see Fig. 1-9 B) also resulted in non-viable cells. A chromosomal loss assay revealed that the ML domain, similar to TOGL1 (Funk, C. et al., submitted), is strongly required for a faithful chromosome segregation, whereas the deletion of D3 and CL only caused a very mild segregation defect (Table 4-1).

strain	viability	chromosome loss per 1000 cells
WT	+	2.4
$\Delta mad2$	+	27.5
<i>stu1</i> Δ TOGL2	-	n.d.
<i>stu1</i> TOGL2-4A	-	n.d.
<i>stu1</i> Δ ML	+	955.6
<i>stu1</i> Δ D3	+	9.4
<i>stu1</i> Δ CL	+	3.2
TOGL2	-	n.d.
TOGL2-ML	+	n.d.

Table 4-1. The integrity of TOGL2 is essential for cell viability whereas ML strongly contributes to correct chromosome segregation.

Indicated Stu1 deletion- and point-mutations were integrated at the endogenous *STU1* locus of a shuffle strain and tested for viability. Chromosomal loss assays were performed determining the loss of a chromosomal fragment.

4.1.2 The role of Stu1 domains for spindle localization and formation in meta- and anaphase

4.1.2.1 The TOGL2 domain is sufficient for tubulin interaction

The conserved intra HEAT-repeat loops of TOG domains have been suggested to bind free tubulin (Al-Bassam, J. et al., 2006, 2010; Ayaz, P. et al., 2012; Wilbur, J. D. et al., 2013) in order to catalyze its incorporation in MTs. Indeed, Stu1 was found to

copurify tubulin when isolated from yeast cells (Fig. 4-2 A). To investigate if this binding is accomplished by the TOGL domains of Stu1, Flag-tagged Stu1 deletion- and point-mutation constructs were immunoprecipitated and analyzed by Western blot for tubulin binding (Fig. 4-2 B and C). The results revealed that the TOGL2 domain alone is sufficient to bind tubulin, whereas deletion of the TOGL2 domain prevented copurification of tubulin. In addition, the mutation of two (K428, K429) or four (W339, R342, K428, K429) conserved amino acids of the intra HEAT-repeat loops of TOGL2 strongly interfered with the tubulin interaction. This suggests that the TOGL2 domain provides the tubulin binding capability of Stu1 via the highly conserved intra-HEAT repeat loops. Notably, immunoprecipitations of TOGL1 did not copurify tubulin and TOGL1 was dispensable for tubulin binding (Funk, C. et al., submitted).

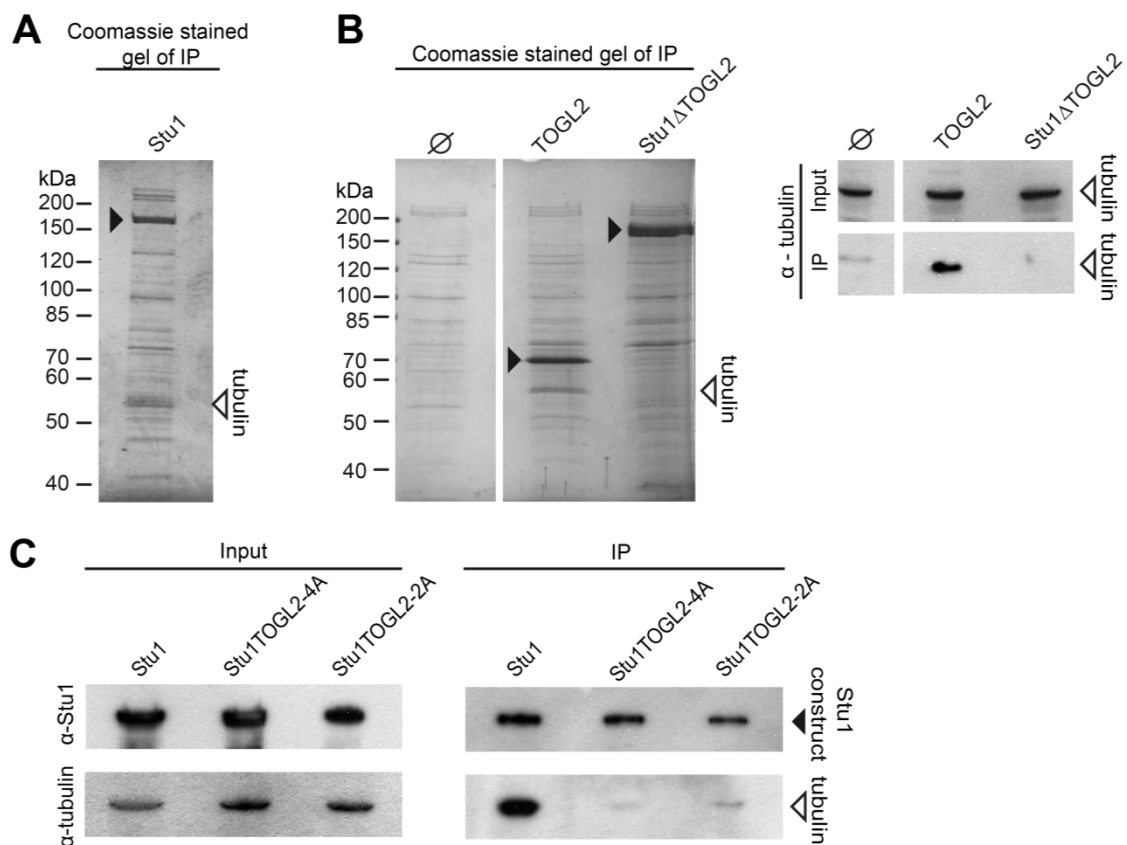


Figure 4-2. The TOGL2 domain is sufficient to bind tubulin via the conserved intra-HEAT repeat loops.

(A) Stu1 binds free tubulin. Flag-Stu1 was expressed from a galactose inducible promoter and immunoprecipitated. Tubulin was identified by mass spectrometry. Black arrows indicate purified Stu1 constructs. (B) TOGL2 is sufficient to copurify tubulin. Cells were treated as in A, except that tubulin was additionally visualized by Western blot analysis. The input represents 0.4 % (\emptyset) and 0.6 % (TOGL2 and Stu1 Δ TOGL2) of the immunoprecipitation (IP). (C) The integrity of the conserved intra HEAT-repeat loops is a prerequisite for tubulin binding via the TOGL2 domain. Cells were treated and analyzed as in B.

Taken together, these data suggest that Stu1, in contrast to other CLASP proteins only requires one TOGL domain to mediate tubulin binding.

4.1.2.2 Stu1 requires the TOGL2 and ML domain for the efficient formation of metaphase spindles

Since Stu1 is required for spindle formation (Yin, H. et al., 2002), the question arose how the individual domains contribute to this important function of Stu1. Very recent work already demonstrated that the dimerization of Stu1 via the D4 domain is important for stable formation of (metaphase) spindles (Funk, C. et al., submitted).

In order to gain more insight in the further domain requirements for Stu1 localization and spindle formation, synchronized cells of Stu1 mutants were analyzed 2 h and 2 h 30 min after release from a G1 arrest (Fig. 4-3 A-C). Subsequently, metaphase (1.3-2 μm length) as well as anaphase ($\geq 2\mu\text{m}$) spindles could be investigated. Due to different requirements for spindle stabilization in meta- and anaphase, different Stu1 domains might be involved to fulfill the corresponding functions in the two cell cycle steps. In metaphase, MTs of the antiparallel overlap need to be crosslinked and bundled to sustain the outward, but also inward forces that operate on the bipolar spindle. In anaphase however, these overlapping MTs have to be able to slide apart, while they still get stabilized.

At first, metaphase spindle formation and localization were addressed in more detail. Therefore, in addition to the release from G1 (Fig. 4-3 A-C), some of the mutant cells were arrested in metaphase by Cdc20 depletion (Fig. 4-3 D). More than 80 % of WT cells showed spindles longer 0.6 μm at both time points after G1 release. About 40 % of cells had prometa- to metaphase spindles of a length between 0.6 and 2 μm (Fig. 4-3 A and C). As expected, Stu1 depletion (Δstu1), but also the deletion of the TOGL2 domain almost completely blocked spindle formation (Fig. 4-3 A and C) and resulted in the formation of only a few spindles with prometaphase length (0.6-1.3 μm). The deletion of the ML domain prevented efficient metaphase spindle formation. Two third of cells failed to elongate their spindles longer than 0.6 μm , and only 29 % managed to form short prometaphase spindles (Fig. 4-3 A and C). Metaphase-arrested *stu1 Δ ML* cells formed spindles with only one third of the length compared to WT cells (Fig. 4-3 D). In contrast, *stu1 Δ D3* and *stu1 Δ CL* cells did not show a significant defect in spindle formation in comparison to WT cells (Fig. 4-3 A, C and D), but a closer look revealed a slightly faster SPB separation in *stu1 Δ CL* cells (Fig. 4-3 C).

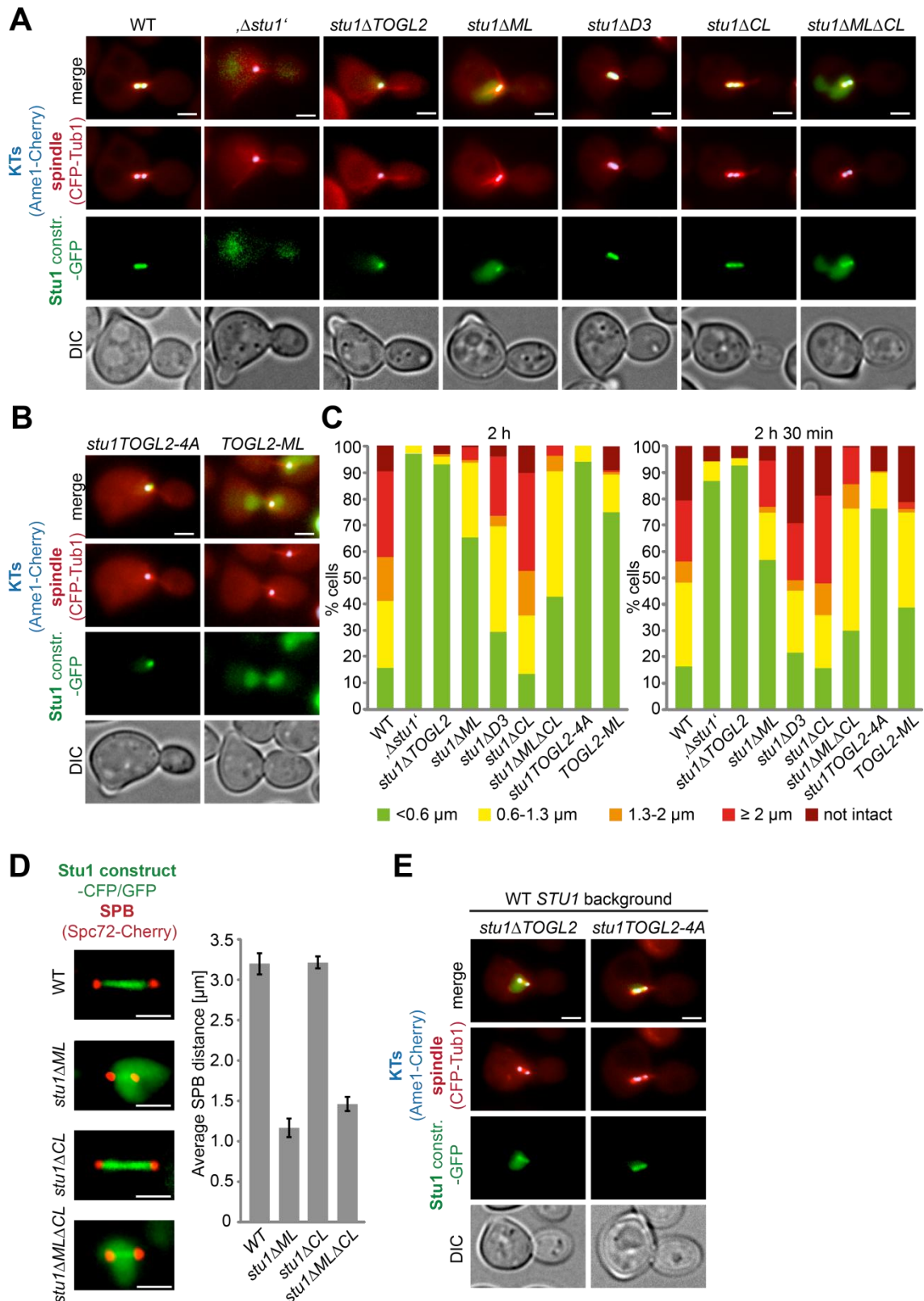


Figure 4-3. TOGL2 is essential for spindle formation in general, whereas ML is specifically required for proper metaphase spindle formation.

(A-C) Cells were released from G1 arrest and analyzed after 120 min and 150 min for spindle formation. For the analysis of nonviable Stu1 constructs shutdown of WT Stu1 was started 3h prior to the addition of α-factor. (A) The TOGL2 and ML domain are required for metaphase spindle formation. Images of indicat-

ed Stu1 mutant cells representing their metaphase spindle phenotype are shown; bar, 2 μm . **(B)** Stu1TOGL2-4A fails to form metaphase spindles. Images of indicated Stu1 mutant cells representing their metaphase spindle phenotype are shown; bar, 2 μm . **(C)** Spindle formation of depicted mutant strains was quantified according to the indicated spindle lengths; $n > 150$. **(D)** The ML domain contributes to metaphase spindle formation. Cells were arrested in metaphase by Cdc20 depletion for 5 h. Spindle length was measured as the distance between two Spc72 signals. Error bars represent the standard deviation for two independent experiments; $n > 100$; bar, 2 μm . **(E)** Stu1 Δ TOGL2 and Stu1TOGL2-4A only weakly localize to the metaphase spindle in WT *STU1* background; bar, 2 μm .

Interestingly, the combined deletion of the ML and the CL domain partially improved the spindle formation compared to *stu1 Δ ML* cells (Fig. 4-3 A and C), but the average SPB distance in metaphase-arrested cells was only slightly longer than in *stu1 Δ ML* cells (Fig. 4-3 D).

Since a part of the TOGL2 and the complete ML domain were determined as the MBD of Stu1 (see Fig. 4-1; Yin, H. et al., 2002), the question arose if a Stu1 localization defect is the reason for the defects in spindle formation in these cells. Indeed, Stu1 Δ ML only very weakly localized to metaphase spindles (Fig. 4-3 A and D). Because *stu1 Δ TOGL2* cells failed to form spindles (Fig. 4-3 A and C), the spindle localization of Stu1 Δ TOGL2 was difficult to determine. Stu1 Δ TOGL2 could be only detected as a faint signal in a region where collapsed SPBs, KTs and MTs reside (Fig. 4-3 A). To overcome this problem, this Stu1 construct was analyzed in the background of WT Stu1. Even when a part of the determined MBD was missing Stu1 Δ TOGL2 still weakly localized to the metaphase spindle under these conditions (Fig. 4-3 E). Stu1TOGL2-4A, which contains an unimpaired MBD domain, localized to the metaphase spindle in a quite similar strength than WT Stu1 (Fig. 4-3 E). A slightly more diffuse signal could be explained by the competition of MT binding of this Stu1 construct with WT Stu1. This indicates that the C-terminal part of the TOGL2 domain contributes to the binding of Stu1 to the MT lattice, but the ML domain has the main MT binding capability.

Although the binding of Stu1TOGL2-4A to the MT lattice was much stronger compared to Stu1 Δ ML, the spindle defect in these cells was much more severe. *stu1TOGL2-4A* cells, similar to *stu1 Δ TOGL2* cells, mostly failed to separate their SPBs beyond 0.6 μm (Fig. 4-3 B and C). This indicates that the interaction of Stu1 with the MT lattice facilitates efficient metaphase spindle formation, but that another function of Stu1 TOGL2 domain is even more important in this respect. Since Stu1TOGL2-4A is not capable to bind free tubulin, the TOGL2 domain might contribute to spindle formation and stabilization by providing free tubulin like other CLASP or XMAP215 proteins (Al-Bassam, J. et al., 2006, 2010; Brouhard, G. J. et al., 2008; Leano, J. B. et al., 2013).

Due to the fact that the ML and the TOGL2 domain are required for spindle formation, it was tested if these two domains are sufficient to fulfill this function on their own. Indeed, the TOGL2-ML construct (Table 4-1) was viable, but was not sufficient to bind to the MT lattice and could only slightly rescue the spindle formation in these cells (Fig. 4-3 B and C). This is in agreement with the finding that Stu1 dimerization via the D4 domain is required for MT lattice binding and efficient metaphase spindle formation (Funk, C. et al., submitted).

In summary, the TOGL2 and the ML domain are required for proper metaphase spindle formation. Thereby, SPB separation and spindle formation is driven by the TOGL2 activity that might provide free tubulin for MT rescue and polymerization. This is substantially facilitated by the MT lattice binding of Stu1 via the ML (and partially TOGL2) domain.

4.1.2.3 The CL domain specifies Stu1 localization to the MT overlap in metaphase

Although spindle formation of *stu1 Δ CL* cells was mostly indistinguishable from WT cells (Fig. 4-3 A, C and D), the localization of Stu1 Δ CL in metaphase arrested cells differed from WT Stu1 (Fig. 4-3 D). Whereas WT Stu1 was more focused in the center of the metaphase spindle, deletion of the CL domain distributed Stu1 Δ CL along the complete spindle in closer vicinity to the ends of the spindle. In WT cells, Stu1 was found to preferentially bind to antiparallel MT overlaps not only in anaphase, but also in metaphase (Funk, C. et al., submitted). This raised the question if the deletion of the CL domain causes metaphase spindles with an extended overlap of antiparallel MTs or if the CL domain specifies Stu1 binding to this overlap region. Therefore, the distribution of Ase1 as an indicator for antiparallel MT overlap (Schuyler, S. C. et al., 2003) was analyzed by measuring the intensity profile of Ase1 along the metaphase spindle axis (Fig. 4-4). The localization of Ase1, indicating the extension of the overlap region, was not severely different in *stu1 Δ CL* cells compared to WT cells (Fig. 4-4 A and B). This indicates that the CL domain indeed specifies the localization of Stu1 to antiparallel interpolar MTs in metaphase.

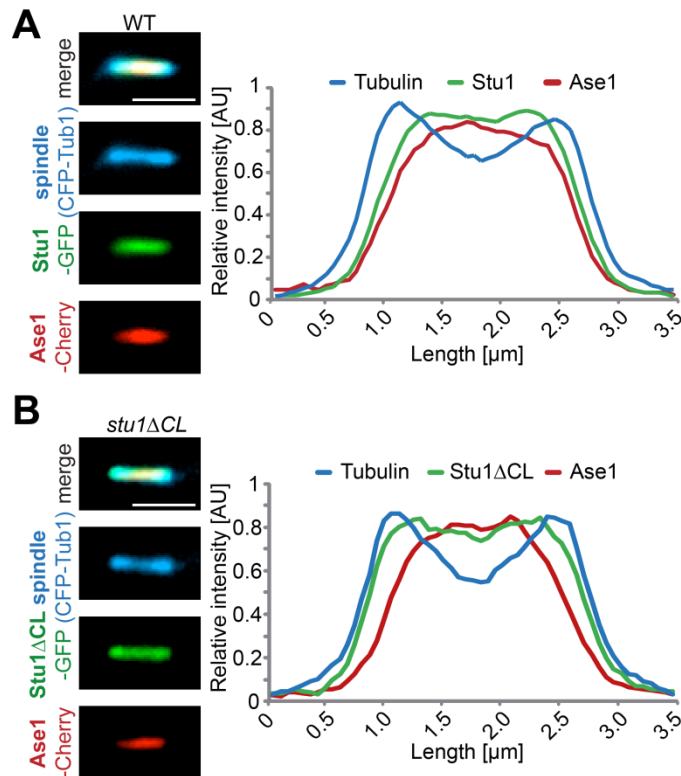


Figure 4-4. The CL domain is required to focus Stu1 to antiparallel MTs in metaphase.

(A-B) Indicated cells were arrested in metaphase by Cdc20 depletion for 2 h. Ase1 is used as a marker for antiparallel MT overlap. Plot profiles were generated by measuring the intensity of tubulin, Ase1 and Stu1 along the spindle axis; $n = 11$ (WT) and 13 (*stu1ΔCL*); bar, 2 μm.

4.1.2.4 The TOGL2 and ML domain are dispensable for midzone localization of Stu1 in anaphase

In anaphase, WT Stu1 was found to localize to the midzone of anaphase spindles to contribute to spindle stability (Yin, H. et al., 2002; Ortiz, J. et al., 2009).

Surprisingly, even though *stu1ΔML* cells were strongly affected in metaphase spindle formation, about 18 % of cells showed intact anaphase spindles when analyzed 2 h 30 min after the release from a G1 arrest (Fig. 4-3 C). This indicates that in anaphase the function of Stu1 in spindle stabilization differs in comparison to metaphase. Indeed, *Stu1ΔML* localized to the midzone of anaphase spindles similar to WT Stu1 (Fig. 4-5 A). This reveals that the interaction with the MT lattice via the ML, which is needed for proper metaphase spindle formation, is not required for Stu1 midzone localization and consequently stable spindle formation during anaphase. Deletion of the D3 or the CL domain had no crucial effect on anaphase spindle formation or Stu1 midzone localization (Fig. 4-3 C, 4-5 A).

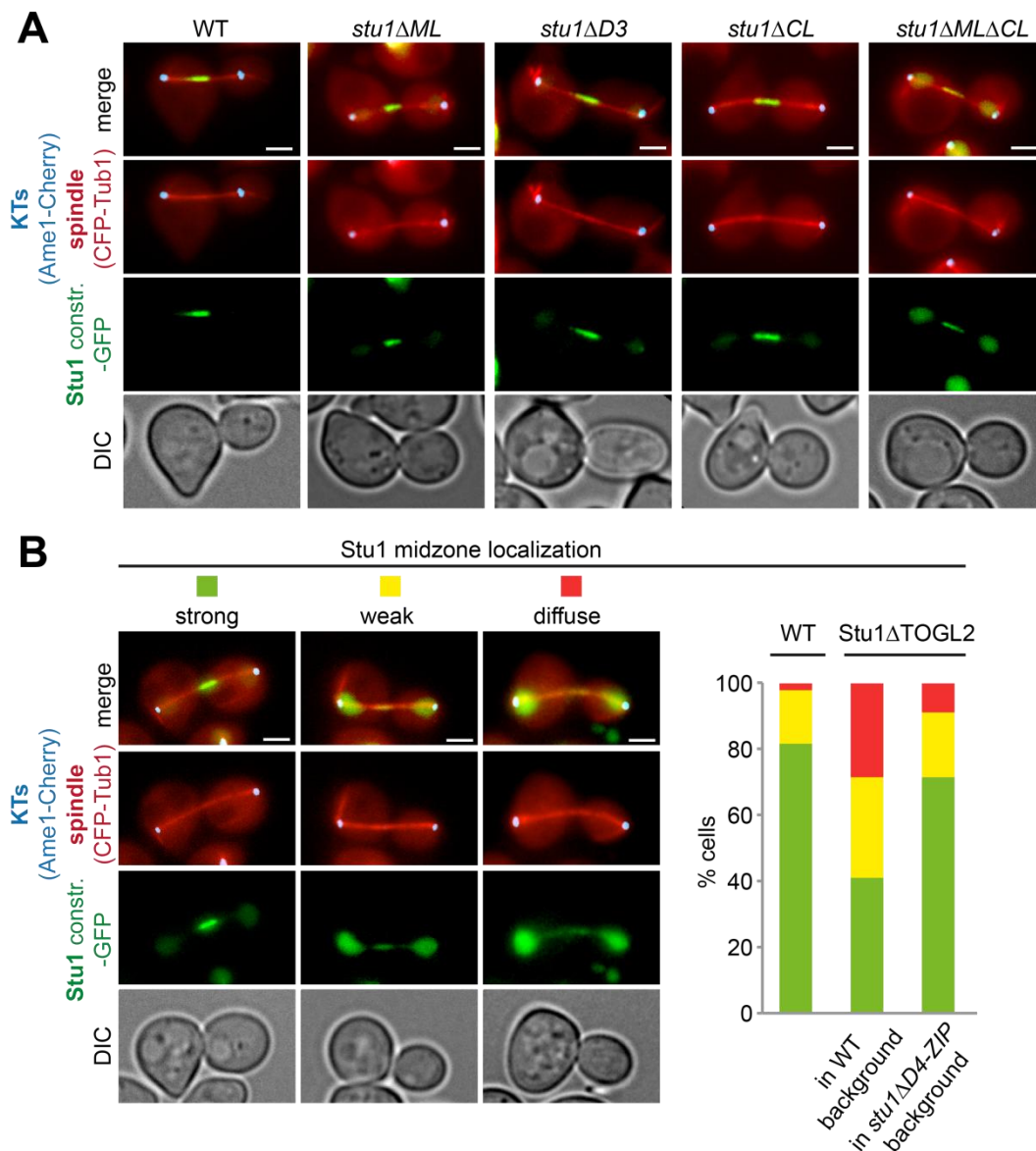


Figure 4-5. The ML and the TOGL2 domain are dispensable for midzone localization of Stu1.

(A) Anaphase spindles of the indicated *STU1* mutant cells are depicted representing the Stu1 midzone localization; bar, 2 μ m. **(B)** The TOGL2 domain is not required for midzone localization of Stu1. Midzone localization of WT Stu1 and Stu1 Δ TOGL2 in the background of WT Stu1 and Stu1 Δ D4-ZIP respectively was analyzed according to the indicated phenotypes. Images were taken 120 min after release from G1 arrest; n > 50; bar, 2 μ m.

Since *stu1* Δ TOGL2 cells were not able to drive spindle formation (Fig. 4-3 C), the localization of Stu1 Δ TOGL2 in anaphase was analyzed in the background of WT Stu1 to enable spindle formation. Quantification revealed that Stu1 Δ TOGL2 localized to the spindle midzone, but somewhat weaker than in WT cells (Fig. 4-5 B). To exclude that Stu1 Δ TOGL2 could only localize to the midzone by forming a heterodimer with WT Stu1, Stu1 Δ TOGL2 localization was also analyzed in the background of Stu1 Δ D4-ZIP.

The Zipper (ZIP) represents an ectopic dimerization domain that allows Stu1 Δ D4 to dimerize, but prevents binding of Stu1 Δ TOGL2 via the D4 dimerization domain. Deletion of the D4 domain usually causes a very severe spindle defect, but 'artificial' dimerization of Stu1 Δ D4 via the ZIP domain enables spindle formation in almost 50 % of cells (Funk, C. et al., submitted). In the Stu1 Δ D4-ZIP background, Stu1 Δ TOGL2 localization to the midzone was quite similar to WT Stu1. This indicates that the TOGL2 domain is also dispensable for midzone localization of Stu1. A possible reason why Stu1 Δ TOGL2 showed a weaker binding to the midzone in the WT background compared to the Stu1 Δ D4 background could be that WT Stu1 and Stu1 Δ TOGL2 compete for the binding site of a certain protein in the midzone. This is not the case in the Stu1 Δ D4-ZIP background. Since the D4 domain is required for midzone localization, Stu1 Δ D4-ZIP consequently fails to bind there (Funk, C. et al., submitted).

Conclusively, neither MT binding via the ML domain, nor the TOGL2 domain is essential for the midzone localization of Stu1. Nevertheless this does not exclude that the TOGL2 activity of midzone localized Stu1 contributes to the stabilization of spindles in anaphase.

4.1.3 The role of Stu1 domains for unattached KT localization

4.1.3.1 The CL domain specifies Stu1 localization to unattached KTs

It has been shown before that Stu1 accumulates at unattached KTs (Ortiz, J. et al., 2009), but also localizes to attached KTs in metaphase (Funk, C. et al., submitted). Very recent experiments revealed that dimerization of Stu1 via the D4 domain and most likely direct binding via the TOGL1 domain are mandatory for KT localization (Funk, C. et al., submitted). Thereby it is unclear how Stu1 distinguishes between an unattached and an attached KT and which role the other domains play in this respect. To provoke a high number of unattached KTs, cells were released from a G1 arrest into media containing the MT-depolymerizing drug nocodazole. Subsequently, Stu1 localization to the generated unattached KTs was analyzed.

Deletion of the TOGL2, the ML or the D3 domain and the point mutations in the Stu1TOGL2-4A construct had no observable effect on the sequestration of Stu1 at unattached KTs compared to WT cells (Fig. 4-6 A). Deletion of the CL domain however caused a severe mispositioning of Stu1 Δ CL to the vicinity of the SPB in about 95 % of cells (Fig. 4-6 A and B). This resulted in no detectable (34 %) or only a weak (61 %) residual Stu1 signal at the unattached KTs. In order to test if the mislocalized Stu1 Δ CL fraction represents Stu1 that is bound to short MTs at the SPB that had resisted the

nocodazole treatment binding to the MT lattice was prevented by the additional deletion of the ML domain. This could partially restore the localization of the major fraction of Stu1 to unattached KTs in about 64 % of cells (Fig. 4-6 A and B). Thus, in the absence of the CL domain MTs more efficiently compete for Stu1 interaction than unattached KTs. Nevertheless it remains unclear where the residual SPB located Stu1 fraction is binding to.

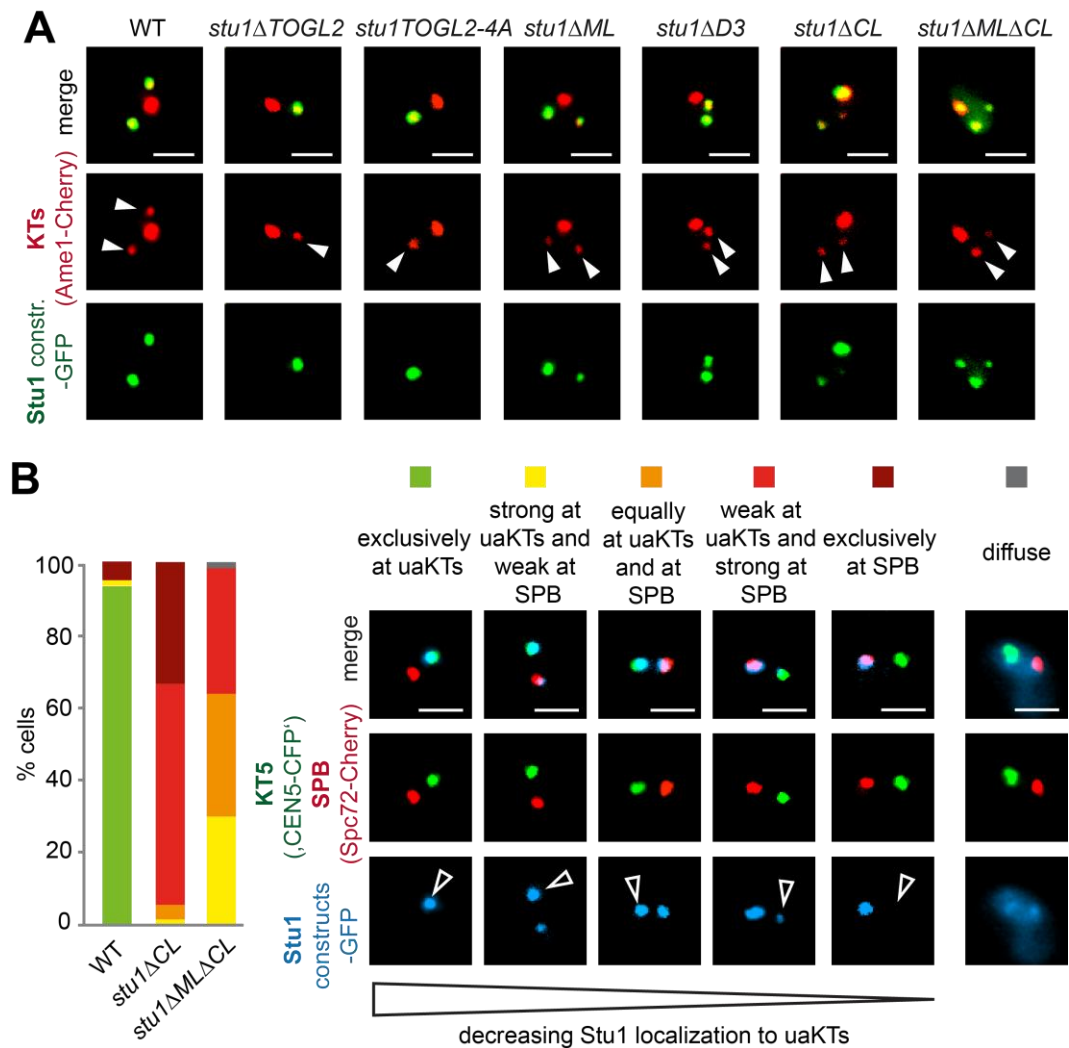


Figure 4-6. The CL domain regulates Stu1's sequestration at unattached KTs.

(A) Localization of indicated Stu1 constructs to unattached KTs (uaKTs). Cells were released from a G1 arrest into nocodazole and analyzed after 3 h. For the nonviable *Stu1ΔTOGL2* or *Stu1TOGL2-4A* constructs shutdown of WT Stu1 was started 3 h prior to the addition of α -factor. White arrows indicate unattached KTs; bar, 2 μ m. **(B)** Additional deletion of the ML domain partially rescued Stu1 localization to unattached KTs in *stu1ΔMLΔCL* cells. Cells were treated as in A and localization of Stu1 to unattached KTs was quantified as indicated. Arrows indicate Stu1 at unattached KTs; n > 100; bar, 2 μ m.

4.1.3.2 Efficient capturing does not require Stu1 localization to unattached KT5 – but TOGL2 activity

A function that has been suggested previously for Stu1 at unattached KT5 is the efficient capturing of unattached KT5 (Ortiz, J. et al., 2009). Therefore, the deletion mutants were analyzed in regards to their capturing capability. In cells containing KT5s labeled by using the tetO/tetR system, unattached KT5s were quantified as signals absent from the SPB signals or the spindle axis.

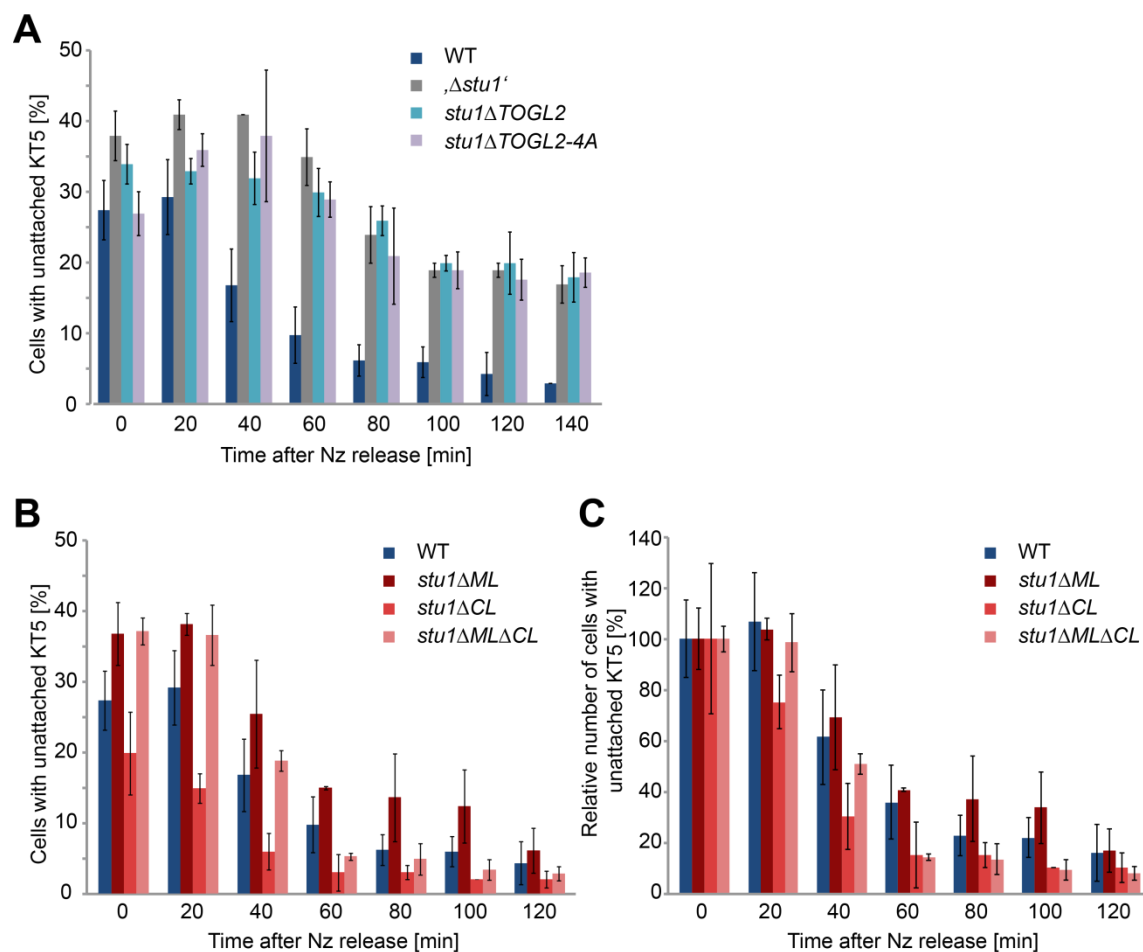


Figure 4-7. The CL domain and localization to unattached KT5 are no prerequisites for capturing, but the TOGL2 activity is essential.

(A) A functional TOGL2 domain is mandatory for efficient capturing. Cells were released from a G1 arrest into nocodazole. After 3 h, nocodazole was washed out and cells were analyzed at the indicated time points. For shutdown of WT Stu1, cells were shifted to glucose 3 h prior the initiation of the α -factor arrest. Unattached KT5s were quantified for each time point; $n > 100$; error bars represent the standard deviation (STD) of minimum three independent experiments. **(B)** The ML domain contributes to efficient KT capture, whereas the CL domain has an inhibitory effect. Cells were treated and analyzed as in A without Stu1 shutdown conditions; $n > 100$; error bars represent the STD of two independent experiments. **(C)** In order to compare capturing of the indicated mutant cells independent of the initial number of unattached KT5, the data derived from experiment B was depicted as relative capturing of KT5. Therefore the number of unattached KT5s at time point 0 min was set to 100 %.

In WT cells that were released from a nocodazole arrest, the majority of the unattached KT5s were captured after 80 min, whereas the depletion of Stu1 resulted in a strong capturing defect (Fig. 4-7 A). These cells showed a higher number of unattached KT5s (38 %) in comparison to WT cells (25 %) at time point 0 min that got only slowly reduced and stagnated at about 18 % of unattached KT5s up to 140 min. Interestingly, cells containing the Stu1 Δ TOGL2 or the Stu1TOGL2-4A construct showed mainly the same defect as Stu1 depletion (Fig. 4-7 A). These results suggest that the TOGL2 activity of binding tubulin is important for efficient capturing of unattached KTs. Deletion of the ML domain also resulted in a high number of unattached KT5s at time point 0 min after nocodazole release (Fig. 4-7 B) and this number slowly decreased to 6 % over time. To be able to compare the velocity of capturing of *stu1* Δ ML and WT cells independent of the initial number of unattached KTs, the percentage of unattached KT5s was calculated relative to the starting number of unattached KT5s (Fig. 4-7 C). Deletion of the ML domain only slightly reduced the velocity of the capturing process in the beginning when compared to WT. But cells maintained a higher intermediate (80 to 100 min) number of unattached KTs (Fig. 4-7 B and C). These data suggest that *stu1* Δ ML cells are able to efficiently capture KTs that are in close proximity to the SPBs, but are impaired in capturing KTs that localize further away. Surprisingly, *stu1* Δ CL cells showed an even improved capturing of unattached KT5s compared to WT cells (Fig. 4-7 B). The already low number of unattached KT5s (20 %) at time point 0 min was reduced down to 3 % within 60 min, indicating that sequestration of Stu1 at unattached KTs is not mandatory for efficient capturing. Interestingly, also the capturing of *stu1* Δ ML Δ CL cells was significantly improved in comparison to *stu1* Δ ML cells, resulting in 95 % proper attached KT5s in cells analyzed 60 min after nocodazole release (Fig. 4-7 B). This proposes that deletion of the CL domain can partially compensate for the defect caused by the deletion of the ML domain.

Taken together, these results suggest that TOGL2, but also the ML domain are required for efficient capturing and KT attachment, whereas the CL domain has an inhibitory function in this respect. The finding that Stu1 function on MTs is more important for efficient capturing than the localization to unattached KTs, suggests that Stu1 regulates the dynamics of capturing kMTs or KT-generated MTs.

4.1.3.3 The TOGL2 domain might be required for the temporal regulation of KT-generated MTs

KT-generated MTs were found to play an important role for the capturing of unattached KTs (Kitamura, E. et al., 2010). In addition, CLASP proteins were suggested to

drive MT rescue or polymerization by recruiting and providing free tubulin that was bound via the TOG domains (Al-Bassam, J. et al., 2010). Our findings that TOGL2 activity is required for efficient capturing raised the question if Stu1 facilitates the nucleation and polymerization of these KT-generated MTs when sequestered at unattached KTs and if this function is stalled in cells with an impaired tubulin binding capability. Accordingly, the *stu1ΔTOGL2* and *stu1TOGL2-4A* mutant cells were analyzed for the nucleation or presence of KT-generated MTs at different time points after the release from nocodazole arrest. Already 40 min after nocodazole washout 95 % of WT cells showed nucleated (25 %) or already polymerized (70 %) KT-generated MTs (Fig. 4-8). However, cells depleted of Stu1 (Δ *stu1*) had only nucleated (6 %) or formed (16 %) KT-generated MTs in 22 % of cells analyzed at the same time. Nevertheless, over time this number increased up to 69 %. Cells containing the *Stu1ΔTOGL2* or the *Stu1TOGL2-4A* construct showed a very similar effect (Fig. 4-8).

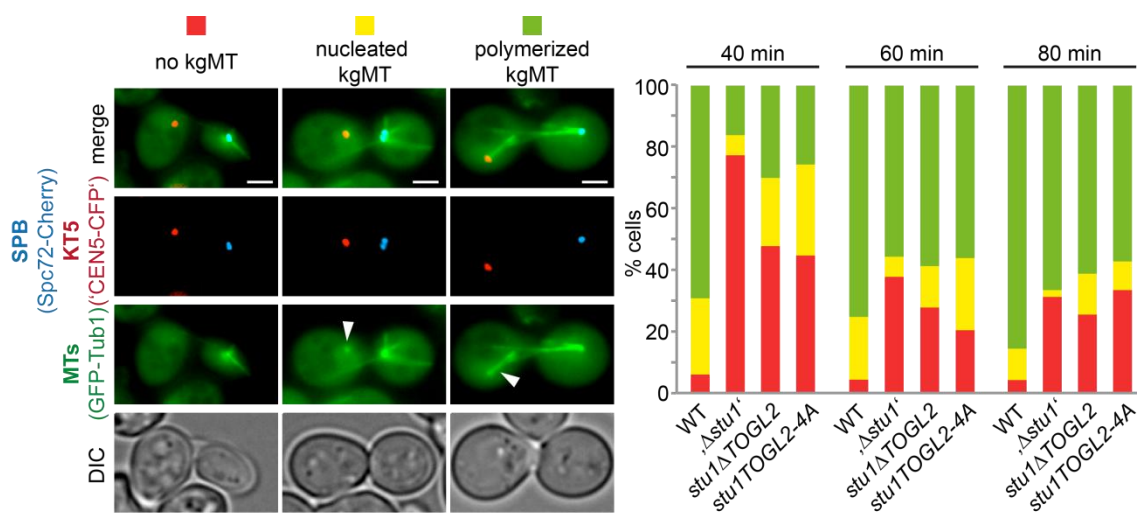


Figure 4-8. Stu1 or rather the TOGL2 activity is important for a temporal efficient formation of KT-generated MTs.

Cells were released from the G1 arrest into nocodazole. After 3 h, nocodazole was washed out and cells were analyzed at the indicated time points. Shutdown of WT Stu1 was started 3 h prior the initiation of the α -factor arrest. Phenotypes of KT-generated MTs (kgMTs) were quantified as depicted. Arrows indicate tubulin signals at unattached KTs; $n > 48$; bar, 2 μ m.

In summary, these results indicate that Stu1 and especially the TOGL2 activity are not essential for the formation of KT-generated MTs in general, but might strongly influence the efficiency and temporal regulation of the generation of these MTs.

4.1.4 Stu1's localization and role at metaphase KT's

4.1.4.1 The ML domain is required for proper KT attachment to MT's

The TOGL2 and to a lesser extent the ML domain are important for efficient capturing of unattached KT's (see 4.1.3.2). Interestingly, cells absent of these domains already showed increased amounts of unattached KT's during a normal cell cycle. To quantify the extent of this defect, *stu1* Δ TOGL2, *stu1*TOGL2-4A and *stu1* Δ ML cells were analyzed 120 min after release from a G1 arrest. In 10 % of cells *Stu1* Δ ML could be detected as a signal completely off the spindle indicating the presence of unattached KT's (Fig. 4-9).

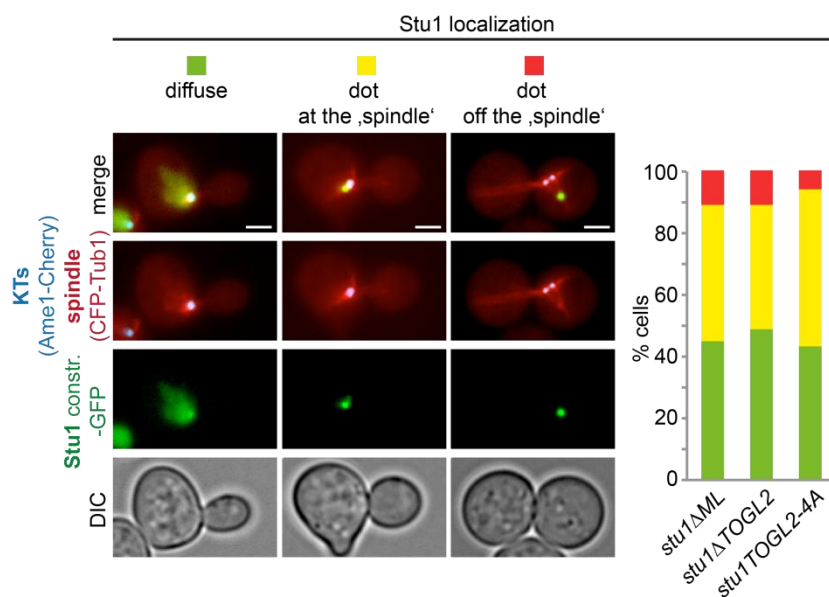


Figure 4-9. The TOGL2 activity and the ML domain might be required for proper KT attachment.

stu1 Δ TOGL2, *stu1*TOGL2-4A and *stu1* Δ ML cells were analyzed 120 min after release from a G1 arrest. The localization of the Stu1 construct was quantified as indicated; n > 100; bar, 2 μ m.

In 44 % of cells *Stu1* Δ ML was visualized as a strong dot in close vicinity to the very short spindle and the major KT signal. The latter may represent a *Stu1* fraction that localizes to KT's that are in close vicinity to the spindle and the SPBs, but were not able to achieve a proper end-on attachment yet. In support of this, CHIP analysis revealed that the ML domain is required for binding to attached KT's in metaphase (Funk, C. et al., submitted). Alternatively, this SPB localized *Stu1* indicates that *Stu1* Δ ML has difficulties to leave attached KT's, due to its weak MT binding capability. *stu1* Δ TOGL2 and *stu1*TOGL2-4A cells showed a very similar defect (Fig. 4-9), indicating that not only the binding of *Stu1* to the MT lattice, but also the binding and providing of free tubulin might be important for a correct attachment of KT's.

unpaired t-test. Asterisks indicate a significant difference compared to WT values with $p < 0.0001$. Bar, 2 μm . **(B)** Scheme representing the values achieved from the analysis shown in A. **(C)** Over-elongation of kMTs in *stu1 Δ CL* cells is independent of tension. Cells were arrested in G1 for 3 h. Distances between SPB and KT5 were measured as the kMT lengths; $n > 150$; error bars represent the STD of two independent experiments. **(D)** Deletion of Cin8 intensified the effect of *Stu1 Δ CL* on the kMT length. Cells were arrested and analyzed as in A; $n > 200$.

When *stu1 Δ CL* cells were arrested in metaphase, cells showed a similar SPB distance than WT cells (Fig. 4-3 D and 4-10 A). However, the length of kMTs was slightly, but reproducibly longer in these cells (Fig. 4-10 A). Consequently, this resulted in a shorter inter-KT distance (Fig. 4-10 A and B). In order to analyze if this effect is dependent on tension of a bipolar spindle, the kMT length of G1 arrested cells was measured. Also under these conditions, the kMT length of *stu1 Δ CL* cells was increased compared to WT cells, indicating that tension, put on the KT-MT interface, is not mandatory for the effect of over-elongated kMTs in *stu1 Δ CL* cells (Fig. 4-10 C).

It was shown before that the assembly of longer kMTs is suppressed by Cin8 to ensure chromosome congression (Gardner, M. K. et al., 2008). Indeed, the additional deletion of Cin8 even increased the effect of *Stu1 Δ CL* on kMTs (Fig. 4-10 D). kMTs elongated even further compared to WT and, most likely as a consequence to keep a minimum level of tension on the KT-MT interface, the average SPB distance increased. This kept the inter-KT distance at a constant minimum length of about 0.5 μm . So indeed, the CL domain seems to attenuate the polymerization of kMTs driven by *Stu1*.

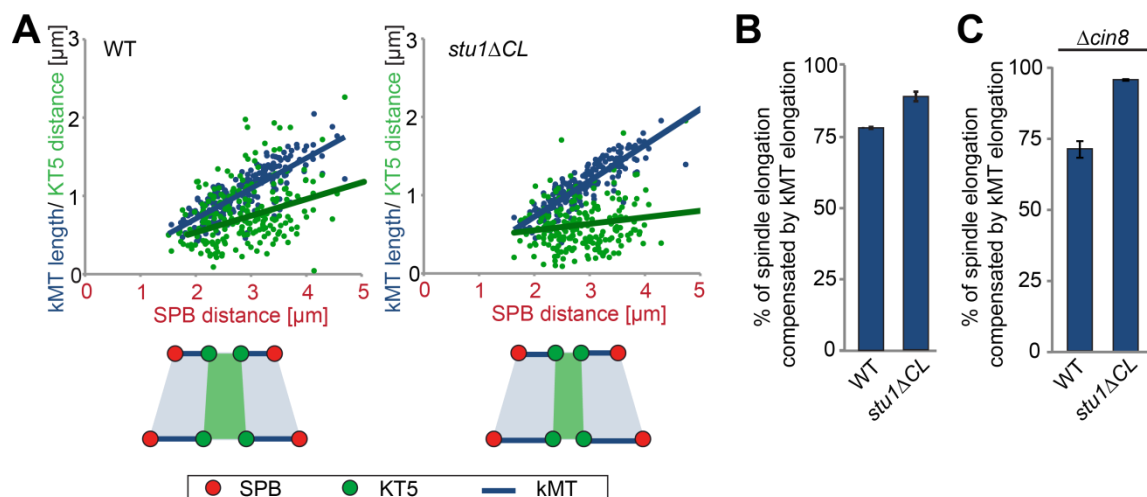


Figure 4-11. The CL domain is required to adapt kMT length to tension on the KT-MT interface.

(A-B) A higher percentage of spindle elongation is compensated by kMT elongation in *stu1 Δ CL* cells compared to WT cells. **(A)** Cells were arrested in metaphase by *Cdc20* depletion for 2 and 5 h. For each cell, values of kMT length and inter-KT distance were plotted against the corresponding SPB distance illustrating to which extent the kMT length or the inter-KT distance increased with increasing spindle length; $n > 200$. **(B)** The percentage of spindle elongation compensated by the elongation of kMTs was obtained by the two-fold slope of the trend line depicted in A. Error bars represent the STD of two independent experi-

ments. **(C)** Upon *Cin8* deletion, the percentage of spindle elongation that is compensated by the elongation of kMTs is even increased in *stu1ΔCL* cells. $\Delta cin8$ strains containing WT or *Stu1ΔCL* were treated and analyzed as described in A and B; $n > 195$. Error bars represent the STD of two independent experiments.

4.1.4.3 The CL domain makes kMT length dependent on tension

Earlier studies revealed that polymerization and stability of kMTs increases with increasing tension on the KT-MT interface, whereas low tension causes enhanced depolymerization (Akiyoshi, B. et al., 2010). To gain more insight in the dependencies between the kMT length and the tension on the KT-MT interface in this mutant, the inter-KT distances and kMT lengths were plotted against the corresponding SPB distances (Fig. 4-11 A). To achieve a broad range of data, we took advantage of the observation that SPB distances increase over time in metaphase arrest. Therefore, the values of 2 h and 5 h of metaphase arrest were combined for this analysis. These analyses revealed that in *stu1ΔCL* cells a higher percentage (89 %) of spindle elongation was compensated by the elongation of the kMTs than in WT cells (78 %) (Fig. 4-11 A and B). As a consequence, the inter-KT distance in *stu1ΔCL* cells only slightly changed, independent of the SPB distance. This effect again was intensified by the additional deletion of *Cin8* (Fig. 4-11 C). In *stu1ΔCL Δcin8* cells, the kMTs almost completely (95 %) compensated the spindle elongation compared to only 71 % in $\Delta cin8$ cells alone (Fig. 4-11 C) and the inter-KT distance was kept at a constant low level of about 0.5 μm (Fig. 4-11 D). This indicates that a very low level of tension was kept on the KT-MT interface that was sufficient to maintain the increased kMT length. In addition, this means that in *stu1ΔCL* cells *Cin8* counteracts the over-polymerizing power of *Stu1ΔCL* at the kMTs. However, in the $\Delta cin8$ background this antagonizing force is missing and kMTs can even elongate further. Taken together, these data suggest that the CL domain of *Stu1* regulates kMT polymerization and makes the kMT length dependent on the tension on the KT-MT interface.

4.1.5 Disturbed (k)MT dynamics result in bipolar attachment defects

The analysis of cells arrested in metaphase revealed that *stu1ΔCL* cells had a slightly increased defect in bipolar attachment in comparison to WT cells (Fig. 4-12 A). This defect was much more severe when cells were released from nocodazole treatment (Fig. 4-12 B). When analyzed 80 min after the nocodazole release, 84 % of *stu1ΔCL* cells with a SPB distance longer than 3 μm still showed monopolar attached KT5s. In WT cells, only 11 % of cells had the same defect. However, only 12 % of *stu1ΔCL* cells that further progressed into G1 after this treatment manifested the bi-

orientation defect and revealed missegregated KT5s, compared to 5 % of WT cells (Fig. 4-12 C). This indicated that the very strong initial bipolar attachment defect could be corrected in the majority of cells, but nevertheless caused an increased number of cells with missegregated KT5s. In addition, it took about 180 min until the majority of *stu1ΔCL* cells had undergone cytokinesis after nocodazole release and were arrested in G1 again, in comparison to about 120 min in WT cells.

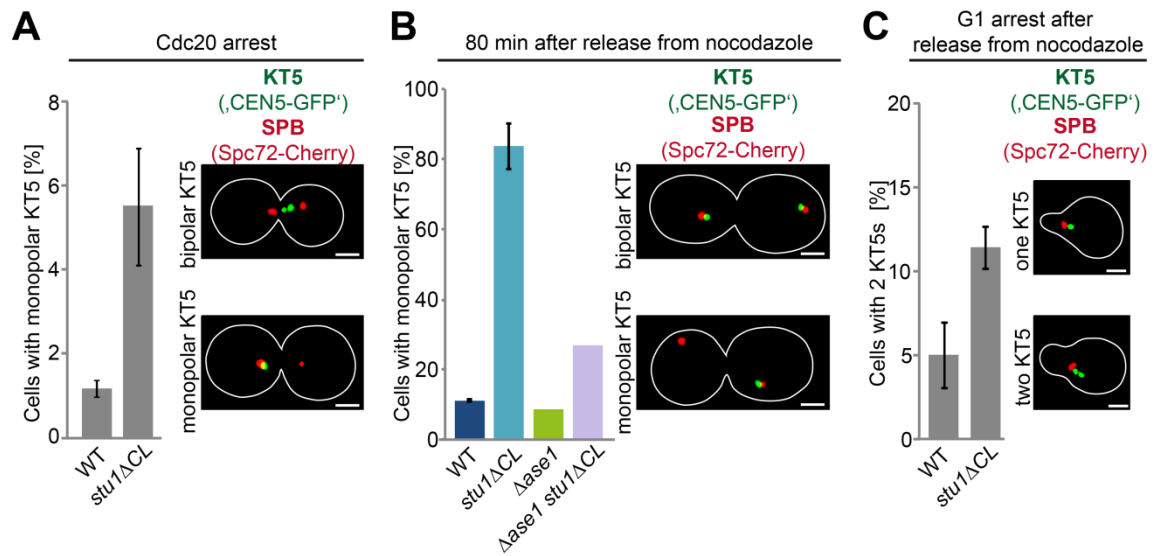


Figure 4-12. Deletion of the CL domain resulted in a bipolar attachment defect.

(A) Deletion of the CL domain resulted in an increased bipolar attachment defect. Cells were arrested in metaphase by Cdc20 depletion for 2 h. KT5 attachment was quantified as indicated; $n > 150$. (B) *stu1ΔCL* cells showed a severe initial attachment defect when released from nocodazole arrest. Additional deletion of Ase1 could mainly rescue this defect. After G1 arrest cells were released into nocodazole. After 3 h, nocodazole was washed out and cells were analyzed 80 min later. Cells with a SPB distance larger than 3 μ m were quantified for monopolar attached KT5; $n > 50$. (C) After nocodazole treatment *stu1ΔCL* cells showed an increased KT missegregation. Cells were treated as in B, but α -factor was added after nocodazole washout. After 3 h, the G1 arrested cells were analyzed. Cells with two KT5 signals were quantified as cells that show missegregation; $n > 380$. (A-C) Error bars represent the STD of two independent experiments; bar, 2 μ m.

Since the CL domain appears as a negative regulator for Stu1 binding or function on MTs, not only the kTMs, but also the spindle dynamics might be influenced by *Stu1ΔCL*. Therefore, the SPB distances were measured after the release from nocodazole treatment. Indeed, *stu1ΔCL* cells separated their SPBs much faster, with an average SPB distance of more than 3 μ m only 40 min after nocodazole release in comparison to 1.1 μ m in WT cells (Fig. 4-13 A). Strikingly, *Stu1ΔCL* localized all along these spindles as described before for metaphase spindles (Fig. 4-13 B). When Ase1 was visualized as an indicator for the overlap of interpolar MTs, it revealed that these spindles had a much more extensive overlap region of interpolar MTs than WT spin-

dles of about the same length (Fig. 4-13 B). This indicated that these spindles, irrespective of their length of up to 5 μm , still had metaphase character and that the *stu1 Δ CL* cells did not prematurely enter anaphase. In order to investigate if the precocious SPB separation could be the reason for the bi-orientation defect in *stu1 Δ CL* cells, Ase1 was deleted to downregulate spindle elongation. Indeed, the deletion of Ase1 in *stu1 Δ CL* cells reduced the rates of SPB separation down to WT levels (Fig. 4-13 A). Analysis of KT bi-orientation in these cells revealed that the number of monopolar attached KT5s was also strongly reduced, but could not be completely lowered to WT levels (Fig. 4-13 B). In conclusion, these data suggest that the premature SPB separation is the main reason for the bi-orientation defect detected in *stu1 Δ CL* cells. While cells try to achieve bipolar attachment, the early spindle elongation might prevent the attachment of KTs to both SPBs due to the spatial distance. Another possible explanation is that a delayed bipolar attachment of KTs enables the SPBs to separate that fast and far. Nevertheless, the disturbed dynamics of the interpolar MTs might not be the sole factor for this defect. Also the dynamics of other MTs, like the kMTs, that seem to be finely regulated by Stu1 via the CL domain, might contribute to faithful chromosome segregation.

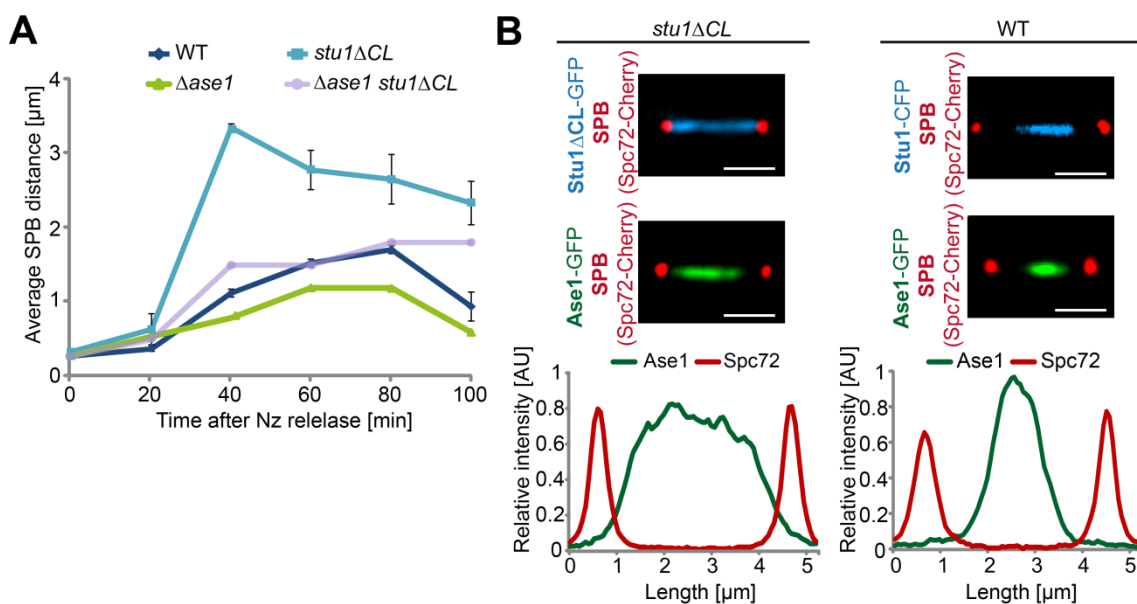


Figure 4-13. Precocious SPB separation is the main reason for the bipolar attachment defect.

(A) Deletion of the CL domain caused a precocious SPB separation after cells were released from nocodazole treatment. Additional deletion of Ase1 almost completely diminished this effect. Cells were treated like in Fig. 4-11 A. Indicated time points after nocodazole washout were analyzed for SPB distances. To exclude the majority of cells that have already initiated anaphase, cells with SPB distances larger than 5 μm were excluded; $n > 80$. Error bars represent the STD of two independent experiments; bar, 2 μm . **(B)** Premature anaphase entry is not the reason for the precocious SPB separation. Cells were treated like in Fig. 4-11 A. Ase1 serves as a marker for interpolar MT overlaps. Plot profiles represent the average intensities of 10 (*stu1 Δ CL*) or 4 (WT) measured cells; bar, 2 μm .

Surprisingly, the deletion of the CL domain did not cause a chromosomal loss as severe as expected considering this observed defect in bi-orientation (Table 4-1). One reason could be that due to the small size of the chromosomal fragment used in this assay the attachment and segregation behavior is altered compared to a regular chromosome. On the other hand, most KT5s could missegregate together with the same SPB. Thus, the loss of the chromosomal fragment would frequently come along with the loss of a regular chromosome. Since all regular chromosomes contain essential genes, these cells would be inviable and overlooked in this assay. To test this hypothesis, *stu1ΔCL* cells that contained two different labeled KT5s (KT5 and KT15) were analyzed in regard to their segregation phenotype. Indeed, in 74 % of *stu1ΔCL* cells in which KT5 and KT15 showed a bi-orientation defect at the same time (48 % of the cell population), both KT5s were attached to the same SPB (Fig. 4-14 A). This finding supports the assumption that in the chromosomal loss assay the loss of the chromosomal fragment might frequently coincide with the loss of a regular chromosome.

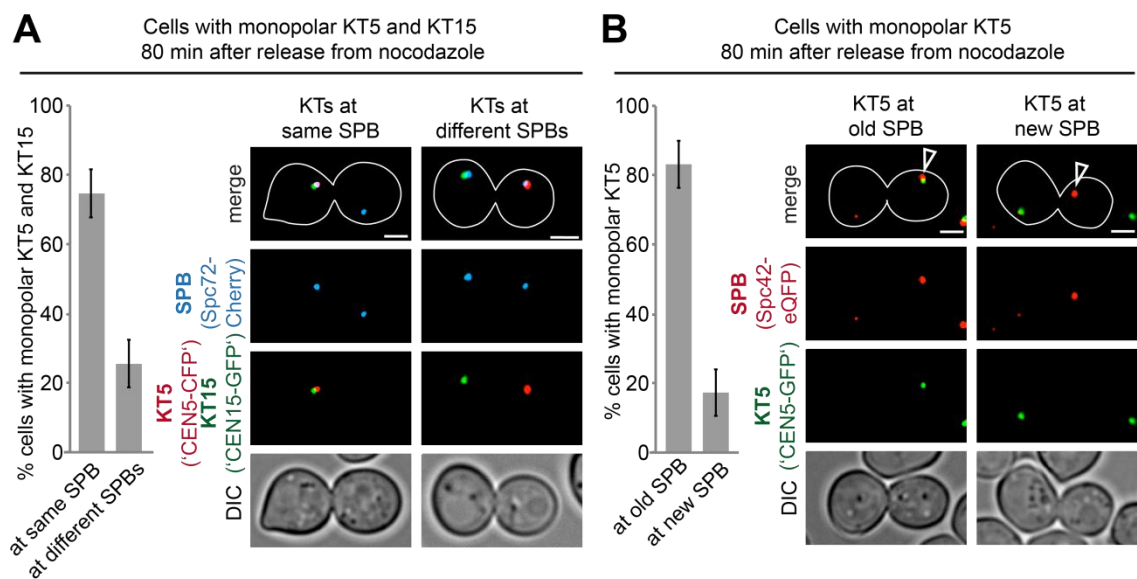


Figure 4-14. Monopolar attached KT5s mainly missegregate together, preferentially to the old SPB.

(A) Two different monopolar KT5s mainly attached to the same SPB. *stu1ΔCL* cells with two labeled KT5s (KT5, KT15) were treated as in Fig. 4-12 A. Cells that contained KT5 and KT15 monopolarly attached were quantified according to their localization to the same or different SPBs; $n > 100$. Error bars represent the STD of two independent experiments; bar, 2 μ m. **(B)** Monopolar KT5s preferentially localize to the old SPB. Cells were released from G1 arrest into nocodazole. After 90 min, nocodazole was washed out and cells were analyzed 80 min later as indicated. Spc42 and its slow maturation after SPB duplication was used as an indicator to distinguish the old and new SPB. Arrows indicate old SPB; bar, 2 μ m.

Analysis of *stu1ΔCL* cells with Spc42 labeled as an indicator to distinguish between the old and the new SPB revealed that more than 80 % of the monopolar attached

KT5s resided with the old SPB (Fig. 4-14 B). Previous studies have shown that defective reorientation from the old to the new SPB in *ipl1* (or *sli15*) mutants causes mono-oriented KTs mainly segregating with the old SPB during anaphase (Tanaka, T. U. et al., 2002). Treatment with nocodazole however tended to abolish the tendency of chromosomes to cosegregate with the old SPB. Based on these findings we assume that most of the KTs get monopolarly attached to the old SPB in *stu1 Δ CL* cells and fail to re-orientate to the new SPB.

4.1.6 Deletion of the TOGL2 domain cannot be rescued by the CLASP1 TOGL2 or Stu2 TOG1 domain

In order to address the question if the TOGL2 domain of Stu1 works like a polymerase like TOG domains of XMAP family members, this domain was replaced by the TOG1 domain of the *S. cerevisiae* XMAP215 homolog Stu2. This chimeric construct however resulted in inviable cells. In order to compare the specific functions of the two TOG domains, the chimeric construct was analyzed in regards to Stu1 function under WT Stu1 shutdown conditions. The Stu2 TOG1 domain could not substitute for the function of the Stu1 TOGL2 domain in spindle formation (Fig. 4-15 A) or KT capture (Fig. 4-15 C). These results suggest that the Stu1 TOGL2 domain does not work in the identical way as the TOG1 domain of the XMAP215 protein Stu2.

Since the TOG domain of a XMAP family member could not compensate for the function of the TOGL2 domain of Stu1, the question raised if a TOGL domain of a CLASP family member can fulfill this function. Therefore, the TOGL2 domain of Stu1 was replaced by the TOGL2 domain of the *H. sapiens* CLASP homolog CLASP1. Surprisingly, also this chimeric construct was not viable and could not rescue the function of Stu1 (Fig. 4-15 A and C). This indicates that the TOGL2 domain of Stu1 does also not work in the identical way as the TOGL domains of higher eukaryotes.

The TOG1 domain of Stu2 and the TOGL2 domain of CLASP1 were determined to be capable of tubulin binding (Al-Bassam, J. et al., 2006; Leano, J. B. et al., 2013) *per se*. But it remains to be tested if these TOG domains are indeed still capable to bind free tubulin when they are embedded within the Stu1 protein structure. The fact that both chimeric Stu1 constructs were able to localize to unattached KTs undistinguishable from WT Stu1 (Fig. 4-15 B) at least demonstrated that the substitution of the TOGL2 domain by these domains did not cause a completely inactive or misfolded Stu1 protein.

In conclusion, the function of the Stu1 TOGL2 domain differs from the function of TOG domains of other XMAP215 proteins or CLASP proteins of higher eukaryotes. Simple binding of free tubulin might not be the only function of the Stu1 TOGL2 domain that is essential for the activity of Stu1 and therefore for the survival of the cell.

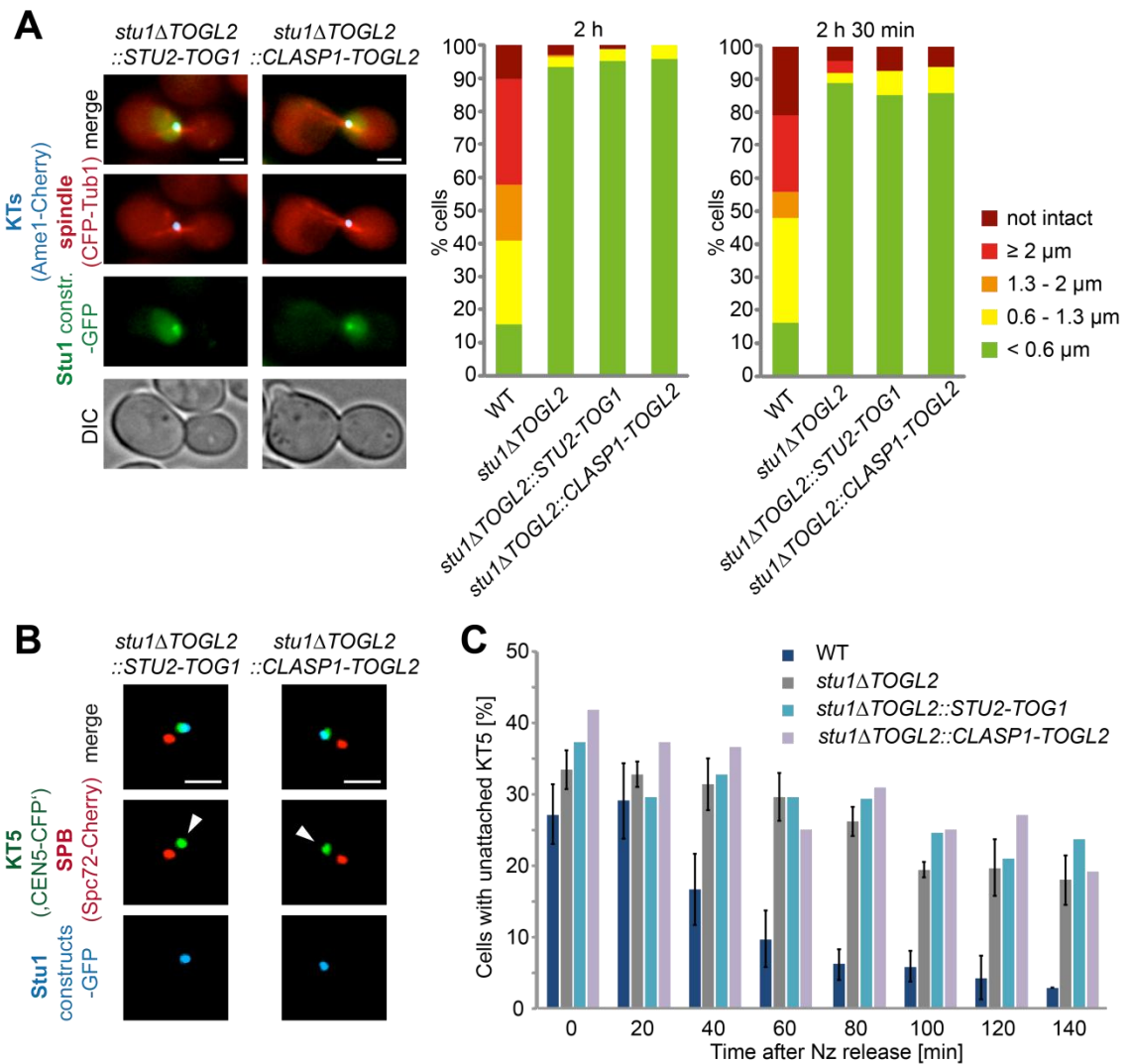


Figure 4-15. Swapping the TOGL2 domain of Stu1 with another TOG domain did not result in cells capable to form spindles or to achieve capturing.

(A-C) The TOGL2 domain of Stu1 was substituted with the TOG1 domain of Stu2 or the TOGL2 domain of CLASP1 respectively. **(A)** Chimeric Stu1 constructs were not able to form spindles. Shutdown of WT Stu1 was started 3 h prior to the initiation of G1 arrest. Cells were released and analyzed for metaphase and anaphase spindle formation at the indicated time points. Data of WT and *stu1* Δ TOGL2 cells are as in Fig. 4-3 C; $n > 130$; bar, 2 μm . **(B)** Chimeric Stu1 constructs localized to unattached KT5. Cells were released from a G1 arrest into nocodazole and analyzed for Stu1 construct localization after 3h. Cells were grown under WT Stu1 shutdown conditions; bar, 2 μm . **(C)** Chimeric Stu1 constructs are not able to facilitate capturing of unattached KT5. Cells were treated under Stu1 shutdown conditions and released from G1 arrest into nocodazole. After 3 h, nocodazole was washed out and cells were analyzed at the indicated time points. Data of WT and *stu1* Δ TOGL2 cells are as in Fig. 4-7 A; $n > 100$.

4.2 Various cell cycle dependent phosphorylations of Stu1 indicate a complex way of regulation

4.2.1 Stu1 phosphorylation in mitosis causes a mobility shift on SDS-PAGE

Analysis of the Stu1 domain mutants already gave more extensive insights in the domain requirements to achieve the various Stu1 localizations (this work; Funk, C. et al., submitted), but the mechanisms that ensure the temporal and spatial regulation of Stu1 remained elusive. Interestingly, Stu1 did not appear as one discrete band when analyzed by Western blot (Fig. 4-16 A). This suggested a post-translational modification of Stu1. Indeed, treatment with calf intestine phosphatase (CIP) revealed that this mobility shift on SDS-PAGE is caused by phosphorylation (Fig. 4-16 A).

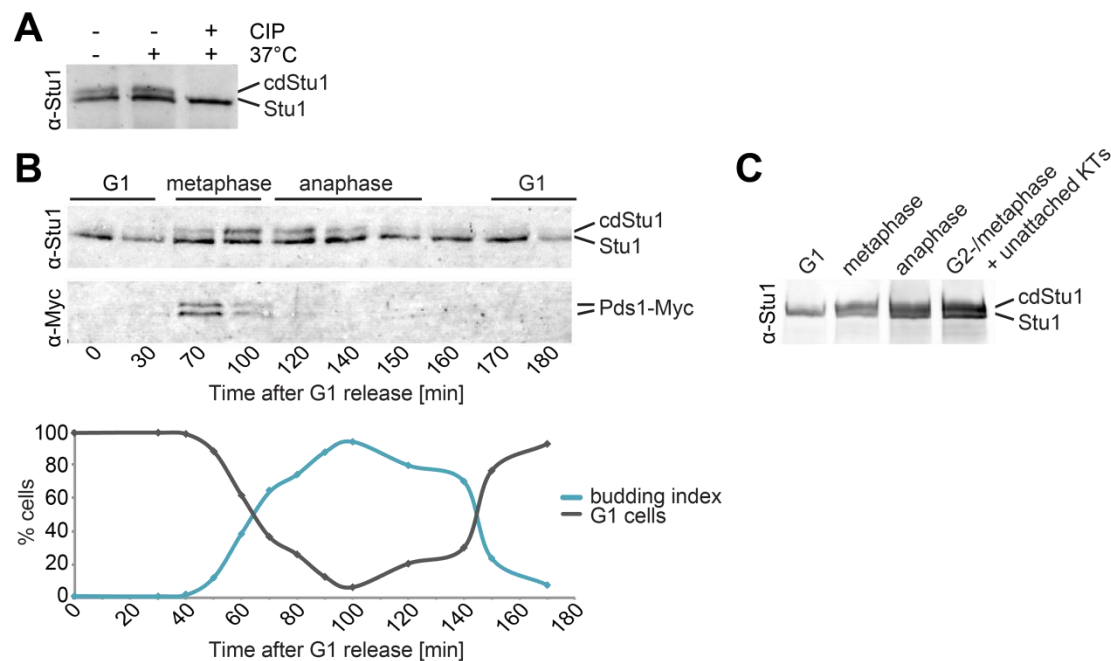


Figure 4-16. Stu1 gets phosphorylated in a cell cycle dependent manner.

(A) The form of Stu1 resulting in a mobility shift on SDS-PAGE was caused by phosphorylation. Protein extracts were isolated from asynchronized WT cells and treated with calf intestine phosphatase (CIP) *in vitro*. Western blot analysis was performed using anti-Stu1 antibody. **(B)** Phosphorylation of Stu1 is cell cycle dependent. WT cells were arrested in G1 and analyzed at the indicated time points after release. α -factor was added 80 min after release to trap the cells in G1 again. Western blot analysis was performed using anti-Stu1 and anti-Myc antibody. The indicated cell cycle stages were determined based on the Pds1 levels and the budding index of the mitotic cells. Pds1 degradation indicates anaphase onset. **(C)** Phosphorylation pattern of Stu1 arrested at indicated cell cycle stages. Stu1-ProtA was affinity purified from cells arrested in G1, metaphase, anaphase and G2-/metaphase with unattached KTs. Western blot analysis was performed using anti-Stu1 antibody.

Following one cell cycle after G1 release demonstrated that this phosphorylated form of Stu1 is not present in G1, but appears at the onset of metaphase and disappears in late anaphase (Fig. 4-16 B), indicating that this particular modified form of Stu1 is cell cycle dependent (cdStu1). This was confirmed by the analyses of Stu1-ProtA affinity-purified from cells arrested in different cell cycle stages (Fig. 4-16 C). Whereas in G1 only one form of Stu1 was visible, Stu1 purified from metaphase or anaphase arrested cells additionally showed the slower migrating Stu1 form. This was also the case when cells were treated with nocodazole to isolate Stu1-ProtA from G2-/metaphase arrested cells with unattached KTs.

Posttranslational protein modifications like phosphorylations are known to fulfill regulatory roles by affecting protein activity, interaction, stability or localization (Fu, J. et al., 2010). The fact that Stu1 gets phosphorylated and dephosphorylated during the cell cycle led to the question for the associated functional relevance of this modification.

4.2.2 Stu1 gets phosphorylated and dephosphorylated throughout the cell cycle

To address the question which sites of Stu1 get phosphorylated, large-scale protein purifications of Protein A-tagged Stu1 were performed using stable isotope labeling of amino acids in cell culture (SILAC). This method allowed to quantitatively analyze the relative phosphorylation of Stu1 at different times and stages of the cell cycle. On the one hand, WT cells arrested in G1 for 2 h were combined with WT cells arrested with nocodazole in G2-/metaphase for 3 h to recruit Stu1 to unattached KTs. On the other hand, WT cells arrested in G1 were mixed with temperature sensitive *cdc15-1* cells arresting in anaphase upon incubation at 37 °C for 3 h. In each case the cultures were combined in an approximate cell number ratio of 1:1 and affinity-purified collectively. Coomassie stained gels show the purified Stu1-ProtA at a size of about 195 kDa (Fig. 4-17 A) which was analyzed by mass spectrometry. Further mass spectrometric analyses of unlabeled Stu1-ProtA purified from cells arrested in G1, metaphase, anaphase or G2-/metaphase with unattached KTs confirmed the SILAC results and identified additional phosphorylation sites (Fig. 4-17 B). In total, 15 phosphorylation sites could be mapped on Stu1 (Fig. 4-17 C). Interestingly, the identified sites were not randomly distributed throughout the protein, but clustered mainly within the ML (or the MBD) and the CL domain. This is in agreement with the finding that both of these do-

mains are mainly unstructured regions and therefore preferentially accessible for modifications.

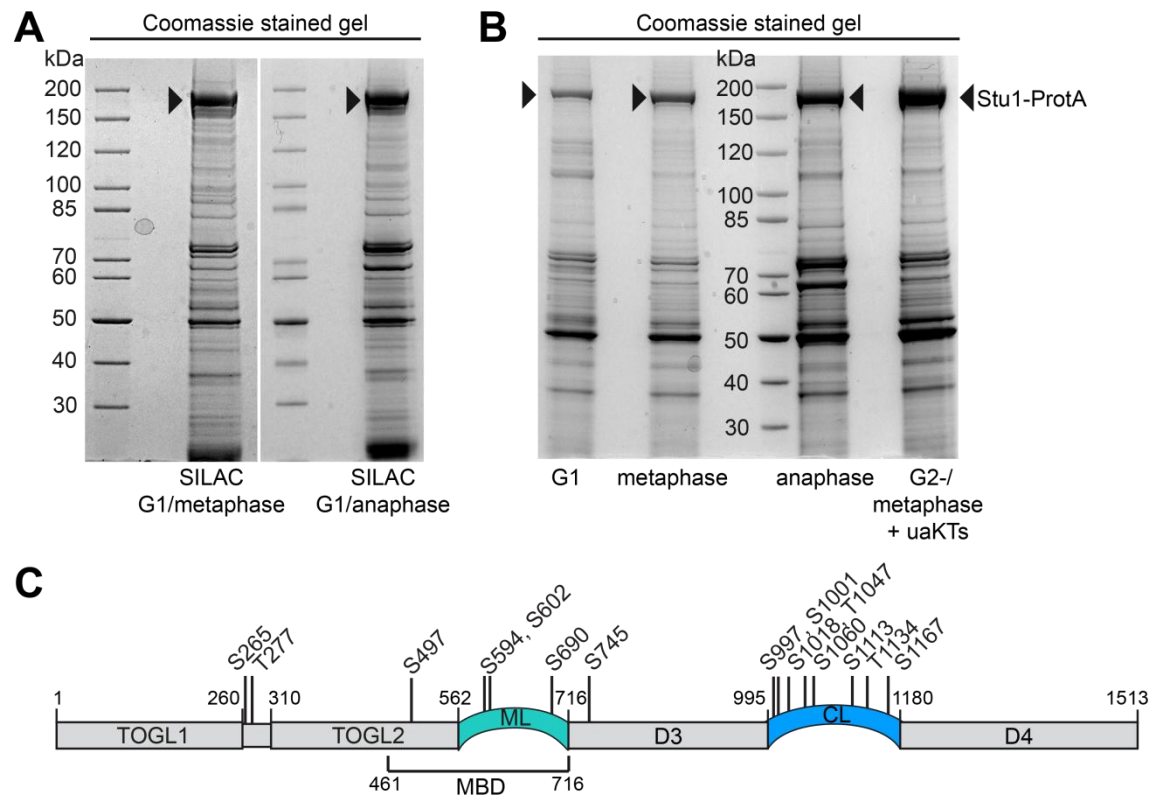


Figure 4-17. Phosphorylation acceptor sites cluster within the ML and the CL domain of Stu1.

(A) Stu1-ProtA was affinity purified using SILAC. Protein A-tagged Stu1 was purified from cells arrested in G1 and in G2-/metaphase (using nocodazole) or in anaphase (using a temperature-sensitive *cdc15-1* mutant) respectively. For each approach cells were combined and processed collectively. Black arrows indicate purified Stu1-ProtA. **(B)** Stu1-ProtA was affinity purified from cells arrested in G1, metaphase, anaphase and G2-/metaphase with unattached KTs. **(C)** Mass spectrometric analyses revealed 15 putative phosphorylation sites predominantly located within the ML and the CL domain. A model of Stu1 with identified phosphorylation sites is shown. The ML and the CL domain are highlighted in green and blue.

Detailed quantitative analysis of the SILAC results showed phosphorylation of Stu1 throughout the cell cycle (Fig. 4-18 A and B). In G1 especially serine 497, located within the TOGL2 domain, was found to be strongly phosphorylated, but was dephosphorylated in nocodazole or anaphase arrested cells. At unattached KTs (represented by results of the G2-/metaphase arrested cells), S745 in the D3 domain and three sites within the CL domain (T1047, S1113, T1134) were found to be more than 10 fold more phosphorylated than in G1. These sites were also accordingly more often phosphorylated in anaphase, indicating that they might get phosphorylated during the onset of mitosis and dephosphorylated after anaphase. In anaphase two additional sites (S265, T277) located between the TOGL1 domain and the TOGL2 domain were found to be strongly phosphorylated in comparison to G1.

Interestingly, the sites S594, S602 and S690 that are mainly located within the ML domain, were found to be phosphorylated in G1 and phosphorylation levels decreased by a factor of three when Stu1 localized to unattached KTs in prometaphase. Comparing phosphorylation levels of these sites from G1 and anaphase however revealed a five-fold increase in phosphorylation of Stu1 in anaphase. Taken together, these results indicate that Stu1 experiences a fifteen-fold increased phosphorylation from metaphase to anaphase at these sites. This alternating phosphorylation during the cell cycle and their location within the ML domain nominates them as interesting candidates to regulate the MT binding ability of Stu1.

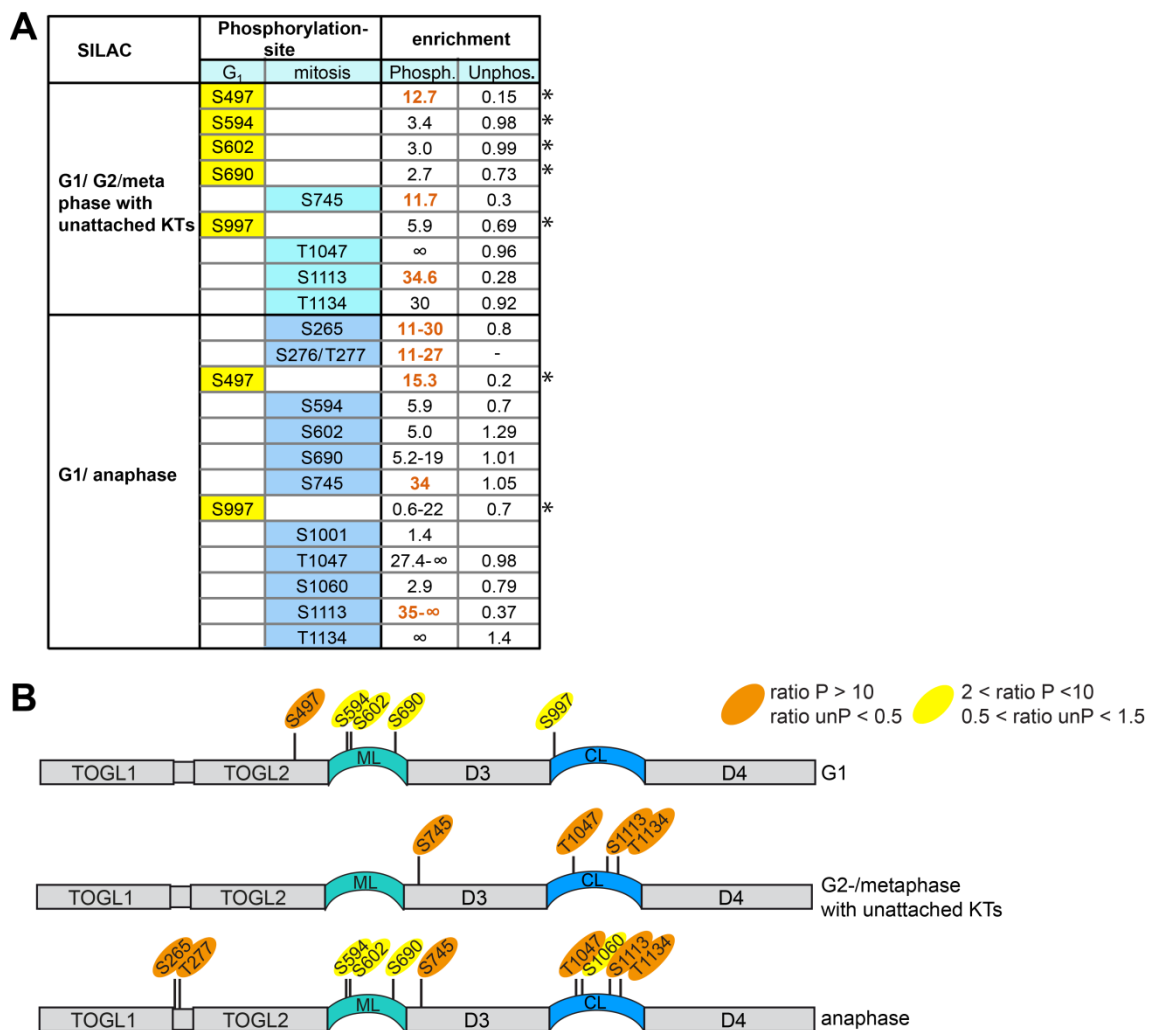


Figure 4-18 SILAC results suggest cell cycle dependent phosphorylation patterns of Stu1.

(A) Sites of Stu1 that were found to be phosphorylated in G1 or mitosis (G2-/metaphase or anaphase respectively) according to the SILAC assays were identified by mass spectrometry. The enrichment in phosphorylation was calculated for each site as the ratio between the intensity of the 'light' (from cells arrested in mitosis) and the 'heavy' (from cells arrested in G1) phosphorylated peptide (M/G1), as well as the corresponding unmodified peptide (for further explanation see 3.4.12). Asterisks indicate when the ratio was calculated vice versa (G1/M). Results were considered to be very significant when the ratio for the phosphorylated peptide (P) was higher than 10 and the ratio for the unphosphorylated peptide (unP)

was smaller than 0.5. These results are highlighted in orange. **(B)** Models of Stu1 in the different cell cycle stages depict the results shown in A. Sites predicted to be phosphorylated with a ratio > 10 are highlighted in orange, the ones with a ratio between 2 and 10 are highlighted in yellow.

Most of the suggested phosphorylation sites contain consensus sequences targeted by different kinases (Fig. 4-19). Sites like S497, S745 or S1167 are predicted phosphorylation sites for Cdk1, the major regulatory kinase of the cell cycle. Phosphorylation of S745 by Cdk1 would make this site suitable to serve as a polo-box binding motif. The sites S1001, T1047 and T1134 that are located within the CL domain could be targets for the polo-like kinase Cdc5. Similar consensus sequences (Fig. 4-19 A) also suggest S1001, T1047, S1113 and T1134 as targets of Mps1 phosphorylation. In addition, T277, S602 (and S690) are possible Ipl1 kinase sites.

A Consensus sequences

Cdk1: [pS/pT]-P or [pS/pT]-P-X-[K/R]
 Ipl1: [R/K]-X-[pS/pT]-[I/L/V]
 polo-like kinase: [D/E]-X-[pS/pT]- ϕ
 polo-box binding motif: S-[pS/pT]-[P/X]
 Mps1: [D/E]-X-[pS/pT]

B

predicted kinase	Cdk1	Ipl1	Rim11/ Ipl1	polo kinase	polo box	Mps1	Ste20	Cka 1/2	?
phospho. site	S497 S745 S1167	T277 S602	S690	S1001 T1047 T1134	S594 S745	S1001 T1047 S1113 T1134	S1060	S1018 S1113	S265 S997

Figure 4-19. Identified sites are predicted to be phosphorylated by different kinases.

(A) The determined consensus sequences for Cdk1 (Nigg, E. A., 1993), Ipl1 (Cheeseman, I. M. et al., 2002), the polo-like kinase (Nakajima, H. et al., 2003) and the polo-box binding motif (Elia, A. E. H. et al., 2003) that resembles a Cdk1 consensus site is depicted. Additionally, the consensus sequence for Mps1 (Dou, Z. et al., 2011) that is similar to the polo-like kinase motif is shown. pS/pT is the phosphorylated serine or threonine, the symbol ϕ indicates a hydrophobic amino acid, X stands for any amino acid. **(B)** Phosphorylation sites were arranged according to their predicted kinases. Kinase predictions are based on their known consensus sites as in A.

In conclusion, Stu1 is a protein that is phosphorylated throughout the cell cycle. The phosphorylation pattern certainly varies during the cell cycle and various kinases might contribute to these concerted modifications.

4.2.3 Ipl1 and Mps1 phosphorylate Stu1 *in vitro*

In order to determine if Stu1 indeed is a substrate of Ipl1 or Mps1, *in vitro* kinase assays with γ -[³²P]-ATP were performed using the N- or C-terminus of Stu1 as substrates. The His-tagged N-terminal (aa1-aa716) and C-terminal part (aa716-aa1513) of

Stu1 was expressed and affinity purified from *E. coli* cells using Ni-NTA beads. Additionally, Ipl1 together with its activator protein Sli15 (Ipl1-6xHis-Sli15-6xHis) and His-Mps1 were expressed and affinity purified. Incorporation of radioactive labeled $^{32}\text{PO}_4$ determined that Ipl1 (Fig. 4-20 A) as well as Mps1 (Fig. 4-20 B) have the capability to phosphorylate both termini of Stu1 *in vitro*. Stu1 N-terminus and Mps1 unfortunately could not be separated on SDS-PAGE due to the same molecular weight. An increase in signal intensity nevertheless suggests the Stu1 N-terminus as a substrate of Mps1 (Fig. 4-20 B). Kinase assays using cold ATP followed by mass spectrometric analysis determined T760, S1034, T1047, S1113 and T1134 as target sites for Mps1 phosphorylation *in vitro*. However, T760 and S1034 were never found to be phosphorylated *in vivo*. Probably due to the low amount of Ipl1 kinase and a low sequence coverage when analyzed by mass spectrometry, no phosphorylation sites could be determined for Ipl1 kinase *in vitro*. Taken together, Ipl1 as well as Mps1 can phosphorylate Stu1 *in vitro*. Both of them target the N-terminal and the C-terminal part of Stu1.

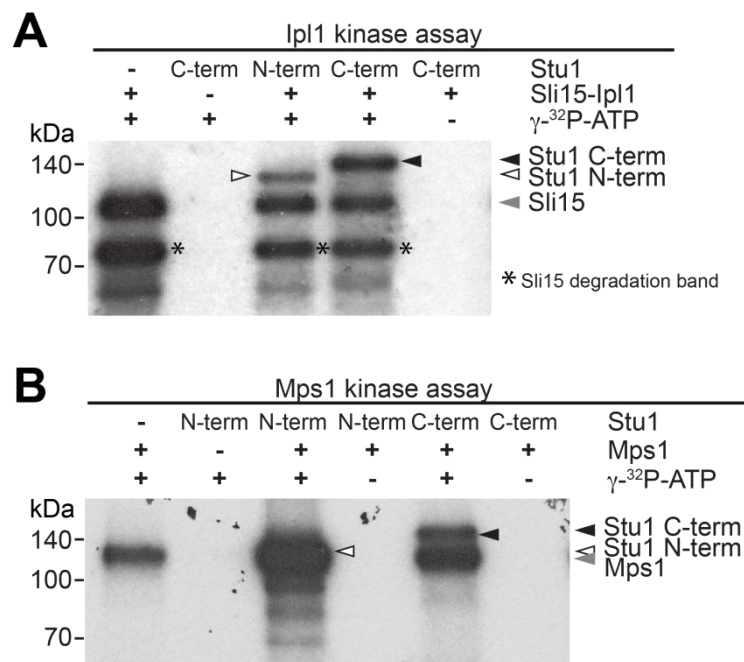


Figure 4-20. Stu1 N- and C-terminus get phosphorylated by Ipl1 and Mps1 *in vitro*.

(A) Ipl1 kinase is capable to phosphorylate Stu1 *in vitro*. His-tagged Stu1 N- and C-terminus and Ipl1-Sli15-His were expressed from *E. coli* cells and purified by Ni-NTA beads. Grey arrow indicates Sli15, also phosphorylated by Ipl1. Asterisks label phosphorylated Sli15 degradation bands. **(B)** Stu1 gets phosphorylated by Mps1 *in vitro*. Stu1 N- and C-terminus and Mps1 were expressed from *E. coli* cells and purified by Ni-NTA beads. Grey arrow indicates autophosphorylated Mps1.

4.2.4 Analysis of Stu1 phosphorylation mutants

As an approach to analyze the effect of Stu1 phosphorylation on the localization and function of the protein, identified phosphorylation sites were mutated to alanine and glutamate respectively. Mutation to alanine abolishes the phosphorylation of Stu1 at this site, whereas mutation to glutamate was used to mimic the negative charge that is created by the phosphorylation of a specific site of the protein. Subsequently, the phosphorylation mutants were analyzed in regards to the function of Stu1 in spindle formation and Stu1 localization to the spindle midzone (Fig. 4-21 A) and to unattached KTs (Fig. 4-21 B). In general the value of one or the average of two clones is depicted for each mutant. Phenotypic examples of spindle defects and Stu1 mislocalizations are depicted (Fig. 4-21) and were quantified accordingly in the following analyses. In some cases the capturing ability, bipolar attachment and SPB separation after nocodazole treatment were tested in addition.

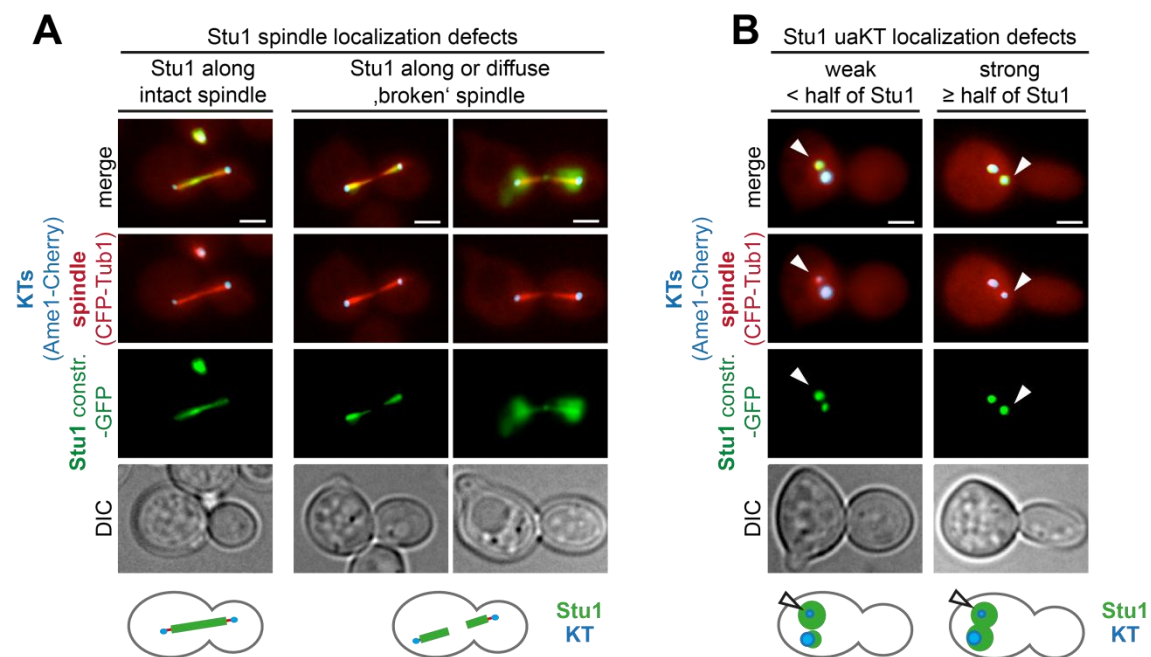


Figure 4-21. Phenotypic examples of spindle and Stu1 localization defects.

(A-B) Representative images of Stu1 localization defects caused by Stu1 mutations are shown; bar, 2 μ m. Schemes represent the phenotypes that are quantified in the following analyses. KTs are depicted in blue and Stu1 is in green. **(A)** Spindle phenotypes and Stu1 localization defects in anaphase. Cells were released from G1 arrest and analyzed after 120 min. **(B)** Stu1 mislocalization phenotypes in the presence of unattached KTs. Cells were released from a G1 arrest into nocodazole and analyzed 3 h later. Arrows indicate Stu1 at unattached KTs.

Simultaneous mutation of the majority of the identified phosphorylation sites (S497A, S602A, S690A, S745A, S1001A, S1018A, T1034A, T1047A, S1060A, S1113A, T1134A and S1167A) resulted in a severe defect in spindle formation and

Stu1 12A localization to the spindle midzone and to unattached KTs (Fig. 4-22). In 12 % of cells with intact spindles Stu1 localized along the spindle (Fig. 4-22 A). 55 % of anaphase spindles were broken and Stu1 localized along these residual spindles. 67 % of cells showed a strong and the residual 33 % a weak mislocalization for Stu1 to the SPB (Fig. 4-22 B). This indicated that phosphorylation indeed has a regulatory function for Stu1 localization, but did not allow further conclusions about the involvement of certain kinases or specific phosphorylation sites.

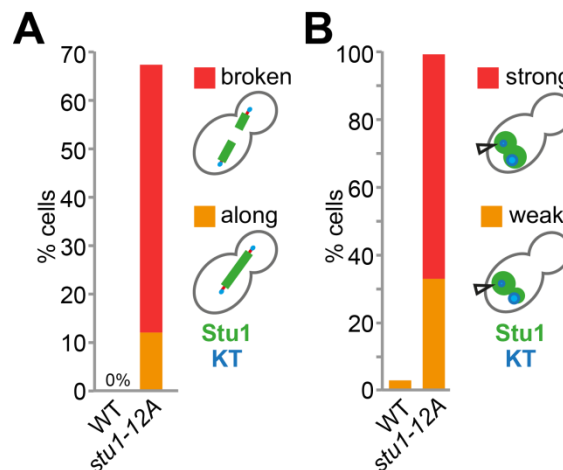


Figure 4-22. Mutation of multiple phosphorylation sites resulted in a severe spindle formation and Stu1 localization defect.

(A) Stu1-12A mislocalizes along the spindle and causes instable spindles. Cells were released from a G1 arrest and analyzed after 120 min. Spindle and Stu1 localization defects (see Fig. 4-21 A) were quantified as depicted. **(B)** Stu1-12A showed a strong localization defect to unattached KTs. Cells were released from a G1 arrest into nocodazole treatment and analyzed after 3 h. Stu1 localization defects (see Fig. 4-21 B) were quantified as depicted. Arrows indicate Stu1 at unattached KTs.

To gain more insight in the functional relevance of each phosphorylation site, mutants were created following different strategies. One approach was to simultaneously mutate phosphorylation sites that are modified during specific cell cycle stages (see Fig. 4-18). Secondly, single substitutions of the most prominent phosphorylation sites were created. Finally, phosphorylation sites were mutated according to the respective predicted kinases and according to their localization within the CL domain.

4.2.4.1 Analysis of Stu1 phosphomutants created according to SILAC results

SILAC results suggested the phosphorylation of S497 in G1 and dephosphorylation of this site in mitosis. The sites S745, T1047, S1113 and T1134 however are supposed to be phosphorylated when Stu1 localizes to unattached KTs in prometaphase and in

anaphase. In addition, sites S265 and T276 get phosphorylated when cells proceed into anaphase.

In order to investigate the biological significance of these sites for the function of Stu1, at first mutants were created that mimic the antagonistic phosphorylation state as predicted for Stu1 at unattached KTs. Therefore the phosphorylation of sites T1047, S1113 and T1134 was prevented by the mutation to alanine, whereas phosphorylation of S497 was mimicked by the mutation to glutamate. Unexpectedly, the mutations in *stu1-E+3A* (S497E, T1047A, S1113A, T1134A) cells caused only a mild average localization defect to unattached KTs (Fig. 4-23 B). Furthermore, the two analyzed clones considerably differed in the localization of Stu1-E+3A to unattached KTs (Fig. 4-23 C). Surprisingly, the additional mutation of S745 to alanine improved the localization of the mutated Stu1-E+4A (S497E, S745A, T1047A, S1113A, T1134A), which harbors mutations in all strong cell cycle dependent sites to WT localization. *stu1-E+7A* (S265A, S276A, T277A, S497E, S745A, T1047A, S1113A, T1134A) cells that harbor all mutations in strong cell cycle dependent sites and particularly mimic the opposite phosphorylation state as found for Stu1 in anaphase, did not cause any mislocalization of the mutated Stu1 (Fig. 4-23 A-C).

As a control, mutations were created that contain the opposite mutations, mimicking the phosphorylation states that Stu1 was predicted to have at unattached KTs and in anaphase respectively. *stu1-A+3E* (S497A, T1047E, S1113E, T1134E) and *stu1-A+4E* (S497A, S745E, T1047E, S1113E, T1134E) cells that mimic the phosphorylation state suggested for Stu1 localizing to unattached KTs showed a mild defect for spindle formation ('broken') and Stu1 localization to the midzone ('along') (Fig. 4-23 A). However, most notably, these mutations resulted in a quite strong localization defect of mutated Stu1 to unattached KTs, especially when additionally S745 was mutated to alanine (Fig. 4-23 B). Furthermore, two clones of *stu1-A+3E* and *stu1-A+4E* cells showed very differently severe phenotypes (Fig. 4-23 C). Moreover, the additional mutation of S265, S276 and T277 to alanine (Stu1-A+7E) resulted in a phenotype very similar to WT Stu1 (Fig. 4-23 A and B). The observed localization defects to unattached KTs are in conflict with the idea that mutations that reflect the phosphorylation of Stu1 at unattached KTs are not expected to cause a localization defect to unattached KTs. A possible explanation for the defects could be that the mutation to glutamate does not precisely reflect the phosphorylation of these sites. Nevertheless, how the additional mutation of certain sites can improve the Stu1 localization in this respect remains unclear.

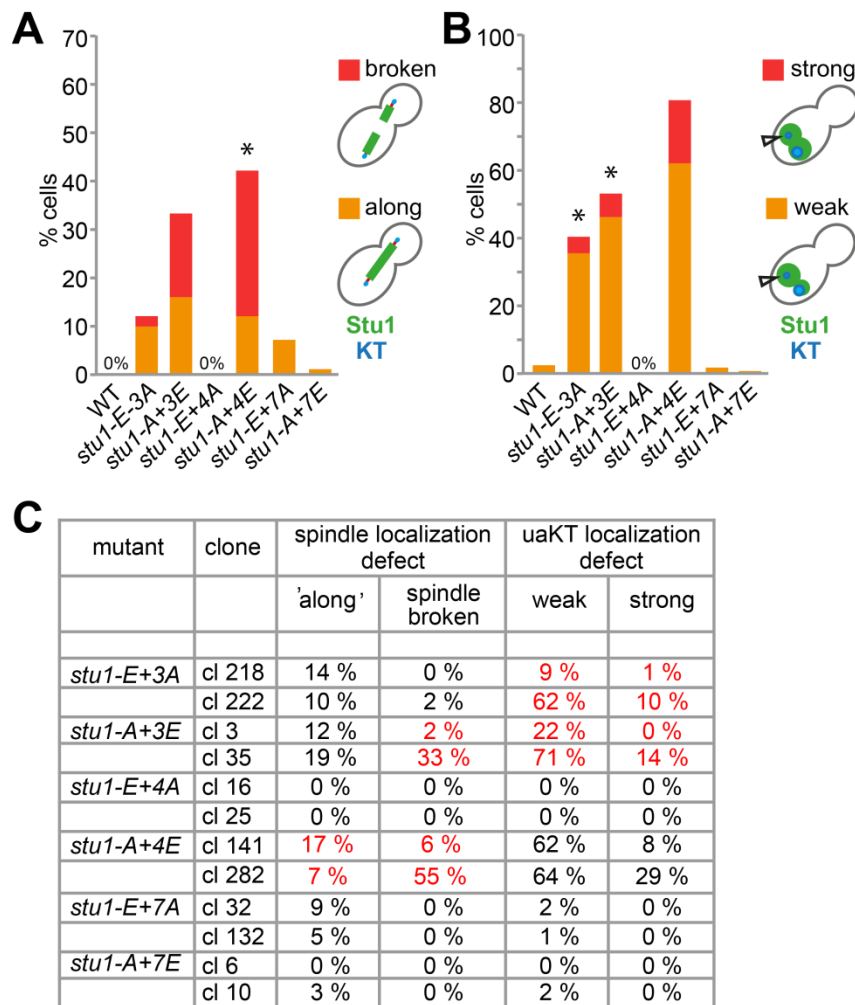


Figure 4-23. Analysis of cell cycle specific phosphomutants of Stu1.

(A) *stu1-A+3E* and *stu1-A+4E* cells showed a defect in spindle formation and Stu1 spindle localization, but *stu1-E+7A* cells did not. Cells were treated as in Fig. 4-21 A. The averaged data of two clones was depicted. Asterisks indicate when two clones showed very different effects; $n > 34$. (B) The Stu1 mutations in the *stu1-A+3E*, *stu1-E+3A* and *stu1-A+4E* cells, but not the *stu1-E+4A* cells resulted in a Stu1 localization defect to unattached KTs. Cells were treated as in Fig. 4-21 B and Stu1 localization defects were quantified. The averaged data of two clones was depicted. Asterisks indicate when two clones showed very different effects; $n > 70$. (C) Different clones of the same mutant had differently severe defects in *stu1-A+3E*, *stu1-E+3A* and *stu1-A+4E* cells. The table lists the values of each analyzed mutant clone. Values that differed severely from one clone to the other are highlighted in red.

In summary, these data propose that the cell cycle dependent phosphorylation of the identified sites that was suggested by the SILAC results does not exhibit the major regulatory function for the examined localizations and functions of Stu1. However, since different clones showed contrasting effects, it is difficult to draw firm conclusions from these investigations.

4.2.4.2 Phosphorylation site S1113 is responsible for the conformational change causing the mobility shift on SDS-PAGE

Analysis of the single substitution of S1113, located within the CL domain, to alanine and glutamate respectively revealed that phosphorylation of this site is solely responsible for the mobility shift of Stu1 on SDS-PAGE (Fig. 4-24 A). Mutation of S1113 to alanine resulted in a faster running protein form, whereas Stu1-S1113E appeared as a slower running form.

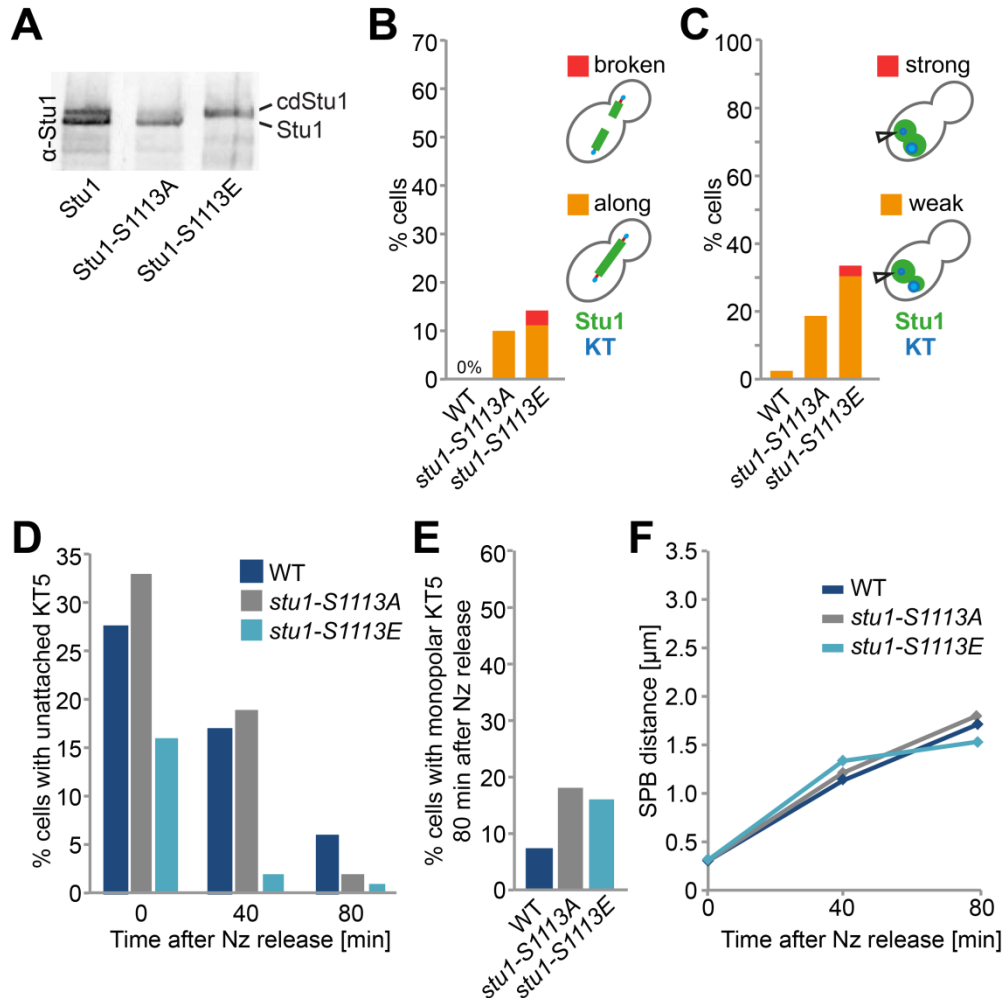


Figure 4-24. Phosphorylation of S1113 affects the mobility shift of Stu1 on SDS-PAGE.

(A) Modification of S1113 determines the mobility of Stu1 on the SDS-PAGE. Stu1-GFP constructs of protein extracts of asynchronized WT, *stu1-S1113A* and *stu1-S1113E* cells were detected using α -Stu1 antibody. **(B)** *stu1-S1113A* and *stu1-S1113E* cells showed only a mild defect in spindle formation and Stu1 spindle localization. Cells were treated as in Fig. 4-21 A. The data represent the average of two different clones; $n > 23$. **(C)** *Stu1-S1113A* and *Stu1-S1113E* caused only a very mild defect in Stu1 localization to unattached KT5. Cells were treated as in Fig. 4-21 B. The data represent the average of two individual clones; $n > 89$. **(D)** Capturing was slightly improved in *stu1-S1113E* cells compared to WT cells. Cells were released from G1 arrest into nocodazole. After 3 h, nocodazole was washed out and cells were analyzed for unattached KT5 at the indicated time points; $n > 67$. **(E)** *stu1-S1113A* and *stu1-S1113E* cells had a slightly increased bi-orientation defect. Cells were treated as in D and analyzed 80 min after nocodazole washout. Cells with a SPB distance larger than 3 μm were quantified for monopolar attached KT5; $n > 33$. **(F)** SPB separation in *stu1-S1113A* and *stu1-S1113E* cells is very similar to WT cells. Cells were treated

as in D, SPB distances were measured at the indicated time points after nocodazole release. To exclude the majority of cells that have already initiated anaphase, cells with SPB distances larger than 5 μm were excluded; $n > 42$.

Phosphorylations are thought to decrease the mobility of a protein due to the inhibited binding of SDS to the phosphorylated protein region. In the case of Stu1 however only one of many phosphorylation sites is responsible for the distinct mobility shift. This suggests that the phosphorylation of S1113 causes a conformational change that can be detected as a mobility shift on SDS-PAGE. Despite the very strong putative effect on the conformation of Stu1, these mutations only caused a very mild defect in Stu1 localization to spindles or to unattached KT5s (Fig. 4-24 B and C). Unexpectedly, the mutation to glutamate (*stu1-S1113E*), which should reflect Stu1 phosphorylation at unattached KT5s, even showed a stronger localization defect to unattached KT5s than the mutation to alanine (Fig. 4-24 C). Consistent with the *stu1 Δ CL* mutant, which also has a defect in unattached KT5 localization, this mislocalization also resulted in an improved capturing phenotype (Fig. 4-24 D). Only 16 % of KT5s detached upon nocodazole treatment in *stu1-S1113E* cells and only 2 % of unattached KT5s were detectable 40 min after nocodazole washout. *stu1-S1113A* cells did not capture much differently than WT cells. Both mutants showed a slightly higher number of monopolar KT5s after nocodazole release (Fig. 4-24 E), but separated their SPBs with a similar timing than WT cells (Fig. 4-24 F).

Conclusively, the strong effect of the modification of serine 1113 on the mobility of Stu1 on SDS-PAGE and therefore most likely on the conformation of Stu1, was not reflected by any of the analyzed Stu1 localization phenotypes or Stu1 functions.

4.2.4.3 Analysis of single mutations of Stu1 phosphorylation sites

To avoid compensatory effects of the multiple mutations based on the SILAC analyses, single mutants of the most prominent phosphorylation sites were analyzed. Cells containing Stu1-S497A, Stu1-S497E, Stu1-S745A or Stu1-S1001A did not show a phenotype distinguishable from WT cells when analyzed for spindle localization and recruitment to unattached KT5s (Fig. 4-25 A and B). *stu1-S745E*, *stu1-T1047A* and *stu1-T1134A* cells had a very mild defect in spindle formation and Stu1 midzone localization in anaphase, but an increased mislocalization of Stu1 to SPBs (Fig. 4-25 A and B). In average, the mutation of S602 to alanine or to glutamate produced a quite severe defect of Stu1 localization to spindles or to unattached KT5, but individual clones revealed differently strong phenotypes (Fig. 4-25 C).

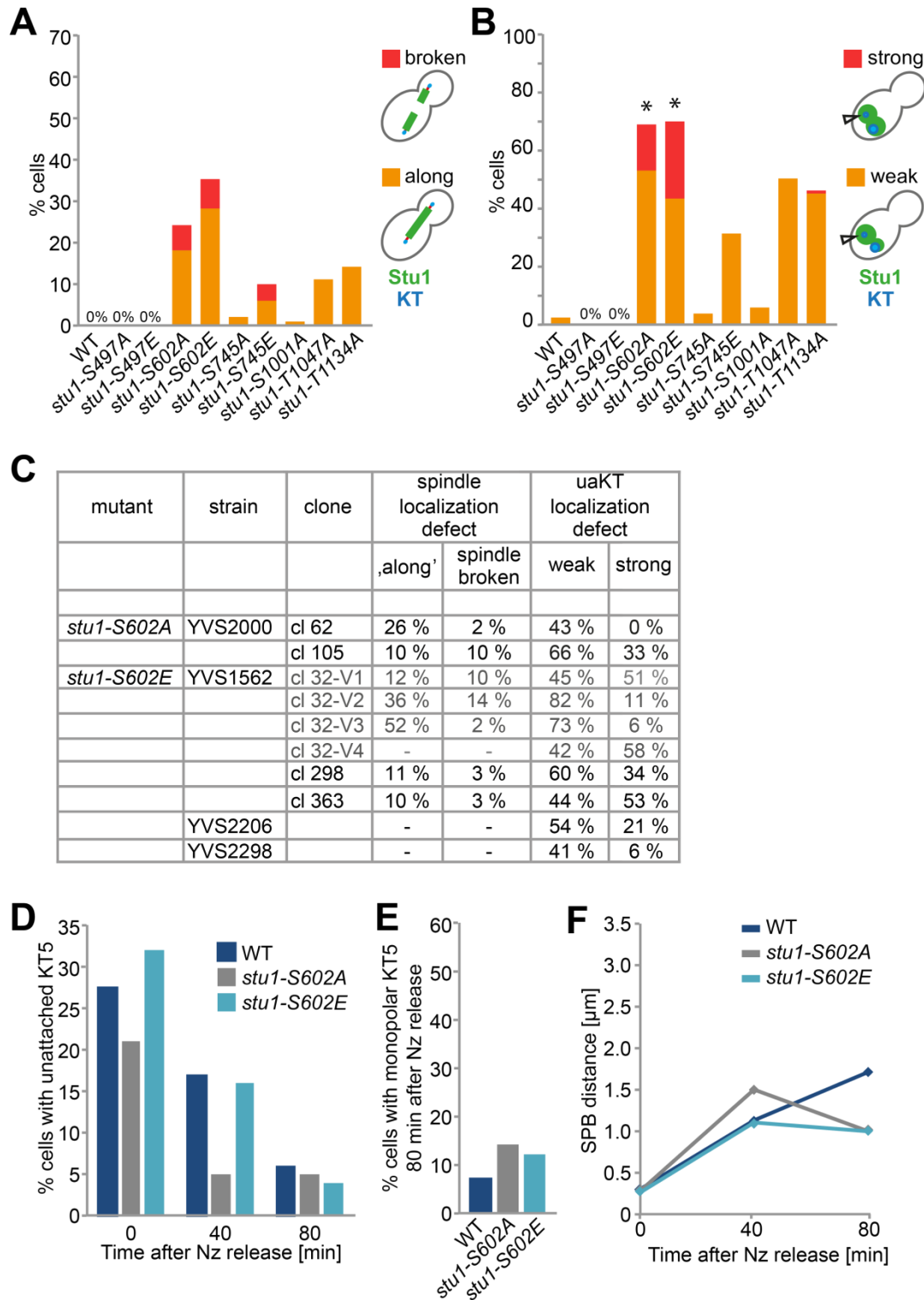


Figure 4-25. Analysis of single phosphomutants of Stu1.

(A) *stu1-S602A* and *stu1-S602E* cells in average showed a defect in spindle formation and Stu1 spindle localization. Cells were treated as in Fig. 4-21 A. The data represent the average of one to three different clones; $n > 31$. **(B)** In average, *stu1-S602A* and *stu1-S602E* cells had a quite strong defect of Stu1 localization to unattached KT5. Mutation of T1047 and T1134 to alanine resulted in a mild mislocalization of Stu1 to SPBs. Cells were treated as in Fig. 4-21 B. The data represent the average of one or more individual clones; $n > 73$. Asterisks indicate that different clone showed differently severe phenotypes. **(C)** Different clones of the same mutant or differently integrated Stu1 constructs varied in the strength of

their defects in *stu1-S602A* or *stu1-S602E* cells. The table lists the values of each analyzed mutant clone. Strain YVS2298 contained Stu1-S602E-GFP integrated at the *LYS2* locus whereas all other Stu1-S602E-GFP constructs were integrated at the endogenous *STU1* locus using the *kITRP1* marker. V1-V4 indicate individual experiments with the same clone 32. **(D-F)** Analyzed cells contain mutated Stu1-GFP constructs integrated in the *LYS2* locus. **(D)** *stu1-S602A* cells captured KT5s slightly faster than WT cells. Cells were treated and analyzed as in Fig. 4-23 C; $n > 116$. **(E)** *stu1-S602A* and *stu1-S602E* cells showed a mild bipolar attachment defect. Cells were treated and analyzed as in Fig. 4-24 E; $n > 42$. **(F)** *stu1-S602A* cells separated their SPBs somewhat faster than WT cells. Cells were treated as in Fig 4-24 F; $n > 62$.

The two analyzed clones of *stu1-S602A* cells already showed differently severe localization defects to unattached KT5s, but this was even more distinct in *stu1-S602E* cells. Weak mislocalization ranged from values of 42 to 82 %, whereas a strong defect was detectable in a range from 6 to 58 % of cells. Not only different clones and strains varied in their phenotypes, but also the same clone in different experiments. This allowed only the conclusion that the mutation of S602 to glutamate might result in a localization defect of Stu1-S602E to unattached KT5s, but the strength of this defect remained unclear.

In agreement with the *Stu1 Δ CL* mutant, the mild mislocalization of Stu1-S602A to the vicinity of the SPB resulted in a slightly faster capturing of unattached KT5s (Fig. 4-25 D), a mild increase in monopolar attached KT5s (Fig. 4-25 E) and a slightly increased velocity of SPB separation (Fig. 4-25 F). However, the same analyses of Stu1-S602E integrated in the *LYS2* locus revealed no significant difference in capturing and bi-orientation or SPB separation when compared to WT cells (Fig. 4-25 D-F). SPBs separated a bit faster than in WT cells, but did not move apart precociously (Fig. 4-25 F). One possible explanation for the varying localization defects of Stu1-S602E could be different expression levels of this Stu1 construct dependent on the way of integration (see discussion).

4.2.4.4 Analysis of Stu1 phosphomutants according to predicted kinases

Another approach to analyze the phosphorylation of Stu1 was to address the phosphorylation sites according to their predicted kinases. Mutation of the putative Cdk1 (S497A, S745A, S1167A) and polo-like kinase (S1001A, T1034A, T1047A, T1134A) sites did not cause any spindle phenotype different from WT cells, but showed a mild localization defect of the mutated Stu1 to unattached KT5s, especially in *stu1-polo-4A* cells (Fig. 4-26 A and B). According to *stu1 Δ CL* cells, mislocalization in *stu1-polo-4A* cells also resulted in improved KT capturing (Fig. 4-26 C) and an increased bi-orientation defect (Fig. 4-26 D), most likely caused by the precocious SPB separation (Fig. 4-26 E). *stu1-Cdk1-3A* cells showed the same phenotypes in a milder extent, but

surprisingly did not separate the SPBs prematurely (Fig. 4-26 C-D). Therefore, the reason for the slightly increased bipolar attachment defect remained unclear.

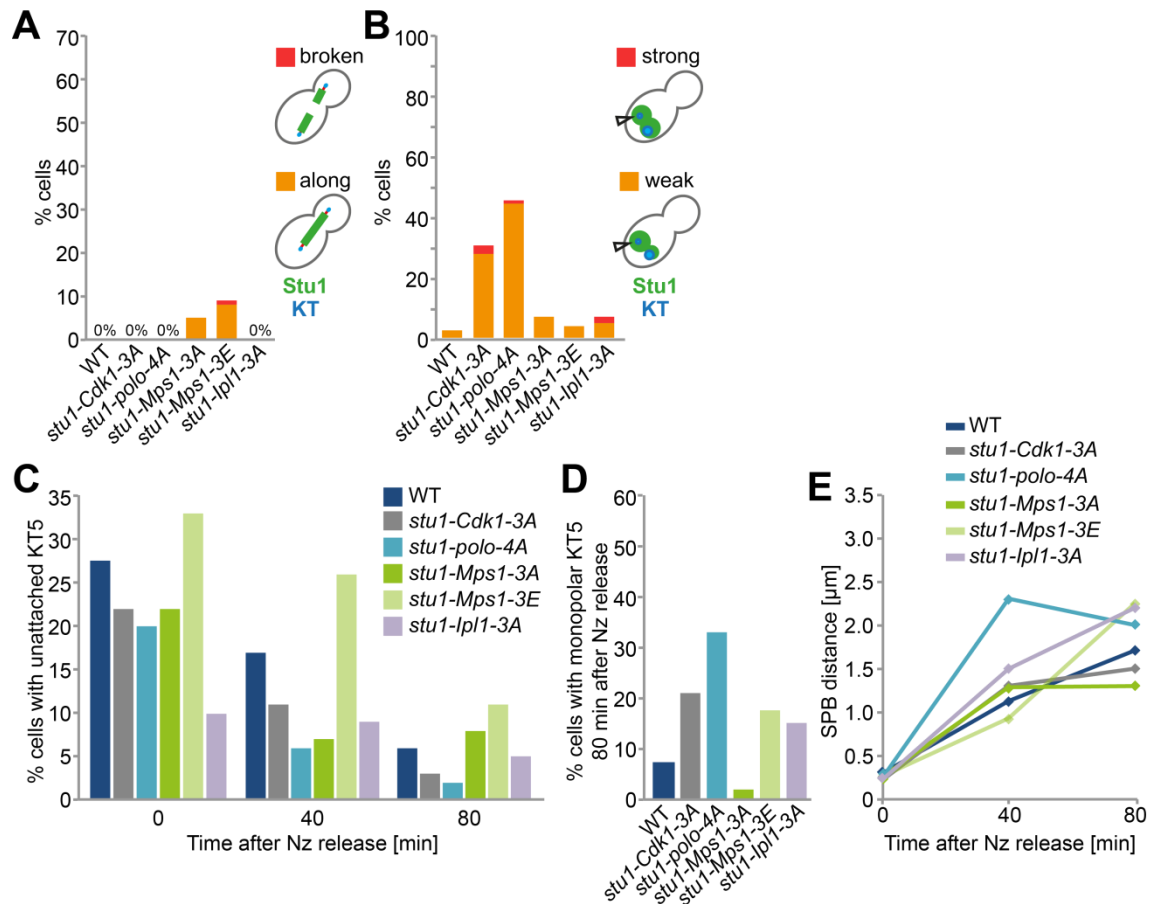


Figure 4-26. Phosphorylation of the CL domain by polo-like kinase might have a regulatory function for Stu1 sequestration at unattached KT5.

(A) *stu1-Mps1-3A* and *stu1-Mps1-3E* cells showed a very mild defect in spindle localization of Stu1. Cells were treated and analyzed as in Fig. 4-21 A; $n > 23$. (B) *stu1-Cdk1-3A* and *stu1-polo-4A* cells showed a defect of Stu1 localization to unattached KT5. Cells were treated as in Fig. 4-21 B; $n > 77$. (C) *stu1-Mps1-3E* cells displayed a capturing defect, whereas *stu1-Cdk1-3A* cells and *stu1-polo-4A* cells showed improved capturing. Cells were treated and analyzed as in Fig. 4-23 D; $n > 76$. (D) Analysis of *stu1-Cdk1-3A* cells and *stu1-polo-4A* cells revealed a mild bipolar attachment defect. Cells were treated and analyzed as in Fig. 4-23 E; $n > 55$. (E) *stu1-polo-4A* cells precociously separated their SPBs. Cells were treated and analyzed as in Fig. 4-23 F; $n > 61$.

Mutation of three possible Mps1 phosphorylation sites (T1047, S1113, T1134) to alanine or glutamate resulted in both cases in a very mild spindle localization defect (Fig. 4-26 A), but no significantly increased localization defect to unattached KT5. *stu1-Mps1-3E* cells showed a high number of unattached KT5s when treated with nocodazole and capturing was slower than in WT cells (Fig. 4-26 C and D). This might also be the reason for the faintly increased bi-orientation defect and the delayed SPB separation (Fig. 4-26 D and E). *stu1-lpl1-3A* cells that contain the sites S276, T277 and

S602 mutated to alanine did not show any severe localization defect to spindles or to unattached KT5s (Fig. 4-26 A and B). Cells started with a low number of unattached KT5s when treated with nocodazole and therefore already had captured most of the KT5s 40 min after nocodazole release (Fig. 4-26 C). This could also explain the somewhat faster SPB separation compared to WT cells (Fig. 4-26 E). Besides that, *stu1-lp1-3A* cells showed a slightly increased bipolar attachment defect.

Taken together, these data suggest that the polo-like kinase could indeed be part of the regulatory machinery that sequesters Stu1 at unattached KT5s in order to prevent precocious SPB separation and to ensure proper bipolar attachment. In addition, the dephosphorylation of phosphorylation sites targeted by Mps1 (or polo-like kinase) could be important to achieve efficient capturing and therefore SPB separation on time.

4.2.4.5 Analysis of Stu1 phosphorylation sites located in the CL domain

The results above indicate that mutations in the CL domain contribute to the regulation of Stu1 localization via the CL domain. To test if this is indeed the case, phosphorylation of the CL domain was mostly prevented by the mutation of 12 potential phosphorylation sites (S997, S1000, S1001, S1003, T1005, S1018, T1034, T1047, S1060, S1113, T1134, S1167) located within the CL domain to alanine.

Stu1-CL-12A localized to the midzone of anaphase spindles like WT *Stu1*, but weakly mislocalized to the vicinity of SPBs in 55 % of cells (Fig. 4-27 A and B). Similar to *stu1-ΔCL* cells, this resulted in an improved capturing of unattached KT5s (Fig. 4-27 C), but a high number of cells with monopolar attached KT5s (55 %) 80 min after cells were released from nocodazole (Fig. 4-27 D). Most likely also in these cells the precocious SPB separation (Fig. 4-27 E) is the main reason for the increased bi-orientation defect.

In conclusion, the phenotype of the *stu1-CL-12A* mutant resembles the phenotype of *stu1-ΔCL* cells, but reveals milder effects. This supports the idea that the CL domain indeed contributes to the regulation of the *Stu1* localization to unattached KT5s and therefore delays precocious SPB separation to allow for KT5s to bipolarly attach. This regulation might be achieved by the multiple phosphorylation of the CL domain.

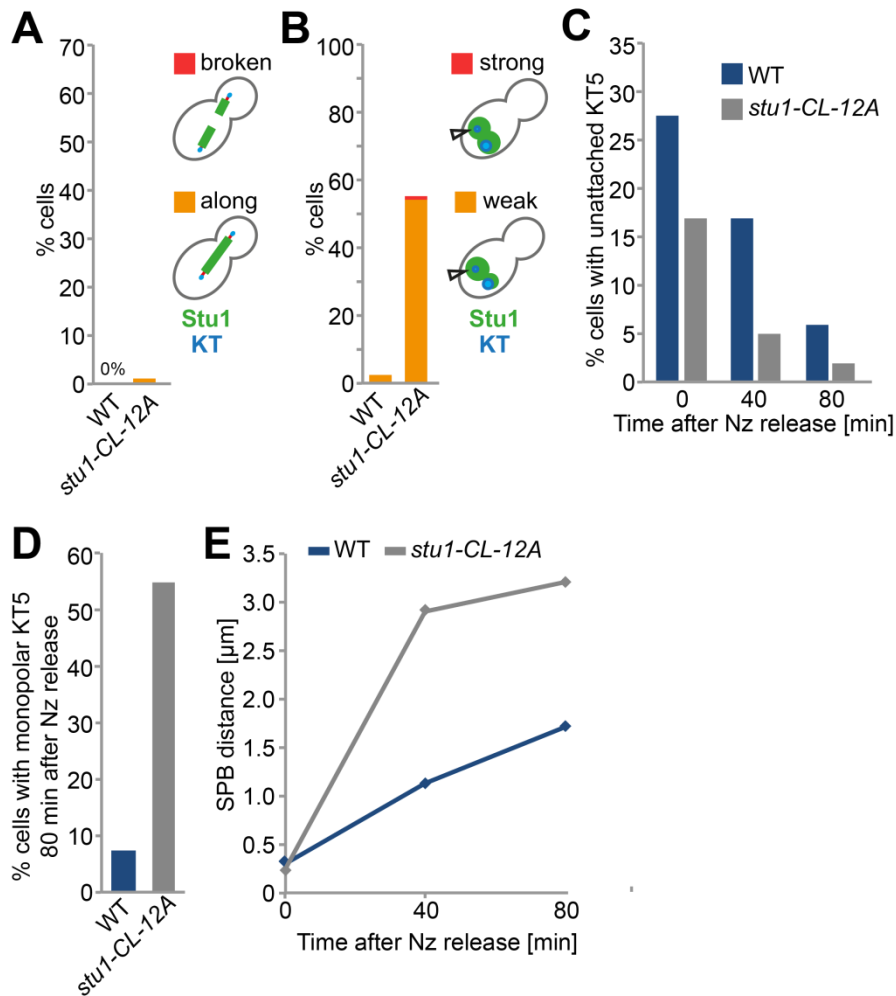


Figure 4-27. Phosphorylation of the CL domain is important for efficient Stu1 sequestration at unattached KTs.

(A) *stu1-CL-12A* cells did not show a defect in Stu1-CL-12A localization to the midzone of anaphase spindles. Cells were treated and analyzed as in Fig. 4-21 A. The data represent the average of two different clones; $n > 33$. **(B)** Stu1-CL-12A weakly mislocalized to SPBs. Cells were treated as in Fig. 4-21 B. The data represent the average of two different clones; $n > 100$. **(C)** *stu1-CL-12A* cells showed improved KT capture. Cells were treated and analyzed as in Fig. 4-23 D; $n > 125$. **(D)** *stu1-CL-12A* cells had a severe bipolar attachment defect. Cells were treated as in Fig. 4-23 E; $n > 66$. **(E)** *stu1-CL-12A* cells precociously separated their SPBs. Cells were treated and analyzed as in Fig. 4-23 F; $n > 73$.

5 DISCUSSION

5.1 An interplay of Stu1 domains regulates Stu1 localization and controls TOGL2 activity

S. cerevisiae Stu1 is an essential protein that was found to have several functions during mitosis. In S-phase Stu1 facilitates capturing of unattached KTs. In metaphase, Stu1 is required to establish and maintain metaphase spindles and kMTs. In anaphase it is found in the midzone of anaphase spindles stabilizing the overlap of interpolar MTs (Funk, C. et al., submitted; Ortiz, J. et al., 2009). In order to be able to fulfill all these diverse functions, Stu1 has to be differently localized during each cell division (see Fig. 5-1). The intention of this work was to gain more insight in the precise and flexible regulation of Stu1 during mitosis.

5.1.1 Metaphase spindle formation requires the TOGL2 activity of binding free tubulin

Stu1 belongs to the family of CLASP proteins which promote MT polymerization and/or rescue by providing free tubulin bound via their TOG domains (Al-Bassam, J. et al., 2010, 2011). Stu1 also forms a stable complex with free tubulin (see 4.1.2.1; Funk, C. et al., submitted). Co-immunoprecipitation revealed that the TOGL2 domain of Stu1 alone is sufficient to bind free tubulin *in vivo* and that the intact intra-HEAT repeat loops of the TOGL2 domain are mandatory for this function. Recent findings showed that the TOGL1 domain, which is less conserved when compared to other homologs, is not able to copurify tubulin (Funk, C. et al., submitted). Thus, Stu1 indeed has a tubulin binding capability as demonstrated for CLASP homologs of other organisms before. However, in contrast to earlier studies on CLASP proteins like the *S. pombe* Cls1 (Al-Bassam, J. et al., 2010) or the related XMAP215 proteins (Al-Bassam, J. et al., 2011), Stu1 only uses the second TOGL domain to achieve the interaction with free tubulin. The result that the TOGL2 domain of Stu1 is sufficient to bind free $\alpha\beta$ -tubulin is in agreement with the findings that the TOG1 (Al-Bassam, J. et al., 2006) and TOG2 (Ayaz, P. et al., 2012) domains of XMAP215 Stu2 can bind free $\alpha\beta$ -tubulin *per se*. The way the TOG1 domain interacts with the tubulin heterodimer even excludes a concurrent binding of the same heterodimer by a second TOG domain (Ayaz, P. et al., 2012), indicating that each TOG domain might bind one $\alpha\beta$ -tubulin on its own. In addition, recent work on the *D. melanogaster* homolog MAST/Orbit revealed that the TOGL1 do-

main, which is also less conserved as it is the case for Stu1, is not able to bind heterotubulin *in vitro* (De la Mora-Rey, T. et al., 2013). This suggests that MAST might also interact with $\alpha\beta$ -tubulin via the TOGL2 domain.

This work revealed that the TOGL2 domain, more precisely the ability of the TOGL2 domain to bind tubulin, is absolutely mandatory for the formation of (metaphase) spindles (see 4.1.2.2). Deletion of the TOGL2 domain or impairing the tubulin binding by the mutation of the TOGL2 tubulin binding interface abolished the separation of SPBs. In support of this finding, not only the TOGL2 domain of Stu1, but especially the ability of this domain to bind tubulin is essential for the cell (see 4.1.1; Funk, C. et al., submitted). Correspondingly, preventing tubulin binding by mutating the same conserved intra-HEAT repeat loops in the *S. pombe* homolog Cls1 also caused nonviable cells and spindle instability (Al-Bassam, J. et al., 2010). Within the XMAP215 family multiple domains, mainly TOG1 and TOG2, contribute to increase the affinity to free tubulin and this affinity correlates with the polymerase activity of the protein (Widlund, P. O. et al., 2011). However, how many TOGL domains contribute to polymerization or rescue activity in CLASP proteins remained unclear so far. The data of this thesis suggest that the *S. cerevisiae* CLASP Stu1 only requires one TOGL domain for the polymerizing activity. The fact that the deletion of the TOGL1 domain did not result in a defective SPB separation and spindle formation (Funk, C. et al., submitted) supports that the TOGL2 domain is not only the sole tubulin binding domain, but also solely responsible for the polymerizing function of Stu1. Taken together, these data emphasize that the function of the Stu1 TOGL2 domain in providing free tubulin is highly important for the formation and maintenance of the spindle and, as a consequence, for the survival of the cell. In addition, these data suggest that the Stu1 TOGL2 domain alone fulfills the function of a MT polymerase or a rescue-promoting factor.

Even when the TOGL2 domain of a Stu1 monomer is sufficient to bind tubulin, the dimerization of Stu1 might enhance the stability of this interaction with free tubulin and improve the function of Stu1 as it was demonstrated for the *S. pombe* CLASP Cls1 and the *S. cerevisiae* XMAP215 Stu2 (Al-Bassam, J. et al., 2006, 2010).

In agreement with the fact that part of the TOGL2 domain was determined to contribute to the MBD domain (Yin, H. et al., 2002), the deletion of the TOGL2 domain weakened the binding of Stu1 to the MT lattice of metaphase spindles. This indicates that (part of) the TOGL2 domain might support the binding to the MT lattice. Such a function was also predicted for the *D. melanogaster* CLASP homolog MAST. Whereas the TOGL1 domain was suggested not to interact with free tubulin (De la Mora-Rey, T. et al., 2013), the TOGL2 domain seems to be able to fulfill two distinct functions. On

the one hand the tubulin binding interface binds to the MT lattice probably by undergoing a conformational change, on the other hand MAST TOGL2 was found to promote MT polymerization *in vitro* (Leano, J. B. et al., 2013). Stu1TOGL2-4A, however, which contains an intact MBD domain, but an impaired tubulin binding interface showed a quite similar localization to the MT lattice as WT Stu1. This indicates that the tubulin binding interface *per se* is not important for the MT lattice binding of Stu1. Therefore, mislocalization of Stu1 is very unlikely to be the reason for the lethal spindle defect, especially because Stu1 Δ ML shows a much more severe localization defect to the MT lattice, but nevertheless is able to form anaphase spindles.

In order to investigate if the function of the TOGL2 domain of Stu1 is evolutionary conserved, chimeric Stu1 constructs were analyzed. Previous findings revealed that the TOG1 domain of *S. cerevisiae* XMAP215 Stu2 and the TOGL2 domain of *H. sapiens* CLASP1 are individually sufficient for tubulin binding (Al-Bassam, J. et al., 2006; Leano, J. B. et al., 2013). However, the chimeric constructs that contain the TOGL2 domain of Stu1 replaced by the Stu2 TOG1 domain and the CLASP1 TOGL2 domain respectively, were not able to achieve spindle formation or capturing, two functions that are strongly impaired in *stu1* Δ *TOGL2* cells. It remains to be tested if these chimeric constructs are indeed still able to bind free tubulin, but it was shown for the TOG1 domain of Stu2 *in vitro* (Al-Bassam, J. et al., 2006) and for Stu1 TOGL2 *in vivo* (this work) that they can bind tubulin independent of the surrounding protein structure.

The data suggest that the TOGL2 domain of Stu1 has a specific essential function that cannot be simply substituted by another tubulin binding TOG domain. This is astonishing, since the intra-HEAT repeat loops of the TOGL2 domain of Stu1 and CLASP1, which form the interface for tubulin interaction, are highly conserved in their amino acid composition (Al-Bassam, J. et al., 2011). On the other hand, slight variations in the sequence of intra-HEAT repeat loops are suggested to determine the different kinetics of tubulin binding and release (Al-Bassam, J. et al., 2011). In addition, despite the strong conservation of tubulin interacting intra-HEAT repeat loops of Stu2 TOG1 and CLASP1 TOGL2, the conformation of the TOG domain and especially the tubulin interaction was predicted to be drastically different between these two domains (Leano, J. B. et al., 2013). These data support the idea that the function of TOG domains is not just simply the binding and release of free tubulin, but that the underlying mechanism and concerted activity of these domains is more complex and regulated.

5.1.2 MT lattice binding via the ML domain is required for metaphase, but not anaphase spindle formation

In addition to the TOGL2 domain, the ML domain is required for the efficient formation of metaphase spindles. In agreement with the fact that this domain is part of the proposed MBD (Yin, H. et al., 2002), the ML domain seems to mainly achieve the binding of Stu1 to the MT lattice. This serine-rich domain is highly basic with a predicted pI of 10.4 and a strongly positive net charge which might be responsible for the affinity to MTs. This is consistent with the findings of the *S. pombe* homolog Cls1 or the *S. cerevisiae* XMAP215 Stu2 – both proteins use a basic linker region to bind to the lattice of MTs (Al-Bassam, J. et al., 2006, 2010).

Together with the finding that dimerization is important for efficient spindle formation (Funk, C. et al., submitted), a possible model would be that the ML domains of a Stu1 dimer (probably supported by the TOGL2 domains) are required for efficient localization of Stu1 to the MT lattice (see Fig. 5-1 E). Being at the right place, the TOGL2 domains could release the bound tubulin and therefore drive efficient spindle polymerization in metaphase. Thereby it is unclear if Stu1 indeed promotes the incorporation of tubulin in the growing MT, serving as a polymerase or if Stu1 releases tubulin to increase the local tubulin dimer concentration which then facilitates MT polymerization.

Although *stu1 Δ ML* cells are compromised in metaphase spindle formation, the ML domain is dispensable for the formation of anaphase spindles (see 4.1.2.4). Neither the ML, nor the TOGL2 domain is required for the localization of Stu1 to the midzone of inter-polar MTs in anaphase. This indicates that midzone positioning of Stu1 is independent of the Stu1 interaction with the MT lattice, but based on another mechanism. In support of this, the interaction with the midzone, in contrast to the localization to the metaphase spindle (Funk, C. et al., submitted), is dependent on Ase1 (Khmelniskii, A. et al., 2007). Since the D4 domain is obligatory for Stu1 midzone localization independent of its dimerizing function (Funk, C. et al., submitted), this domain might directly provide the interaction with another midzone protein (see Fig. 5-1 H). For instance, the midzone localization of the *S. pombe* homolog Cls1 is mediated by a direct interaction with Ase1 (Bratman, S. V. et al., 2007) and the *X. laevis* homolog CLASP was found to copurify with Ase1/PRC1 when isolated from *Xenopus* egg extracts (Patel, K. et al., 2012). Since there is no evidence for a direct interaction of Stu1 and Ase1 so far, further studies will be required to detect the interaction partner of Stu1 at the spindle midzone.

These data suggest that the way Stu1 is binding to MTs changes during meta- to anaphase transition. In metaphase, spindles have to stay short, but resist the antagonizing forces of tension on the KT-MT interface to prevent SPB collapse. Thereby, a Stu1 dimer could stabilize the spindle by crosslinking or bundling antiparallel MTs and providing tubulin (see Fig. 5-1 D and E). Upon cleavage of cohesin at anaphase onset, this rigid crosslinking would be a hindrance for the fast elongation of anaphase spindles by the gliding of antiparallel MTs. Therefore, Stu1 dissociates from MTs, but midzone localization is ensured by the interaction with another protein (see Fig. 5-1 G and H). This allows gliding, but at the same time stabilizes the interpolar MT overlap by providing free tubulin. A previous study already suggested that CLASP proteins support midzone stability by contributing to the incorporation of tubulin at the plus-ends of the overlapping interpolar MTs (Pereira, A. L. et al., 2006).

5.1.3 Stu1 localizes to attached KTs in metaphase and regulates kMT formation

CHIP analyses revealed that Stu1 does not only accumulate at unattached KTs (Ortiz, J. et al., 2009), but also localizes to attached KTs in metaphase (Funk, C. et al., submitted). This localization is dependent on dimerization of Stu1 and the TOGL1 domain (Funk, C. et al., submitted). Interestingly, in contrast to unattached KTs, the ML domain, but not the CL domain is required for the interaction with attached KTs (Funk, C. et al., submitted), indicating that a simultaneous interaction with the MT lattice might be required for the binding of Stu1 to attached KTs. The absence of Stu1 from attached KTs in *stu1 Δ TOGL1* cells resulted in very short kMTs (Funk, C. et al., submitted), indicating that Stu1 and its KT localization is important for the polymerization of these MTs. This is in agreement with the previous findings that depletion of CLASP homologs in *Drosophila* or human cells resulted in the formation of monopolar asters with chromosomes close to the collapsed centrosomes, indicating that kMTs are very short (Maiato, H. et al., 2002, 2003). In addition, CLASP proteins are suggested to regulate the dynamics of kMTs by mediating the incorporation of MT subunits at the KTs (Maiato, H. et al., 2005). Since yeast CLASPs were not found to localize to plus-ends of MTs, the attached KT could serve as a factor to accumulate Stu1 in close proximity to kMT plus-ends. This might be necessary to ensure efficient Stu1 activity for kMT polymerization. For instance, only certain local concentrations of *S. pombe* CLASP molecules are sufficient to induce MT rescue events *in vitro* (Al-Bassam, J. et al., 2010).

Interestingly, *stu1* Δ *CL* cells showed slightly longer kMTs than WT cells (see 4.1.4.2). This effect was even increased upon the deletion of Cin8, a protein suggested to have a depolymerizing function on kMTs (Gardner, M. K. et al., 2008). Cin8 promotes plus-end disassembly of kMTs specifically in response to an increasing kMT length. This length-dependent regulation of kMT assembly allows chromosome congression, but also a balanced tension on the KT-MT interface (Gardner, M. K. et al., 2008). In agreement with this, the findings suggest that the CL domain of Stu1 has an inhibitory function on the polymerizing or rescue activity of Stu1 that is antagonized at least partially by Cin8. Upon the additional deletion of Cin8 the equilibrium between polymerization by Stu1 and depolymerization is shifted, resulting in over-elongated kMTs. Since the polymerization of kMTs does not seem to be unlimited, other depolymerizing proteins might still counteract the polymerizing activity of Stu1. Kip1 for example was also found to suppress kMT plus-end assembly, but to a lesser extent than Cin8 (Gardner, M. K. et al., 2008). Analysis of the kMT dynamics in WT cells revealed, as expected, that spindle elongation in metaphase is compensated partially by the elongation of the kMTs as well as an increased inter-KT distance, resulting in a higher level of tension on the KT-MT interface (see 4.1.4.3). However, when the CL domain is deleted, kMTs over-elongate and SPBs only separate to an extent that keeps the inter-KT distance at a minimum of about 0.5 μ m. This might represent the minimum level of tension on the KT-MT interface that is sufficient to satisfy the tension checkpoint. This indicates that less tension is required to keep the kMTs polymerized. Conclusively, the CL domain seems to make kMT elongation dependent on the tension on the KT-MT interface.

Thereby it is unclear, if the kMTs over-elongate because the CL domain usually has a direct inhibitory effect on the incorporation of tubulin in the kMTs or because of the indirect effect that the CL domain is usually concentrating Stu1 preferentially at the region of overlapping interpolar MTs in metaphase (see 4.1.2.3). Since deletion of the CL domain seems to increase the amount of Stu1 on the kMTs, higher amounts of free tubulin might be provided to the KT-MT interface for incorporation. The fact that KT localization of Stu1 is absolutely mandatory for kMT polymerization makes the first theory more likely, but does not exclude the second one.

In summary, these data suggest that Stu1 has to bind to attached KTs via the TOGL1 and ML domain to promote the incorporation of tubulin in kMT plus-ends and that the CL domain fine-tunes the polymerizing activity of Stu1 to optimize the balance between tension and kMT elongation (see Fig. 5-1 F). Correspondingly, CHIP analysis could not detect Stu1 at attached KTs in anaphase when kMTs are very short and keep

the attached KTs close to the SPB to ensure faithful segregation into mother and daughter (Ortiz, J. et al., 2009). Therefore, not only solving the precise mechanism that regulates kMT elongation, but also the mechanism that controls the detachment of Stu1 from KTs at anaphase onset is an interesting goal for future studies.

5.1.4 The CL domain specifies Stu1 for unattached KTs

Stu1 gets sequestered at the reassembled, but unattached KT after centromeric DNA replication (Ortiz, J. et al., 2009). Very recent studies revealed that similar to attached KTs this recruitment is dependent on Stu1 dimerization and the binding to KTs via the TOGL1 domain (Funk, C. et al., submitted; see Fig. 5-1 A and C). In contrast to attached KTs, the ML domain is dispensable for this localization (see 4.1.3.1), strongly suggesting that the binding to unattached KTs differs from the binding to attached KTs. This is in agreement with the fact that Stu1 has a strong preference in binding to unattached KTs even in the presence of attached KTs and MTs (Ortiz, J. et al., 2009). Interestingly, the CL domain was found to have a regulatory function in this respect. The deletion of the CL domain mislocalized the majority of Stu1 Δ CL to the vicinity of the SPB, but additional deletion of the ML domain could partially rescue the localization to unattached KTs. Therefore, the CL domain could specify Stu1 for the sequestration to unattached KTs in different possible ways that are not mutually exclusive. One possibility is that the CL domain serves as an additional direct (weaker) binding site for unattached KTs, whereas a second possibility is that the CL domain initiates a certain conformational change of Stu1 that allows Stu1 sequestration at unattached KTs. As a third possibility the CL domain might reduce the MT affinity of Stu1 by the direct inhibition of the MT-binding ML domain, specifying Stu1 for the binding to unattached KTs.

5.1.5 TOGL2 activity and the ML domain, but not KT localization are prerequisites for efficient capturing of unattached KTs

One suggested function of Stu1, accumulated at unattached KTs, is that it facilitates efficient capturing of unattached KTs (Ortiz, J. et al., 2009). Indeed, this work reveals that the TOGL2 activity of tubulin binding (and providing) plays a crucial role for the capturing of unattached KTs, since cells with an impaired TOGL2 activity were as defective in capturing as cells depleted of Stu1. Preventing the binding to the MT lattice by the deletion of the ML domain also diminished the capturing of unattached KTs. This suggests that the TOGL2 activity, but also MT binding of Stu1 are important requirements for efficient KT capturing. Surprisingly, the analysis of the *stu1* Δ CL strain re-

vealed that the sequestration of Stu1 to unattached KT is not a prerequisite for efficient capturing. Although the majority of Stu1 Δ CL mislocalized to MTs or attached KTs in the vicinity of the SPB, these cells captured unattached KTs even faster than WT cells. In agreement with this, also the deletion of the TOGL1 domain, which prevents Stu1 localization to unattached KTs in favor of MT binding, resulted in an improved capturing of unattached KTs (unpublished data, Funk, C.). These results suggest that an unimpaired action of Stu1 on MTs is more important for efficient capturing than the localization of Stu1 at unattached KTs. On the other hand, in the *stu1* Δ CL and *stu1* Δ TOGL1 cells the defective KT localization that would *per se* interfere with capturing might be compensated by the ectopic binding and function of Stu1 Δ CL and Stu1 Δ TOGL1 on MTs.

These data raise the question how Stu1 influences MTs to facilitate KT capturing. Two types of MTs, the KT-generated MTs and the capturing kMTs emanating from the SPB, are directly involved in the capturing process (Kitamura, E. et al., 2010) and could be regulated by Stu1. KT-generated MTs were found to form at unattached KTs to facilitate the capturing process by initiating a parallel or antiparallel contact with the capturing kMTs (Kitamura, E. et al., 2010). Since Stu1, more precisely the TOGL2 activity, is important for the formation and polymerization of kMTs and interpolar MTs, it is conclusive that also the polymerization of KT-generated MTs might be affected by the mutation of Stu1. Although the mutation of the TOGL2 domain of Stu1 did not prevent the formation of KT-generated MTs completely, the polymerization of KT-generated MTs was substantially delayed (see 4.1.3.3). In agreement with this, CLASP1 is also dispensable for the formation of K-fibres, the bundles of kMTs elongating from KTs in *Drosophila* cells, in general, but is required to maintain their length by providing tubulin for a mechanism called the MT subunit flux (Maiato, H. et al., 2005). Hereby, KT-generated MTs undergo constant depolymerization from the non-anchored minus-end and polymerization at the plus-end that is facing the KT. Even though in *S. cerevisiae* the minus-end of KT-generated MTs is at the KT (Kitamura, E. et al., 2010) and no MT subunit flux was detected at the KT-generated MTs in these cells, Stu1 might contribute to the incorporation of tubulin at KT-generated MT plus-ends facing away from the KT. Consistent with this, the XMAP215 ortholog Stu2 was found to provide the nucleation and elongation of KT-generated MTs at unattached KTs (Kitamura, E. et al., 2010). Conclusively, these data indicate that Stu1 is not mandatory for the nucleation of KT-generated MTs, but facilitates their rapid formation by providing tubulin.

Stu1 was found to support the elongation of kMTs in metaphase (see 4.1.4.2; Funk, C. et al., submitted). Therefore, it is likely that the dynamics of the capturing kMTs are also regulated by the Stu1 activity. Until now, Stu1 was found to work on MT bundles or overlaps in meta- and anaphase and at KT to regulate MTs from there. Particularly when the localization of Stu1 to KT is disturbed in *stu1 Δ CL* (and *stu1 Δ TOGL1*) cells, Stu1 also operates on single MTs (this work; Funk, C. et al., submitted). In WT cells however, Stu1 strongly localizes to unattached KTs and is not visible at MTs, but nevertheless the TOGL2 activity is highly important for the capturing process. One possibility is that small amounts of Stu1 nevertheless operate on capturing kMTs that are not detectable by the applied microscopic approach. Unfortunately, approaches to gain more insight in the dynamics of capturing kMTs using the *stu1 Δ TOGL2* or the *stu1TOGL2-4A* cells were difficult due to unexplained effects on cytoplasmic MTs. Although the formation of spindle MTs was impaired upon Stu1 depletion or the mutation of the TOGL2 domain, unusually long and numerous MTs emanated from the collapsed SPBs of these cells. A similar effect was observed when spindle formation was inhibited in the *stu1-5* temperature sensitive mutant (Yin, H. et al., 2002). Most of these MTs might be cytoplasmic and therefore astral MTs (Yin, H. et al., 2002), but some also could be capturing kMTs. Unfortunately, it was not possible to establish a tool that allowed a reliable determination of the types of MTs so far. This restricted further approaches to analyze the influence of Stu1 on the dynamics of the capturing kMTs. Taken together, Stu1 may indeed have a function on MTs for the capturing of unattached KTs, but the exact role of Stu1 in this process is still poorly understood.

5.1.6 The TOGL2 and ML domain contribute to faithful KT attachment

Supportive to the theory that undisturbed MT dynamics are important for efficient capturing, all mutant cells that revealed defective spindle formation and capturing (*stu1 Δ TOGL2*, *stu1TOGL2-4A*, *stu1 Δ ML*), also displayed unattached KTs during a regular cell cycle when released from G1 arrest (see 4.1.4.1). Besides the quite moderate amount of unattached KTs that were completely off the spindle, a lot of cells showed a strong Stu1 signal in the close vicinity of the spindle and the major KT signal respectively. The fact that the majority of WT Stu1 usually leaves the KT as soon as monopolar attachment is achieved (Ortiz, J. et al., 2009), suggests that these KTs are not end-on, but only lateral attached to kMTs.

A possible explanation for this effect in *stu1 Δ ML* cells could be that Stu1 Δ ML is impaired in achieving proper end-on attachment of KT and MTs. The finding that the ML domain is important for the localization of Stu1 to attached KTs in metaphase suggests that a proper KT-MT end-on attachment requires KT binding via the TOGL1 domain and MT binding via the ML domain, probably bridging the gap between the two structures (see Fig. 5-1 F). A failure in MT binding might destabilize the KT-MT interaction in metaphase.

A more general explanation for all these mutants would be that due to the lack of tension on the KT-MT interface, which results from the impaired spindle formation, the tension-checkpoint constantly creates unattached KTs. This could be verified by the analysis of these mutants in the background of an *Ipl1* mutant that is defective to respond to a lack of tension on the KT-MT interface.

Another possible explanation is that the mutated Stu1 constructs have difficulties to leave the KT after attachment to MTs due to their lower MT binding affinity. An intact Dam1 complex was shown to be required for the majority of Stu1 to leave the captured KT and move on to the spindle (Ortiz, J. et al., 2009), indicating that end-on attachment is a prerequisite for the dissociation of Stu1 from KTs. Vice versa an impaired dissociation of Stu1 might also interfere with the Dam1-KT association. Thus, the accumulation of Stu1 at the KT could hinder a proper end-on attachment to MTs by occupying required interaction sites on the KT interface. As a consequence, the only lateral attached KTs more frequently detach and cause unattached KTs. This theory is supported by the observation that overexpression of a Stu1 mutant lacking the MT-binding domain (Stu1 Δ MDB) provokes unattached KTs during a normal cell cycle even in the presence of WT Stu1 (Ortiz, J. et al., 2009). Since Stu1 Δ MDB competes for WT Stu1 at unattached KTs and thus supplies a pool of Stu1 for proper spindle formation, unattached KTs are provoked even under conditions that would allow tension on the KT-MT interface.

Taken together these data propose that either the impact of Stu1 on the MT and spindle stability is important for a proper KT-MT attachment or more likely that the majority of Stu1 has to leave the KT after reaching the SPB to ensure a proper MT end-on attachment of KTs.

5.1.7 Sequestration of Stu1 at unattached KT's prevents precocious SPB separation to ensure bipolar attachment

This work demonstrated that the localization of Stu1 to unattached KT's is not a prerequisite for successful KT capturing (see 4.1.3.2). Therefore, it is unclear why WT Stu1 gets sequestered at unattached KT's even when preferred MT binding seems to be an advantage for capturing of these unattached KT's. Defects in the bi-orientation of KT's in *stu1 Δ CL* cells however emphasize that the, most likely, higher affinity of Stu1 Δ CL to MT's also comes along with deficiencies in correct chromosome segregation (see 4.1.5). These caveats have only a weak effect during a regular cell cycle, but become much more evident after the treatment with nocodazole. Upon the release from nocodazole, spindles form and elongate remarkably fast in these cells, associated with a severe initial bi-orientation defect. This defect is corrected over time in the majority of cells, but results in a massive delay in cell cycle progression. During that time, the majority of spindles in these cells have still metaphase character with Stu1 Δ CL completely along the spindle and an extended interpolar MT overlap indicated by an extended Ase1 signal. Both effects verify that the cells did not prematurely enter anaphase, but that an intact tension checkpoint delays anaphase onset to allow for the correction of the erroneous attachments. There are various explanations for the precocious SPB separation and spindle elongation in *stu1 Δ CL* cells. The three most likely ones that are not mutually exclusive are discussed in the following.

One possibility is that *stu1 Δ CL* cells prematurely drive spindle formation and elongation due to a stronger polymerizing activity of Stu1 Δ CL. The large distance between the SPBs then impedes bi-orientation of KT's. This is in agreement with the finding that precocious SPB separation causes defects in bipolar attachment after nocodazole release (Liang, H. et al., 2012). Evidence that the precocious SPB separation is indeed the main reason for the initial bipolar attachment defect is given by the improved bi-orientation of KT's when spindle length was decreased close to WT levels by the additional deletion of Ase1.

Vice versa, another explanation is that Stu1 Δ CL delays the bi-orientation of KT's by a so far unknown defect. The presence of many monopolar attached KT's reduces the inward forces that keep SPBs in close proximity and spindles can elongate further than under WT conditions (Liu, H. et al., 2008). This could explain the slightly higher number of monopolar KT's compared to WT cells even after abrogation of the premature SPB separation in Δ *ase1 stu1 Δ CL* cells.

In addition, the possibility that not only the spindle length, but also the dynamics of kMT's play a role for efficient bipolar attachment, could also explain the still slightly in-

creased bi-orientation defect in $\Delta ase1 stu1\Delta CL$ cells when compared to WT cells. Analyses of β -tubulin mutants revealed that decreased MT dynamics cause a defect in bi-orientation (Huang, B. et al., 2006). Since kMTs are over-elongated and most likely hyper-stable in $stu1\Delta CL$ cells in metaphase, their dynamics might be also altered after nocodazole release. However, in contrast to β -tubulin mutants $stu1\Delta CL$ cells did not have a defect in capturing of unattached KTs.

It is astonishing why the defect in bi-orientation is much more severe in $stu1\Delta CL$ cells after nocodazole treatment than during a regular cell cycle. This is similar to the findings in mammalian cells that the effect of merotelic attached KTs, which are frequently found during early mitosis, is strongly intensified in cells released from nocodazole treatment, because they display a delay in KT bi-orientation (Cimini, D. et al., 2003).

Analyses in budding yeast also revealed that Cdk1 is required for efficient bi-orientation after recovery from a nocodazole arrest to prevent premature SPB separation, but is dispensable during normal S-phase (Liang, H. et al., 2012). This indicates that the conditions required to achieve bipolar attachment are different after nocodazole arrest. A possible explanation could be that during a normal S-phase, centrosomes get replicated early and reassembled KTs attach already to the old SPB while the new SPB still needs time to mature (Kitamura, E. et al., 2007). When the new SPB starts to emanate MTs, bipolar attachment and formation of the overlap of inter-polar MTs might happen mainly simultaneously, so SPBs cannot be pushed apart prematurely. However, when cells get released from a metaphase arrest with nocodazole, both SPBs are already mature and the outward pulling forces have to be stalled until all KTs are captured and bipolar attached. Thereby the CL domain seems to play an important role. This indicates that a delay in bi-orientation emerging from the nocodazole treatment causes the premature SPB separation in $stu1\Delta CL$ cells, which is prevented by the simultaneous bi-orientation and SPB separation during an unperturbed cell cycle.

The findings that the monopolar KTs are preferentially attached to the old SPB in $stu1\Delta CL$ cells released from nocodazole treatment suggest that most of the KTs get monopolar attached to the old SPB and fail to reorient to the new SPB. Previous studies revealed that mono-oriented KTs mainly segregate with the old SPB during anaphase when the reorientation from the old to the new SPB is defective in *ipl1* (or *sli15*) mutants (McCarroll, R. M. et al., 1988; Tanaka, T. U. et al., 2002, 2005). It is suggested that KTs of replicated chromosomes preferentially attach to the old SPB, because rep-

lication of the centromeric DNA is completed early in S-phase before the new SPB is fully operative. After nocodazole treatment however, the unattached KT's usually randomly attach to the old or the new SPB in WT and *ipl1* mutant cells (Tanaka, T. U. et al., 2002). Considering this, the aberrant phenotype in *stu1ΔCL* cells could be explained by different, not mutually exclusive effects. One reason might be that the reorientation of the monopolarly attached KT's by the tension checkpoint machinery is complicated in *stu1ΔCL* cells because spindles elongate very fast after nocodazole wash-out. A more interesting explanation would be that most of the KT's that got attached to the old SPB right after replication fail to reorient during nocodazole treatment when SPBs would be close because the correction by *Ipl1* works in a CL domain dependent manner. Phosphorylation of the CL domain by *Ipl1* might regulate the interaction between the CL and the ML domain and therefore destabilize the KT-MT interaction. On the other hand phosphorylation of the CL domain could also be involved in the recruitment of *Ipl1* to the monopolar attached KT.

All these described defects support the suggested theory that the sequestration of *Stu1* by unattached KT's has the function to inhibit premature localization of *Stu1* to the spindle to prevent precocious spindle elongation (Ortiz, J. et al., 2009; see Fig. 5-1 A-C). Keeping the SPBs in close proximity until all chromosomes are bipolarly attached and the tension checkpoint is satisfied, facilitates the reorientation of KT's and therefore ensures faithful chromosome segregation.

Nevertheless, the biological function that underlies this mechanism that only gets important after nocodazole treatment is unclear. A possible explanation is that outside the controlled laboratory conditions cells are exposed to a higher environmental stress that more easily generates unattached KT's. For instance a fluctuating temperature could impair MT polymerization that results in delayed KT capturing after replication and therefore necessitates a mechanisms that controls premature spindle elongation.

5.1.8 The regulatory interplay between the CL domain and the ML domain

Various observations throughout the analyzed cell cycle events suggest that the CL domain has an inhibitory function on the localization of *Stu1* to the MT lattice. In G1, in contrast to WT *Stu1*, *Stu1ΔCL* can be found slightly bound to kMT's (data not shown), in metaphase *Stu1ΔCL* localizes not only to the overlap region of interpolar MT's, but also along non-overlapping MT's. In nocodazole arrested cells, *Stu1ΔCL* mislocalizes to the MT's close to the SPBs and after release from nocodazole *Stu1ΔCL* could be found

along the entire spindle. Supportively, a truncated version of Stu1, lacking the 797 C-terminal amino acids including the CL domain, was found to have a higher affinity for MTs than full-length Stu1 *in vitro* (Yin, H. et al., 2002). Since it cannot be completely excluded that the additionally lacking D4 domain contributes to this effect in this case, further MT co-sedimentation assays would be required to confirm the influence of the CL domain on the MT affinity of Stu1. In summary, the CL domain might fine-tune the affinity of Stu1 to the MT lattice, probably by an intramolecular mechanism. This intramolecular regulation could take place by a direct interaction of the CL domain and the ML domain. Since the net charge of the ML domain is strongly positive (Yin, H. et al., 2002) with an pI of 10.4 whereas the CL domain has an overall strongly negative net charge with an pI of 4.4, such an interaction could be accomplished by electrostatic forces.

It is unclear if the over-elongation of kMTs in G1 and metaphase or the precocious spindle elongation after nocodazole treatment is only a consequence of the higher MT affinity of Stu1 that results in an increased amount of Stu1 at MTs providing free tubulin. Another possibility is that the CL domain also inhibits the Stu1 TOGL2 activity to ensure a regulated incorporation of $\alpha\beta$ -tubulin.

Upon anaphase onset however, Stu1 Δ CL, like WT Stu1, leaves the length of the spindle and localizes to the spindle midzone. This suggests that, in favor of midzone localization in anaphase, unspecific MT binding by the ML domain is inhibited by a mechanism independent of the CL domain (see Fig. 5-1 H).

Taken together, all the data support the theory that Stu1, similar to other CLASP proteins (Mimori-Kiyosue, Y. et al., 2006), acts as a local modulator for MT dynamics and stability. While the TOGL2 domain accomplishes the essential function of tubulin incorporation in MT plus-ends, the other domains are required to regulate the localization of Stu1 and (probably therefore) control the MT polymerizing activity. Thereby, the CL domain specifies the localization of Stu1 to the MT overlap or to unattached KTMs in metaphase, probably by a direct inhibiting function on the ML domain. In addition, the CL domain seems to make the incorporation of free tubulin in kMTs dependent on the tension on the KT-MT interface.

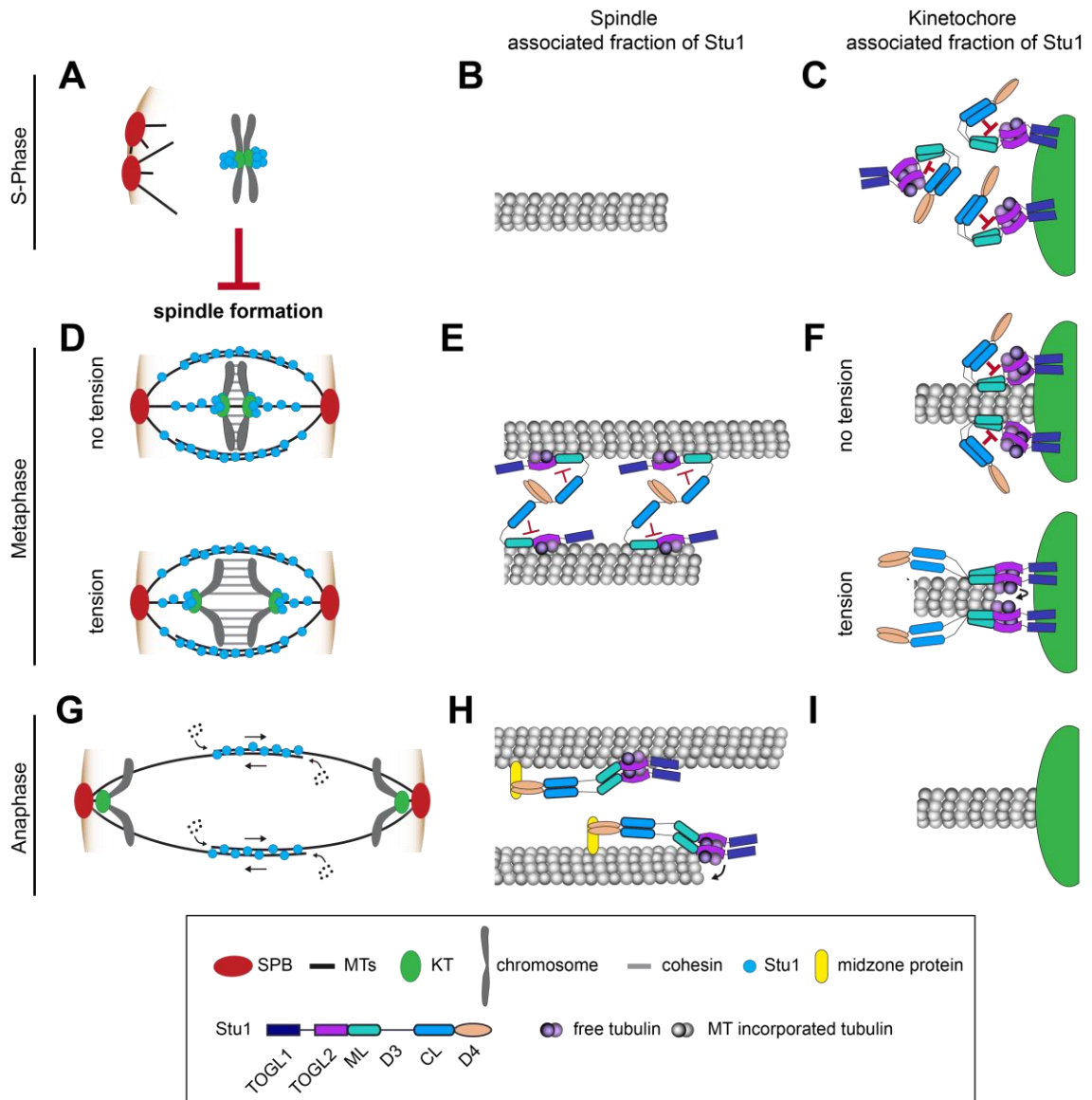


Fig. 5-1. Model of the domain requirements for Stu1 localization and function.

(A-B) Sequestration of Stu1 by unattached KTs prevents spindle formation. Thereby Stu1, dimerized by the D4 domain, binds to unattached KTs via the TOGL1 domain. **(C)** The CL domain specifies the localization of Stu1 to unattached KTs by inhibiting the ML domain for MT binding. **(D)** Regulated spindle dynamics supported by the TOGL2 activity and the ML domain of Stu1 ensure the efficient capturing of unattached KTs. After all KTs are attached, the TOGL2 activity and Stu1 localization to the MT lattice via the ML domain are required to drive spindle formation. **(E)** In metaphase, a Stu1 dimer binds the MT lattice of preferably overlapping interpolar MTs via the ML domain. Thereby, Stu1 might serve as a stabilizing cross-linker that antagonizes the outward forces of the spindle. Spindle stability might be also supported by the TOGL2 activity. **(F)** In addition, a Stu1 dimer localizes to attached KTs in a TOGL1 and ML domain dependent manner. KT localization is a prerequisite for kMT polymerization which might be regulated by the CL domain. Upon low or no tension on the KT-MT interface, the CL domain inhibits the TOGL2 activity. However, when tension is applied, the inhibitory effect of the CL domain is reduced and the TOGL2 domain can provide $\alpha\beta$ -tubulin for the incorporation in the kMT plus-end. This contributes to a tension-dependent regulation of kMT elongation. **(G-H)** At anaphase onset, binding to the MT lattice is prevented

by a mechanism independent of the CL domain. Stu1 interacts with the spindle midzone via the D4 domain, most likely by the interaction with another midzone protein. Thereby, the TOGL2 activity might contribute to midzone stability. **(I)** Stu1 leaves attached KTs that are dragged to the SPBs by the depolymerization of kMTs. The model is mainly based on the findings of this work, Funk, C. et al. (submitted), Yin, H. et al. (2000), Ortiz, J. et al. (2009) and Al-Bassam, J. et al. (2010).

5.2 Phosphorylation might contribute to regulate the MT affinity of Stu1

Stu1 is a protein that undergoes various changes in localization during each cell cycle. This work suggests that the CL domain regulates the specificity of Stu1 localization by fine-tuning the MT binding affinity of the ML domain. In addition, Stu1 is phosphorylated in a cell cycle dependent manner (see 4.2.1 and 4.2.2). Phosphorylation is suggested to regulate MT association of several MAP proteins, especially CLASP proteins, with phosphorylation within the MT-binding domain reducing the affinity for MTs (Akhmanova, A. et al., 2001; Cassimeris, L. et al., 2001). Therefore, it is very likely that a concerted series of phosphorylation and dephosphorylation events ensures the localization and proper activity of Stu1. Thereby, an interplay of temporally and locally active kinases and phosphatases might contribute to the regulatory mechanisms of Stu1.

5.2.1 Cell cycle specific phosphorylations within the ML and the CL domain contribute to regulate Stu1 localization

Mass spectrometric analyses identified 15 phosphorylation sites that were mainly located within the ML domain (and the MBD respectively) and the CL domain of Stu1 (see 4.2.1). Both domains are predicted to be mainly unstructured, making them easily accessible for post-translational modifications. Some of the sites (S276, S497, S690, S997, S1001, S1018, T1047 and S1167) were also found by a global screen for phosphorylation sites of modified proteins in *S. cerevisiae* cells after DNA damage (Albuquerque, C. P. et al., 2008). Furthermore, SILAC results propose that Stu1 is phosphorylated and dephosphorylated throughout the cell cycle. The determined phosphorylation sites represent the consensus sequences of several different kinases, namely Cdk1, polo-like kinase, Ipl1 kinase, Mps1 kinase and casein kinase.

stu1-12A cells, carrying 12 of the identified phosphorylation sites mutated to alanine (S497A, S602A, S690A, S745A, S1001A, S1018A, T1034A, T1047A, S1060A, S1113A, T1134A, S1167A), revealed a defect in specific Stu1 midzone localization. In addition, the localization to unattached KTs was strongly diminished. These findings

showed that preventing the modification of the main Stu1 phosphorylation sites completely disturbed the regulated localization of Stu1. This supported the idea that the phosphorylation of primarily the ML and the CL domain is indeed involved in the regulation of Stu1, but the numerous mutated sites did not allow a specification of certain responsible phosphorylation sites.

5.2.2 Phosphorylation of the CL domain might contribute to a balanced Stu1 sequestration at unattached KTs

Stu1 sites that were dominantly phosphorylated in G2-/metaphase after nocodazole treatment and in anaphase are T1047, S1113 and T1134. All three sites are located within the CL domain and are predicted targets of the polo-like kinase (T1047 and T1134) or Mps1 (T1047, S1113 and T1134). Indeed, sites T1047, S1113 and T1134 were confirmed to be Mps1 targets *in vitro* (see 4.2.3).

Interestingly, the single mutation of the serine 1113 revealed that this site alone determines the conformational change of Stu1 that can be detected as a distinct mobility shift on SDS-PAGE. It is intriguing that the modification of one single site has such a strong impact on the running behavior on SDS-PAGE, whereas all the other mutations have not. One explanation would be that phosphorylation of site S1113 causes a conformational change of Stu1 that results in decreased mobility on SDS-PAGE. If this potential conformational change is prevented, one would expect a strong defect of Stu1 localization and/or function. Therefore, it was disappointing that mutation of this site to alanine had no effect on Stu1 localization and function. Moreover, the mutation to glutamate unexpectedly resulted in a weak localization defect, to the MT midzone as well as to unattached KTs.

The single mutation of T1047 and T1134 to alanine caused a slightly increased defect in midzone localization in anaphase and a mild delocalization from unattached KTs. Unexpectedly, the phenotype of cells containing all three sites (T1047, S1113, T1134) mutated to alanine (*stu1-Mps1-3A*) was mainly indistinguishable from WT cells. *stu1-Mps1-3A* cells showed normal capturing and bipolar attachment and a slightly faster SPB separation. Upon mutation of these three sites to glutamate, as expected, the localization was similar to WT, but capturing of unattached KTs was severely decelerated in these cells. Most likely as a consequence, bi-orientation and SPB separation were also slightly delayed compared to WT cells. This suggests that inhibited dephosphorylation of these sites implies a stronger KT binding of Stu1 which could be a hindrance for efficient KT capturing (see 5.1.6). This would be in agreement with the

suggested model that the CL domain has an inhibitory function on the MT affinity of the ML domain. Mimicking constant phosphorylation increases the negative charge of the CL domain and therefore might increase the inhibitory effect of the CL domain. Accordingly, Mps1 and Ipl1 are highly active at incorrect attached KT-MT interactions, but KT substrates have to get dephosphorylated to allow KT-MT attachment of unattached KTs (Jelluma, N. et al., 2010; Funabiki, H. et al., 2013).

Preventing the phosphorylation of the putative polo-like kinase sites S1001, T1034, T1047 and T1134 together, revealed a mild delocalization from unattached KTs, that resulted in accordingly faster capturing and increased monopolar attached KTs, most likely as a consequence of a faster SPB separation.

In summary, this emphasizes that phosphorylation of the CL domain by the polo-like kinase and Mps1 might contribute to the regulation of Stu1 localization to unattached KTs and therefore controls SPB separation and spindle elongation to ensure bi-orientation of chromosomes. The main target sites that are important for this regulation might be T1047 and T1134.

Similar to the *stu1 Δ CL* mutant, the *stu1-CL-12A* mutant that contained the majority of possible phosphorylation sites within the CL domain (S997, S1000, S1001, S1003, T1005, S1018, T1034, T1047, S1060, S1113, T1134, S1167) mutated to alanine showed the strongest delocalization from unattached KTs of all CL domain mutants. This resulted in a faster capturing of unattached KTs, but also in a quite high defect in bi-orientation, most likely again as a result of the precocious SPB separation. Notably, the relatively mild mislocalization to the vicinity of the SPB in nocodazole treated cells had a quite strong impact on SPB separation and the bi-orientation of the KTs. Therefore, preventing the phosphorylation of the CL domain indeed resulted in a very similar, but somewhat milder defect than the complete deletion of the CL domain. This supports the hypothesis that the MT affinity of the ML domain is controlled by the CL domain and that the strength of inhibition is regulated by the phosphorylation of the CL domain.

In summary, analyses of mutants affecting phosphorylation sites within the CL domain support the idea that the CL domain has a regulatory impact on the MT binding affinity of the ML domain (see Fig. 5-2). This activity might be controlled by the phosphorylation of the CL domain. The more the CL domain is phosphorylated, the more negative is the overall net charge of the CL domain. This might increase the inhibitory impact on the positively charged ML domain. However, analyses of the phosphomutants could not determine specific phosphorylation sites or kinases to be solely responsible for this fine-tuned regulation, but sites within the CL domain at least

seem to contribute to this mechanism. Maybe the interplay between the two domains is primarily based on numerous electrostatic interactions, suggesting that the concerted modification of multiple sites is important, but not a specific single site could be determined to be critical. A similar phenomenon was observed for the N-terminal tail of Ndc80 (Akiyoshi, B. et al., 2009a). The overall charge state, but not a specific site, is suggested to be important for the function of Ndc80. This would indicate that concerted phosphorylation events on the CL domain, accomplished by the interplay of different kinases, increase the inhibitory effect of the CL domain on the MT affinity of the ML domain. This enables cells to balance the inhibitory effect on Stu1 MT binding to fulfill two functions: sufficient capturing by supporting MT dynamics, but also sequestration of the majority of Stu1 at unattached KT to prevent precocious spindle elongation and to ensure bi-orientation of sister chromatids.

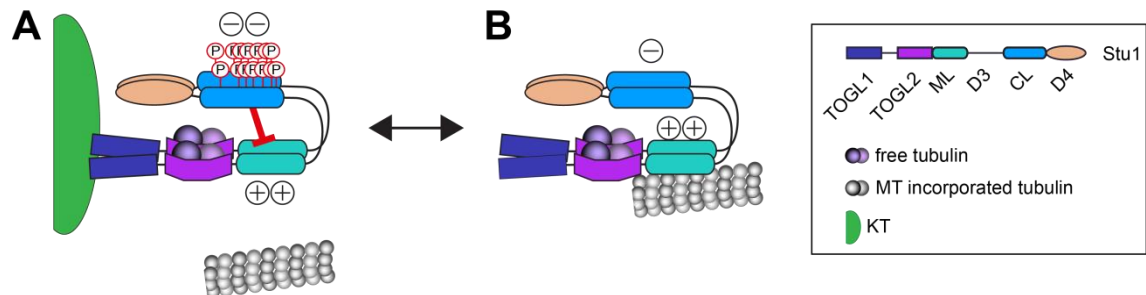


Fig. 5-2. Model of the impact of phosphorylation within the CL domain on the MT affinity of the ML domain.

(A) Phosphorylation of the CL domain enhances its negative net charge resulting in a strong inhibitory impact on the overall strongly positive charged ML domain. This prevents MT binding and ensures sequestration of Stu1 at unattached KTs. **(B)** Preventing the phosphorylation of the CL domain reduces the inhibitory effect of the CL on the ML domain. Therefore, Stu1 has a higher affinity for MT binding.

5.2.3 Phosphorylation of Stu1 in the ML domain

Interesting phosphorylation sites are S594, S602 and S690 because their phosphorylation status was found to fluctuate during mitosis with a minimum in nocodazole treated cells. All three sites are located within the ML domain and therefore could be important candidates to regulate the MT affinity of Stu1. In general, the ML domain has a strongly positive net charge that is suitable for the binding to the overall negatively charged MTs (Yin, H. et al., 2002), as it was also described for the MT-binding domains of other MAP proteins before (Akhmanova, A. et al., 2001; Cassimeris, L. et al., 2001). As a consequence, one would expect that phosphorylation of the positively

charged ML domain attenuates the MT affinity of the ML domain by making it more negative (Akhmanova, A. et al., 2001; Cassimeris, L. et al., 2001).

Therefore, it was surprising that these sites were found to be non-phosphorylated in G2-/metaphase under nocodazole treatment. Under these conditions, Stu1 exclusively localizes to unattached KTs and not to MTs. One explanation is that the inhibitory interaction of the under these conditions phosphorylated and therefore strongly negative CL domain is sufficient to sequester the majority of Stu1 at unattached KTs. Phosphorylation of the ML domain would interfere with the putative crosstalk between the CL and the ML domain and increase the MT affinity of the Stu1 ML domain.

In addition, the site S602 and probably also S690 locate within the consensus site of the Ipl1 kinase. Since unattached KTs are not under tension, one would expect that also in this case these sites should be phosphorylated by Ipl1 under nocodazole treatment. According to the SILAC results however, this is not the case. Anyhow, Ipl1 kinase is suggested to be active at monopolar attached KTs that are not under tension (Tanaka, T. U. et al., 2002; Dewar, H. et al., 2004), but not at completely unattached KTs. It would be logical that Ipl1 is active at monopolar attached KTs to facilitate their detachment, but is inactive at unattached KTs to enable capturing and KT-MT attachment. This would explain why Stu1 is non-phosphorylated at these putative Ipl1 sites at unattached KTs.

In contrast to expectations, the mutation of site S602 to alanine resulted in a quite strong localization defect to unattached KTs and a strong interaction with MTs. Mutation of this site to glutamate resulted in a very similar defect, which would be expected of the mutant that mimics constitutive phosphorylation of S602 at unattached KTs, but not in anaphase. In addition, the results of different clones were quite contradictory for both mutants. This is discussed in more detail below. Overall, these contradictions made a clear conclusion impossible.

Taken together, SILAC results suggest a fluctuating phosphorylation of sites located within the ML domain of Stu1 during the cell cycle with a minimum in nocodazole treated cells and a maximum in anaphase. Sequestration of Stu1 at unattached KTs therefore might be achieved by a direct interaction of the overall negatively charged CL domain and the unphosphorylated and therefore strongly positively charged ML domain (see Fig. 5-2). This decreases the MT affinity of the ML domain and therefore fine-tunes the localization of Stu1 to the KT.

In anaphase however, these sites within the ML domain were shown to be phosphorylated. Since Stu1 does not interact with the anaphase midzone via the MT lattice,

but most likely by the interaction with another midzone protein via the D4 domain (Funk, C. et al., submitted), MT binding has to be prevented in anaphase. Considering the fact that the CL domain is dispensable for midzone localization (see 4.1.2.4), the CL domain cannot inhibit MT binding of the ML domain in anaphase. As suggested by the SILAC results, phosphorylation events within the ML domain might be sufficient to lower the affinity of the ML domain to MTs in favor of midzone localization in anaphase. Unfortunately analyses of neither the phosphorylation mutants of site S602, nor the Ipl1 sites allow any convincing conclusions in this respect.

The question if phosphorylation events within the ML and/or the CL domain contribute to the severe change of localization from the KT to the MT lattice after attachment of all KTs in metaphase remains completely unclear. Since Stu1 midzone localization in anaphase emerged to be independent of MT interaction (see 4.1.2.4), detailed analysis of the phosphorylation pattern of Stu1 binding to the MT lattice is missing. Therefore, it would be interesting to perform SILAC analyses comparing the phosphorylation state of Stu1 from cells arrested in metaphase when Stu1 localizes to the MT lattice with cells arrested in G1 or in anaphase. Possibly this would give more insight in the phosphorylation or dephosphorylation events that enable the ML domain to efficiently interact with the MT lattice.

5.2.4 Phosphorylation of putative Cdk1 sites

One Cdk1 (Cdc28) site, S497, is suggested to be significantly phosphorylated in G1, but is not found phosphorylated in the later analyzed cell cycle steps, indicating that it might get dephosphorylated at the beginning of mitosis. Neither the mutation of this site to alanine nor to glutamate had an effect on Stu1 localization to the anaphase spindle or to unattached KTs. Another suggested Cdk1 site, S745 was found to be phosphorylated in G2-/metaphase and anaphase, indicating that this site gets phosphorylated at the beginning of mitosis. Interestingly, upon phosphorylation this site becomes a polo-box binding site. Within various organisms and proteins, CDK was detected as the 'priming' kinase that phosphorylates the S-pS/pT-P motif to initiate subsequent phosphorylation by the polo-like kinase (Cdc5 in budding yeast) (Elia, A. E. H. et al., 2003; Litvak, V. et al., 2004; Preisinger, C. et al., 2005; Qi, W. et al., 2006). For instance, 'priming' phosphorylation of CLASP2 by CDK1 is required for an efficient recruitment of Plk1 (polo-like kinase in mammalian cells) to the KT (Maia, A. R. R. et al., 2012). This suggests that the phosphorylation of S745 by Cdk1 at the beginning of mitosis could be the 'priming' phosphorylation for modifications by the polo-like kinase. However, pre-

venting the phosphorylation of this site did not have any effect on Stu1 function. Mutation to glutamate slightly increased Stu1 binding to the MTs in anaphase, increased the number of broken spindles and showed a very mild mislocalization from unattached KTs. Therefore, there is no evidence for a distinct relevance of S745 as a 'priming' Cdk1 site.

Concerted mutation of the predicted Cdk1 sites (S497, S745 and S1167) to alanine did not affect Stu1 localization to the midzone, but caused a mild delocalization from unattached KTs in favor of the vicinity of the SPB. Similar to the *stu1 Δ CL* mutant, but in a substantially milder extent, these cells also showed a faster capturing and a defect in bipolar attachment, most likely caused by the slightly faster SPB separation. These data suggest that phosphorylation by the Cdk1 could be part of the regulation for Stu1 sequestration at unattached KTs, but that the investigated sites only slightly contribute to the regulatory mechanism.

5.2.5 Phosphorylation of the main cell cycle dependent sites

Mutants that were created according to the SILAC results contain mutations of the most prominent cell cycle dependent phosphorylation sites to prevent or mimic the phosphorylation pattern of Stu1 at different cell cycle stages. Unexpectedly, neither *stu1-E+4A* (S497E, S745A, T1047A, S1113A, T1134A), nor *stu1-E+7A* (S265A, S276A, T277A, S497E, S745A, T1047A, S1113A, T1134A) cells did show any Stu1 localization defect. Thereby, the first construct mimics the opposite phosphorylation state as suggested for Stu1 at unattached KTs, whereas the second one mimics the converse phosphorylation state as proposed for Stu1 at the midzone. Therefore, for both constructs a localization defect was expected. In contrast, mimicking the phosphorylation state predicted for Stu1 at unattached KTs (*stu1-A+3E*, *stu1-A+4E*) resulted in a strong localization defect to unattached KTs and in a strong average spindle defect. In addition, two different clones showed very different phenotypes, which is discussed in more detail below. Moreover, adding further mutations to create *stu1-A+7E* cells completely improved the Stu1 localization close to the WT phenotype. Taken together, analyses of Stu1 phosphorylation mutants created according to the SILAC results were too contradictory to contribute to the understanding of the regulatory mechanisms of Stu1.

5.2.6 Problems of reproducibility due to strain variations

As mentioned before, to some extent, the evaluation of the phosphorylation mutants was very contradictive. Especially the analyses of the single mutant S602 and the mutants created according to the SILAC results gave very inconclusive results. Various clones showed very diverse results, and moreover, in case of the S602E mutant, the same clone even revealed differently strong defects in individual experiments. Possible reasons for this are discussed in the following.

(1) Recent FRAP analyses indicated that the localization of Stu1 to unattached KTs is usually very static in WT cells (Ortiz, J. et al., 2009). Therefore, one possibility could be that some of the mutations like S602 to glutamate resulted in a Stu1 construct that shows a very dynamic localization. The mutated Stu1 construct is not stably sequestered at unattached KTs, but dynamically localizes to unattached KTs and to the vicinity of the SPBs. This would explain the inconsistent localization phenotypes of Stu1.

(2) Another possibility could be a dosage-dependent effect. The background strain used for these integrations carried only a N-terminal deletion of the *TRP1* marker (*trp1-Δ63*) and no complete knock-out (Sikorski, R. S. et al., 1989). Positive clones selected for the integration of the Stu1 construct in the endogenous DNA-locus using the *kITRP1* marker (replacing the *HIS3MX6* marker) therefore could erroneously integrate an additional copy of the Stu1 construct in the *TRP1* locus. Twice the content of the Stu1 construct could explain why different clones showed diverse phenotypes and sometimes also variable strong Stu1 signals. Noticeably, the transformation of the linearised plasmids containing the *kITRP1* marker, in contrast to the *KanMX* marker, resulted in a high number of false positive clones. They were positive for growth on plates devoid of tryptophane and showed a Stu1-GFP signal by microscopy, but could still grow on plates devoid of histidine. To avoid this caveat in future strain constructions, other integration mechanisms using the *KanMX* marker or integration of the *STU1* construct in the *LYS2* locus might be advisable.

6 REFERENCES

- Adams, I.R. and Kilmartin, J. V. 1999. "Localization of Core Spindle Pole Body (SPB) Components During SPB Duplication in *Saccharomyces Cerevisiae*." *The Journal of cell biology* 145(4): 809–23.
- Akhmanova, A. and Hoogenraad, C.C. 2005. "Microtubule Plus-End-Tracking Proteins: Mechanisms and Functions." *Current opinion in cell biology* 17(1): 47–54.
- Akhmanova, A., Hoogenraad, C.C., Drabek, K., Stepanova, T., Dortland, B., Verkerk, T., Vermeulen, W., Burgering, B.M., De Zeeuw, C.I., Grosveld, F. and Galjart, N. 2001. "Clasps Are CLIP-115 and -170 Associating Proteins Involved in the Regional Regulation of Microtubule Dynamics in Motile Fibroblasts." *Cell* 104(6): 923–35.
- Akiyoshi, B., Nelson, C.R., Ranish, J.A. and Biggins, S. 2009a. "Analysis of Ipl1-Mediated Phosphorylation of the Ndc80 Kinetochore Protein in *Saccharomyces Cerevisiae*." *Genetics* 183(4): 1591–95.
- Akiyoshi, B., Nelson, C.R., Ranish, J.A. and Biggins, S. 2009b. "Quantitative Proteomic Analysis of Purified Yeast Kinetochores Identifies a PP1 Regulatory Subunit." *Genes & development* 23(24): 2887–99.
- Akiyoshi, B., Sarangapani, K.K., Powers, A.F., Nelson, C.R., Reichow, S.L., Arellano-Santoyo, H., Gonen, T., Ranish, J.A., Asbury, C.L. and Biggins, S. 2010. "Tension Directly Stabilizes Reconstituted Kinetochore-Microtubule Attachments." *Nature* 468(7323): 576–79.
- Al-Bassam, J., van Breugel, M., Harrison, S.C. and Hyman, A. 2006. "Stu2p Binds Tubulin and Undergoes an Open-to-Closed Conformational Change." *The Journal of cell biology* 172(7): 1009–22.
- Al-Bassam, J. and Chang, F. 2011. "Regulation of Microtubule Dynamics by TOG-Domain Proteins XMAP215/Dis1 and CLASP." *Trends in cell biology* 21(10): 604–14.
- Al-Bassam, J., Kim, H., Brouhard, G., van Oijen, A., Harrison, S.C. and Chang, F. 2010. "CLASP Promotes Microtubule Rescue by Recruiting Tubulin Dimers to the Microtubule." *Developmental cell* 19(2): 245–58.
- Albuquerque, C.P., Smolka, M.B., Payne, S.H., Bafna, V., Eng, J. and Zhou, H. 2008. "A Multidimensional Chromatography Technology for in-Depth Phosphoproteome Analysis." *Molecular & cellular proteomics : MCP* 7(7): 1389–96.
- Andrade, M.A. and Bork, P. 1995. "HEAT Repeats in the Huntington's Disease Protein." *Nature genetics* 11: 115–16.
- Antoni, A. De, Pearson, C.G., Cimini, D., Canman, J.C., Sala, V., Nezi, L., Mapelli, M., Sironi, L., Faretta, M., Salmon, E.D., Musacchio, A., Ripamonti, V., Hall, F., Hill, C.

- and Carolina, N. 2005. "The Mad1 / Mad2 Complex as a Template for Mad2 Activation in the Spindle Assembly Checkpoint." *Current Biology* 15: 214–25.
- Ayaz, P., Ye, X., Huddleston, P., Brautigam, C.A. and Rice, L.M. 2012. "A TOG:αβ-Tubulin Complex Structure Reveals Conformation-Based Mechanisms for a Microtubule Polymerase." *Science (New York, N.Y.)* 337(6096): 857–60.
- Baskerville, C., Segal, M. and Reed, S.I. 2008. "The Protease Activity of Yeast Separase (esp1) Is Required for Anaphase Spindle Elongation Independently of Its Role in Cleavage of Cohesin." *Genetics* 178(4): 2361–72.
- Biggins, S. 2013. "The Composition, Functions, and Regulation of the Budding Yeast Kinetochores." *Genetics* 194(4): 817–46.
- Biggins, S., Severin, F.F., Bhalla, N., Sassoon, I., Hyman, A.A. and Murray, A.W. 1999. "The Conserved Protein Kinase Ipl1 Regulates Microtubule Binding to Kinetochores in Budding Yeast." *Genes & Development* 13: 532–44.
- Birnboim, H. C. and Doly, J. 1979. "A Rapid Alkaline Extraction Procedure for Screening Recombinant Plasmid DNA." *Nucleic acids research* 7(6).
- Bjellqvist, B., Basse, B., Olsen, E. and Celis, J. 1994. "Reference Points for Comparisons of Two-Dimensional Maps of Proteins from Different Human Cell Types Defined in a pH Scale Where Isoelectric Points Correlate with Polypeptide Compositions." *Electrophoresis* 15(3-4): 529–39.
- Bjellqvist, B., Hughes, H., Pasquali, C., Paquet, N., Ravier, F., Sanchez, J., Frutiger, S. and Hochstrasser, D. 1993. "The Focusing Positions of Polypeptides in Immobilized pH Gradients Can Be Predicted from Their Amino Acid Sequences." *Electrophoresis* 14(10): 1023–31.
- Bouck, D. C. and Bloom, K.S. 2005. "The Kinetochores Protein Ndc10p Is Required for Spindle Stability and Cytokinesis in Yeast." *Proceedings of the National Academy of Sciences of the United States of America* 102(15): 5408–13.
- Bratman, S. V. and Chang, F. 2007. "Stabilization of Overlapping Microtubules by Fission Yeast CLASP." *Developmental cell* 13(6): 812–27.
- Brouhard, G.J., Stear, J.H., Noetzel, T.L., Al-Bassam, J., Harrison, S.C., Howard, J. and Hyman, A.A. 2008. "XMAP215 Is a Processive Microtubule Polymerase." *Cell* 132(1): 79–88.
- Bullitt, E., Rout, M.P., Kilmartin, J. V and Akey, C.W. 1997. "The Yeast Spindle Pole Body Is Assembled Around a Central Crystal of Spc42p." *Cell* 89(7): 1077–86.
- Buvelot, S., Tatsutani, S.Y., Vermaak, D. and Biggins, S. 2003. "The Budding Yeast Ipl1/Aurora Protein Kinase Regulates Mitotic Spindle Disassembly." *The Journal of cell biology* 160(3): 329–39.
- Byers, B. and Goetsch, L. 1975. "Behavior of Spindles and Spindle Plaques in the Cell Cycle and Conjugation of *Saccharomyces Cerevisiae*." *Journal of bacteriology* 124(1): 511.

- Cai, M. and Davis, R.W. 1990. "Yeast Centromere Binding Protein CBF1, of the Helix-Loop-Helix Protein Family, Is Required for Chromosome Stability and Methionine Prototrophy." *Cell* 61: 437–46.
- Campbell, C.S. and Desai, A. 2013. "Tension Sensing by Aurora B Kinase Is Independent of Survivin-Based Centromere Localization." *Nature* 15: 1–5.
- Carmena, M., Ruchaud, S. and Earnshaw, W.C. 2009. "Making the Auroras Glow: Regulation of Aurora A and B Kinase Function by Interacting Proteins." *Current opinion in cell biology* 21(6): 796–805.
- Cassimeris, L. and Spittle, C. 2001. "Regulation of Microtubule-Associated Proteins." *International Review of Cytology* 210: 163–226.
- Caydasi, A.K., Ibrahim, B. and Pereira, G. 2010. "Monitoring Spindle Orientation: Spindle Position Checkpoint in Charge." *Cell division* 5(1): 28.
- Caydasi, A.K. and Pereira, G. 2012. "SPOC Alert--When Chromosomes Get the Wrong Direction." *Experimental cell research* 318(12): 1421–27.
- Cheeseman, I.M., Anderson, S., Jwa, M., Green, E.M., Kang, J.S., Yates, J.R., Chan, C.S.M., Drubin, D.G. and Barnes, G. 2002. "Phosphoregulation of Kinetochore-Microtubule Attachments by the Aurora Kinase Ipl1p." *Cell* 111(2): 163–72.
- Cheeseman, I.M., Chappie, J.S., Wilson-Kubalek, E.M. and Desai, A. 2006. "The Conserved KMN Network Constitutes the Core Microtubule-Binding Site of the Kinetochore." *Cell* 127(5): 983–97.
- Cho, U.-S. and Harrison, S.C. 2012. "Ndc10 Is a Platform for Inner Kinetochore Assembly in Budding Yeast." *Nature structural & molecular biology* 19(1): 48–55.
- Ciferri, C., Pasqualato, S., Screpanti, E., Varetto, G., Santaguida, S., Dos Reis, G., Maiolica, A., Polka, J., De Luca, J.G., De Wulf, P., Salek, M., Rappsilber, J., Moores, C. a, Salmon, E.D. and Musacchio, A. 2008. "Implications for Kinetochore-Microtubule Attachment from the Structure of an Engineered Ndc80 Complex." *Cell* 133(3): 427–39.
- Cimini, D., Moree, B., Canman, J.C. and Salmon, E.D. 2003. "Merotelic Kinetochore Orientation Occurs Frequently During Early Mitosis in Mammalian Tissue Cells and Error Correction Is Achieved by Two Different Mechanisms." *Journal of cell science* 116(Pt 20): 4213–25.
- Ciosk, R., Zachariae, W., Michaelis, C., Shevchenko, A., Mann, M. and Nasmyth, K. 1998. "An ESP1/PDS1 Complex Regulates Loss of Sister Chromatid Cohesion at the Metaphase to Anaphase Transition in Yeast." *Cell* 93(6): 1067–76.
- Clarke, L. 1998. "Centromeres: Proteins, Protein Complexes, and Repeated Domains at Centromeres of Simple Eukaryotes." *Current opinion in genetics & development* 8(2): 212–18.
- Cohen-Fix, O., Peters, J.M., Kirschner, M.W. and Koshland, D. 1996. "Anaphase Initiation in *Saccharomyces Cerevisiae* Is Controlled by the APC-Dependent

- Degradation of the Anaphase Inhibitor Pds1p." *Genes & Development* 10(24): 3081–93.
- Connelly, C. and Hieter, P. 1996. "Budding Yeast SKP1 Encodes an Evolutionarily Conserved Kinetochores Protein Required for Cell Cycle Progression." *Cell* 86(2): 275–85.
- Cottarel, G., Shero, J.H., Hieter, P. and Hegemann, J.H. 1989. "A 125-Base-Pair CEN6 DNA Fragment Is Sufficient for Complete Meiotic and Mitotic Centromere Functions in *Saccharomyces Cerevisiae*." *Molecular and cellular biology* 9(8): 3342.
- Cottingham, F.R., Gheber, L., Miller, D.L. and Hoyt, M.A. 1999. "Novel Roles for *Saccharomyces Cerevisiae* Mitotic Spindle Motors." *The Journal of cell biology* 147(2): 335–50.
- Dewar, H., Tanaka, K., Nasmyth, K. and Tanaka, T.U. 2004. "Tension Between Two Kinetochores Suffices for Their Bi-Orientation on the Mitotic Spindle." *Nature* 428: 93–97.
- Dou, Z., von Schubert, C., Körner, R., Santamaria, A., Elowe, S. and Nigg, E.A. 2011. "Quantitative Mass Spectrometry Analysis Reveals Similar Substrate Consensus Motif for Human Mps1 Kinase and Plk1." *PLoS one* 6(4): e18793.
- Dumitrescu, T.P. and Saunders, W.S. 2002. "The FEAR Before MEN." *Cell cycle* 1(5): 304–7.
- Elia, A.E.H., Rellos, P., Haire, L.F., Chao, J.W., Ivins, F.J., Hoepker, K., Mohammad, D., Cantley, L.C., Smerdon, S.J. and Yaffe, M.B. 2003. "The Molecular Basis for Phosphodependent Substrate Targeting and Regulation of Plks by the Polo-Box Domain." *Cell* 115(1): 83–95.
- Francisco, L., Wang, W. and Chan, C.S. 1994. "Type 1 Protein Phosphatase Acts in Opposition to Ipl1 Protein Kinase in Regulating Yeast Chromosome Segregation." *Molecular and cellular biology* 14(7): 4731–40.
- Franco, A., Meadows, J.C. and Millar, J.B. a. 2007. "The Dam1/DASH Complex Is Required for the Retrieval of Unclustered Kinetochores in Fission Yeast." *Journal of cell science* 120(Pt 19): 3345–51.
- Fu, J., Jiang, Q. and Zhang, C. 2010. "Collaboration of Mitotic Kinases in Cell Cycle Control." *Nature Education* 3(9): 82.
- Funabiki, H. and Wynne, D.J. 2013. "Making an Effective Switch at the Kinetochores by Phosphorylation and Dephosphorylation." *Chromosoma* 122(3): 135–58.
- Funk, C., Schmeiser, V., Ortiz, J. and Lechner, J. "Multiple CLASP Domains Cooperate to Drive Spindle Formation and Chromosome Segregation in Budding Yeast." *The Journal of cell biology* (submitted).
- Gachet, Y., Courthe, T., Goldstone, S., Gay, G. and Tournier, S. 2008. "Sister Kinetochores Recapture in Fission Yeast Occurs by Two Distinct Mechanisms , Both Requiring Dam1 and Klp2." *Molecular biology of the cell* 19(April): 1646–62.

- Gardner, M.K., Bouck, D.C., Paliulis, L. V, Meehl, J.B., O'Toole, E.T., Haase, J., Soubry, A., Joglekar, A.P., Winey, M., Salmon, E.D., Bloom, K. and Odde, D.J. 2008. "Chromosome Congression by Kinesin-5 Motor-Mediated Disassembly of Longer Kinetochore Microtubules." *Cell* 135(5): 894–906.
- Gasteiger, E., Hoogland, C., Gattiker, A., Duvaud, S., Wilkins, M.R., Appel, R.D. and Bairoch, A. 2005. "Protein Identification and Analysis Tools on the ExPASy Server." *The Proteomics Protocols Handbook, Humana Press*: 571–607.
- Gietz, D.R., Schiestl, R.H., Willems, A.R. and Woods, R.A. 1995. "Studies on the Transformation of Intact Yeast Cells by the LiAc/SS-DNA/PEG Procedure." *Yeast* 11(4): 355 – 360.
- Gillett, E.S., Espelin, C.W. and Sorger, P.K. 2004. "Spindle Checkpoint Proteins and Chromosome-Microtubule Attachment in Budding Yeast." *The Journal of cell biology* 164(4): 535–46.
- Glotzer, M. 2009. "The 3Ms of Central Spindle Assembly: Microtubules, Motors and MAPs." *Nature reviews. Molecular cell biology* 10(1): 9–20.
- Guacci, V., Hogan, E. and Koshland, D. 1997. "Centromere Position in Budding Yeast: Evidence for Anaphase A." *Molecular biology of the cell* 8(6): 957–72.
- Harrison, J.C. and Haber, J.E. 2006. "Surviving the Breakup: The DNA Damage Checkpoint." *Annual review of genetics* 40: 209–35.
- Hayden, J.H., Bowser, S.S. and Rieder, C.L. 1990. "Kinetochores Capture Astral Microtubules During Chromosome Attachment to the Mitotic Spindle: Direct Visualization in Live Newt Lung Cells." *The Journal of cell biology* 111(3): 1039–45.
- Hieter, P., Pridmore, D., Hegemann, J.H., Thomas, M., Davis, R.W. and Philippsent, P. 1985. "Functional Selection and Analysis of Yeast Centromeric DNA." *Cell* 42(October): 913–21.
- Ho, S.N., Hunt, H.D., Horton, R.M., Pullen, J.K. and Pease, L.R. 1989. "Site-Directed Mutagenesis by Overlap Extension Using the Polymerase Chain Reaction." *Gene* 77(1): 51–59.
- Howell, B.J., McEwen, B.F., Canman, J.C., Hoffman, D.B., Farrar, E.M., Rieder, C.L. and Salmon, E.D. 2001. "Cytoplasmic Dynein/dynactin Drives Kinetochore Protein Transport to the Spindle Poles and Has a Role in Mitotic Spindle Checkpoint Inactivation." *The Journal of cell biology* 155(7): 1159–72.
- Hoyt, M.A., He, L., Loo, K.K. and Saunders, W.S. 1992. "Two *Saccharomyces Cerevisiae* Kinesin-Related Gene Products Required for Mitotic Spindle Assembly." *The Journal of cell biology* 118(1): 109–20.
- Hoyt, M.A., He, L., Totis, L. and William, S. 1993. "Loss of Function of *Saccharomyces Cerevisiae* Kinesin-Related CIN8 and KIPI Is Suppressed by KAR3 Motor Domain Mutations." *Genetics* 135: 35–44.

- Hoyt, M.A., Totis, L. and Roberts, B.T. 1991. "S. Cerevisiae Genes Required for Cell Cycle Arrest in Response to Loss of Microtubule Function." *Cell* 66(3): 507–17.
- Huang, B. and Huffaker, T.C. 2006. "Dynamic Microtubules Are Essential for Efficient Chromosome Capture and Biorientation in S. Cerevisiae." *The Journal of cell biology* 175(1): 17–23.
- Indjeian, V.B. and Murray, A.W. 2007. "Budding Yeast Mitotic Chromosomes Have an Intrinsic Bias to Biorient on the Spindle." *Current biology* 17(21): 1837–46.
- Inoue, H., Nojima, H. and Okayama, H. 1990. "High Efficiency Transformation of Escherichia Coli with Plasmids." *Gene* 96: 23–28.
- Inoué, S. and Salmon, E.D. 1995. "Force Generation by Microtubule Assembly/disassembly in Mitosis and Related Movements." *Molecular biology of the cell* 6(12): 1619–40.
- Inoue, Y.H., do Carmo Avides, M., Shiraki, M., Deak, P., Yamaguchi, M., Nishimoto, Y., Matsukage, A. and Glover, D.M. 2000. "Orbit, a Novel Microtubule-Associated Protein Essential for Mitosis in Drosophila Melanogaster." *The Journal of cell biology* 149(1): 153–66.
- Israels, E.D. 2000. "The Cell Cycle." *The Oncologist* 5(6): 510–13.
- Jacobs, C.W., Adams, A.E.M., Szaniszló, P.J. and John, R. 1988. "Functions of Microtubules in the Saccharomyces Cerevisiae Cell Cycle." *The Journal of cell biology* 107(October): 1409–26.
- Janke, C., Ortíz, J., Tanaka, T.U., Lechner, J. and Schiebel, E. 2002. "Four New Subunits of the Dam1-Duo1 Complex Reveal Novel Functions in Sister Kinetochores Biorientation." *The EMBO journal* 21(1-2): 181–93.
- Jaspersen, S.L., Charles, J.F., Tinker-Kulberg, R.L. and Morgan, D.O. 1998. "A Late Mitotic Regulatory Network Controlling Cyclin Destruction in Saccharomyces Cerevisiae." *Molecular biology of the cell* 9(10): 2803–17.
- Jaspersen, S.L. and Winey, M. 2004. "The Budding Yeast Spindle Pole Body: Structure, Duplication, and Function." *Annual review of cell and developmental biology* 20: 1–28.
- Jelluma, N., Dansen, T.B., Sliedrecht, T., Kwiatkowski, N.P. and Kops, G.J.P.L. 2010. "Release of Mps1 from Kinetochores Is Crucial for Timely Anaphase Onset." *The Journal of Cell Biology* 191(2): 281–90.
- Jelluma, Nannette, Brenkman, A.B., van den Broek, N.J.F., Crujisen, C.W.A., van Osch, M.H.J., Lens, S.M.A., Medema, R.H. and Kops, G.J.P.L. 2008. "Mps1 Phosphorylates Borealin to Control Aurora B Activity and Chromosome Alignment." *Cell* 132(2): 233–46.
- Jin, Q.W., Fuchs, J. and Loidl, J. 2000. "Centromere Clustering Is a Major Determinant of Yeast Interphase Nuclear Organization." *Journal of cell science* 113 (Pt 1: 1903–12.

- Juang, Y.-L. 1997. "APC-Mediated Proteolysis of Ase1 and the Morphogenesis of the Mitotic Spindle." *Science* 275(5304): 1311–14.
- Kahana, J.A., Schnapp, B.J. and Silver, P.A. 1995. "Kinetics of Spindle Pole Body Separation in Budding Yeast." *Proceedings of the National Academy of Sciences of the United States of America* 92(21): 9707–11.
- Kaiser, C., Michaelis, S. and Mitchell, A. 1994. "Methods in Yeast Genetics: a Cold Spring Harbor Laboratory Course Manual." *Cold Spring Harbor Laboratory Press* 1994 editi: 234.
- Kawashima, S.A., Tsukahara, T., Langeegger, M., Hauf, S., Kitajima, T.S. and Watanabe, Y. 2007. "Shugoshin Enables Tension-Generating Attachment of Kinetochores by Loading Aurora to Centromeres." *Genes & development* 21(4): 420–35.
- Kawashima, S.A., Yamagishi, Y., Honda, T., Ishiguro, K. and Watanabe, Y. 2010. "Phosphorylation of H2A by Bub1 Prevents Chromosomal Instability through Localizing Shugoshin." *Science* 327(5962): 172–77.
- Kemmler, S., Stach, M., Knapp, M., Ortiz, J., Pfannstiel, J., Ruppert, T. and Lechner, J. 2009. "Mimicking Ndc80 Phosphorylation Triggers Spindle Assembly Checkpoint Signalling." *The EMBO journal* 28(8): 1099–1110.
- Khmelinskii, A., Lawrence, C., Roostalu, J. and Schiebel, E. 2007. "Cdc14-Regulated Midzone Assembly Controls Anaphase B." *The Journal of cell biology* 177(6): 981–93.
- Khmelinskii, A., Roostalu, J., Roque, H., Antony, C. and Schiebel, E. 2009. "Phosphorylation-Dependent Protein Interactions at the Spindle Midzone Mediate Cell Cycle Regulation of Spindle Elongation." *Developmental cell* 17(2): 244–56.
- Khmelinskii, A. and Schiebel, E. 2008. "Assembling the Spindle Midzone in the Right Place at the Right Time." *Cell cycle* 7(3): 283–86.
- King, E.M.J., Rachidi, N., Morrice, N., Hardwick, K.G. and Stark, M.J.R. 2007. "Ipl1p-Dependent Phosphorylation of Mad3p Is Required for the Spindle Checkpoint Response to Lack of Tension at Kinetochores." *Genes & development* 21(10): 1163–68.
- King, J.M., Hays, T.S. and Nicklas, R.B. 2000. "Dynein Is a Transient Kinetochores Component Whose Binding Is Regulated by Microtubule Attachment, Not Tension." *The Journal of cell biology* 151(4): 739–48.
- King, R.W., Peters, J.M., Tugendreich, S., Rolfe, M., Hieter, P. and Kirschner, M.W. 1995. "A 20S Complex Containing CDC27 and CDC16 Catalyzes the Mitosis-Specific Conjugation of Ubiquitin to Cyclin B." *Cell* 81(2): 279–88.
- King, R.W., Jackson, P.K. and Kirschner, M.W. 1994. "Mitosis in Transition." *Cell* 79: 563–71.

- Kitamura, E., Tanaka, K., Kitamura, Y. and Tanaka, T.U. 2007. "Kinetochore – Microtubule Interaction During S Phase in *Saccharomyces Cerevisiae*." *Genes & development* 21: 3319–30.
- Kitamura, E., Tanaka, K., Komoto, S., Kitamura, Y., Antony, C. and Tanaka, T.U. 2010. "Kinetochores Generate Microtubules with Distal Plus Ends: Their Roles and Limited Lifetime in Mitosis." *Developmental cell* 18(2): 248–59.
- Kiyomitsu, T., Obuse, C. and Yanagida, M. 2007. "Human Blinkin/AF15q14 Is Required for Chromosome Alignment and the Mitotic Checkpoint through Direct Interaction with Bub1 and BubR1." *Developmental cell* 13(5): 663–76.
- Knockleby, J. and Vogel, J. 2009. "The COMA Complex Is Required for Sli15/INCENP-Mediated Correction of Defective Kinetochore Attachments." *Cell cycle* 8(16): 2570–77.
- Kotwaliwale, C. V., Frei, S.B., Stern, B.M. and Biggins, S. 2007. "A Pathway Containing the Ipl1/Aurora Protein Kinase and the Spindle Midzone Protein Ase1 Regulates Yeast Spindle Assembly." *Dev Cell*. 13(3): 433–45.
- Krishnan, V., Nirantar, S., Crasta, K., Cheng, A.Y.H. and Surana, U. 2004. "DNA Replication Checkpoint Prevents Precocious Chromosome Segregation by Regulating Spindle Behavior." *Molecular cell* 16(5): 687–700.
- De la Mora-Rey, T., Guenther, B.D. and Finzel, B.C. 2013. "The Structure of the TOG-Like Domain of *Drosophila Melanogaster* Mast / Orbit." *Acta Crystallographica* F69: 723–29.
- Laemmli, U.K. 1970. "Cleavage of Structural Proteins During the Assembly of the Head of Bacteriophage T4." *Nature* 227: 680–85.
- Lampson, M.A. and Cheeseman, I.M. 2011. "Sensing Centromere Tension: Aurora B and the Regulation of Kinetochore Function." *Trends Cell Biol* 21(3): 133–40.
- Leano, J.B., Rogers, S.L. and Slep, K.C. 2013. "A Cryptic TOG Domain with a Distinct Architecture Underlies CLASP-Dependent Bipolar Spindle Formation." *Structure* 21(6): 939–50.
- Lechner, J. and Carbon, J. 1991. "A 240 Kd Multisubunit Protein Complex, CBF3, Is a Major Component of the Budding Yeast Centromere." *Cell* 64(4): 717–25.
- Li, R. and Murray, A.W. 1991. "Feedback Control of Mitosis in Budding Yeast." *Cell* 66(3): 519–31.
- Li, Y., Bachant, J., Alcasabas, A.A., Wang, Y., Qin, J. and Elledge, S.J. 2002. "The Mitotic Spindle Is Required for Loading of the DASH Complex onto the Kinetochore." *Genes & development* 16(2): 183–97.
- Liang, F., Jin, F., Liu, H. and Wang, Y. 2009. "The Molecular Function of the Yeast Polo-Like Kinase Cdc5 in Cdc14 Release During Early Anaphase." *Molecular biology of the cell* 20: 3671–79.

- Liang, H., Lim, H.H., Venkitaraman, A. and Surana, U. 2012. "Cdk1 Promotes Kinetochore Bi-Orientation and Regulates Cdc20 Expression During Recovery from Spindle Checkpoint Arrest." *The EMBO journal* 31(2): 403–16.
- Lim, H.H., Goh, P.-Y. and Surana, U. 1996. "Spindle Pole Body Separation in *Saccharomyces Cerevisiae* Requires Dephosphorylation of the Tyrosine 19 Residue of Cdc28." *Molecular and cellular biology* 16(11): 6385.
- Lim, H.H., Zhang, T. and Surana, U. 2009. "Regulation of Centrosome Separation in Yeast and Vertebrates: Common Threads." *Trends in cell biology* 19(7): 325–33.
- Lin, H., de Carvalho, P., Kho, D., Tai, C.Y., Pierre, P., Fink, G.R. and Pellman, D. 2001. "Polyploids Require Bik1 for Kinetochore-Microtubule Attachment." *The Journal of cell biology* 155(7): 1173–84.
- Litvak, V., Argov, R., Dahan, N., Ramachandran, S., Amarilio, R., Shainskaya, A. and Lev, S. 2004. "Mitotic Phosphorylation of the Peripheral Golgi Protein Nir2 by Cdk1 Provides a Docking Mechanism for Plk1 and Affects Cytokinesis Completion." *Molecular cell* 14(3): 319–30.
- Liu, D., Vader, G., Vromans, M.J.M., Lampson, M.A. and Lens, S.M.A. 2009. "Sensing Chromosome Bi-Orientation by Spatial Separation of Aurora B Kinase from Kinetochore Substrates." *Science* 323(March): 1350–53.
- Liu, D., Vleugel, M., Backer, C.B., Hori, T., Fukagawa, T., Cheeseman, I.M. and Lampson, M.A. 2010. "Regulated Targeting of Protein Phosphatase 1 to the Outer Kinetochore by KNL1 Opposes Aurora B Kinase." *The Journal of cell biology* 188(6): 809–20.
- Liu, H., Liang, F., Jin, F. and Wang, Y. 2008. "The Coordination of Centromere Replication, Spindle Formation, and Kinetochore-Microtubule Interaction in Budding Yeast." *PLoS genetics* 4(11): e1000262.
- London, N., Ceto, S., Ranish, J.A. and Biggins, S. 2012. "Phosphoregulation of Spc105 by Mps1 and PP1 Regulates Bub1 Localization to Kinetochores." *Current biology: CB* 22(10): 900–906.
- Longtine, M., McKenzie, A. 3rd, Demarini, D., Shah, N., Wach, A., Brachat, A., Philippsen, P. and Pringle, J. 1998. "Additional Modules for Versatile and Economical PCR-Based Gene Deletion and Modification in *Saccharomyces Cerevisiae*." *Yeast* 14(10): 956–61.
- Luo, X., Tang, Z., Rizo, J. and Yu, H. 2002. "The Mad2 Spindle Checkpoint Protein Undergoes Similar Major Conformational Changes Upon Binding to Either Mad1 or Cdc20." *Molecular cell* 9(1): 59–71.
- Maia, A.R.R., Garcia, Z., Kabeche, L., Barisic, M., Maffini, S., Macedo-Ribeiro, S., Cheeseman, I.M., Compton, D.A., Kaverina, I. and Maiato, H. 2012. "Cdk1 and Plk1 Mediate a CLASP2 Phospho-Switch That Stabilizes Kinetochore-Microtubule Attachments." *The Journal of Cell Biology* 199(2): 285–301.

- Maiato, H., Fairley, E.A.L., Rieder, C.L., Swedlow, J.R., Sunkel, C.E. and Earnshaw, W.C. 2003. "Human CLASP1 Is an Outer Kinetochore Component That Regulates Spindle Microtubule Dynamics." *Cell* 113(7): 891–904.
- Maiato, H., Khodjakov, A. and Rieder, C.L. 2005. "Drosophila CLASP Is Required for the Incorporation of Microtubule Subunits into Fluxing Kinetochore Fibres." *Nature cell biology* 7(1): 42–47.
- Maiato, H., Rieder, C.L. and Khodjakov, A. 2004. "Kinetochore-Driven Formation of Kinetochore Fibers Contributes to Spindle Assembly During Animal Mitosis." *The Journal of cell biology* 167(5): 831–40.
- Maiato, H., Sampaio, P., Lemos, C.L., Findlay, J., Carmena, M., Earnshaw, W.C. and Sunkel, C.E. 2002. "MAST/Orbit Has a Role in Microtubule-Kinetochore Attachment and Is Essential for Chromosome Alignment and Maintenance of Spindle Bipolarity." *The Journal of cell biology* 157(5): 749–60.
- Manchado, E., Guillaumot, M. and Malumbres, M. 2012. "Killing Cells by Targeting Mitosis." *Cell death and differentiation* 19(3): 369–77.
- Mapelli, M., Massimiliano, L., Santaguida, S. and Musacchio, A. 2007. "The Mad2 Conformational Dimer: Structure and Implications for the Spindle Assembly Checkpoint." *Cell* 131(4): 730–43.
- Maskell, D.P., Hu, X.-W. and Singleton, M.R. 2010. "Molecular Architecture and Assembly of the Yeast Kinetochore MIND Complex." *The Journal of cell biology* 190(5): 823–34.
- Matson, D.R., Demirel, P.B., Stukenberg, P.T. and Burke, D.J. 2012. "A Conserved Role for COMA/CENP-H/I/N Kinetochore Proteins in the Spindle Checkpoint." *Genes & development* 26(6): 542–47.
- Maure, J.-F., Kitamura, E. and Tanaka, T.U. 2007. "Mps1 Kinase Promotes Sister-Kinetochore Bi-Orientation by a Tension-Dependent Mechanism." *Current biology : CB* 17(24): 2175–82.
- Maure, J.-F., Komoto, S., Oku, Y., Mino, A., Pasqualato, S., Natsume, K., Clayton, L., Musacchio, A. and Tanaka, T.U. 2011. "The Ndc80 Loop Region Facilitates Formation of Kinetochore Attachment to the Dynamic Microtubule Plus End." *Current biology : CB* 21(3): 207–13.
- McCarroll, R.M. and Fangman, W.L. 1988. "Time of Replication of Yeast Centromeres and Telomeres." *Cell* 54(4): 505–13.
- McClelland, M.L., Gardner, R.D., Kallio, M.J., Daum, J.R., Gorbsky, G.J., Burke, D.J. and Stukenberg, P.T. 2003. "The Highly Conserved Ndc80 Complex Is Required for Kinetochore Assembly, Chromosome Congression, and Spindle Checkpoint Activity." *Genes & development* 17(1): 101–14.
- Meeks-Wagner, D., Wood, J.S., Garvik, B. and Hartwell, L.H. 1986. "Isolation of Two Genes That Affect Mitotic Chromosome Transmission in *S. Cerevisiae*." *Cell* 44(1): 53–63.

- Meitinger, F., Palani, S. and Pereira, G. 2012. "The Power of MEN in Cytokinesis." *Cell cycle* 1: 219–28.
- Meluh, P.B. and Koshland, D. 1995. "Evidence That the MIF2 Gene of *Saccharomyces Cerevisiae* Encodes a Centromere Protein with Homology to the Mammalian Centromere Protein CENP-C." *Molecular biology of the cell* 6(7): 793–807.
- Michaelis, C., Ciosk, R. and Nasmyth, K. 1997. "Cohesins: Chromosomal Proteins That Prevent Premature Separation of Sister Chromatids." *Cell* 91(1): 35–45.
- Mimori-Kiyosue, Y., Grigoriev, I., Sasaki, H., Matsui, C., Akhmanova, A., Tsukita, S. and Vorobjev, I. 2006. "Mammalian CLASPs Are Required for Mitotic Spindle Organization and Kinetochore Alignment." *Genes to cells: devoted to molecular & cellular mechanisms* 11(8): 845–57.
- Miranda, J.J.L., De Wulf, P., Sorger, P.K. and Harrison, S.C. 2005. "The Yeast DASH Complex Forms Closed Rings on Microtubules." *Nature structural & molecular biology* 12(2): 138–43.
- Musacchio, A. and Salmon, E.D. 2007. "The Spindle-Assembly Checkpoint in Space and Time." *Nature reviews. Molecular cell biology* 8(5): 379–93.
- Nakajima, H., Toyoshima-Morimoto, F., Taniguchi, E. and Nishida, E. 2003. "Identification of a Consensus Motif for Plk (Polo-Like Kinase) Phosphorylation Reveals Myt1 as a Plk1 Substrate." *The Journal of biological chemistry* 278(28): 25277–80.
- Nakajima, Y., Cormier, A., Tyers, R.G., Pigula, A., Peng, Y., Drubin, D.G. and Barnes, G. 2011. "Ipl1/Aurora-Dependent Phosphorylation of Sli15/INCENP Regulates CPC-Spindle Interaction to Ensure Proper Microtubule Dynamics." *The Journal of cell biology* 194(1): 137–53.
- Nasmyth, K. 1993. "Control of the Yeast Cell Cycle by the Cdc28 Protein Kinase." *Current opinion in cell biology* (5): 166–79.
- Nasmyth, K. 1996a. "At the Heart of the Budding Yeast Cell Cycle." *Trends in genetics: TIG* 12(10): 405–12.
- Nasmyth, K. 1996b. "Viewpoint: Putting the Cell Cycle in Order." *Science (New York, N.Y.)* 274(5293): 1643–45.
- Navadgi-Patil, V.M. and Burgers, P.M. 2011. "Cell-Cycle-Specific Activators of the Mec1/ATR Checkpoint Kinase." *Biochemical Society transactions* 39(2): 600–605.
- Neuwald, A.F. 2000. "HEAT Repeats Associated with Condensins, Cohesins, and Other Complexes Involved in Chromosome-Related Functions." *Genome Research* 10(10): 1445–52.
- Nezi, L., Rancati, G., De Antoni, A., Pasqualato, S., Piatti, S. and Musacchio, A. 2006. "Accumulation of Mad2-Cdc20 Complex During Spindle Checkpoint Activation Requires Binding of Open and Closed Conformers of Mad2 in *Saccharomyces Cerevisiae*." *The Journal of cell biology* 174(1): 39–51.

- Nicklas, R.B. and Koch, C.A. 1969. "Chromosome Micromanipulation. 3. Spindle Fiber Tension and the Reorientation of Mal-Oriented Chromosomes." *The Journal of cell biology* 43(1): 40–50.
- Nigg, E.A. 1993. "Cellular Substrates of P34(cdc2) and Its Companion Cyclin-Dependent Kinases." *Trends in cell biology* 3(9): 296–301.
- Nurse, P. 1990. "Universal Control Mechanism Regulating Onset of M-Phase." *Nature* 344: 503–8.
- Ohkura, H., Garcia, M.A. and Toda, T. 2001. "Dis1/TOG Universal Microtubule Adaptors - One MAP for All?" *Journal of cell science* 114(Pt 21): 3805–12.
- Ortiz, J., Funk, C., Schäfer, A. and Lechner, J. 2009. "Stu1 Inversely Regulates Kinetochore Capture and Spindle Stability." *Genes & development* 23(23): 2778–91.
- Ortiz, J., Stemmann, O., Rank, S. and Lechner, J. 1999. "A Putative Protein Complex Consisting of Ctf19, Mcm21, and Okp1 Represents a Missing Link in the Budding Yeast Kinetochore." *Genes & development* 13: 1140–55.
- Östergren, G. 1951. "The Mechanism of Co-Orientation in Bivalents and Multivalents." *Hereditas* 37: 85–156.
- Palmer, D.K., O'Day, K., Wener, M.H., Andrews, B.S. and Margolis, R.L. 1987. "A 17-kD Centromere Protein (CENP-A) Copurifies with Nucleosome Core Particles and with Histones." *The Journal of cell biology* 104(4): 805–15.
- Pasqualone, D. and Huffaker, T.C. 1994. "STU1, a Suppressor of a Beta-Tubulin Mutation, Encodes a Novel and Essential Component of the Yeast Mitotic Spindle." *The Journal of cell biology* 127(6 Pt 2): 1973–84.
- Patel, K., Nogales, E. and Heald, R. 2012. "Multiple Domains of Human CLASP Contribute to Microtubule Dynamics and Organization in Vitro and in Xenopus Egg Extracts." *Cytoskeleton (Hoboken, N.J.)* 69(3): 155–65.
- Pearson, C.G., Yeh, E., Gardner, M., Odde, D., Salmon, E.D. and Bloom, K. 2004. "Stable Kinetochore-Microtubule Attachment Constrains Centromere Positioning in Metaphase." *Current Biology* 14: 1962–67.
- Pereira, A.L., Pereira, A.J., Maia, A.R.R., Drabek, K., Sayas, C.L., Hergert, P.J., Lincefaria, M., Matos, I., Duque, C., Stepanova, T., Rieder, C.L., Earnshaw, W.C., Galjart, N. and Maiato, H. 2006. "Mammalian CLASP1 and CLASP2 Cooperate to Ensure Mitotic Fidelity by Regulating Spindle and Kinetochore Function." *Molecular Biology of the Cell* 17(October): 4526–42.
- Pereira, G., Tanaka, T.U., Nasmyth, K. and Schiebel, E. 2001. "Modes of Spindle Pole Body Inheritance and Segregation of the Bfa1p-Bub2p Checkpoint Protein Complex." *The EMBO journal* 20(22): 6359–70.
- Peters, J.-M. 2002. "The Anaphase-Promoting Complex: Proteolysis in Mitosis and Beyond." *Molecular cell* 9(5): 931–43.

- Pinheiro, D. and Sunkel, C. 2012. "Mechanisms of Cell Cycle Control." *canalbg* 9: 4–17.
- Pinsky, B.A., Kotwaliwale, C. V, Sean, Y., Breed, C.A., Biggins, S. and Tatsutani, S.Y. 2006. "Glc7 / Protein Phosphatase 1 Regulatory Subunits Can Oppose the Ipl1 / Aurora Protein Kinase by Redistributing Glc7." *Molecular and cellular biology* Vol. 26(No. 7): 2648–60.
- Pinsky, B.A., Kung, C., Shokat, K.M. and Biggins, S. 2006. "The Ipl1-Aurora Protein Kinase Activates the Spindle Checkpoint by Creating Unattached Kinetochores." *Nature cell biology* 8(1): 78–83.
- Porollo, A.A., Adamczak, R. and Meller, J. 2004. "POLYVIEW: a Flexible Visualization Tool for Structural and Functional Annotations of Proteins." *Bioinformatics* 20(15): 2460–62.
- Preisinger, C., Körner, R., Wind, M., Lehmann, W.D., Kopajtich, R. and Barr, F.A. 2005. "Plk1 Docking to GRASP65 Phosphorylated by Cdk1 Suggests a Mechanism for Golgi Checkpoint Signalling." *The EMBO journal* 24(4): 753–65.
- Qi, W., Tang, Z. and Yu, H. 2006. "Phosphorylation- and Polo-Box – Dependent Binding of Plk1 to Bub1 Is Required for the Kinetochores Localization of Plk1." *Molecular biology of the cell* 17(August): 3705–16.
- Renshaw, M.J., Ward, J.J., Kanemaki, M., Natsume, K., Nédélec, F.J. and Tanaka, T.U. 2010. "Condensins Promote Chromosome Recoiling During Early Anaphase to Complete Sister Chromatid Separation." *Developmental cell* 19(2): 232–44.
- Rieder, C.L. and Alexander, S.P. 1990. "Kinetochores Are Transported Poleward Along a Single Astral Microtubule During Chromosome Attachment to the Spindle in Newt Lung Cells." *The Journal of cell biology* 110(1): 81–95.
- Rieder, C.L., Cole, R.W., Khodjakov, A. and Sluder, G. 1995. "The Checkpoint Delaying Anaphase in Response to Chromosome Monoorientation Is Mediated by an Inhibitory Signal Produced by Unattached Kinetochores." *The Journal of cell biology* 130(4): 941–48.
- Roof, D.M., Meluh, P.B. and Rose, M.D. 1992. "Kinesin-Related Proteins Required for Assembly of the Mitotic Spindle." *The Journal of cell biology* 118(1): 95–108.
- Rosasco-Nitcher, S.E., Lan, W., Khorasanizadeh, S. and Stukenberg, P.T. 2008. "Centromeric Aurora-B Activation Requires TD-60, Microtubules, and Substrate Priming Phosphorylation." *Science* 319(5862): 469–72.
- Rosenberg, J.S., Cross, F.R. and Funabiki, H. 2011. "KNL1/Spc105 Recruits PP1 to Silence the Spindle Assembly Checkpoint." *Current biology : CB* 21(11): 942–47.
- Rosenfeld, J., Capdevielle, J., Guillemot, J.C. and Ferrara, P. 1992. "In-Gel Digestion of Proteins for Internal Sequence Analysis after One- or Two-Dimensional Gel Electrophoresis." *Analytical biochemistry* 203(1): 173–79.
- Ruchaud, S., Carmena, M. and Earnshaw, W.C. 2007. "Chromosomal Passengers: Conducting Cell Division." *Nature reviews. Molecular cell biology* 8(10): 798–812.

- Sakuno, T., Tada, K. and Watanabe, Y. 2009. "Kinetochore Geometry Defined by Cohesion Within the Centromere." *Nature* 458(7240): 852–58.
- Sanchez, Y. 1999. "Control of the DNA Damage Checkpoint by Chk1 and Rad53 Protein Kinases Through Distinct Mechanisms." *Science* 286(5442): 1166–71.
- Sandall, S., Severin, F., McLeod, I.X., Yates, J.R., Oegema, K., Hyman, A. and Desai, A. 2006. "A Bir1-Sli15 Complex Connects Centromeres to Microtubules and Is Required to Sense Kinetochore Tension." *Cell* 127(6): 1179–91.
- Santocanale, C. and Diffley, J.F. 1998. "A Mec1- and Rad53-Dependent Checkpoint Controls Late-Firing Origins of DNA Replication." *Nature* 395(6702): 615–18.
- Sarangapani, K.K., Akiyoshi, B., Duggan, N.M., Biggins, S. and Asbury, C.L. 2013. "Phosphoregulation Promotes Release of Kinetochores from Dynamic Microtubules via Multiple Mechanisms." *PNAS* 110(18): 7282–87.
- Saunders, W., Lengyel, V. and Hoyt, M.A. 1997. "Mitotic Spindle Function in *Saccharomyces Cerevisiae* Requires a Balance Between Different Types of Kinesin-Related Motors." *Molecular biology of the cell* 8(6): 1025–33.
- Saunders, W.S. and Hoyt, M.A. 1992. "Kinesin-Related Proteins Required for Structural Integrity of the Mitotic Spindle." *Cell* 70(3): 451–58.
- Schuyler, S.C., Liu, J.Y. and Pellman, D. 2003. "The Molecular Function of Ase1p: Evidence for a MAP-Dependent Midzone-Specific Spindle Matrix." *The Journal of cell biology* 160(4): 517–28.
- Schuyler, S.C. and Pellman, D. 2001. "Microtubule 'Plus-End-Tracking Proteins': The End Is Just the Beginning." *Cell* 105(May 18): 421–24.
- Segurado, M. and Tercero, J.A. 2009. "The S-Phase Checkpoint: Targeting the Replication Fork." *Biology of the cell* 101(11): 617–27.
- Shah, J. V, Botvinick, E., Bonday, Z., Furnari, F., Berns, M. and Cleveland, D.W. 2004. "Dynamics of Centromere and Kinetochore Proteins: Implications for Checkpoint Signaling and Silencing." *Current Biology* 14: 942–52.
- Shepherd, L.A., Meadows, J.C., Sochaj, A.M., Lancaster, T.C., Zou, J., Buttrick, G.J., Rappsilber, J., Hardwick, K.G. and Millar, J.B. a. 2012. "Phosphodependent Recruitment of Bub1 and Bub3 to Spc7/KNL1 by Mph1 Kinase Maintains the Spindle Checkpoint." *Current biology: CB* 22(10): 891–99.
- Shero, J., McCormick, M., Antonarakis, S. and Hieter, P. 1991. "Yeast Artificial Chromosome Vectors for Efficient Clone Manipulation, and Mapping." *Genomics* in press.
- Shimogawa, M.M., Graczyk, B., Gardner, M.K., Francis, S.E., White, E.A., Ess, M., Molk, J.N., Ruse, C., Niessen, S., Yates, J.R., Muller, E.G.D., Bloom, K., Odde, D.J. and Davis, T.N. 2006. "Mps1 Phosphorylation of Dam1 Couples Kinetochores to Microtubule Plus Ends at Metaphase." *Current biology: CB* 16(15): 1489–1501.

- Sikorski, R.S. and Hieter, P. 1989. "A System of Shuttle Vectors and Yeast Host Strains Designed for Efficient Manipulation of DNA In *Saccharomyces Cerevisiae*." *Genetics* 122: 19–27.
- Skibbens, R. V, Skeen, V.P. and Salmon, E.D. 1993. "Directional Instability of Kinetochore Motility During Chromosome Congression and Segregation in Mitotic Newt Lung Cells: a Push-Pull Mechanism." *The Journal of cell biology* 122(4): 859–75.
- Stegmeier, F., Visintin, R. and Amon, A. 2002. "Separase, Polo Kinase, the Kinetochore Protein Slk19, and Spo12 Function in a Network That Controls Cdc14 Localization During Early Anaphase." *Cell* 108(2): 207–20.
- Stoler, S., Keith, K.C., Curnick, K.E. and Fitzgerald-Hayes, M. 1995. "A Mutation in CSE4, an Essential Gene Encoding a Novel Chromatin-Associated Protein in Yeast, Causes Chromosome Nondisjunction and Cell Cycle Arrest at Mitosis." *Genes & Development* 9(5): 573–86.
- Storchová, Z., Becker, J.S., Talarek, N., Kögelsberger, S. and Pellman, D. 2011. "Bub1, Sgo1, and Mps1 Mediate a Distinct Pathway for Chromosome Biorientation in Budding Yeast." *Molecular biology of the cell* 22(9): 1473–85.
- Straight, A.F., Belmont, A., Robinett, C.C. and Murray, A.W. 1996. "GFP Tagging of Budding Yeast Chromosomes Reveals That Protein-Protein Interactions Can Mediate Sister Chromatid Cohesion." *Current biology: CB* 6(12): 1599–1608.
- Sudakin, V., Chan, G.K. and Yen, T.J. 2001. "Checkpoint Inhibition of the APC/C in HeLa Cells Is Mediated by a Complex of BUBR1, BUB3, CDC20, and MAD2." *The Journal of cell biology* 154(5): 925–36.
- Sullivan, M. and Uhlmann, F. 2003. "A Non-Proteolytic Function of Separase Links the Onset of Anaphase to Mitotic Exit." *Nature cell biology* 5(3): 249–54.
- Tanaka, K., Kitamura, E., Kitamura, Y. and Tanaka, T.U. 2007. "Molecular Mechanisms of Microtubule-Dependent Kinetochore Transport Toward Spindle Poles." *The Journal of cell biology* 178(2): 269–81.
- Tanaka, K., Mukae, N., Dewar, H., van Breugel, M., James, E.K., Prescott, A.R., Antony, C. and Tanaka, T.U. 2005. "Molecular Mechanisms of Kinetochore Capture by Spindle Microtubules." *Nature* 434(7036): 987–94.
- Tanaka, T.U. 2008. "Bi-Orienting Chromosomes: Acrobatics on the Mitotic Spindle." *Chromosoma* 117(6): 521–33.
- Tanaka, T.U. 2010. "Kinetochore-Microtubule Interactions: Steps Towards Bi-Orientation." *The EMBO journal* 29(24): 4070–82.
- Tanaka, T.U., Fuchs, J., Loidl, J. and Nasmyth, K. 2000. "Cohesin Ensures Bipolar Attachment of Microtubules to Sister Centromeres and Resists Their Precocious Separation." *Nature cell biology* 2(8): 492–99.
- Tanaka, T.U., Rachidi, N., Janke, C., Pereira, G., Galova, M., Schiebel, E., Stark, M.J.R. and Nasmyth, K. 2002. "Evidence That the Ipl1-Sli15 (Aurora Kinase-

- INCENP) Complex Promotes Chromosome Bi-Orientation by Altering Kinetochore-Spindle Pole Connections." *Cell* 108(3): 317–29.
- Tanaka, T.U., Stark, M.J.R. and Tanaka, K. 2005. "Kinetochore Capture and Bi-Orientation on the Mitotic Spindle." *Nature reviews. Molecular cell biology* 6(12): 929–42.
- Toole, E.T.O., Winey, M. and Mcintosh, J.R. 1999. "High-Voltage Electron Tomography of Spindle Pole Bodies and Early Mitotic Spindles in the Yeast." *Molecular biology of the cell* 10(June): 2017–31.
- Torres-Rosell, J., Machín, F. and Aragón, L. 2005. "Cdc14 and the Temporal Coordination Between Mitotic Exit and Chromosome Segregation." *Cell cycle* (January): 109–12.
- Tytell, J.D. and Sorger, P.K. 2006. "Analysis of Kinesin Motor Function at Budding Yeast Kinetochores." *The Journal of cell biology* 172(6): 861–74.
- Uhlmann, F., Lottspeich, F. and Nasmyth, K. 1999. "Sister-Chromatid Separation at Anaphase Onset Is Promoted by Cleavage of the Cohesin Subunit Scc1." *Nature* 400(6739): 37–42.
- Varga, V., Helenius, J., Tanaka, K., Hyman, A.A., Tanaka, T.U. and Howard, J. 2006. "Yeast Kinesin-8 Depolymerizes Microtubules in a Length-Dependent Manner." *Nature cell biology* 8(9): 957–62.
- Van der Waal, M.S., Saurin, A.T., Vromans, M.J.M., Vleugel, M., Wurzenberger, C., Gerlich, D.W., Medema, R.H., Kops, G.J.P.L. and Lens, S.M. a. 2012. "Mps1 Promotes Rapid Centromere Accumulation of Aurora B." *EMBO reports* 13(9): 847–54.
- Wargacki, M., Tay, J., Muller, E., Asbury, C. and Davis, T. 2010. "Kip3, the Yeast Kinesin-8, Is Required for Clustering of Kinetochores at Metaphase." *Cell Cycle* 9(13): 76–75.
- Waters, J.C., Chen, R.H., Murray, A.W. and Salmon, E.D. 1998. "Localization of Mad2 to Kinetochores Depends on Microtubule Attachment, Not Tension." *The Journal of cell biology* 141(5): 1181–91.
- Wei, R.R., Sorger, P.K. and Harrison, S.C. 2005. "Molecular Organization of the Ndc80 Complex, an Essential Kinetochore Component." *PNAS* 102(15): 5363–67.
- Weiss, E. and Winey, M. 1996. "The *Saccharomyces Cerevisiae* Spindle Pole Body Duplication Gene MPS1 Is Part of a Mitotic Checkpoint." *The Journal of cell biology* 132(1-2): 111–23.
- Welburn, J.P.I., Vleugel, M., Liu, D., Yates, J.R., Lampson, M.A., Fukagawa, T. and Cheeseman, I.M. 2010. "Aurora B Phosphorylates Spatially Distinct Targets to Differentially Regulate the Kinetochore-Microtubule Interface." *Molecular cell* 38(3): 383–92.
- Westermann, S., Avila-Sakar, A., Wang, H.-W., Niederstrasser, H., Wong, J., Drubin, D.G., Nogales, E. and Barnes, G. 2005. "Formation of a Dynamic Kinetochore-

- Microtubule Interface through Assembly of the Dam1 Ring Complex." *Molecular cell* 17(2): 277–90.
- Westermann, S., Drubin, D.G. and Barnes, G. 2007. "Structures and Functions of Yeast Kinetochore Complexes." *Annual review of biochemistry* 76: 563–91.
- Widlund, P.O., Stear, J.H., Pozniakovsky, A., Zanic, M., Reber, S., Brouhard, G.J., Hyman, A.A. and Howard, J. 2011. "XMAP215 Polymerase Activity Is Built by Combining Multiple Tubulin-Binding TOG Domains and a Basic Lattice-Binding Region." *PNAS* 108(7): 2741–46.
- Wilbur, J.D. and Heald, R. 2013. "Cryptic No Longer: Arrays of CLASP1 TOG Domains." *Structure* 21(6): 869–70.
- Winey, M, Mamay, C.L., O'Toole, E.T., Mastronarde, D.N., Giddings, T.H.J., McDonald, K.L. and McIntosh, J.R. 1995. "Three-Dimensional Ultrastructural Analysis of the *Saccharomyces Cerevisiae* Mitotic Spindle." *The Journal of cell biology* 129(6): 1601–15.
- Winey, M and O'Toole, E.T. 2001. "The Spindle Cycle in Budding Yeast." *Nature cell biology* 3(1): E23–7.
- Winey, M. and Bloom, K.S. 2012. "Mitotic Spindle Form and Function." *Genetics* 190(4): 1197–1224.
- Wojcik, E., Basto, R., Serr, M., Scaërou, F., Karess, R. and Hays, T. 2001. "Kinetochore Dynein: Its Dynamics and Role in the Transport of the Rough Deal Checkpoint Protein." *Nature cell biology* 3(11): 1001–7.
- Wollman, R., Cytrynbaum, E.N., Jones, J.T., Meyer, T., Scholey, J.M. and Mogilner, A. 2005. "Efficient Chromosome Capture Requires a Bias in the 'Search-and-Capture' Process During Mitotic-Spindle Assembly." *Current biology: CB* 15(9): 828–32.
- Wolyniak, M.J., Blake-hodek, K., Kosco, K., Hwang, E., You, L. and Huffaker, T.C. 2006. "The Regulation of Microtubule Dynamics in *Saccharomyces Cerevisiae* by Three Interacting Plus-End Tracking Proteins." *Molecular Biology of the Cell* 17(June): 2789–98.
- De Wulf, P., McAinsh, A.D. and Sorger, P.K. 2003. "Hierarchical Assembly of the Budding Yeast Kinetochore from Multiple Subcomplexes." *Genes & development* 17(23): 2902–21.
- Yamagishi, Y., Honda, T., Tanno, Y. and Watanabe, Y. 2010. "Two Histone Marks Establish the Inner Centromere and Chromosome Bi-Orientation." *Science* 330(6001): 239–43.
- Yamagishi, Y., Yang, C.-H., Tanno, Y. and Watanabe, Y. 2012. "MPS1/Mph1 Phosphorylates the Kinetochore Protein KNL1/Spc7 to Recruit SAC Components." *Nature cell biology* 14(7): 746–52.

- Yang, Z., Tulu, U.S., Wadsworth, P. and Rieder, C.L. 2007. "Kinetochore Dynein Is Required for Chromosome Motion and Congression Independent of the Spindle Checkpoint." *Current biology : CB* 17(11): 973–80.
- Yeh, E., Skibbens, R. V, Cheng, J.W., Salmon, E.D. and Bloom, K. 1995. "Spindle Dynamics and Cell Cycle Regulation of Dynein in the Budding Yeast, *Saccharomyces Cerevisiae*." *The Journal of cell biology* 130(3): 687–700.
- Yin, H., You, L., Pasqualone, D., Kopski, K.M. and Huffaker, T.C. 2002. "Stu1p Is Physically Associated with β -Tubulin and Is Required for Structural Integrity of the Mitotic Spindle." *Molecular Biology of the Cell* 13(June): 1881–92.
- Yoon, H. and Carbon, J. 1999. "Participation of Bir1p, a Member of the Inhibitor of Apoptosis Family, in Yeast Chromosome Segregation Events." *PNAS* 96(23): 13208–13.
- Yu, H. 2007. "Cdc20: a WD40 Activator for a Cell Cycle Degradation Machine." *Molecular cell* 27(1): 3–16.
- Zhang, K., Lin, W., Latham, J.A., Riefler, G.M., Schumacher, J.M., Chan, C., Tatchell, K., Hawke, D.H., Kobayashi, R. and Dent, S.Y.R. 2005. "The Set1 Methyltransferase Opposes Ipl1 Aurora Kinase Functions in Chromosome Segregation." *Cell* 122(5): 723–34.

ACKNOWLEDGEMENT/DANKSAGUNG

An dieser Stelle möchte ich mich bei all denjenigen bedanken, die mich während meiner Promotion auf unterschiedlichste Weise unterstützt haben und somit maßgeblich zum Gelingen dieser Arbeit beigetragen haben.

Mein besonderer Dank geht dabei an PD Dr. Johannes Lechner, der mir die Gelegenheit gegeben hat, an diesem sehr spannenden, aber auch komplexen Thema zu arbeiten und mir dabei stets mit Rat und Diskussionsbereitschaft zur Seite stand.

Prof. Dr. Felix Wieland danke ich für die Übernahme des Erstgutachtens.

Besonders möchte ich Jennifer Ortiz und Caroline Funk für ihre fortwährende Hilfsbereitschaft und unzählige Diskussionen danken, die mir eine schnelle Einarbeitung im neuen Thema ermöglichten und maßgeblich zu den Projektentwicklungen beigetragen haben.

Allen aktuellen und ehemaligen Mitarbeitern der AG Lechner möchte ich für ihre Unterstützung und Hilfe im Laboralltag danken. Genannt seien dabei Jennifer Ortiz, Caroline Funk, Britta Klem, Maria Delasauce, Manuel Stach und Ana Stelkic. Vielen Dank an Jürgen Reichert, Petra Ihrig, Jvelina Kadiyska und Susanne Eisel nicht nur für die Analyse meiner Massenspektrometrie-Proben.

Ich möchte mich an dieser Stelle auch bei Dr. Dimitris Liakopoulos und seiner Gruppe für viele interessante Literaturseminare und die Bereitstellung von Stämmen, Vektoren und Oligonukleotiden bedanken.

Ein ganz persönlicher Dank geht an meine Familie und meine Freunde, die mich auf meinem Weg immer unterstützt und motiviert haben. Besonders möchte ich Martin danken, dass er immer für mich da war und an mich geglaubt hat.

VIELEN DANK!

Heidelberg, im Januar 2014